Applying an integrated ecotoxicological approach to assess stress from exposure to trace metals and UVB radiation

Chloe Lucy Eastabrook

140135446

A Thesis submitted for the Degree of Doctor of Philosophy

School of Natural and Environmental Sciences

Newcastle University

March 2022

Abstract

Coastal marine organisms are impacted by combinations of chemical and non-chemical stressors, including exposure to metals and elevated UVB radiation. The impacts of chemical mixtures upon these are largely unknown, as are the links between exposure and biological effects. Regulatory guidelines are often based on single effect data and concentration addition (CA) modelling that assumes an additive response, thereby overlooking possible synergistic or antagonistic interactions. In this thesis, a harpacticoid copepod (*Tisbe battagliai* Volkmann-Rocco, 1972) and a chlorophyte microalga *Tetraselmis suecica* (Kylin) Butcher, 1959 were applied as models to characterise the toxicity and determine observed adverse effects of copper, nickel, and zinc chlorides (copepod and alga) or UVB (copepod only). An integrated toxicity characterisation for singular and combined metal exposures were conducted using endpoints across different levels of biological organisation, informed by metal concentrations previously determined from Kaldvellfjorden, Norway. For the combined studies, a form of resolution IV design (Definitive Screening Design, DSD) was implemented, using the EC_{20}, EC_{50} and EC_{80} values from single exposure data. Additionally, CA and independent action (IA) models predict combined effects of mixtures. The UVB-induced effects were quantified using a cyclobutene pyrimidine dimer (CPD) DNA damage induced toxicity pathway, resulting in increased reactive oxygen species (ROS), CPD-DNA damage, short-term reproductive problems, developmental delays, and mortality. Single metal studies characterised toxicity along a metal-induced toxicity pathway that increased ROS production, oxidative DNA damage and apoptosis leading to reduced survival. *T. battagliai* survival was most impacted by copper (48h LC_{50} 1.66 µM), followed by zinc (48h LC_{50} 4.53 µM) and nickel (48h LC_{50} 27.70 µM). All three metals were identified as significant effect drivers within the three-metal mixture, influencing survival after 24 and 48 hours. Significant interactions were found between the pairs copper and zinc, and copper and nickel after 24 hours. These mixtures were compared to CA (48h EC_{50} 16.73 µM) and IA (48h EC_{50} 23.32 µM) models that predicted copper would

be the main risk driver at low mixture concentrations and zinc at high mixture concentrations. The observed mixtures were identified as having a non-interactive effect (additive) or an antagonistic interaction. *T. suecica* growth was most sensitive to zinc and copper after seven days of single exposure, but all three metals were significant effect drivers within the three-metal mixture. When comparing the two species sensitivity to these metals, *T. battagliai* was more sensitive to copper but less sensitive to nickel than *T. suecica*. This integrated ecotoxicological approach provides greater insight into how the interactions between metals influence mixture toxicity of copper, nickel, and zinc at different levels of biological organisation. Following stressor-specific toxicity pathways allowed stressor-specific endpoints to be developed and conducted. For some endpoints, the high variability in observed effects over time shows the complexity of interpreting toxicity from chemical and non-chemical stressors.

Acknowledgements

I would like to thank my supervisors Dr Gary Caldwell, Dr Knut Erik Tollefsen, Dr Hans-Christian Teien and Dr You Song for their knowledge, encouragement, and patience over the last four years. Without their support and guidance, I would not be the researcher I am today. Thank you to all the staff in Ridley 2, specifically Charlotte Andersen, Peter McParlin and David Whitaker for their technical support and to the Ecotoxicology and Risk Assessment Section at the Norwegian Institute of Water Research (NIVA) for hosting me whilst visiting Norway. I am grateful to the MixRisk project (268294) at NIVA, the Centre for Environmental Radioactivity (CERAD) and the School of Environmental Sciences at Newcastle University for the funding that they provided for my PhD. Thanks as well to the Enviresearch Foundation to awarding two bursaries to support a summer project in 2019 and research trip to Oslo in 2020.

The discussions had with Dr Li Xie, Dr Karina Petersen, Dr Raoul Wolf, and Emil Jarosz were invaluable to the development of this work and my professional development. I would have been lost without the support of Dr Li Xie when conducting UVB exposures. Thank you for always helping me set up the instrument and answering many questions at the same time. Particularly, I want to thank Emil Jarosz for spending long days in the labs with me in Norway, and for being a good friend during these trips.

It's very true that the people make the place, and for that reason I have so much thanks and love for Kat Howton, Charlie Vagg, Paul Whitworth, Jess Clarke, Charlie Beighton and Dr John Finley for making the labs and Ridley 2 a great place to work. Without the kindness, support, and conversations from my office mate Cassie Bakshani I would not have achieved as much. Thank you for always listening to my rants about work and a hundred other topics. And finally, to Sophie Mentzel, for making my trips to Oslo so much fun and for being my writing buddy over the last few months.

I wouldn’t be able to put into the words all the thanks I owe to my wonderful parents Pam and Kev, and to my sister Sophie, for always supporting me in pursuing a career that I love. Without them I wouldn’t be where I am today.

Finally, to my partner Kieran for being with me every step of the way and proofreading many chapter drafts. Not only has he always had my back, but he has encouraged me to be the best version of myself throughout this PhD process. I wouldn’t be the person I am today without him.

I dedicate this thesis to my late grandad Robert Davis, who inspired me to become a marine biologist when I was ten years old.

Declaration

This thesis was written by Chloe Eastabrook, with editing and feedback provided by Dr Gary Caldwell on all Chapters, Dr Knut Erik Tollefsen on the systematic review and all data Chapters, Dr Hans-Christian Teien on Chapters four and five, and Dr You Song and Dr Li Xie on the draft manuscript of Chapter six.

Protocols for completing *Tisbe battagliai* metal single and combined experiments were co-developed by Chloe Eastabrook, Emil Jarosz and Dr Li Xie. All ICP-MS samples were analysed on an ICP-MS instrument by Emil Jarosz, a technician at NMBU and Dr Shannon Flynn, as well as guidance on analysing the metal concentration data and ICP-MS methods for data chapters. The water analysis kits were kindly donated by Matthew Pickersgill. Modelling guidance and support for concentration addition and independent action was provided by Dr Karina Petersen. The script used in the systematic review was written by Kieran Cutting. All other experimental work and data collection were conducted by Chloe Eastabrook.

COVID Impact Statement

The research underpinning this thesis was significantly impacted by the COVID-19 pandemic and its associated public health measures, resulting in large changes to the planned scheme of work. The restrictions on movement between the UK and Norway meant that not all the work that had been intended to be completed at the Norwegian Institute for Water Research (NIVA) was able to go ahead.

Notably, the thesis was originally meant to include an additional data chapter focused on the combined interactions of chemical and non-chemical stressors (trace metal exposure and UVB radiation). To collect the data for this chapter, I needed to return to the NIVA for a final data collection trip in order to make use of the UVB incubator within their radiation lab. No suitable radiation facilities were identified within easy reach during the pandemic; as such, this chapter had to be cut. As there is a dearth of research focusing on the interactions between chemical and non-chemical stressors, this chapter would have been a strong end to the thesis, as it would have synthesised the research into a final study to show the importance of combined chemical/non-chemical hazard assessment.

There are also a small number of gaps in data due to the restrictions on movement. When the pandemic began, I was in the middle of a research trip in Norway which had to be cut short to safely return to the UK whilst covered by Newcastle University's insurance. This meant that work which was in progress at the time could not be completed. In Chapter 4, gene expression samples for *T. battagliai* were collected and frozen pending later RNA extraction and qPCR. I had also planned to collect gene expression data for combined metals in Chapter 5. Both were unable to go ahead as I was unable to return to Norway. This was also the case for oxidative DNA damage for UVB radiation in Chapter 6.

Publications and conferences

Publications:

Eastabrook C. L., Song Y., Xie L., Caldwell G. S., and Tollefsen K. E. (In prep). Assembling a toxicity pathway for UVB radiation-induced effects on *Tisbe battagliai*. Journal of Ecotoxicology and Environmental Safety.

Jarosz E., Eastabrook C. L., Byrnes I., Lind O. C., Skipperud L., Wolf R., Tollefsen K. E., and Teien H. C. (In prep). Effect of salinity on speciation, uptake and toxicity in marine copepod *Tisbe battagliai* exposed to Al, Cu, Zn and Ni.

Conferences:

- Poster presentation at the 8th Young Environmental Scientist meeting, of the Society of Environmental Toxicology and Chemistry (SETAC), in Ghent, Belgium in February 2019. Poster titled 'UV-induced stress response of the marine copepod *Tisbe battagliai*: DNA damage and gene expression'. (Chapter 6)

- Two poster presentations at the 29th SETAC Europe Annual Meeting in Helsinki, Finland in May 2019. Posters titled:
  - 'Single and multiple stressor effects in *Tisbe battagliai* – toolbox and adverse outcome pathway development'.
  - 'UV-induced stress response of the marine copepod *Tisbe battagliai*: DNA damage and gene expression'. (Chapter 6)

- Platform presentation at the 30th SETAC Europe Annual Meeting, online in May 2020. Platform presentation titled 'Source to outcome pathways – a way forward in integrating marine exposure and impact assessment?'. (Chapter 4)

- Platform presentation at the 31st SETAC Europe Annual Meeting, online in May 2021. Platform presentation titled 'Using definitive screening design to

conduct complex experimental testing of chemical and non-chemical mixtures'. (Chapter 5)

- Poster presentation at the 31st SETAC Europe Annual Meeting, online in May 2021. Poster titled 'Validating the use of definitive screening design to conduct metal mixture effects assessments with marine microalgae'. (Chapter 3)

- Platform presentation at the 32nd SETAC Europe Annual Meeting in Copenhagen, Denmark in May 2022. 'Integrated exposure and effects assessment of three trace metals on a marine copepod *Tisbe battagliai'*. (Chapter 5, 7)

Table of Contents

List of figures

List of tables

Abbreviations used

AChE	Acetylcholinesterase
AO	Adverse outcome
ASW	Artificial sea water
CAT	Catalase
EC_x	Effective concentration that results in x% of mortality
EPS	Extracellular Polymeric Substances
ETR	Electron Transfer Rate
F	Relative fluorescence yield
FA	Fatty acids
Fm	Maximum fluorescence yield after dark adaption
Fm'	Maximum fluorescence yield after illumination
Ft	Current fluorescence yield
GPx	Glutathione peroxidase
GPX2	Glutathione peroxidase 2
GR	Glucocorticoid receptor
GST	Glutathione S-transferase
GSH	Glutathione
HSP	Heat shock protein
ICP-MS	Inductively Coupled Plasma Mass Spectrometry

KE	Key Event
L	Litre
LC_x	Lethal concentration that results in x% of mortality
LI_x	Lethal irradiance that results in x% of mortality
LOEC	Lowest observed effective concentration
LMM	Low Molecular Mass
LPO	Lipid peroxidation
µL	Microlitres
µM	Micromoles
M	Moles
mL	Millilitre
MoA	Mode of Action
MIE	Molecular Initiating Event
MT	Metallothionein
NOEC	No observed effective concentration
NPQ	Non-photochemical quenching
PAR	Photosynthetically Active Radiation
PCA	Principal component analysis
PETC	Photosynthetic electron transport chain
ppt	Parts per thousand

PSI	Photosystem I
PSII	Photosystem II
qN	Coefficient of non-photochemical quenching
qP	Coefficient of photochemical quenching
ROS	Reactive oxygen species
SOD	Superoxide dismutase
Vg	Vitellogenin
YII	Quantum yield

Chapter 1. Introduction

1.1 Background

Although risk assessments were initially conducted for insurance purposes as far back as 1720 (Christopher, 2007), it wasn't until the establishment of the Environmental Protection Agency (EPA) in 1970 in the United States of America (USA) that quantitative ecological risk assessments became a routine part of regulatory decision making (Suter II, 2008). The 1970s saw a swathe of developments in the methods and practice of quantitative ecological risk assessment (ERA), such as the publication of the Interim Procedures and Guidelines for Health Risk and Economic Impact Assessments of Suspected Carcinogens, that described a general framework for standardised analysis of cancer risks from pesticides (Farland, 1992). There began to be a divergence in practice as the methods developed, with different regulatory agencies interpreting risk assessments differently and working to different standards. In response, the National Academy of Science (NAS) released the 'Red Book' in 1983 that outlined how risk assessments should be understood and managed, including a four-step framework for human health risk assessment: hazard identification, exposure assessment, dose-response assessment, and risk characterisation (NRC, 1983). This was later modified by Environment Canada to focus on exposure assessment, receptor characterisation, hazard assessment and risk characterisation (Gaudet *et al.*, 1995). To this day, this remains the dominant approach for conducting ERAs worldwide.

ERAs have enabled the evaluation of the likelihood of adverse ecological consequences occurring as a result of exposure to a chemical or non-chemical hazard (stressor), focusing at an individual level (Van den Brink, 2008). Chemical stressors include organics, metals, pesticides, and emerging contaminants of concern, whereas non-chemical stressors include temperature, noise, and radiation. ERAs can help identify environmental issues, establish regulatory priorities, and provide scientific evidence for policy makers. Following this, suitable regulatory guidelines on usage, release and/or exposure can be established. To achieve this, the hazard assessment stage is integral, as the

hazard or toxicity of a stressor must be known and understood before risk can be assessed. Hazard assessments determine and characterise the capacity of a stressor to cause adverse effects (Hope, 2006). This can be achieved by identifying toxicological activity within an organism. A mechanistic approach can be taken here, which identifies modes of action and the adverse outcomes of the stressor. An integrated hazard assessment combines measured effects from different levels of biological organisation (molecular, cellular, and individual) to understand how the toxicity at initial levels triggers the observed adverse outcomes at an individual level.

The focus of risk assessments more generally is shifting to cumulative risk assessments (CRA), which has pressured regulatory agencies to simultaneously consider the importance of both chemical and non-chemical stressors. It is therefore important to understand the complexity of mixtures and their interactions (Lewis *et al.*, 2011). The National Research Council's 'Science and Decisions' report, released in 2009, noted that both chemical and non-chemical stressors should be included in cumulative risk efforts, as primary focus is usually given to chemical stressors (NRC, 2009). Traditional risk assessment methodologies have been focused on single chemical stressors, which has meant that quantitative evidence base for combined studies using non-chemical stressors is lacking.

The combined effects of complex mixtures and multiple stressors are often not known or characterised for many common environmental stressors. Combined hazard assessment can therefore provide these missing adverse effects data on combined stressors, as a key component of CRA. Combined hazard assessment can also consider potential interactions between stressors. Combined experiments in the laboratory and field are complex; therefore, predictive models have been useful in taking already known single toxicity data and providing the predicted toxicity of combined stressors. However, measured combined data are needed to understand whether these interactions are acting in the assumed way, or whether this is under- or over-predicting potential combined effects. To harmonise ERA of combined exposure to multiple chemicals, Committee *et al.* (2019) suggest that hazard assessments for the characterisation of mixtures can

be achieved using a whole mixture approach and/or a component-based approach. The whole mixture approach is holistic as all components are considered as contributors to the overall mixture toxicity.

Despite the move towards CRA, there remains a dearth of research focusing on how mixtures interact and cause toxicity in marine contexts. In this thesis, an integrated ecotoxicological approach is taken to assess stress from exposure to trace metals in two marine species, a copepod (*Tisbe battagliai*) and a microalga (*Tetraselmis suecica*), and to UVB radiation for *T. battagliai*. These lower trophic level marine organisms are used to provide a detailed mechanistic understanding of how microalgae and copepods respond to chemical and non-chemical stressors. Microalgae are vital as a base for most marine food webs, and copepods as the most numerous multicellular organisms on Earth, have a critical role in transferring energy between this base to higher trophic levels (Jones and Henderson, 1987; Paffenhöfer, 1993; Stibor *et al.*, 2004; Turner, 2004; Schminke, 2007). Although dominated by planktonic species, those occupying a more benthonic niche, including the Harpacticoida, help to regulate meiobenthic communities and are essential food sources for the juveniles of many commercially important fish (Gee, 1989). Coastal harpacticoid copepods (inhabiting the littoral and infralittoral zones) have been widely used in toxicology studies (Bengtsson, 1978) and for ecological and ecosystem health and risk assessments (ISO, 1999). Furthermore, increased use of such species in risk assessment will help to reduce vertebrate testing in aquatic ecotoxicology.

Both chemical (trace metals) and non-chemical (UVB radiation) stressors are used to complete hazard assessments in singular exposures and combined stressor exposures. For the single stressors, a stressor-specific toxicity pathway is used to characterise the adverse effects at different levels of biological organisation. For combined stressors, specific endpoints are measured along a toxicity pathway to characterise the toxicity because of stressor interactions. Alongside these hazard assessments, the metal fractions within the exposure solutions are determined to better understand what the test species is exposed to and the implications for toxicity.

Metals are chemical elements that have metallic luster, are malleable and ductile, form cations, have basic oxides and are electrical conductors (Ali, Khan and Ilahi, 2019b). There are many different terms for metals, including heavy metal, trace metal and essential metal. Heavy metal is commonly used in ecotoxicology; however, this can lead to assumptions that these metals are always toxic and will cause ecological hazard (Duffus, 2002). Therefore, in this thesis, the term trace metal will be used throughout, to include metals that are often found in the environment at low concentrations and have the potential to cause toxicity whether it is an essential or non-essential element in biological systems and pathways (Rainbow, 2018b).

1.2 Aims and objectives

This thesis forms part of a larger Norwegian Research Council funded project, Cumulative Hazard and Risk Assessment of Complex Mixtures and Multiple Stressors (MixRisk), which used five coastal case studies in Norway to characterise the hazard and risk of chemical and non-chemical stressors. The metals studies within the MixRisk project were based on Kaldvellfjorden in Southern Norway. Kaldvellfjorden was heavily polluted by metal rich runoff into the fjord after the construction of highway E18. Water samples were taken in 2016 and analysed using inductively coupled plasma mass spectrometry (ICP-MS) to identify 29 metals present (Teien *et al.*, 2017). These metals were used in a cumulative risk assessment using NIVA's Risk Assessment database (NIVA, 2019) to identify the most susceptible taxonomic groups (the three most susceptible groups in the fjord were fish, molluscs, and crustaceans) and to determine the main risk drivers for each group. For crustaceans, the main risk drivers in descending order of acute risk were identified as cobalt, aluminium, vanadium, copper, zinc, and nickel. From these, copper, nickel, and zinc were selected as they are well studied as single stressors in crustaceans, specifically copepods, with known mechanisms of action, making them good contenders for cumulative effects and risk assessment evaluation. Further, copper, nickel, and zinc are among the most common metals associated with toxicity in marine environments (Jara-Marini, Soto-Jiménez and Páez-Osuna, 2009; Sharma,

Sarvalingam and Marigoudar, 2021; Arifin, Puspitasari and Miyazaki, 2012; Cardwell *et al.*, 2013).

Within MixRisk, the aims of this thesis are to:

1. Characterise the toxicity of trace metals copper, nickel and zinc, and UVB radiation in single exposure, following a toxicity pathway;
2. Characterise the toxicity of combined stressors;
3. Determine the types of interactions occurring between stressors, and how these impact toxicity.

To achieve these aims, the objectives of this thesis are to:

1. Identify the relevant toxicity pathways for metals and UVB radiation using already published literature;
2. Develop an effects toolbox of targeted bioassays and endpoints related to the mode of action and adverse outcomes of each stressor for the test species;
3. Conduct a hazard assessment for metals and UVB radiation to populate a chosen toxicity pathway with measured responses;
4. Conduct a combined hazard assessment using the same targeted bioassays for comparisons to single toxicity responses;
5. Characterise the interactions occurring between the stressors within a mixture by comparing to predicted mixture responses.

1.3 Research questions

The research questions for this thesis are:

1. What are the effects of metals and UVB radiation on lower trophic level marine organisms when exposed to mixture scenarios?
2. What are the different ways that the test species respond to the same mixture scenarios?
3. Does the presence of other metals in an exposure solution change the effects experienced in these organisms, and if so how?

4. How can we do easier, quicker, and cheaper ecotoxicological testing of mixtures in a laboratory setting?

1.4 Outline of thesis

In Chapter two, a systematic review is conducted to provide insights into the current understanding of metal effects on aquatic copepods and where gaps exist in relation to the mechanistic understanding of metal toxicity. Effect responses show the variability and susceptibility of different metals to marine, brackish and freshwater copepods. The potential modes of action underlying adversity and the factors that influence metal toxicity are discussed. This provides a base for further investigating oxidative stress-induced effects in marine organisms.

Using a toolbox of targeted bioassays, Chapter three investigates the photosynthetic responses of *T. suecica* exposed to copper, nickel, and zinc as single and combined stressors. The combined metal exposures are completed using a design of experiments statistical approach to reduce the number of concentrations needed and provide information on whether there are interactions within the mixtures contributing to the adverse effects on growth.

In Chapter four, toxicity characterisations of copper, nickel, and zinc on the marine copepod *T. battagliai* are conducted, using a toolbox of targeted bioassays to follow a stressor-specific toxicity pathway. Alongside effect endpoints, metal fractionation is measured to understand whether different size fractions are impacting on toxicity.

In Chapter five, the combined effects of the three trace metals are characterised on *T. battagliai* using a design of experiments statistical approach to reduce the amount of testing required. These measured responses at the individual level are compared to predictive models, to determine how the mixture components are interacting and the impact on toxicity.

In Chapter six, toxicity characterisation of the non-chemical stressor UVB radiation on *T. battagliai* is conducted after an acute, short-term exposure using a realistic light, UV and darkness set up. Using stressor-specific bioassays, the responses are assembled into a potential toxicity pathway.

Chapter seven synthesises the findings of this thesis and compares toxicity between the two test species. Reflections on how microalgae and copepod interactions can transfer toxicity along food webs, alongside the exposure and hazard interactions presented in a realistic scenario, are included as a conceptual diagram. Future recommendations for hazard assessments are made for combined chemical and non-chemical stressors and better integration of hazard and exposure assessments to fully characterise toxicity.

Chapter 2. Determining the effects of trace metals in free-living copepods: A Systematic Review

2.1 Introduction

Metals are common chemical contaminants in aquatic and marine environments, originating from multiple geological and anthropogenic sources (Ali and Khan, 2019). Copepods are an important class of crustaceans that play crucial roles in marine and aquatic food webs, transferring energy between primary producers and higher secondary consumers. Copepods uptake trace metals from solution via adsorption onto the exoskeleton and absorption across respiratory surfaces (Rainbow, 2018a). As copepods lack gills, gaseous exchange takes place through pores in the integument and hindgut (Blaxter *et al.*, 1998). Metals can also be taken up in particulate form alongside suspended particulate matter from the water column, sediment or food (Villagran *et al.*, 2019). Copepods typically feed on microalgae which co-exist in the same contaminated environments (although not exclusively), affording an additional uptake mechanism – a trophic transfer of metals between biota known as bioaccumulation (Ali and Khan, 2019).

Toxicity depends on the concentration of a metal and its route of exposure, as some metals at low concentrations (essential metals) are required for normal function of many metabolic and signalling pathways. Toxicity mechanisms for metals include displacing other metals from binding sites on proteins and DNA, resulting in cellular misfunctioning and generating reactive radical species that impact enzyme activity and damage lipids and DNA. These toxicity mechanisms can cause copepods to react by activating internal defence systems (including metabolic enzymes) against oxidative and cellular damage (Kozlowsky-Suzuki *et al.*, 2009). Stress responses can be triggered in other cellular components when these defences are overwhelmed or damaged by metal exposure. These molecular and cellular effects can indicate a metal's mode of action (MoA) and, alongside adverse outcomes (AO) at the individual level, form a pathway of toxicity from initial exposure to adverse outcome. Hazard assessment in marine and aquatic environments has typically focused on the impacts of chemical stressors on higher trophic organisms (particularly those of economic

importance), for example, fish. This taxonomic bias has created gaps in our understanding of chemical stressors in lower trophic organisms, including copepods exposed to trace metals.

2.1.1 Toxicity mechanisms of metals

Although metals are known to cause oxidative stress in many marine and aquatic invertebrates (Jeong *et al.*, 2019), much of the necessary detailed mechanistic understanding remains missing. Metals can react with biological systems by voluntarily losing electrons to form metal cations that have affinity to the nucleophilic sites of vital macromolecules, for example proteins and DNA (Balali-Mood *et al.*, 2021). Metals bind to macromolecule sites that are not intended for them by displacing the intended metal from its binding site (Jaishankar *et al.*, 2014). This is known as a pseudo metal which can interfere with metabolic processes, leading to cellular dysfunction. This interaction of metals with proteins and DNA is thought to cause oxidative deterioration of these macromolecules (Flora, Mittal and Mehta, 2008).

Metal-induced responses in aquatic organisms include: (1) exposure effects such as reactive oxygen species (ROS) generation, (2) detoxification responses including antioxidant enzymes and antioxidant production, (3) toxicity responses – the induction of oxidative stress, DNA damage and repair and apoptosis, and (4) adverse effects at the individual level with mortality, impaired reproduction and development, and growth. First, metals can generate reactive radical species that cause reduced enzyme activity and damage lipid bilayers and DNA. These reactive radical species include oxygen, nitrogen, carbon and sulphur radicals that can originate from two sources: (1) superoxide radical, hydrogen peroxide and lipid peroxides, and (2) chelates of amino acids, peptides and proteins complexed with harmful metals (Flora, Mittal and Mehta, 2008). ROS are most frequently reported for metals, including singlet oxygen, superoxide anion, hydrogen peroxide and hydroxyl radical (Valavanidis *et al.*, 2006; Lauritano, Procaccini and Ianora, 2012). ROS are integral to metabolism, being continuously formed in cells and acting as important signalling molecules (Sharma *et al.*, 2012; Wang *et al.*, 2017). At low intracellular concentrations, ROS can be detoxified by efficient scavenging systems and converted into less

reactive species; however, when concentrations are high the equilibrium between ROS formation and scavenging shifts off balance and leads to damage of macromolecules (Caramujo *et al.*, 2012).

Specifically, copper can facilitate the Haber-Weiss and Fenton reactions, which converts a superoxide anion to a highly reactive hydroxyl radical. If these radicals cannot be removed or the production process inhibited, the antioxidant balance in the cell will be disrupted and overwhelmed with radicals, leading to oxidative stress and cellular damages (Valavanidis *et al.*, 2006). Relatedly, heat shock proteins (HSP) that provide defence against oxidative stress, can undergo transcriptional changes following metal exposure to copper, cadmium and zinc (Kim *et al.*, 2014a). Additionally, free copper ions (Cu^{2+}) can compete with other cations at ion channels, interfering with osmoregulation and enzyme activity (Heuschele *et al.*, 2022).

Similarly, a major mechanism of cadmium toxicity is oxidative stress, as cadmium can increase cellular ROS, such as superoxide anions and hydrogen peroxide, and reduce the antioxidant capacity of the cell (Ensibi and Daly Yahia, 2017). This leads to lipid peroxidation, DNA damage and cellular damage (Wang *et al.*, 2012). Cellular thiols and protein sulfhydryl groups can maintain the intracellular redox homeostasis and protein functions by reacting with ROS (Hu *et al.*, 2019). However, cadmium can deplete sulfhydryl groups and combine with thiol proteins, disrupting the neutralisation of ROS and normal protein function. Relatedly, calcium-mediated intracellular signalling processes and homeostasis can be disrupted by cadmium, by activating transcription to reduce calcium ion stores within a cell (Tvermoes, Bird and Freedman, 2011). Calcium ions are a major signalling molecular during cell signal transduction, which when altered by a trace metal like cadmium, can disrupt energy output regulation and cellular metabolism, often inducing apoptotic cellular death (George and Orrenius, 1999). Further, cadmium can cause neurotoxicity as it interferes with cholinesterase enzymes (ChEs), which includes acetylcholinesterase (AChE). AChE inhibition disrupts nervous system functions, resulting in impacted respiration, feeding and behaviour. ChEs can be inhibited by metals including cadmium, copper, and zinc.

Following on from ChE inhibition, zinc is also known to cause toxicity by interfering with antioxidant defences. Zinc can inhibit glutathione reductase, an enzyme involved in maintaining the supply of reduced glutathione (a cellular reducing thiol) for the control of cellular ROS (Trevisan *et al.*, 2014).

Finally, according to Brix, Schlekat and Garman (2017), there are five potential toxicity mechanisms for nickel in aquatic environments, three of which are the disruption of homeostasis for calcium, magnesium, and iron. Magnesium plays an important catalytic role in stabilising nucleic acids and protein functions in enzymatic reactions, mainly involved in ATP production. Nickel can disrupt magnesium homeostasis by inhibiting the uptake of magnesium ions at the cellular and organ levels (Brix, Schlekat and Garman, 2017). Similarly, iron is an electron donor and receptor in cellular processes including ATP and DNA synthesis. Nickel can impact the expression of genes involved in iron homeostasis, including transferrin receptors, transferrin and ferritin, leading to iron deficiency and reduced oxygen transfer (Brix, Schlekat and Garman, 2017). Nickel has been reported to reduce oxygen consumption rates in aquatic invertebrates (Pane *et al.*, 2003). As described for copper and cadmium, nickel can contribute to the formation of ROS and associated oxidative damage, by denaturing and interfering with antioxidant enzymes such as catalase, glutathione-S-transferases, and glutathione peroxidases (Tlili *et al.*, 2016).

2.1.2 Defence and repair mechanisms

Defence and repair mechanisms can assist in restoring ROS-induced DNA and protein damage in copepods (Sahlmann *et al.*, 2017). Cells contain detoxification systems that use endogenous antioxidants including catalase (CAT), superoxide dismutase (SOD) and glutathione peroxidase (GPx) to inhibit or quench free radical reactions (Nimse and Pal, 2015). In short, these enzymatic antioxidants work by breaking down and removing free radicals by converting them into hydrogen peroxide, then splitting the hydrogen peroxide into a harmless water molecule and divalent oxygen. There are two types of antioxidants – small-molecule and large-molecule. Small-molecule antioxidants e.g., glutathione (GSH) are scavengers that can physically remove ROS. Large-molecule antioxidants (e.g., CAT, SOD and GPx enzymes) absorb ROS to prevent protein

damage (Nimse and Pal, 2015). Additionally, HSP provide protein defence following metal induced oxidative stress. HSP are widely known as chaperone proteins as one of their functions is to interrupt aggregations of proteins which can occur under oxidative stress (Sørensen, Kristensen and Loeschcke, 2003). HSP can also secure functional conformation of proteins and can reverse misfolded or degraded proteins (Wang *et al.*, 2017). Protein synthesis can be temporarily paused in copepods when HSP are expressed to avoid further misfolding or degradation during oxidative stress (Hakimzadeh and Bradley, 1990). Measurements of these responses can indicate whether there was a stress response from the organism and whether the species can naturally deal with that stress. This helps to characterise toxicity and provide explanations for a species' sensitivity.

2.1.3 Toxicity characterisation

Metal toxicity can cause adverse outcomes for affected species, including compromised reproduction, development, and survival. Adverse outcomes are commonly measured in hazard assessments as they represent the toxicity impact on the individual and the growth of the population, with both impacting overall community structure and functioning. The lethal concentration that causes 50% mortality (LC_{50}) value has become a well-accepted value to compare the effects of metals between species, and easily determine a species' metal sensitivity. As adverse outcomes are the result of both molecular and cellular toxicity, these effects can be organised into a toxicity pathway to provide a mechanistic understanding of metal toxicity. Measurements of gene expression or cellular components that are changed during toxicity (e.g., ROS formation and enzyme activity) can be determined alongside life history assays (e.g., fecundity and developmental delays).

2.1.4 Aims of review

Metals were chosen as the stressors of interest for this systematic review as they are major chemical contaminants found in all marine and aquatic environments and are known to cause toxicity and activate stress responses. Copepods are known to be good indicators of how ecosystems will respond to environmental

change (Wang *et al.*, 2018), making them ideal candidates for hazard assessments. Within hazard assessment, there is a need to capture data in a standardised, structural, and transparent way to allow assembly, integration, interpretation, and reporting of these data.

The aims of this review were to assess copepod species sensitivity to different metals and to provide a mechanistic understanding of metal toxicity. To achieve this, measured effects after metal exposure in laboratory studies were organised into possible molecular initiating events (MIE), and cellular responses and adverse outcomes. Potential links between effects are discussed.

2.2 Materials and Methods

A systematic review collects published empirical evidence to answer a specific research question. To achieve this, a database search was conducted to collate studies to be reviewed using carefully selected key words that relate to the research question and aims. These studies were then assessed for eligibility and reliability, using inclusion and exclusion criteria, and the remaining studies were used for qualitive data analysis.

2.2.1 Identification of studies

The research question for this review was, ‘what are the effects of metals on free-living copepods?’ A pilot study was conducted to check that the chosen key words for the database search and criteria for including and excluding papers at each screening level were suitable. Using Scopus as the chosen electronic database, the search was performed without restrictions using the advanced search settings and query string:

> *TITLE-ABS-KEY(copepods AND metal AND effect) TITLE-ABS-KEY(copepods AND metals OR effect).*

Using the programming language node.js, a script was written to query the Scopus Search API for papers matching the query string. This code (see appendix A) retrieved all necessary metadata (title, authors, abstract, journal, date published, DOI) and was outputted into a .csv file. This .csv file was the

basis for data screening. The search was performed on 4th October 2021, and initially included papers from 1972 until 2021.

2.2.2 Assessment of study eligibility

All downloaded studies were screened for eligibility at three levels following specific inclusion and exclusion criteria. Firstly, studies were screened at the title and abstract levels and were included if they met the inclusion criteria: (1) specified a crustacean species was used, (2) a metal was used in a laboratory test, using terms such as LC/EC_X values, MoA or AO, and (3) was written in English. This generated a list of papers to be read in more detail and further screened using more specific criteria.

The inclusion criteria for full texts were as follows: (1) a marine, brackish or freshwater copepod was used in a laboratory experiment, (2) an ecotoxicology study was conducted using a metal(s) added to the media or food, and (3) reported toxicity endpoints were measured. The exclusion criteria for full texts were as follows: (1) a marine, brackish or freshwater copepod was used in a field or mesocosm experiment, (2) an ecotoxicology study was conducted using another chemical stressor, and (3) no toxicity endpoints were measured. For the screening of full texts, a record was kept of why each paper was rejected. Review articles were excluded. Following this, this list of papers to be included was used in the reliability and quality assessment.

2.2.3 Reliability and quality assessment

Reliability and quality assessment of the full texts that passed the inclusion criteria were conducted using the Toxicological data reliability assessment tool (ToxRTool) (Schneider *et al.*, 2009). This tool is publicly available for use and can be downloaded and used in Microsoft Excel (version 16.58). ToxRTool has two software tools – an in vivo and an in vitro evaluation tool – this review only used the in vivo software tool. To answer the 21 criteria of ToxRTool, a binary response was implemented, giving the answer zero when the criteria was not met and one when the criteria was met. These were totalled and given an overall score that related to one of three Klimisch reliability categories (Klimisch, Andreae and Tillmann, 1997). Category one represents studies that are reliable

without restrictions, as studies were carried out following accepted test guidelines or close to these guidelines. Category two represents studies that are reliable with restrictions, as these studies do not follow accepted test guidelines but have sufficient methodological details and are well documented approaches. Category three includes not reliable studies as they used methods that are not accepted, there was insufficient information provided for the assessment, or the test substance or organism/system were not relevant for the research questions. A score of three indicated that the paper was not reliable enough to be included in this review and was removed before data extraction.

2.2.4 From identification to inclusion

The selection of studies included in this review can be seen in a PRISMA flow diagram – Preferred Reporting Items for Systematic reviews and Meta-Analyses (Figure 2.1). This review began with 269 studies and excluded 212 studies after title, abstract and full text eligibly assessment. Full texts couldn't be found for nine papers, after contacting the authors via ResearchGate where possible, causing these to be removed. The 57 full texts were assessed for reliability, resulting in 19 papers being excluded as they scored three and the remaining 20 papers scoring one and 18 papers scoring two that were included in this review. These final 38 studies were included in qualitative data analysis.

2.2.5 Data extraction

Data extraction was completed in Microsoft Excel (version 16.58), to include the relevant information for effect endpoint comparisons, including year of publication, metals used in exposure, species name, LC_{50} values if present and effect endpoints measured. These data were imported into GraphPad Prism 9 for qualitative data analysis, including non-linear regressions and Pearson correlation analysis when relevant.

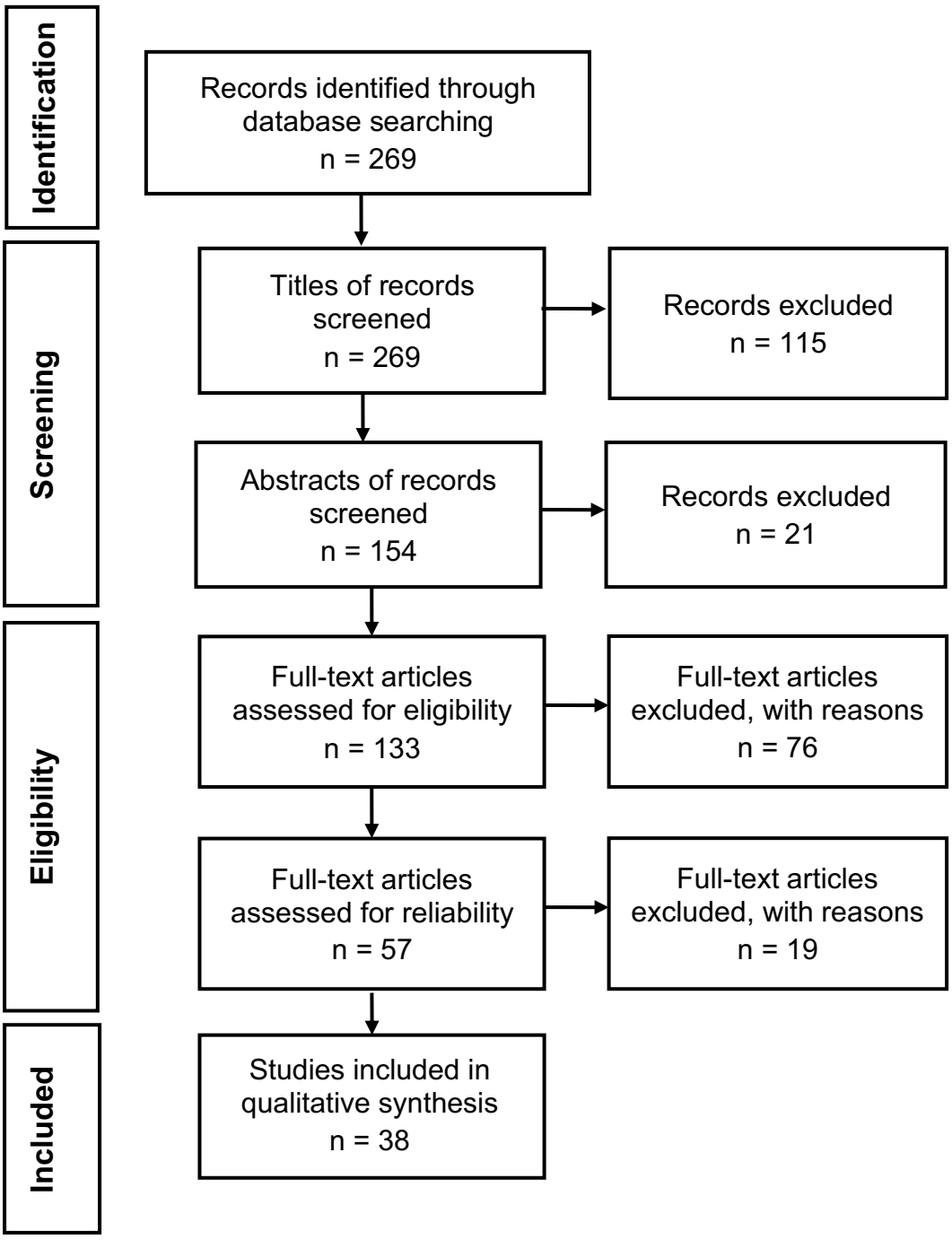

Figure 2.1. PRISMA flow through depicting the screening process for the selection of records included in the review for metals. Some studies reported multiple metals or species, producing multiple data entries into the review, making the number of studies shown here different to the number of data entries. Adapted from Liberati *et al.* (2009).

2.3 Results and Discussion

In this systematic review, 38 studies measured toxicity endpoints during and after exposure to metals in laboratory studies. The metals included in this review are metals of concern for researchers and environmental hazard assessments because of their bioavailability, their difficulty to eliminate from marine and aquatic environments and for their population health effects on commercially and regulatory important species (Briffa, Sinagra and Blundell, 2020; Tian *et al.*, 2020; Jeong *et al.*, 2019).

2.3.1 Frequency of studies over time

Since the early 1980s the number of papers published exposing metals to copepods there has increased (Figure 2.2). There was a significant positive correlation between the year and the number of papers published (Pearson correlation, P = 0.02). This correlation between the number of papers published and the year of publication seems representative of the increasing risk and understanding of metal contamination over that period. Recently, the interest in understanding metal occurrence, behaviour, interactions, and effects has increased due to growing industrial and anthropogenic activities near marine and aquatic environments, particularly coastal environments (Balali-Mood *et al.*, 2021; Ali, Khan and Ilahi, 2019b).

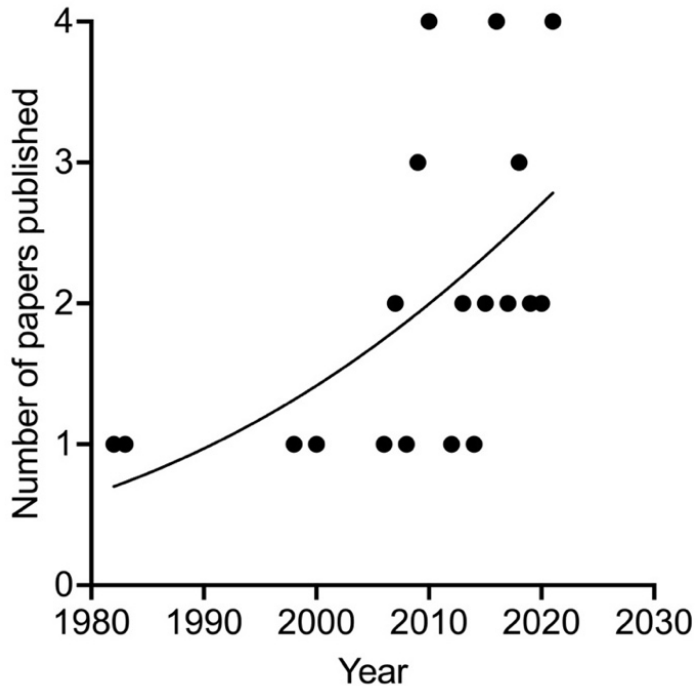

Figure 2.2. Frequency of papers published between 1982 and 2021, fitted with a non-linear regression (R^2 = 0.31).

2.3.2 Frequency of species and metals

Of the 38 studies included in this review, 30 were marine, including 22 different copepod species; there were four brackish species across seven studies and only one freshwater species in a single study (Figure 2.3A); although 16 of the 22 marine species were only reported once. The most tested marine species were harpacticoids; *Tigriopus japonicus*, *T. brevicornis* and *T. fulvus* (Figure 2.3C).

Copper was the most studied of the 11 metals, closely followed by cadmium (Figure 2.3B). This is not surprising considering that copper and cadmium are two of the most persistent metals found in many marine environments. Seven metals were only reported once or twice, including lead, manganese, and cobalt. Silver only featured in brackish studies.

2.3.3 Frequency of effects measured

Survival was the most measured endpoint, followed by reproductive and developmental endpoints (Figure 2.4). These life history endpoints were included in marine, brackish, and freshwater studies, whereas the molecular and cellular

endpoints were mostly included in marine studies. The most common cellular endpoint was antioxidant enzyme activity, but this was only included in marine studies (Figure 2.4). Genetic and proteomic expression were recorded for both marine and brackish copepods, yet no molecular or cellular endpoints were measured in the freshwater study (Figure 2.4). Because of this and the low number of freshwater studies found, in this review the effects of freshwater copepods were limited to life history discussions. Freshwater environments and species are common for ecotoxicological assessments, suggesting that the focus on copepods is lacking. This could be due to wide acceptance of other model freshwater species that are recommended in testing guidelines, including the water flea *Daphnia magna* and zebrafish *Danio rerio*. Metal toxicity and effects are well understood in fish and *Daphnia*, but this level of understanding for copepods is lacking.

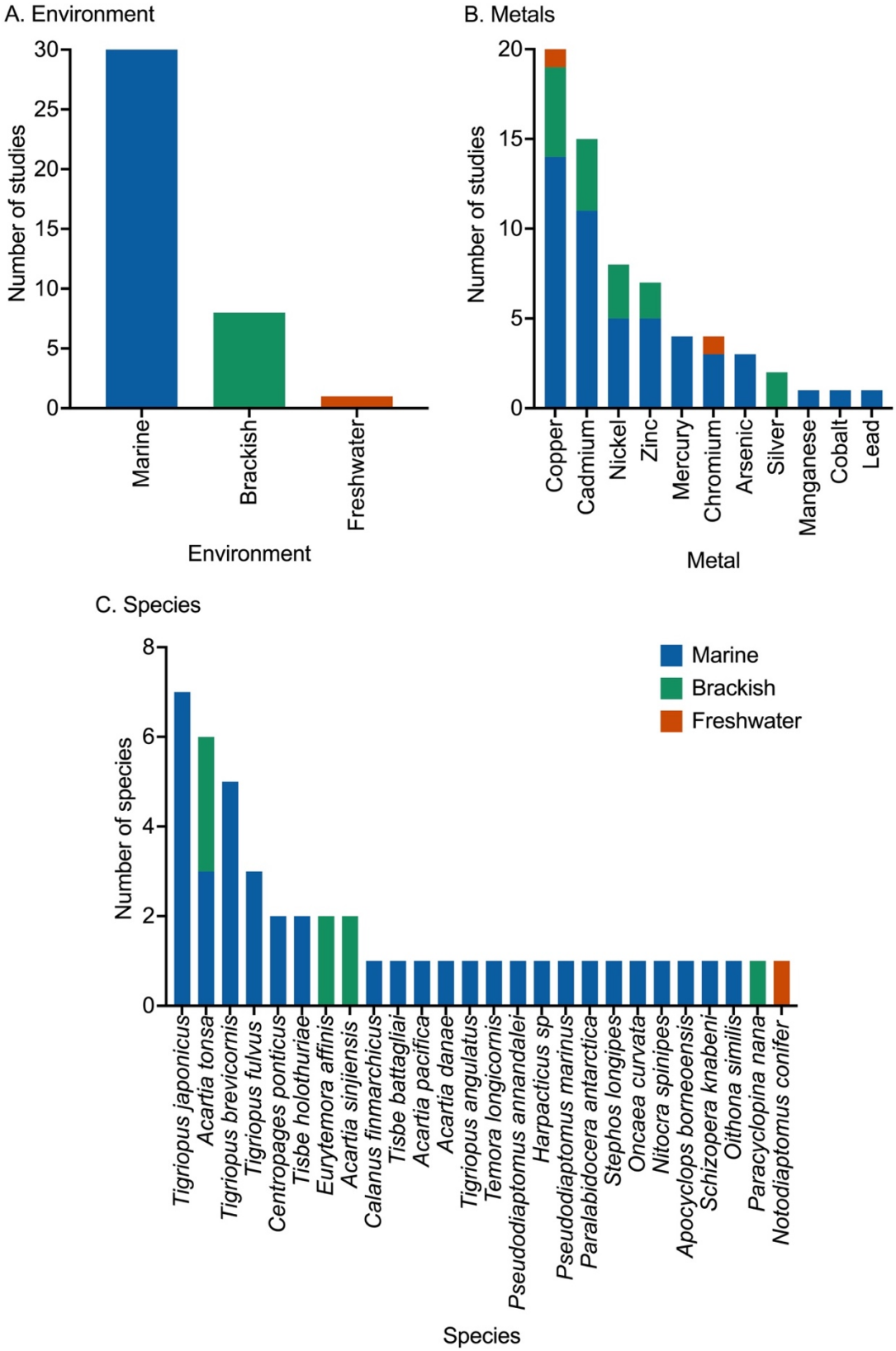

Figure 2.3. Frequency of marine (blue), brackish (green) and freshwater (orange) copepods. (A) Type of environment studied, (B) metals studied and (C) species studied. Some studies included multiple species or metals, making the total number of studies vary between (A) and (B).

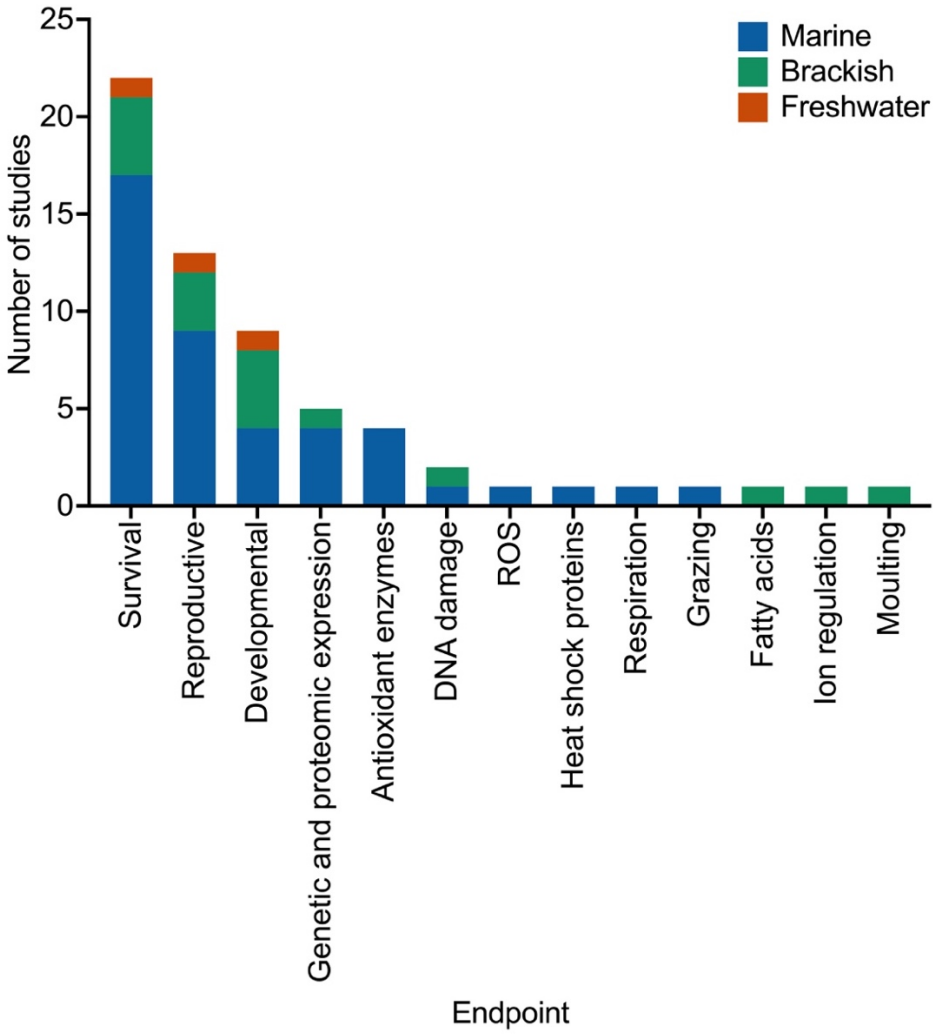

Figure 2.4. Frequency of biological endpoints measured. The total number of endpoints does not equal the total number of studies as some studies included multiple endpoints. ROS = reactive oxygen species.

2.3.4 Copepod sensitivity to metals

Species sensitivity to adversity was described in many studies in this review (n = 22). LC_{50} values were compiled for the top four genera studied to compare sensitivity (Figure 2.5). *Tigriopus* had LC_{50} values for seven metals, over different time points, and was the most resilient genus to chromium, nickel, and cadmium. *Eurytemora* had LC_{50} values for only three metals but was the most sensitive genus to all three (nickel, cadmium, and copper).

For the most studied species (*T. japonicus*) copper was the most toxic metal, followed by lead, zinc, arsenic, cadmium, nickel, and chromium. This review found a similar trend in the order of metal toxicity for other marine species

including *T. battagliai* and *T. holothuriae*, although not all the same metals were tested. Copper is an essential metal and according to Barka, Pavillon and Amiard (2001), essential metals often have higher toxicities than non-essential metals. This did not hold true for all metals, as nickel is essential yet was less toxic than non-essential lead.

Copper was the most toxic metal measured for marine, brackish and freshwater adversity (Figure 2.6). This finding must be considered within the limitations of this metal being the only metal where survival, reproduction and development were measured in all three species groups, as well as being the most studied metal overall. This main finding supports other published literature comparing metal sensitivity outside of the criteria for this review (Verriopoulos and Moraïtou-Apostolopoulou, 1982; Hagopian-Schlekat, Chandler and Shaw, 2001).

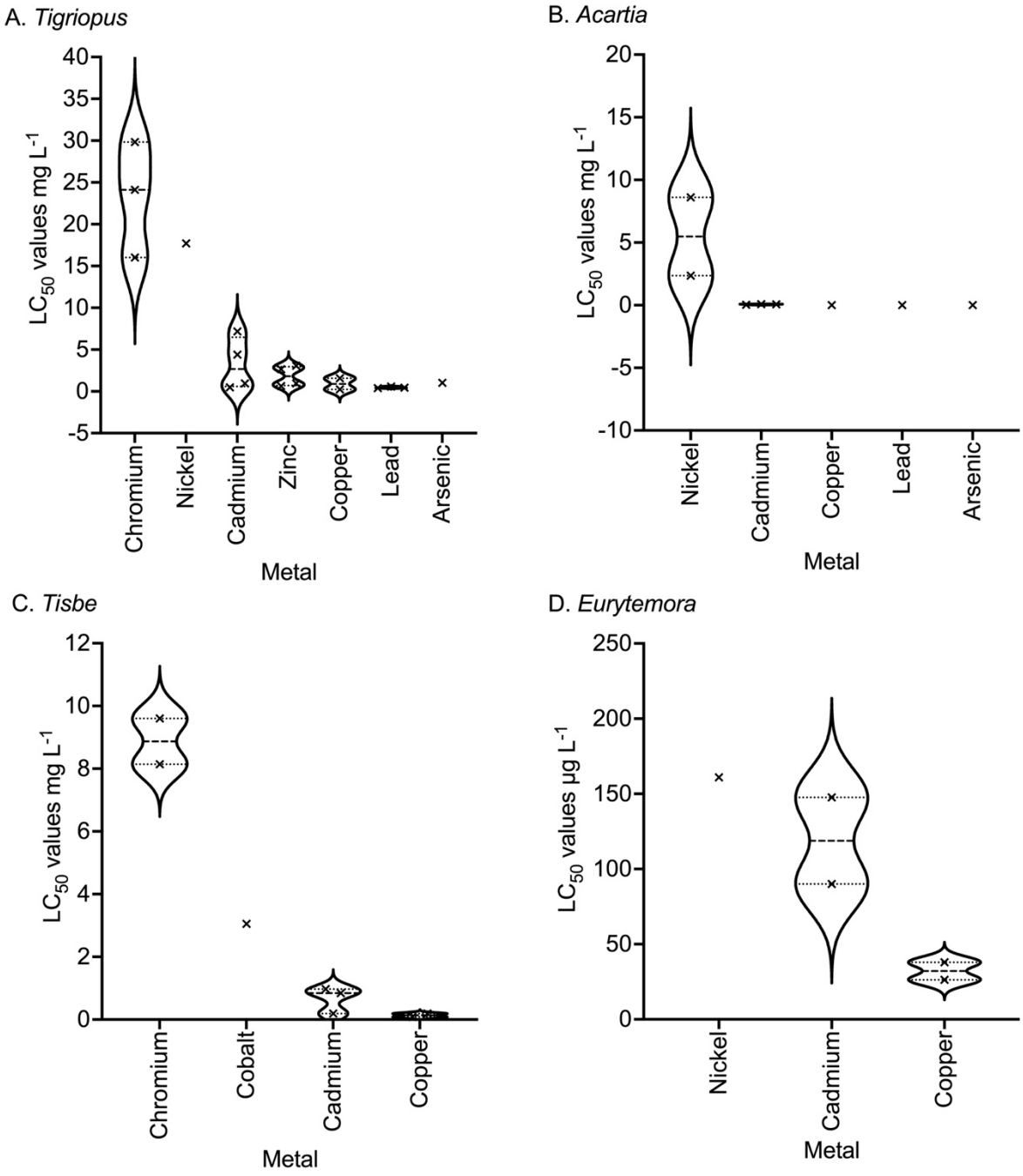

Figure 2.5. Lethal concentrations that cause 50% mortality (LC_{50} values) after (A) *Tigriopus*, (B) *Acartia*, (C) *Tisbe* and (D) *Eurytemora* genera are exposed to trace metals. Trace metals include chromium, nickel, cadmium, zinc, copper, lead, arsenic, and cobalt. Each cross represents one LC_{50} value taken from a study. The spread of LC_{50} values per metal shows different LC_{50} values calculated at different time points. The greater the width of the violin outline, the more data points were available. The width is relative to the number of metals measured per genus and is therefore only comparable within each genus figure.

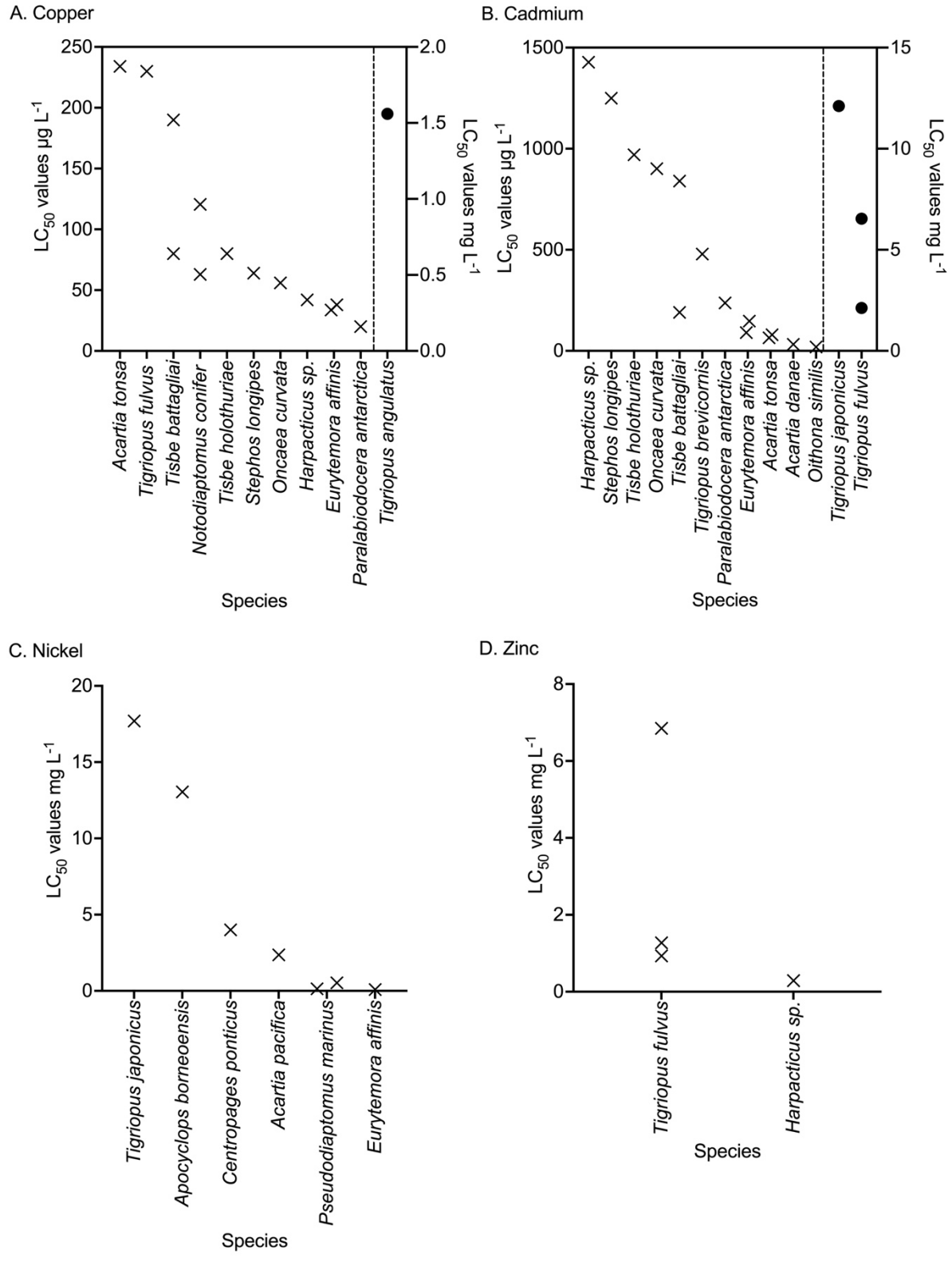

Figure 2.6. Lethal concentrations that cause 50% mortality (LC_{50} values) for copepod species after exposure to (A) copper, (B) cadmium, (C) nickel, and (D) zinc. The cross-data points are for species with LC_{50} values shown on the left-hand y-axis, and filled circle data points are for species with LC_{50} values on the right-hand y-axis. The dashed line on the x-axis divides these two groups.

2.3.5 Copper toxicity

Copper caused the upregulation of anti-oxidative enzymes GST, GPx and SOD and heat shock proteins (HSP) 20 and 70 at 10 and 100 µg L^{-1} in *T. japonicus*, alongside genes coding for detoxification, antioxidant defence and HSP at 10 µg L^{-1}. However, no ROS formation at the same concentrations were measured in *T. japonicus* and no increase in DNA damage in two other *Tigriopus* species were reported at 6 and 60 µg L^{-1}, albeit this study also reported high background DNA damage that could explain the lack of significant difference between controls and exposed *Tigriopus* species (Table 2.1). ROS formation and DNA damage at lower concentrations than mortality would be expected. However, *T. angulatus* had a high sensitivity to copper and had the highest LC_{50} value reported in this review for copper (1.56 mg L^{-1}) (Figure 2.6).

These responses suggest that anti-oxidative enzymes are effectively managing ROS formation in *T. japonicus* as copper is a redox metal known to directly form superoxide and hydrogen peroxide from the Fenton reaction (Chaitanya, Shashank and Sridevi, 2016). However, it is surprising that a measurement of increased ROS was not reported, as shown in other marine species (Nguyen *et al.*, 2018; Rhee *et al.*, 2013b; Bopp, Abicht and Knauer, 2008). This lack of ROS formation could explain the lack of change in DNA damage, measured using the comet assay in three species (Sahlmann *et al.*, 2019). This assay measures double strand breaks, single strand breaks, oxidative base damage, and DNA cross-linking. Copper exposure has been shown to cause oxidative base damage after build-up of free radicals and ROS in cells. A study outside of this review found that DNA damage occurred after metal exposure in three marine copepods, with copper being associated with some of the highest DNA damage (Goswami *et al.*, 2014), suggesting that changes in DNA damage in Sahlmann *et al.* (2019) might have been missed due to the high background DNA damage. As 50% mortality was seen for *A. tonsa* at 234 µg L^{-1}, DNA damage at a lower concentration would be expected before mortality.

Contrary to the lack of DNA damage reported in Sahlmann *et al.* (2019), HSP20 and HSP70 were significantly overexpressed at 10 and 100 µg L^{-1} in *T. japonicus* (Table 2.1). HSP are often overexpressed in response to genotoxic stress, as a

mechanism to protect cells and preserve cell integrity (Dubrez *et al.*, 2020). However, HSPs are also known to respond to a form of cell death called intrinsic apoptosis, which occurs in response to cellular stresses by mitochondrial signalling. These cellular stresses include ROS and the accumulation of mis-folded proteins (Menze *et al.*, 2010b). Here HSP overexpression could be to protect the cells from apoptosis, as one of their main roles is to correct mis-folded proteins. Though apoptosis was not measured in any of these reviewed studies, it is a common response to metal exposure and can be one of the final stages of toxicity at the cellular level, before adverse outcomes.

Furthermore, fatty acids (FA) are involved in protecting cells against diseases (Boissonnot *et al.*, 2016) and were measured in *Acartia tonsa* under copper exposure of 109 µg L^{-1}, showing compositional changes including a lack of monounsaturated fatty acids (MUFA) and polyunsaturated fatty acids (PUFA) (Table 2.1). FAs are involved in metabolism and a change in composition can trigger reduced reproductive success, notably through compromised egg viability (Irigoien *et al.*, 2000). Although egg viability was not measured, reproductive success did decrease following copper exposure, with impacts occurring on the presence of egg sacs (fecundity) and the number of nauplii released (hatching success).

Respiration was measured for two marine species, with opposing results. There were no changes in respiration rates after 12 hours of 23 µg L^{-1} copper exposure to *Calanus finmarchicus* yet *T. brevicornis* displayed increased respiration in one study but exhibited no change in a second (Table 2.1). Lode *et al.* (2021) suggested this difference was due to the number of individuals used per replicate, as an increase was only found when low densities were used (1-2 individuals per replicate). Changes in respiration rates can have important consequences for energy availability for growth and reproduction.

At the adverse outcome level, following copper exposure, reproductive and developmental endpoints showed significant effects after exposure to low concentrations over both short and long time periods, from one to 30 days. For the marine species *Nitocra spinipes* that was exposed to copper via sediment contamination, there were 50% fewer nauplii produced at 37 and 740 mg kg^{-1}.

Even when the copper concentration increased 20 times, the same percentage reduction in nauplii production was shown. The change in silt percentage in the sediment could therefore be contributing to the lack of change in nauplii production, or the additional copper cannot be up taken and increase toxicity impacts. Larval development was reduced in a marine and an estuarine copepod following both constant and pulsed exposure at concentrations of 1.7, 13 and 28 μg L^{-1} and up to 25 μg L^{-1} respectively (Table 2.1). Relatedly, the expression of vitellogenin (Vg) genes Vg1 and Vg2 following a higher 400 μg L^{-1} exposure after 2, 3 and 4 days showed significant induction in the marine copepod *Paracyclopina nana*, whilst the freshwater *Notodiaptomus conifer* produced no egg sacs (Table 2.1). Although the concentrations for these studies were quite different, the impacts on developmental success were linked to Vg expression levels as Vg is important for energy availability for embryonic development, as it is the starting protein of the egg yolk vitellin (Lauritano, Procaccini and Ianora, 2012).

Copper exposure was not always detrimental for reproduction as *N. conifer* experienced an increase in the number of eggs per female at low copper concentrations of 0.4 – 0.8 μg L^{-1}. As copper is an essential metal this suggests that the individuals were able to utilise the additional copper up to a certain threshold value. Above this threshold, the concentration of copper exceeded what was needed for essential cellular processes, like reproduction, and instead had a damaging effect. This was shown for *N. conifer* that had no egg sac at a copper concentration of 3 μg L^{-1}. Further, *N. conifer* had a LC_{50} value of 120.5 and 62.9 μg L^{-1} that are higher than any concentrations used in this reproductive study, suggesting that although *N. conifer* can survive higher copper concentrations, their reproduction is negatively impacted at much lower concentrations.

Overall, copper toxicity from these papers indicated a relationship to oxidative stress that caused anti-oxidative enzymes, HSPs and FAs to react at a molecular and cellular levels. Once copper toxicity was established, both reproductive and developmental endpoints highlighted the high impact at relatively low copper concentrations, suggesting that copepods are very sensitive to copper.

Table 2.1. Summary of biological endpoints measured in studies that exposed copepods to copper, except for survival or LC_{50} values. For the environment column, blue represents marine species, green represents brackish species and orange represents freshwater species. ROS = reactive oxygen species, GPx = glutathione peroxidase, GST = glutathione S-transferase, GSH = glutathione, GR = glucocorticoid receptor, SOD = superoxide dismutase, CYP13A = cytochrome P13A, CYP4C20 = cytochrome P4C20, HSP = heat shock protein, FA = fatty acids, PUFA = polyunsaturated fatty acid, HUFA = highly unsaturated fatty acids, Vg = vitellogenin.

Environment	Species	Endpoint	Time	Concentration ($\mu g\ L^{-1}$ unless otherwise stated)	Response	Reference
	Tigriopus japonicus	Gene expression	6h	10	138 genes upregulated – detoxification, antioxidant defence, heat shock proteins, GPx, GST, CYP13A and CYP4C20. 375 genes downregulated – structure, growth, development, Vg and cuticle proteins.	(Ki *et al.*, 2009)
	T. japonicus	GST expression	6h	10 50	No change Increased	(Lee *et al.*, 2007)
	T. japonicus	ROS formation	4d	10 and 100	No sig. change	(Kim *et al.*, 2014b)
		GSH and GR			No sig. change	
		GST, GPx and SOD			Concentration dependent significant increases compared to controls	
		HSP40			Downregulated	
		HSP20 and 70			Upregulated	
	T. brevicornis *T. longicornis* *Acartia tonsa*	DNA strand breaks	6h and 3d	0, 6 and 60	No increase in DNA strand break but high background DNA strand break reported	(Sahlmann *et al.*, 2019)
	A. tonsa	FA profile	2d	109	No PUFAs or HUFAs present	(Filimonova *et al.*, 2016)
	T. brevicornis	Respiration	12h	23	Increase at low copepod densities per replicate (1 or 2 individuals)	(Lode *et al.*, 2021)
	T. brevicornis	Respiration	12h	23	No change	

	Calanus finmarchicus					(Lode *et al.*, 2020)
	Nitocra spinipes	Number of nauplii	10d	Sediment 10% silt = 37 mg kg^{-1} Sediment 91% silt = 740 mg kg^{-1} Water = 68	50% fewer nauplii produced 50% fewer nauplii produced No change	(Campana *et al.*, 2012)
	A. sinjiensis	Larval development	1d 2d 3d	28 13 1.7	Chronic EC_{50} value following 3h pulse Chronic EC_{50} value following 3h pulse Chronic EC_{50} value following continuous exposure	(Stone *et al.*, 2021)
	Paracyclopina nana	Vg1 and 2 expression	0, 1, 2, 3, 4d	400	Significant induction of Vg1 at all time points when compared to 0-day Significant induction of Vg2 at 2, 3 and 4 days	(Hwang *et al.*, 2010)
	A. tonsa	Number of nauplii	7d	Dietary exposure = 1.2	20% fewer nauplii	(Bielmyer, Grosell and Brix, 2006)
	Eurytemora affinis	Developmental rates	2d	> 25	Suppressed developmental rates	(Sullivan *et al.*, 1983)
	Notodiaptomus conifer	Fecundity	19 – 30d	0.4 – 1.6	Higher than controls = 5.67 ± 1.14 Exposed = 7 – 11.2	(Gutierrez, Gagneten and Paggi, 2010)
		Time of first clutch		0.4 – 1.6	Increased time for clutch presence of 4.2 – 4.8 days compared to controls 3.8 ± 0.83	
		Presence of clutch		3	No egg sac	
		Number of eggs per female		0.4 – 0.8 1.6	7 2.5	

2.3.6 Cadmium toxicity

Cadmium exposure at 100 and 1000 µg L^{-1} did not increase ROS production in *T. japonicus* and only stimulated SOD, GST and GPx enzyme activity in *T. japonicus* at the same concentrations (Kim *et al.*, 2014b) and at lower concentrations of 0.2 and 0.4 µg L^{-1} for *C. ponticus* (Ensibi and Daly Yahia, 2017) (Table 2.2). Redox-inactive metals (e.g., cadmium, arsenic and lead) cannot form ROS and free radicals themselves, but can deplete glutathione and bond to sulfhydryl groups of proteins including glutathione (Valko *et al.*, 2016). This can disrupt and intervene with enzyme activity involved in detoxification, and as a result can allow more ROS to accumulate uncontrollably within cells. This could explain why high concentrations of cadmium did not increase GR and GSH and suggest that ROS formation was controlled by other enzyme activities that were increased (CAT and SOD). These data align with *T. japonicus* survival data and the LC_{50} value of 12.11 mg L^{-1} (Figure 2.6) and suggest that this species has a low sensitivity to cadmium.

Both DNA damage and HSPs increased following cadmium exposure, especially the upregulation of HSP20 and HSP70 in *T. japonicus* at high concentrations of 100 and 1000 µg L^{-1} (Kim *et al.*, 2014b). For DNA damage, this review saw that a relatively low cadmium concentration of 9.57 µg L^{-1} caused over 60% DNA damage in the brackish species *A. tonsa* (Pavlaki *et al.*, 2016a). *A. tonsa* had a LC_{50} value of 64.6 µg L^{-1}, which alongside high DNA damage at 9.57 µg L^{-1} suggests that *A. tonsa* is a sensitive species to cadmium. Another *Acartia* species, *A. danae* had a similar response with high mortality and a similarly low LC_{50} value of 32 µg L^{-1} (Figure 2.6). HSPs are known to upregulate in response to DNA damage and mis-folded proteins (Menze *et al.*, 2010b); therefore, these responses suggest a possible DNA damage-induced toxicity mechanism for cadmium. HSP20 is known as the small molecular HSP as the molecular weights are below 42 kDa, which are evolutionarily conserved and have a role in protein homeostasis, while HSP70 is a large HSP. Both have been identified as potential molecular biomarkers for metal toxicity in marine and aquatic environments as they play protective roles in many species (Jung and Lee, 2012). In support, gene expression in *T. japonicus* was upregulated in genes related to diseases and oxidative phosphorylation following exposure to 50 µg L^{-1}(Wang, Zhang and Lee, 2018). Relatedly to DNA damage, lipid peroxidation (LPO) is a main indicator of damage to a cellular membrane following metal exposure, as structural lipids are a target for toxicity (Sobrino-Figueroa, Hernández and Álvarez, 2020).

Cadmium was found to cause this damage in *C. ponticus*, with a concentration dependent increase at relatively low concentrations of 0.2 and 0.4 µg L^{-1} (Ensibi and Daly Yahia, 2017).

Neurotoxicity can be inferred from acetylcholinesterase (AChE) enzyme activity. For *C. ponticus*, AChE activity also initially increased at relatively low concentrations of 0.2 and 0.4 µg L^{-1}, suggesting cadmium is involved in neurotoxicity (Ensibi and Daly Yahia, 2017). This enzyme controls acetylcholine, the primary neurotransmitter in most copepods, that without regulation can result in excessive nerve and muscle fibre stimulation and death (Forget, Beliaeff and Bocquené, 2003). As cadmium is not an essential metal, this could explain the initial response even at low concentrations, as the metal does not need to be scavenged when present at a concentration slightly higher than normal, although AChE activity reduced after 72 hours. AChE inhibition has been linked to neurotoxicity in copepods exposed to other contaminants, suggesting that longer exposures to cadmium could result in neurotoxicity (Forget, Beliaeff and Bocquené, 2003). Although *C. ponticus* was not included in a survival assay in this review, the AChE assay being conducted at very low concentrations of 0.2 and 0.4 µg L^{-1} is a very different experimental design set up compared to the survival assays for other copepod species. Eight species had LC_{50} values above 840 ug L^{-1}, with only two species having very low survival at low cadmium concentrations (Figure 2.6). This suggests that *C. ponticus* would be as sensitive to cadmium as *Acartia danae* and *Oithona similis*. These three species are pelagic, whereas *T. japonicus* and *T. fulvus* are benthic species and have the highest sensitivity to cadmium in this review (Figure 2.6). This suggests that the habitat or adaptations to the habitat could influence cadmium sensitivity.

Vg expression can impact reproduction and development. This was seen for cadmium in two estuarine copepods at the molecular and cellular level, with changes in Vg expression for *P. nana* at 100 µg L^{-1} (Hwang *et al.*, 2010) and suppressed developmental rates for nauplii for *E. affinis* at a slightly higher concentration of 116 µg L^{-1} (Sullivan *et al.*, 1983). Other papers have also reported Vg expression induction following cadmium exposure in the marine copepod *T. japonicus* (Lee *et al.*, 2008). These three species (*P. nana, E. affinis* and *T. japonicus*) are different copepods in terms of their environment (estuarine or marine) and where they live within that environment (pelagic, epipelagic, and benthic respectively); however, they all experienced an induction of Vg to similar levels of cadmium.

Cadmium also impacts copepod physiology, including feeding rates, developmental rates, and reproductive timings. Feeding rates of *S. knabeni* were studied in a sediment experiment, showing short term (four-hour) significant impacts at concentrations up to 49 mg kg^{-1} and no grazing at higher concentrations of 98, 106 and 157 mg kg^{-1} (Silva *et al.*, 2009). As a result, energy requirements can be impacted, often causing energy diversions from reproductive processes during stress. Reproductive outputs were found to be significantly impacted by cadmium for brackish species (Table 2.2), with a hatching success EC_{50} value of 1940 µg L^{-1} for *A. tonsa* and larval development ratio EC_{50} value of 690 µg L^{-1} (Pavlaki *et al.*, 2016a). At a lower cadmium concentration of 116 µg L^{-1} the developmental rates for *E. affinis* were supressed. Although both estuarine species, these species live in different environments that could contribute this difference in tolerance (*A. tonsa* is pelagic and often at the ocean surface, while *E. affinis* is epipelagic and can live in sediment or water).

For two marine species of *Tigriopus*, the number of clutches, number of nauplii, nauplii per clutch and fecundity all decreased at concentrations of 2.5, 5, 10, 50 and 300 µg L^{-1} when compared to controls (Pane *et al.*, 2008; Wang, Zhang and Lee, 2018). These results show that cadmium exposure will impact overall population growth, but once hatched *T. japonicus* nauplii survival did not significantly change up to cadmium concentrations of 50 µg L^{-1}. Similarly, when *T. japonicus* and *T. fulvus* are adults, they are not particularly sensitive to cadmium, with high survival and LC_{50} values of 12.11 mg L^{-1} and 6.54 mg L^{-1} respectively (Figure 2.6). Yet their reproductive systems are very sensitive to cadmium, as shown by significant decreases happening from 2.5 to 300 µg L^{-1}. However, if the cadmium contamination is short-lived, the recovery could take only one to two generations, as shown in Wang, Zhang and Lee (2018). Here, after cadmium exposure was stopped for the 5^{th} and 6^{th} generations of *T. japonicus*, there was no significant difference from the controls. This quick recovery could allow population numbers to recover in areas experiencing one-off contamination events. Overall, cadmium exposures to copepods suggests that the mode of action occurs from prolonged oxidative stress (LPO induced) causing increased DNA damage, in turn impacting physiological rates, including feeding rates, reproductive rates and developmental rates.

Table 2.2. Summary of biological endpoints measured in studies that exposed copepods to cadmium, except for survival or LC_{50} values. For the environment column, blue represents marine species, and green represents brackish species. ROS = reactive oxygen species, GPx = glutathione peroxidase, GST = glutathione S-transferase, GSH = glutathione, GR = glucocorticoid receptor, SOD = superoxide dismutase, CAT = catalase, AChE = Acetylcholinesterase, HSP = heat shock protein, Vg = vitellogenin.

Environment	Species	Endpoint	Time (days, unless otherwise stated)	Concentration (µg L^{-1} unless otherwise stated)	Response	Reference
	Tigriopus japonicus	ROS formation	4	100 and 1000	No significant change compared to controls	(Kim *et al.*, 2014b)
		GSH and GR				
		GST and SOD			Significant increase at both concentrations	
		GPx			Significant increase at 1000 only	
		HSP10			Downregulated	
		HSP20 and HSP70			Upregulated	
	Centropages ponticus	GPx	3	0, 0.2 and 0.4	Concentration dependent increase	(Ensibi and Daly Yahia, 2017)
		CAT, GR, GST and AChE			Biphasic response – increasing at 24h or 48h and decreasing by 72h	
		Protein and lipid peroxidation			Concentration dependent	
	Tigriopus japonicus	Gene expression	1^{st} – 4^{th} generations	50	28 genes upregulated – metabolic pathways, oxidative phosphorylation, and diseases 30 genes downregulated – neuroactive ligand-receptor interaction, protein digestion, and absorption	(Wang, Zhang and Lee, 2018)
	Tigriopus japonicus	Nauplii survival	1^{st} – 4^{th} generations	0, 2.5, 5, 10 and 50	No change	(Wang, Zhang and Lee, 2018)
		Time in the naupliar phase			Concentration dependent increase for all generations	
		Developmental time				

		Number of clutches			4th generation impacted at 5, 10 and 50 µg L^{-1}	
		Fecundity			Concentration dependent decrease for all generations	
		Recovery	5th – 6th generations		No significant differences to controls	
	Tigriopus fulvus	Number of clutches	2	300	Reduced from 7 ± 0.7 in controls to 4.2 ± 1.1	(Pane *et al.*, 2008)
		Number of nauplii			Reduced from 96.4 ± 14 in controls to 22.5 ± 7.8	
		Nauplii per clutch			Reduced from 13.7 ± 1.5 in controls to 5.3 ± 1.2	
		Nauplii per female per day			Reduced from 3.2 ± 0.5 in controls to 0.7 ± 0.2	
	Schizopera knabeni	Feeding rates	4h	> 49 mg kg^{-1} dry sediment	Significantly reduced	(Silva *et al.*, 2009)
				98, 106 and 157 mg kg^{-1} dry sediment	No grazing observed	
	Paracyclopina nana	Vg1 and 2 expression	0, 1, 2, 3, 4	100	Significant induction of both Vg1 and Vg2 from 1 day	(Hwang *et al.*, 2010)
	Acartia tonsa	DNA damage	2	9.57	> 60% DNA damage	(Pavlaki *et al.*, 2016a)
		Hatching success	1	1940	50% hatching success	
		Larval development ratio	1	690	50% LDR	
	Eurytemora affinis	Developmental rates	2	116	Supressed	(Sullivan *et al.*, 1983)

2.3.7 Nickel toxicity

As shown in Table 2.3, nickel toxicity was measured at the molecular and cellular levels using endpoints for antioxidant enzymes, AChE activity, LPO, and metallothionein (MT). These endpoints are related to oxidative stress, with mainly concentration dependent increases for most enzyme activity. Two different marine species *T. japonicus* and *C. ponticus* showed similar increases for the enzymes SOD at nickel concentrations 0.75 mg L^{-1} and 0.002 to 2 mg L^{-1} respectively and GST at nickel concentrations of 3 mg L^{-1} and 0.002 to 2 mg L^{-1} respectively (Wang and Wang, 2010; Djebbi *et al.*, 2021). Nickel cannot directly produce ROS, but it can interfere with enzyme activity which leads to ROS formation being uncontrolled. All related enzyme activities (e.g., SOD, GST, GPx, and CAT) were increased by nickel exposure of 3 mg L^{-1} and up to 2 mg L^{-1} depending on the species, except for GSH that reduced lower than controls from 0.25 – 3 mg L^{-1}.

Relatedly, MT was significantly increased in response to nickel exposure from 0.125 to 3 mg L^{-1} in *T. japonicus* (Wang and Wang, 2010). MTs are a family of cysteine-rich metal binding proteins that are commonly associated with metal exposure and providing protection against oxidative stress. When MT synthesis capacities are overcome, LPO and DNA damage can occur, making MT a useful bioindicator of general oxidative stress. However, LPO was significantly reduced in *T. japonicus* when exposed to 0.75 and 3 mg L^{-1} of nickel (Wang and Wang, 2010). LPO is often induced by free radicals and ROS; therefore, this response is surprising when other oxidative stress indicators have increased. This suggests that LPO factors might not depend on the antioxidant system. Interestingly, both LPO and GSH decreases occurred at the same concentration, hinting at a possible interaction. A similar reduced LPO was noted after 14 days of nickel exposure to *Apocyclops borneoensis* by Mohammed (2013) – a study not included within this review.

Two brackish species exposed to nickel experienced reproductive and developmental delays. For *A. tonsa*, the number of nauplii per female reduced by 20% after a low dietary exposure of nickel at 2.4 µg L^{-1} (Bielmyer, Grosell and Brix, 2006). For *A. sinjiensis*, both larval and naupliar developments were impacted, with a 50% reduction in larval development at 8.6 µg L^{-1} and no copepodites developed at 16 µg L^{-1} (Gissi *et al.*, 2018); similar trends were found for other *Acartia* species (Mohammed, Wang and Jiang, 2010; Stone *et al.*, 2021). Pulse exposures were

trialled at 71 and 130 µg L^{-1} with *A. sinjiensis* in Stone *et al.* (2021), resulting in lower EC_{50} values than continuous exposure, which is not surprising but provides more insightful responses for environments where pulse exposures would provide a more accurate understanding of toxicity. In other marine species, the number of nauplii per female for *T. japonicus* and *Apocyclops borneoensis* reduced from 45 to 20 and 5 respectively after 1 mg L^{-1} of nickel exposure (Mohammed, Wang and Jiang, 2010). In the same study, another species *A. pacifica* had a reduction in the number of eggs per female from 23 to 3 and a reduced hatching success from 80% to around 30% at the same nickel concentration. All three species were included in a survival assay, where lethality sensitivity was low for *T. japonicus* (LC_{50} value of 17.70 mg L^{-1}), followed by *A. borneoensis* (LC_{50} value of 13.05 mg L^{-1}) and *A. pacifica* (LC_{50} value of 2.36 mg L^{-1}). The same order of sensitivity for reproduction was seen for *T. japonicus* and *A. borneoensis*. Another marine copepod *C. ponticus* suffered reduced reproductive success, egg production and hatching success reduced at relatively low nickel concentrations of 0.02 and 2 mg L^{-1}, particularly when compared to LC_{50} value of 4.0 mg L^{-1} for adult survival (Djebbi *et al.*, 2021). This suggests that reproduction and development are more sensitive endpoints to nickel exposure than lethality.

When comparing nickel species sensitivity to copper, cadmium and zinc, nickel had the largest range of LC_{50} values from 17.70 mg L^{-1} to 0.090 mg L^{-1}. The highest LC_{50} value reported in this review belongs to the benthic *T. japonicus*, yet the lowest nickel LC_{50} value is for an epipelagic species *E. affinis*. As both these species are associated with the sediment, it is surprising that their sensitivity to nickel ranges so much. The second highest LC_{50} of 13.05 mg L^{-1} is a pelagic cyclopoid species *Apocyclops borneoensis*, suggesting that where the copepod inhibits might not be a major factor for species sensitivity to nickel and other factors are responsible.

Overall, nickel toxicity in marine copepods appears to be driven by oxidative stress and neurotoxicity, although mostly oxidative stress related endpoints were included at the cellular levels in the studies featured in this review. Further experiments with nickel should be completed to be able to fully understand and characterise the mode of action for copepods. At the adverse outcome level there were more assays completed and for both marine and brackish species, showing that both reproduction and development were impacted by nickel exposure at much lower concentrations than were causing 50% mortality in adults.

Table 2.3. Summary of biological endpoints measured in studies that exposed copepods to nickel, except for survival or LC_{50} values. For the environment column, blue represents marine species and green represents brackish species. MT = Metallothionein, GPx = glutathione peroxidase, GST = glutathione S-transferase, GSH = glutathione, SOD = superoxide dismutase, CAT = catalase, AChE = Acetylcholinesterase.

Environment	Species	Endpoint	Time (days)	Concentration (mg L^{-1})	Response	Reference
	Tigriopus japonicus	MT	12	0, 0.125, 0.25, 0.75 and 3	Significantly higher, between 19 – 21 µg per mg protein, than controls = ~12 µg per mg protein	(Wang and Wang, 2010)
		Lipid peroxidation		0.75 and 3	Significantly reduced approximately two-fold lower than controls	
		SOD		0.75	Over two-fold increase compared to controls	
		GST		3	~1.7-fold increase compared to controls	
		GPx		3	Over two-fold lower than controls	
		GSH		0.125 0.75	Higher than controls Lower than controls	
		AChE		0.25 and 3	Increase in activity	
	Centropages ponticus	SOD and GST	2	0, 0.002, 0.02, 0.2 and 2	Concentration dependent increase	(Djebbi *et al.*, 2021)
		CAT and AChE			Biphasic response, decreasing at higher concentrations	
		Reproductive success		0.02, 0.2 and 2	Significant negative effects	
		Egg production		0.02 and 2	46% and 82%	
		Hatching success		2	79% reduction from controls from 8.3 ± 1.1 and 1.5 ± 0.2 eggs $female^{-1}$ day^{-1}	
	Acartia sinjiensis	Larval development ratio	1 2	0.071 0.130	Chronic EC_{50} value following 3h pulse Chronic EC_{50} value following 3h pulse	(Stone *et al.*, 2021)

			3	0.0086	Chronic EC_{50} value following continuous exposure	
	T. japonicus	Number of nauplii per female	10	1	Reduced from 45 to 20	(Mohammed, Wang and Jiang, 2010)
	Apocyclops borneoensis				Reduced from 45 to 5	
	Acartia pacifica	Number of eggs per female			Reduced from 23 to 6	
		Hatching success			Reduced from 80 to ~30%	
	Acartia tonsa	Number of nauplii per female	7	Dietary exposure = 0.0024	20% reduction compared to the controls	(Bielmyer, Grosell and Brix, 2006)
	Acartia sinjiensis	Larval development ratio	3	0.0086	50% reduction	(Gissi *et al.*, 2018)
		Naupliar development		0.016	No copepodites developed	

2.3.8 Zinc toxicity

Exposure to zinc at 50 and 250 µg L^{-1} did not promote ROS production or simulate GSH activity in *T. japonicus* (Kim *et al.*, 2014a) (Table 2.4). Zinc is a redox-inert metal that is an essential component of oxidative stress proteins, and therefore could indicate a similar explanation as cadmium (Chaitanya, Shashank and Sridevi, 2016). In contrast, zinc nanoparticles were reported to increase ROS production in *T. japonicus* (Wong *et al.*, 2020). HSPs related to oxidative stress, HSP20 and HSP70 were upregulated following 100 µg L^{-1} of zinc. This, alongside GR, SOD, GST, GPx and AChE activity increases at 50 and 250 µg L^{-1}, suggests oxidative damage and neurotoxicity from zinc exposure.

Most of the endpoints measured were related to reproduction and development changes (Table 2.4). In two different studies *T. fulvus* was exposed to zinc; in one study as nanoparticles. Nanoparticle exposure between 100 and 250 µg L^{-1} resulted in a significantly reduced clutch formation, number of nauplii per clutch and total number of nauplii per female, while a high percentage of non-viable eggs per female occurred at only 0.15 µg L^{-1} (Prato *et al.*, 2020). For the same species, similar reductions were noted for the number of nauplii per clutch at 400 µg L^{-1}, but clutch formation was not as affected at this higher concentration (Pane *et al.*, 2008). Nanoparticle exposure to *A. tonsa* resulted in similar outcomes, with a concentration of 263 µg L^{-1} decreasing fecundity and the number of nauplii in half (Jarvis *et al.*, 2013). This study reported an EC_{20} value for reproduction of 143 µg L^{-1}. Although *A. tonsa* was not included in a zinc survival assay in this review, *T. fulvus* had much higher LC_{50} values of 6.85 to 0.93 mg L^{-1}. For zinc, the lethal sensitivity ranged from 6.85 to 0.29 mg L^{-1}, with *Harpacticus sp*. having a higher mortality for zinc than most concentrations used in these reproduction assays.

Alongside acute media exposure, zinc was exposed in the diet and in a chronic assay. Dietary exposure to *A. tonsa* resulted with 20% fewer nauplii per female after one week of exposure (Bielmyer, Grosell and Brix, 2006). A similar species A. *sinjiensis* had a larval development EC_{50} value of 0.7 µg L^{-1}. These responses highlighted that water-borne exposure caused greater reductions in the number of nauplii per female than dietary exposure, yet all types and routes of exposure did have an impact.

Overall, zinc toxicity was observed as oxidative and neurotoxicity damage and therefore could be a potential route to reduced reproduction and development in marine copepods. The data gaps for understanding and characterising zinc toxicity are evident, with a greater focus on life-history endpoints in this review.

Table 2.4. Summary of biological endpoints measured in studies that exposed copepods to zinc, except for survival or LC_{50} values. For the environment column, blue represents marine species, and green represents brackish species. ROS = reactive oxygen species, GPx = glutathione peroxidase, GST = glutathione S-transferase, GSH = glutathione, GR = glucocorticoid receptor, SOD = superoxide dismutase, AChE = Acetylcholinesterase, HSP = heat shock protein.

Environment	Species	Endpoint	Time (days)	Concentration (µg L^{-1})	Response	Reference
	Tigriopus japonicus	ROS formation	4	50 and 250	No significant impact	(Kim *et al.*, 2014b)
		GSH				
		GR			Significant increase only at 50	
		SOD, GST, GPx and AChE			Significant increase	
		HSP10		100	Downregulated	
		HSP20 and HSP70			Upregulated	
	Tigriopus fulvus	Clutch formation	2	400	Reduced from 7 ± 0.7 in controls to 6.4 ± 1.4	(Pane *et al.*, 2008)
		Nauplii produced			Reduced from 96.4 ± 14 in controls to 41.8 ± 14.5	
		Number of nauplii per clutch			Reduced from 13.7 ± 1.5 in controls to 6.4 ± 1.8	
		Number of nauplii per female per day			Reduced from 3.2 ± 0.5 in controls to 1.4 ± 0.5	
		Clutch formation	28	Nanoparticles = 50, 100, 150, 200 and 250	One day delay in females becoming ovigerous	(Prato *et al.*, 2020)
		Number of nauplii per clutch			Significantly reduced from 100 µg L^{-1}, in a concentration dependent manner	
		Mean total number of nauplii per female			Significantly reduced at all exposed concentrations	
		% non-viable eggs per female			Significantly increased from 0.15 µg L^{-1}, with 0.25 µg L^{-1} having ~ 70%	
	Acartia tonsa	Fecundity	7	Nanoparticles = 263	Significant decrease by half – effects only seen at the highest concentration	(Jarvis *et al.*, 2013)

		Number of nauplii per female			Reduced from 24 nauplii per female for controls to 12 at highest concentration	
		Reproduction		Nanoparticles = 143	EC_{20} value for reproduction	
	Acartia sinjiensis	Larval development	3	0.7	Chronic EC_{50} value to continuous exposure	(Stone *et al.*, 2021)
	Acartia tonsa	Number of nauplii per female	7	Dietary exposure = 0.3	20% reduction compared to the controls	(Bielmyer, Grosell and Brix, 2006)

2.3.9 Toxicity of other metals

In addition to copper, cadmium, nickel, and zinc, there were seven other metals measured in papers included in this review. These seven metals were less frequently used and only five of the metals highlight specific toxicity responses for marine and estuarine copepods in addition to survival. These responses provide support for the routes of toxicity discussed above for copper, cadmium, nickel, and zinc.

The euryhaline copepod *A. tonsa* requires effective ion regulation for survival; however, the 48-hour acute effects of silver found that whole body Na^+, K^+ -ATPase activity reduced significantly when exposed to LC_{10}, LC_{30} and LC_{50} values at three salinities – 5, 15 and 30 ppt (Pedroso *et al.*, 2007). The same trend was seen at all three salinities, with all controls having short of 4 μM ADP per mg protein h^{-1} and highest concentrations reducing by approximately 50% across all salinities. Na^+ at high intracellular concentrations is toxic to the cell and impacts internal homeostasis and cellular functions, like mitochondrial functions, potentially leading to neurotoxicity.

T. japonicus exposed to manganese had increased GST expression after exposure to 100 μg L^{-1} for six hours or 50 μg L^{-1} for 12 hours (Lee *et al.*, 2007). Expression at 48 hours decreased at both concentrations, suggesting that the need to respond to oxidative stress or neurological diseases reduced or the metal impaired GST expression.

Also using *T. japonicus*, arsenic and silver were part of a larger study by Kim *et al.* (2014b) to determine oxidative stress and HSP expression. Silver caused concentration dependent increases for ROS formation, GSH, GST, GR, GPx and SOD activities. The highest concentrations of metals (100 μg L^{-1}) resulted in mixed responses of HSP genes, with HSP10 being down-regulated by silver, while HSP60 was down-regulated by silver and arsenic. Both HSP10 and HSP60 reside in the mitochondria, and facilitate mitochondrial protein folding, suggesting that these metals will result in abnormal mitochondrial protein homeostasis and mitochondrial-related diseases. Both metals also caused high transcriptional levels of HSP20 and HSP70 over 96 hours, which aligns with responses from copper, cadmium, and zinc. Further, *P. nana* had significant induction of Vg1 and Vg2 after exposure to arsenic (Hwang *et al.*, 2010), which is known to impact reproduction and was seen for

cadmium exposure as well. As arsenic and cadmium are both redox-inactive metals, this could be a shared toxicity mechanism.

After a short five-hour exposure to mercury, whole transcriptome analysis responses also included the upregulation of genes related to HSP for *T. japonicus* and *P. annandalei* (Wang *et al.*, 2017). Interestingly, the most up-regulated genes for both species differed, with stress response genes being the focus of *P. annadalei* and stress alongside life-history parameters for *T. japonicus*. This could show the initial response of *T. japonicus* to continue and increase reproduction during metal stress. *T. japonicus* was included in a multigenerational life cycle test in Li *et al.* (2015) that showed no effect of 50 μg L^{-1} on the number of clutches produced. However, there were reductions in fecundity and the number of nauplii per clutch. Pane *et al.* (2008) looked at the effects of mercury and chromium on *T. fulvus*. Mercury (0.2 mg L^{-1}) caused the lowest egg sac (2.8 ± 0.7) and nauplii production (13 ± 2.9) resulting in 4.8 ± 1.5 nauplii per egg sac and 0.4 ± 0.1 nauplii per female per day. In comparison, chromium was less toxic to these endpoints, with 5.7 ± 0.6 and 6.4 ± 1.4 egg sacs produced and 44.4 ± 11.7 and 41.8 ± 14.5 nauplii produced, resulting in 7.8 ± 1.8 and 6.4 ± 1.8 nauplii per egg sac and 1.5 ± 0.4 and 1.4 ± 0.5 nauplii per female per day respectively.

Chromium exposure caused no egg sacs to be produced and developmental delays in the freshwater species *N. conifer* (Gutierrez, Gagneten and Paggi, 2010). This was also seen for the marine species *T. holothuriae* - although an egg sac was produced, the negative reproductive impacts were seen with lower nauplii numbers per egg sac and reduced survival (Miliou *et al.*, 2000). Interestingly, trace metals measured in the marine copepod *Euchaeta concinna* showed that chromium concentrations were higher in egg sacs than female or male bodies, suggesting either an accumulation or elimination from the main body is occurring in the egg sac (Hsiao and Fang, 2013). This study (and species) was not included in this review but could explain the large impacts on reproductive outputs at low chromium concentrations.

2.3.10 Factors influencing toxicity

Most studies in this review featured water-borne metal exposure, although two studies used contaminated sediment, one study used diet-borne metal exposure, and another used pulsed water exposure. Reproductive responses depended on the exposure route, albeit from a relatively small sample size, with dietary exposure

having the largest impact on the number of nauplii released per female. The opposite was found in Lauer and Bianchini (2010), where the reproductive response to chronic copper exposure also did vary due to the route of exposure, with hatching rate EC_{50} values lower after media exposure when compared to media and diet exposure combined.

Moreover, the use of nano-sized particles of zinc and nickel highlighted the difference in toxicity with metal size. Nickel nanoparticles were more toxic than other nickel forms, whereas zinc nanoparticles had both higher and lower toxicity to ionic zinc. In Griffitt *et al.* (2008), nanoparticles of five metals (including nickel) were found to be less toxic than dissolved metals in freshwater species, including *D. magna*. Most studies in this review used total, dissolved, or ionic concentrations. Ions are thought to be the most bioavailable form of the metal due to their metal charges; therefore, ions have the potential to cause the most toxicity (Gagnon and Vigneault, 2013). However, copepods might be able to uptake larger uncharged particles due to their feeding mechanisms to gather and uptake microalgae cells (Rainbow, 2018a). This could have led to some toxicity being missed due to the exclusion of larger particles. According to Campana *et al.* (2012), the particulate copper exposure in the sediment was shown to be the significant route of exposure for *N. spinipes* and another invertebrate species, with dissolved copper in the overlaying water not being responsible for the observed reproductive impacts. Additionally, salinity can impact metal speciation, which is important to consider when comparing environments with levels of dissolved minerals and salinities, as shown by changes to cadmium speciation in Pavlaki *et al.* (2017). According to Hall *et al.* (1995), a salinity increase from 5ppt to 25ppt reduced ionic cadmium from 20% to 4.5%. Copepods in freshwater and lower salinity estuarine environments could be exposed to a higher ionic concentration of metal than marine copepods, with the same total concentration. The impacts of this on copepod metal uptake are not clear, as many metal species can be up taken and cause toxicity.

Effects varied depending on life stage. In the copepod life cycle, nauplii are often the most sensitive to environmental stressors, for example Medina *et al.* (2002) found that nauplii were 28 times more sensitive to a pesticide than adults. When comparing sex specific sensitivities, male copepods are often more sensitive than females (Dayras *et al.*, 2020). However, *E. affinis* females were more sensitive than males after cadmium exposure (Kadiene *et al.*, 2017). The use of different life stages and

adult sexes is not included in most hazard assessment guidelines, potentially missing effects to the most sensitive stages of a copepod.

2.4 Limitations

Due to the nature of this review, there is a risk of bias due to being assessed by only one investigator. This is not common in these types of reviews, due to the screening and eligibility steps being subjective; however, there are examples of published systematic reviews completed by a solo investigator (Cedergreen, 2014). To help manage this bias, ToxRTool was implemented after screening and eligibility, to check the studies reliability whilst removing some of the subjectivity. ToxRTool has been implemented in other systematic reviews focused on ecotoxicological questions (Nagy *et al.*, 2020). In addition, the criteria for inclusion and exclusion at each stage of the review were trialled in the pilot study to make sure they were as targeted as possible on quantifiable outcomes, for example a laboratory study using a metal. Another limitation is the narrow search source, as only one database was used for this review. This was decided after completing the pilot study and understanding the requirements needed to complete a review with one investigator. Choosing specific databases have been decided in other systematic reviews, for example in Nagy *et al.* (2020) Scopus and PubMed were selected as sources, including a similar number of studies in the final qualitative analysis (n = 36).

2.5 Conclusion

For organisms such as fish and mussels, it is well-established in the literature that metal effects are initiated by oxidative stress. This review also substantiated these findings for copepods, identifying that the effects of most metals were either oxidative stress-induced or DNA damage-induced, leading to increased mortality and limited reproduction and development. The genotoxic impact of trace metals on copepods was not the focus of many studies, with greater attention on adverse outcomes. In this review, genotoxicity was measured in situ after exposure to metals, allowing a level of understanding for toxicity mechanisms, particularly for copper and cadmium. The main genus reviewed was *Tigriopus*, which included effects at multiple biological levels, enabling a better understanding of metal toxicity for copper and cadmium. Interestingly, the genus *Tisbe* was the third most common for metal adversity studies, yet no information was included about the molecular and cellular responses to these

metals. Although it is difficult to conclude on responses from freshwater copepods, both marine and brackish copepods had similar responses suggesting that metals have shared MoAs and toxicity mechanisms between these two groups.

The relevance of these laboratory responses to realistic exposure scenarios is varied, as for some effects, the studies often go far beyond environmental concentrations. This is common for effects such as survival that require concentrations that equal full mortality to depict a complete concentration response curve. That said, effects on DNA damage, gene expression and developmental outputs were seen at relatively low concentrations for most metals, suggesting a potential field application. When using copepods for metal hazard assessments, including a range of effect endpoints across different levels of biological organisation provides information to be used in toxicity characterisation and understanding possible mechanisms of action. Further information on possible effects and interactions arising from combined metals would provide a more realistic hazard assessment for marine and aquatic environments.

Chapter 3. Effects of single and combined trace metals on *Tetraselmis suecica*

3.1 Introduction

Marine algae are the foundation of most marine ecosystems, producing oxygen, energy and recycling nutrients (Gomes *et al.*, 2017). Without algae, the structure and function of marine ecosystems would collapse due to oxygen depletion and reduced primary productivity. The stability and balance of algae communities — particularly in coastal waters — is under threat from increased chemical (including metals) and nutrient runoff, exacerbated by climate change (Ajitha *et al.*, 2021). Due to their trophic position and their need to utilise trace metals for numerous biochemical processes (e.g., photosynthetic electron transport chain; PETC), microalgae may be considered as the first target of metal toxicity. Microalgae have evolved metal detoxification mechanisms to control metal uptake, thereby allowing algae to adapt to metal contaminated waters. Metal toxicity occurs once these systems are no longer sufficient. Algae therefore represent important indicators of environmental metal contamination (Satoh *et al.*, 2005; Debelius *et al.*, 2009).

Mixtures of metals from natural and anthropogenic sources persist in many marine environments, yet research efforts have tended to focus on the effects of single metals, with a bias towards the impacts on freshwater species (Ceschin, Bellini and Scalici, 2021). Even then, the use of aquatic algae and plants are limited when compared to bacteria, invertebrates, and fish for single stressor ecotoxicological tests (Ceschin, Bellini and Scalici, 2021). The characterisation of metal toxicity in realistic mixtures is needed for marine species; however, mixture experiments can be complex, expensive and time consuming. A statistical design of experiments approach can be used to simplify complex mixture experiments and provide a structured format for mixture responses. Combining this approach with rapid fluorescence parameters can allow quick data collection on metal-induced stress in photosystem II (PSII) and related chlorophyll parameters.

Tetraselmis suecica was chosen as the microalga species of interest as it is easy to grow under laboratory conditions, is a well-studied species in ecotoxicology (Stachowski-Haberkorn *et al.*, 2013), is an industrial and aquaculture relevant species, and has a worldwide distribution (Nassiri *et al.*, 1996). Copper, nickel, and

zinc were selected as the metals of interest for mixture studies as they are global contaminants. In coastal waters in the North Atlantic Ocean and English Channel, copper and nickel concentrations have been increasing over the last 31 years, yet zinc concentrations have been remained stable (Richir *et al.*, 2021). The measured concentrations ranged massively, as the area covered was large, from 0.4 to 4,007 mg kg^{-1} for copper, 0.1 to 274 mg kg^{-1} for nickel and 1.3 to 10,900 mg kg^{-1} for zinc. In the North Sea, copper has been reported reaching 63 nM (total concentration) in the coastal waters by the Humber (Balls, 1985). More recently, an assessment conducted in 2015, the average concentration of copper in Northeast Atlantic sediment was 33 mg kg^{-1} (OSPAR, 2016). For zinc, there are a range of concentrations reported for the North Sea, from 3.2 nM to 571 nM during other contamination events (Prego and Cobelo-García, 2003). In the surface waters of the North Atlantic Sub-Polar Mode Water, nickel was found at a concentration of 3.49 ± 0.02 nM, but in the deeper water the concentrations reached 7.72 ± 0.02 nM (Middag *et al.*, 2020). Furthermore, these metals have known information regarding mode of action (MoA) as single stressors, making them ideal for a cumulative toxicity study. Initially, a single metal toxicity study was conducted to establish information on metal interactions. These data provided comparisons for mixture responses to determine whether the toxicity observed from mixture effects were interacting or not (i.e., additive).

3.1.1 Metal uptake for microalgae

Trace metals are known to be taken up and accumulated by microalgae. As some trace metals are essential, microalgae have evolved specialised transport corridors or transmembrane carriers to facility uptake. However, these carriers can similarly uptake non-essential metals; for example, cobalt, nickel and zinc use a magnesium ion channel (Jahan *et al.*, 2004).

Additionally, metals can actively bioaccumulate in algae by a passive extracellular biosorption mechanism, which can occur using adsorption reactions at bindings sites in the cell wall or in extracellular polymeric substances (EPS). EPS are biopolymers produced by microalgae as an adaptive self-defence mechanism, as they can form a protective barrier on the cell surface to prevent intracellular toxicity and maintain cellular integrity (Naveed *et al.*, 2019). The adsorption reaction depends on the functional group on the binding site and the chemical properties of the metal trying to

bind. Microalgae have a high metal-binding capacity as positively charged metal ions in the media are attracted to the negatively charged functional groups within cell walls (Monteiro, Castro and Malcata, 2012). This intrinsic composition acts as a self-defence mechanism and allows active bioaccumulation of metal ions to prevent metal toxicity. Furthermore, the cell wall takes positively charged ions from the surrounding water (e.g., Na^+, K^+, Ca^{2+} and Mg^{2+}) which can be substituted by metal ions (Danouche, El Ghachtouli and El Arroussi, 2021). This is known as ion exchange and involves active transport and followed by passive diffusion. These absorption and accumulation processes can ensure that microalgae can maintain growth during metal exposure up to a certain concentration, which is metal specific. However, essential metals can become toxic once their concentration reaches a threshold, driving the evolution of mechanisms to detoxify metals (Danouche, El Ghachtouli and El Arroussi, 2021).

3.1.2 Metal toxicity on microalgae

According to Nowicka (2022), there are four modes of action (MoA) of metal ions on microalgae: (1) disrupting structures and reducing activity by reacting with thiol, histidyl and carboxyl protein groups and glutathione; (2) competing with, and dislodging essential metal cations from enzyme active sites; (3) having a similar chemical structure to functional groups; and, (4) via the formation of reactive oxygen species (ROS). Most metals cause toxicity via one or two of these MoAs; for example, copper, nickel and zinc can displace essential metal cations, but copper can also generate ROS and nickel can react with thioyl histidyl or carboxyl groups (Nowicka, 2022). Nickel and zinc cannot directly form ROS but are known co-factors for enzymes that produce ROS as by-products; nickel participates in urease oxidising urea to form nitrogen and zinc affects carbon dioxide fixation, DNA transcription and phosphorus acquisition (Expósito *et al.*, 2017). These MoAs can often interrupt cellular division and inhibit growth (Balaji *et al.*, 2016; Ouyang *et al.*, 2012), inhibit photosynthesis (Hussain *et al.*, 2021; Kumar *et al.*, 2014; Guanzon, Nakahara and Yoshida, 1994) and cause oxidative stress due to the overproduction of ROS and compromise enzyme activity (Ameri *et al.*, 2020; Sabatini *et al.*, 2009).

Growth inhibition can occur when the concentration of intracellular metal ions or those bound to the cell surface disrupts the functioning of metabolic processes, specifically photosynthesis. Photosystems II (PSII) and I (PSI) are the two sites of

photosynthesis, which is a light-driven process to produce adenosine triphosphate (ATP) and nicotinamide adenine dinucleotide phosphate (NADPH) for active cellular processes. ATP production is coupled with the Mehler reaction when oxygen is reduced to hydrogen peroxide in chloroplasts (Foyer, 2018). PSII is a large protein complex found in the chloroplast thylakoid membrane, which catalyses a reduction in plastoquinone by electrons that oxidise water into oxygen (Knauert and Knauer, 2008). Metals (e.g., copper) can inactivate PSII reaction centres, inhibiting PSII activity and in turn ATP generation (Cid *et al.*, 1995). Pulse amplitude modulation (PAM) fluorometry can be used to determine inhibitory effects on the photosystems.

Chloroplasts are a main site of ROS formation, as the PETC uses oxygen as an electron acceptor to produce superoxide anion ($\bullet O_2^-$). When cells are stressed the light independent reactions of photosynthesis slow down and the electron chain elements are reduced (Nowicka, 2022). This results in superoxide anion forming in PSII reaction centres and increased electron leakage out of Fe-S centres of PSI or from the Mehler reaction (Gechev *et al.*, 2006; Foyer, 2018). Under normal conditions, superoxide anion can be rapidly metabolised into hydrogen peroxide by superoxide dismutase (SOD). ROS are a natural by-product of aerobic metabolism and have become useful to cells as growth signalling molecules, specifically signalling for cell proliferation and cell death. However, excessive ROS can cause photooxidative damage to macromolecules (e.g., DNA, proteins, and lipids) and may lead to cell death. Copper is required in the light-harvesting complex of PSII, providing an example of an essential metal that can become toxic, by directly generating ROS.

3.1.3 Mixture study design

To better inform risk assessments and regulatory guidelines, hazard assessments that understand and characterise the toxicity of metals must be conducted, followed by a cumulative hazard assessment to understand how mixtures can disrupt and change toxicity. However, mixture toxicity studies can be difficult to conduct, with resource, time, and financial limitations. Many of these limitations can be mitigated with a Design of Experiments approach which offers considerable efficiency gains relative to a full factorial design, as shown in figure 3.1 (Jankovic, Chaudhary and Goia, 2021). One option is the Definitive Screening Design (DSD) that samples a subset of mixture component settings in a multidimensional design space (Jones and

Nachtsheim, 2011). DSD can be used for screening and characterising complex processes with multiple factors and interactions (Jankovic, Chaudhary and Goia, 2021). Using measured mixture responses from low and high concentrations of each mixture component, a definitive screening fit can be applied to determine the main toxicity drivers within the mixture (i.e., whether it is a single component or the interaction of two components). By adding a centre point concentration to the design matrix, information regarding curvature can be added to the model, and replicated in the design to provide reliability. Additional models can be used to further explore the interaction of mixture components, including the least squares model that fits a regression to predict the behaviour of dependent components.

The outcome of choosing a DSD approach is that a three-factor mixture with two controls that is replicated three times totals 48 experimental runs to analyse, whereas the equivalent full factorial design would require 81 experiment runs without including replicated controls. This systematic approach has been commonly used to optimise and understand multifaceted bioengineering processes by modelling complex systems, for example optimising and screening biodiesel production (Hundie and Akuma, 2022; Felix *et al.*, 2019). It has been successfully implemented in pharmaceutical and molecular biology fields, ranging from optimising liquid extractions from seaweeds (Heavisides *et al.*, 2018), enzyme production (Uhoraningoga *et al.*, 2019) and improving robustness of cell-free protein synthesis (Banks *et al.*, 2022).

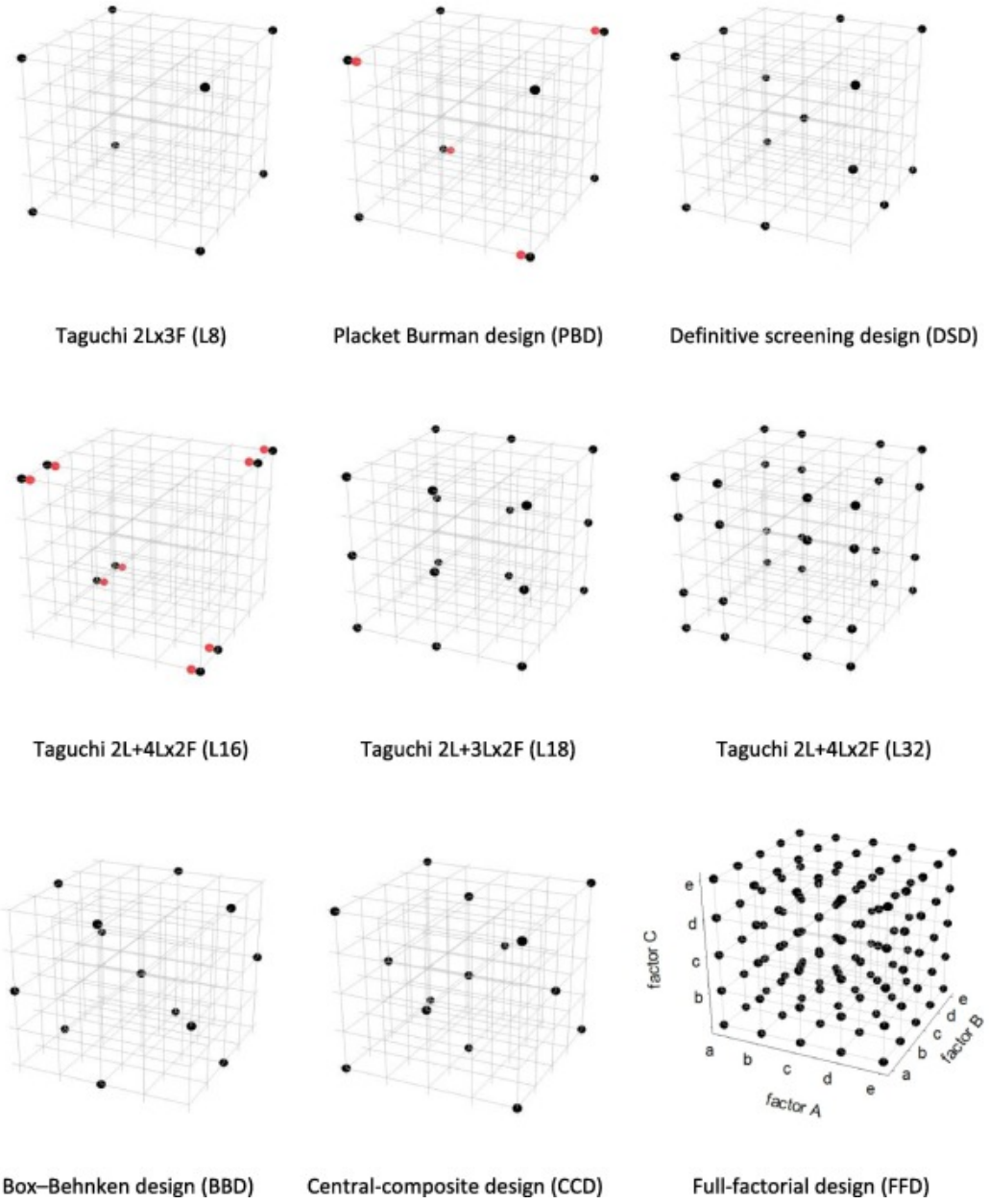

Figure 3.1. Three-factor model designs, reproduced from Jankovic, Chaudhary and Goia (2021) under a creative commons license. Where the lines intersect indicates possible combinations in a three-factor design, with the dots showing which combinations the design would instruct to measure. Red dots show additional repeats needed to reach the minimum number of tests required for the model.

The implementation of a DSD approach in a mixture toxicity study could provide quick statistical information on mixture interactions and which (if any) components are toxicity drivers. Specifically for algae and plants, the Imaging PAM (IPAM) is also used in ecotoxicology to quickly gather high quality data on complex systems. An IPAM can quickly assess several functional parameters at once that relate to stress in PSII using a rapid light curve, in a non-destructive manner that can show trends over time or with increasing photosynthetically active radiation (PAR) (Expósito *et al.*,

2021). Conducting mixture experiments using a DSD approach and rapid stress assessments such as PAM fluorometry, could be useful in cumulative hazard assessments of microalgae, macroalgae and plants. There is a considerable need in cumulative hazard assessments to provide information to meet the demands of quicker and cheaper ecotoxicological testing for complex mixtures. There are an infinite number of chemical combinations in marine environments, which will vary on a local scale and from species to species. Finding new approaches to cumulative hazard assessment that provide structured, organised, and comparable data is a huge undertaking.

3.1.4 Aims and objectives

The aims of this Chapter were to characterise the toxicity of three trace metals on *T. suecica*, in singular and combined exposures, focusing on how ROS-induced stress affects photosynthesis inhibition. This was achieved using a combination of rapid fluorescence parameters to measure responses to metals in PSII and the DSD approach for streamlined mixture experiments. Moreover, the single metal effects data gave the opportunity to populate a toxicity pathway and, using well-informed literature, begin to understand potential links to other effects to produce a conceptual network of toxicity pathways.

3.2 Materials and Methods

3.2.1 Tetraselmis suecica *cultures*

Tetraselmis suecica stock cultures were obtained from long term, established cultures in the marine biology department within the School of Natural of Environmental Sciences at Newcastle University. *T. suecica* cultures were maintained in modified F2 medium according to the method of Guillard and Ryther (1962) except for removing ethylenediaminetetraacetic acid (EDTA) in the trace elements to prevent metal coagulation. Filtered (0.22 µm) artificial seawater (Tropic Marin Pro Reef Salt) was used at 30 ppt salinity (ATC refractometer) and pH 8.1±0.2 and was autoclaved before adding vitamins. Vitamins were sterilised via filtration through a 0.22 µm filter in a biological safety cabinet. All stock and experimental cultures were kept in a light and temperature-controlled room under a 16:8-hour photoperiod, with a light intensity of 33 µM photons m^{-2} s^{-1} at 20 ± 2 °C, on a gyrating rocker (Bibby Stuart™ Gyro-Rocker STR9 platform shaker) set to 5 rev min^{-1}.

3.2.2 Single metal exposure set up

All metal salts used were chlorides – copper chloride ($CuCl_2$, 99% Sigma-Aldrich, CAS number 7447-39-4), nickel chloride ($NiCl_2$, ≤98% Sigma-Aldrich, CAS number 7791-20-0) and zinc chloride ($ZnCl_2$, ≤98% Fisher Scientific, CAS number 7646-85-7). All stock cultures and experiments were conducted in a light and temperature-controlled room. Stock solutions (1 mM) of copper, nickel, and zinc were added to F2 medium to make six exposure solutions per metal, alongside a control, which were replicated five times (n=5). The measured concentrations used were 16.8, 24.84, 59.52, 138.65, 310.36 and 637.71 µM for copper exposure, 5.01, 6.80, 19.39, 26.31, 65.08 and 298.56 µM for zinc exposure and 4.03, 7.09, 29.79, 32.20, 250.81 and 406.20 µM for nickel exposure. These concentrations were the same for each bioassay conducted. Eighteen millilitres of exposure medium and 1 mL of metal solution were added to each cell culture flask (Thermo Scientific BioLite cell culture treated flasks, working volume of 25 mL) and inoculated with 1 mL of exponentially growing *T. suecica*, with a starting concentration of 5.15 – 5.5 $x10^5$ cells mL^{-1}, to total 20 mL. The experimental flasks were placed on a 3D gyrating rocker for the entire exposures, set to five rev min^{-1}. The exposure lasted for seven days, with samples taken during this period for cell counts and endpoint measurements (Table 3.1). During method development, experiments were conducted in borosilicate flasks, which were acid washed before use with diluted 10% nitric acid (70% purity, >99.999% trace metals basis, Sigma Aldrich).

Table 3.1. An effects toolbox for acute trace metal exposure to *Tetraselmis suecica*. ROS = reactive oxygen species and PAM = photosynthetic active radiation.

Category	Method	Endpoint	Sampling
Whole population toxicity test	Modified toxicity tests	Growth	In situ
Targeted assay	H_2DCFDA assay	Cellular ROS formation	In situ
	Imaging PAM	Photosynthesis efficiency	In situ

3.2.3 Combined metal exposure set up

All metal stock solutions and F2 medium were made up following the same process as 3.2.2. Combined metal exposures were designed and prepared following the

DSD. The mixture concentrations were chosen using the single metal concentration response curves for growth. The slope values from these concentration response curves are used to calculated effective concentrations (EC_x values), that represent a concentration at which a specific response is seen, for example the EC_{50} value for growth is the concentration where there is a 50% reduction in growth. At first, the nominal growth EC_{20}, EC_{50} and EC_{80} concentrations for each single metal cell density were inputted into JMP Pro software version 15.2.0 (SAS Institute, NC, USA) and the software calculated 14 mixture exposure solutions that contained a different ratio and concentration of copper, nickel, and zinc. Each exposure solution had either the least forcing (lower concentration), the centre point (mid concentration) or the most forcing (higher concentration) concentrations of copper, nickel, and zinc (Table 3.2). Solutions four and eleven were replicates and contained the same concentrations of each metal (all at their centre points), to add centre points into the design to check the curvature of the line. Controls were added, making 15 solutions in total that were all conducted in triplicate, although control data couldn't be added into the model.

Table 3.2. Definitive screening mixture design for *Tetraselmis suecica* and total concentrations (μM) of copper, nickel, and zinc added to each run (solution) at the beginning of the exposures (day zero). The mixture design for each metal is shown, with minus (-) indicating the least forcing, zero (0) indicating the centre point, and plus (+) indicating the most forcing concentration. The total concentration (μM) is the addition of copper, nickel, and zinc concentrations in each solution.

Run	**Block**	**Copper concentration μM**		**Nickel concentration μM**		**Zinc concentration μM**		**Total concentration μM**
1	1	-	40	-	85	-	20	145
2	1	-	40	+	130	0	57.5	227.5
3	1	0	70	-	85	-	20	175
4	1	0	70	0	107.5	0	57.5	235
5	1	0	70	+	130	+	95	295
6	1	+	100	-	85	0	57.5	242.5
7	1	+	100	+	130	+	95	325
8	2	-	40	-	85	+	95	220
9	2	-	40	0	107.5	+	95	242.5
10	2	-	40	+	130	-	20	190
11	2	0	70	0	107.5	0	57.5	235
12	2	+	100	-	85	+	95	280
13	2	+	100	0	107.5	-	20	227.5
14	2	+	100	+	130	-	20	250
Control	1 & 2	Control	0.00	Control	0.00	Control	0.00	0.00

3.2.4 Metal concentration determination

Metal concentrations for all experiments were determined using a photometer method using LCK cuvette tests (Hach Lange, CO, USA). For samples at the beginning of the experiment, 1 mL of exposure solution was pipetted and stored in 15mL Sarstedt tubes for analysis. To determine the metal concentration at the end of the experiment, the exposure cultures were poured into sterile 50 mL Falcon tubes and centrifuged at 2500 rpm and room temperature for ten minutes to separate the exposure solution and algal cells, and 1 mL of exposure solution per replicate was stored at room temperature in darkness. This same method was used for single and combined metal experiments, to know how much of each metal was present in each mixture solution. Using these data, each solutions total metal concentration was calculated by adding the concentrations of copper, nickel, and zinc (Table 3.2).

Separate kits were used for each metal – LCK 329 for copper with a 0.1 – 8 mg L^{-1} measurement range, LCK 337 for nickel with a 0.1 – 6 mg L^{-1} range, and LCK 360 for zinc with a 0.2 – 6 mg L^{-1} range. Samples were diluted if necessary to ensure the metal concentration was present within these ranges. Each metal kit contained the barcoded vials for that metal, and any additional powders and chemicals needed to measure the metal concentrations. Any powders came pre-dosed in the cap of the vials, separate to any solution already present in the vials. One barcoded vial was used per replicate. The barcode allowed automatic recognition from the photometer to know which metal was being measured. The sample preparation steps were followed according to the manufacturer's instructions for each metal measurement kit. Solution A – which arrived in the kit – was the only chemical that needed to be added to the vials when adding the samples. This was only necessary for the nickel and zinc kits. If necessary, the samples were diluted to fall between the measurement range using reverse osmosis (RO) water. Afterwards, any diluted samples were back calculated, and concentrations were converted to micromolar (µM) to allow single and combined metal effects to be compared more easily.

To measure the copper concentrations, the sample was added to the vial and inverted five times to mix the sample with the powder that arrives in the kit in the vial. After three minutes, the samples were read on a photometer (Hach Lange DR2800 laboratory analysis spectrophotometer) by placing the samples into the cell holder. The photometer automatically turns the vial to read the barcode and measure the metal concentration present as mg L^{-1}.

For the nickel measurements, 2 mL of each sample were pipetted into each vial and inverted five times to dissolve the freeze-dried chemical that arrives in the kit in the vial. Then 200 µL of solution A was added to the vial and inverted five times. When nickel was detected, the solution in the vial turns an orange/brown colour as the nickel ions react with dimethylglyoxime in the vial. The vial was added into the cell holder in the photometer to measure the nickel concentration present.

To measure zinc concentrations, the foil on top of the cap was removed and the cap removed from the vial. 0.2 mL of the sample was added to the vial, along with 0.2 mL of solution A. The cap was immediately screwed back on and shaken to make sure the powder under the foil in the cap was added into the solution in the vial. Each vial was measured three minutes after adding the sample. For zinc, there was a zero-cuvette to blank the instrument before measuring samples. When zinc was present in the sample, the solution turned an orange/red colour as it formed a complex with 4-(2-pyridylazo-)resorcin.

3.2.5 Combined metal models

Following the combined metal experiments, the mean responses of each mixture solution to the measured endpoints were added into the DSD data table in JMP Pro 15. First, a definitive screening was fitted to the data to identify any main effect drivers – i.e., a single metal driving the mixture effects – and second order effect drivers – i.e., whether metal pairs within the three-metal mixture were driving the mixture effects. The second order effects were determined from the three possible pairs of metals in these mixtures: (1) copper and nickel, (2) copper and zinc, and (3) nickel and zinc. Secondly, a standard least squares combined model was ran to produce prediction profilers, surface profilers and interaction plots (Jones and Nachtsheim, 2011). The standard least squares combined model could only be run when interactions had been identified between the metals in the mixture.

3.2.6 Growth

All cell counts for inoculating stock and experimental cultures and during exposures were conducted using a BD Accuri™ C5 flow cytometer (blue laser 488 nm) on days one, two, five, and seven. The RO water was run through the instrument for five minutes on the fast flow rate (66 µL min^{-1}) before running any samples. The instrument was backflushed, and the number of drips and angle of the stream of

water was monitored as this can indicate whether the sip is blocked. For a successful backflush, the instrument should drip three times followed by a stream of water falling vertically and another three drops. RO water was run for another two minutes on the fast flow rate before samples were measured and the events per µL were checked. Samples were only measured once the instrument was deemed to be at an acceptable level of cleanliness, which was determined by a successful backflush and low events per µL (>10) measured after running RO water. Milli-Q® water was used as sheath fluid and calibration beads were measured before instrument use, either weekly or daily depending on how often the instrument was being used. The instrument was deemed to be calibrated when >75% of the beads fell between pre-determined ranges from the manufacturer, and CV values were <5%, meaning that the instrument was clean and the lasers were aligned within the manufacturer's acceptable range.

Each sample was measured in a new area of interest on the software (BD Accuri™ C6 software version 1.0.264.21), with backflushes between each replicate for each metal concentration and RO water run after a set of replicates per concentration per metal. When finished, RO water was run for two minutes followed by decontamination solution for two minutes. The sip was left covered in clean RO water before shutting down the instrument.

To determine the cell count in each replicate, the forward scatter (FSC) and side scatter (SSC) were used as a proxy for cell number and cell size respectively. After each sample, gates around the algae cells were drawn to distinguish these counts from bacterial cells and any possible contamination when loading the samples (e.g., dust). To help ensure the gates were successfully plotted around the algal cells, the FL3 and FL4 fluorescence measurements were used to separate cells depending on their chlorophyll fluorescence. The FL3 can be used as a proxy for chlorophyll *a*; therefore, cells containing higher (algae), and lower (bacteria) chlorophyll fluorescence are differentiated. The gates from FL1 and FL2 plots can be shown on FL3 and FL4 plots to see whether the selected sized cells have a relatively high or low chlorophyll fluorescence. Cell count data were converted to cell density (cells mL^{-1}). Mean growth rates and percentage growth inhibition at each metal concentration over the seven day period were calculated using these equations (OECD, 2011):

$$\text{Mean growth rate day}^{-1} = \frac{\ln X_j - \ln X_i}{t_j - t_i} \text{ ----- [1]}$$

Where X_j is the biomass at time *j* (t_j) and X_i is the biomass at time *i* (t_i).

$$\text{Percentage inhibition of growth rate} = \frac{u_c - u_t}{u_c} \times 100 \text{ ----- [2],}$$

Where u_c is the mean value for mean specific growth rate in the control group and u_t is the mean specific growth rate for the treatment replicate.

3.2.7 Reactive oxygen species formation

The fluorescence probe H_2DCFDA (Invitrogen, Molecular Probes Inc., Eugene, OR, USA) was used to assess cellular reactive oxygen species (ROS) formation. This probe is a chemically reduced form of fluorescein that does not fluoresce, but when it is converted inside the cell into 2',7'-dichlorofluorescein (DCF), DCF fluoresces at specific wavelengths. H_2DCFDA is taken up by the cells and intracellular esterase's cleave the diacetate groups, forcing the anion to be retained by the cell and undergo two-electron oxidation (oxidation by ROS) to form DCF (Rodogiannis, Duong and Kovarik, 2018). H_2DCFDA is a nonspecific ROS indicator able to detect superoxide, peroxide, and nitric oxide; therefore, it is a useful tool for detecting multiple forms of ROS in a single measurement. To optimise this assay to this species, a pilot test was conducted with 20 different concentrations of probe, increasing in large concentrations increments at first, and then 10 smaller increments in concentration, to see which concentration was best suited without high background fluorescence. After, the time needed to incubate the probe was worked out by seeing when the increasing fluorescence stopped, and the plateau began.

A 200 mM stock solution was diluted upon arrival in DMSO and aliquoted for long term storage at 20 mM and stored at -18 °C in darkness. Working solutions were prepared on the day of analysis to a concentration of 5 mM by dilution in RO water in darkness. One millilitre of algae in exposure solution was taken on day seven from each replicated exposure flask and centrifuged at 1500 rcf for three minutes to form a pellet. The pellet was reconstituted in 200 µL of clean F2 medium without any metals. Each control replicate, single metal exposed replicate, and 14 mixture replicates were pipetted into individual wells of a black 96-well clear flat bottom microplate (Corning Inc., NY, USA) on day seven of their exposure, not using the outer columns due to observed high evaporation (Figure 3.2). These outer columns were filled with F2 medium to protect the samples from evaporation and associated stress. A final volume of 200 µL per well was used containing the algae sample and 3.2 µL of the

probe working solution (final concentration of 80 µM per well). Once each replicate and probe were added to the microplate, the plate was covered in aluminium foil to protect from light and kept for one hour at 20 °C before measured using a FLUOstar Optima fluorescence plate reader (BMG Labtech, Ortenberg, Germany). The plate reader recorded relative fluorescence units for each replicate, including blank F2 medium replicates containing probe and no probe for background, and hydrogen peroxide as a positive control, at excitation 485 nm and emission 538 nm. The gain was set to 1518 for all single and combined metal exposures, taken from a pilot test to work out optimum ROS probe concentration and timings. In this pilot test, concentrations from 5 – 100 µM were tested, informed from previously published literature (Stachowski-Haberkorn *et al.*, 2013; Peperzak and Brussaard, 2011). The background fluorescence containing the probe was subtracted during data analysis from each sample to remove any background or contaminating fluorescence. The relative fluorescence value for each replicate of each metal concentration and mixture were displayed as fold change compared to the controls. The data were normalised to cell densities calculated from day seven samples measured on the flow cytometer.

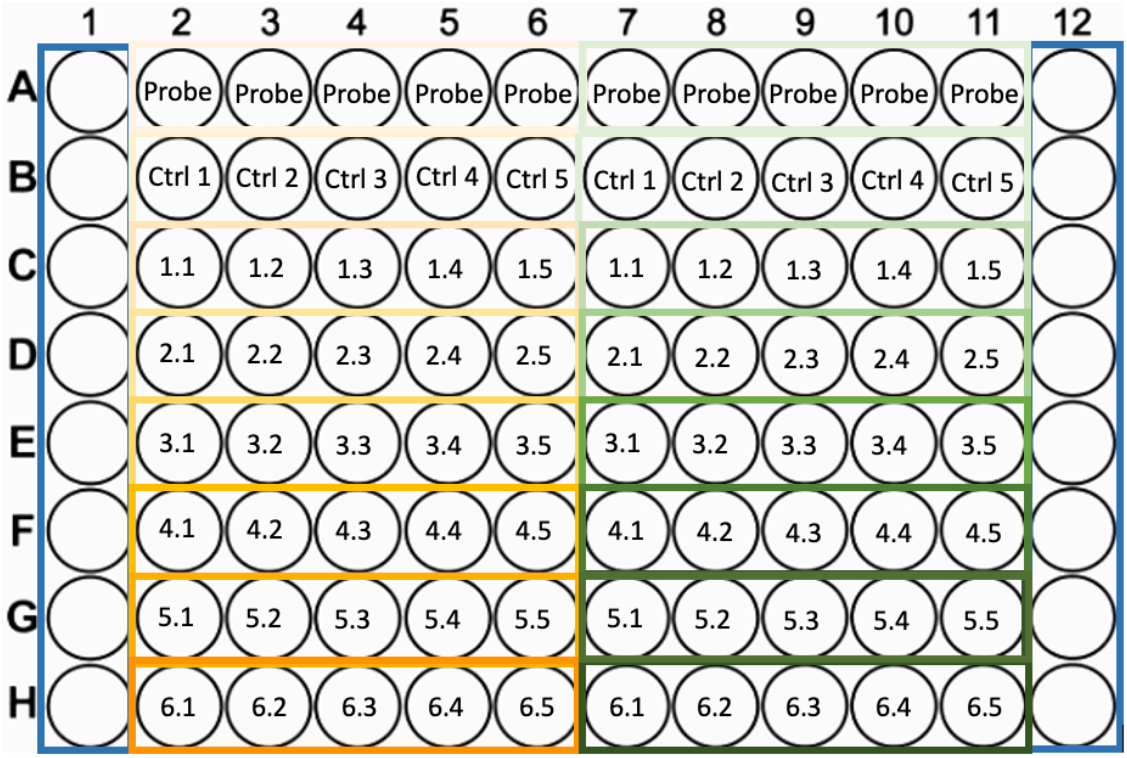

Figure 3.2. 96-well microplate layout for reactive oxygen species formation measurements. Each colour represents one single metal exposure, starting at a low concentration (1) and increasing to a high concentration (6). Ctrl = controls and blue highlighted columns = F2 medium added to protect samples from evaporation.

3.2.8 Photosynthesis II efficiency

Photosystem II efficiency of *T. suecica* exposed to single and combined solutions of copper, nickel, and zinc were determined using a Maxi-Imaging PAM (IPAM; Heinz Walz GmbH, Germany). The IPAM measures chlorophyll a fluorescence in vivo, using a non-destructive, pulse amplitude modulated (PAM) fluorometry that emits short wavelength light to excite photosystem II (PSII), which emits red to far-red light that can be measured (Schreiber *et al.*, 2007; Stock *et al.*, 2019). As the IPAM has a CCD camera, it can image and record samples in a 96-well plate in one measurement. The fluorescence signal can be easily distinguished between wells and the use of a black well, clear bottom microplate improved the contamination between neighbouring wells. To optimise this assay for *T. suecica*, a pilot study was conducted to ensure each exciting saturating pulse of light from the IPAM was within measuring range for the instrument. Further, the number of cells needed per well was calculated using a stock culture that was serially diluted from a highly concentrated sample to a low concentrated sample. A minimum concentration of cells was determined, which limited IPAM measurements to only the 7-day samples, as the earlier time points did not contain enough cells.

The same methods were conducted for both single metal and combined metal samples. One millilitre samples were taken from the metal exposed cultures after seven days and centrifuged following the same process as in 3.2.7. Each replicate was added to individual wells of a black 96-well clear flat bottom microplate (Corning Inc., NY, USA). The cell density of each replicate ranged between $6.6 \times 10^5 – 1.2 \times 10^6$ cells mL^{-1}. One microplate was measured at one time and was placed in the same location under the camera and LED lights, ensuring the microplate was pushed against the back bar and against the left-hand side pin. The samples were left to dark adapt for 30 minutes to allow PSII reaction centres to fully oxidise. After loading the ImagingWinGigE software and selecting MAXI as the measuring head on the instrument, the pulse-modulated fluorescence measuring light was automatically switched on, giving relatively weak measuring light pulses at low repetition rate (ca. 1Hz) that does not impact the samples but allows the user to define settings, select areas of interest and adjust gain. The aperture lens on the camera was set to 1.4 to give the best depth of field and the zoom and focus were adjusted for each microplate. The areas of interest were selected for each replicated control and metal concentration. The measuring light intensity, measuring light frequency and gain

were adjusted to ensure that all samples had a current fluorescence yield (F_t) greater than 0.1 relative units. The measuring light frequency was increased to between 4 – 8, and the intensity remained no greater than three to avoid problems with causing higher than expected F_o values, which would affect subsequent F_v/F_m values. Gain was increased to ten and damping to five (reduces background noise). Samples with a F_t value higher than 0.6 were diluted 10-fold and the dark adaption was completed again.

F_o, F_m determination was conducted, and the same value was used for both the kinetics and rapid light curve data collection. Firstly, measurements for dark-light induction were collected, which applied a saturation pulse to the samples to determine the maximum fluorescent yield after dark adaption (F_m) (Figure 3.3). Actinic light was then used at an intensity of five (=18 PAR mM m^{-2} s^{-1}) and width of zero, to excite samples every 20 seconds for 320 seconds. During this induction, the current fluorescence yield (F_t) and the maximum fluorescence yield after illumination (F_m') were recorded. Secondly, measurements for rapid light responses were collected, which steadily increased the photosynthetic active radiation (PAR) every 20 seconds, until reaching a PAR value of 701 - 703. During this light response, relative fluorescence yield (F), non-photochemical quenching (NPQ), coefficient of non-photochemical quenching (qN), coefficient of photochemical quenching (qP), the effective PSII quantum yield (YII) and relative photosynthetic electron transport rate (ETR) values were recorded. All measurements were recorded and presented as relative units for each parameter.

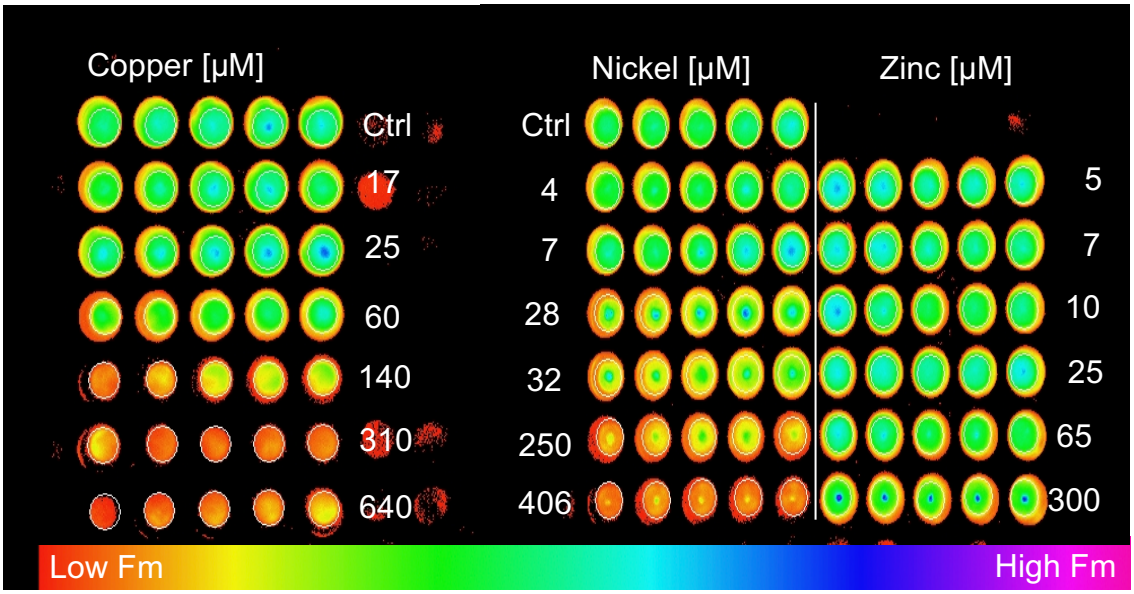

Figure 3.3. Imaging PAM F_m parameter measurements after seven days. F_m = Maximal fluorescence yield of dark-adapted sample with all PSII centres closed.

3.2.9 Statistical analysis

Dose response curves for cell density (cells mL^{-1}) after treatment were created using GraphPad Prism 9 (GraphPad Software Inc., California, USA). A non-linear regression allowed EC_{50} values to be calculated after seven days for *T. suecica* exposed to each metal. All statistical analyses for fluorescence endpoints were conducted using GraphPad Prism 9, including checking for normality using the Kolmogorov-Smirnov test and log_{10} transformation when needed. Data conforming to normality were further analysed using a one- (1W ANOVA) or two-way analysis of variance (2W ANOVA) depending on the assay, to determine significance for time, concentration and the interaction between time and concentration. After, Tukey's HSD Post Hoc tests were used to determine significant differences between concentrations and time points ($P < 0.05$). ANOVA could not be used when there were missing values for endpoints. When these situations arose, a mixed effects model was selected as it is capable of handling missing values and similar to a 2W ANOVA, provides information on which factors were significantly different. Following a mixed effects model, the Sidak's multiple comparisons test determined significant differences between concentrations and time points ($P < 0.05$). A principal component analysis (PCA) was applied to the full data set to characterise relationships between endpoints using XLSTAT (Addinsoft, Paris, France). Pearson's correlation coefficients were also calculated using XLSTAT as an estimate of the strength of association between the different endpoints ($P \leq 0.05$).

To analyse the combined metals data, the measured responses for each endpoint were imported into JMP Pro 15.2 (SAS Institute, Cary, North Carolina, USA), which included cell density, growth rates, percentage growth inhibition, ROS formation and IPAM parameters. Firstly, definitive screening was fitted to the data, providing main effect, and second order effect estimates and accompanying P-values. If there were main effects present within the mixture, the least squares model was fitted to the data, and surface profiler and interaction plots were produced. Data were also analysed in GraphPad Prism 9 to perform Pearson correlation coefficients using the total mixture solution concentration. Total mixture solution was calculated by adding all three metal concentrations together (Table 3.2).

3.3 Results

3.3.1 Exposure characteristics

The medium physiochemical exposure parameters measured at the beginning and end of the exposures showed that salinity remained constant and there was a decrease in pH for combined metal solutions from 8.21 ± 0.1 at zero days to 8.00 ± 0.1 at seven days.

Total metal concentrations were measured at the beginning and end of each exposure for copper, nickel, zinc, and combined metals. As shown in figure 3.4, copper had the largest change in concentration between days 0 and 7, with the highest four concentrations being significantly different, whereas nickel and zinc had only two significantly different concentrations (Table 3.3). The concentration throughout the combined metal exposure also reduced over seven days, with all the concentrations being significantly different between the time points.

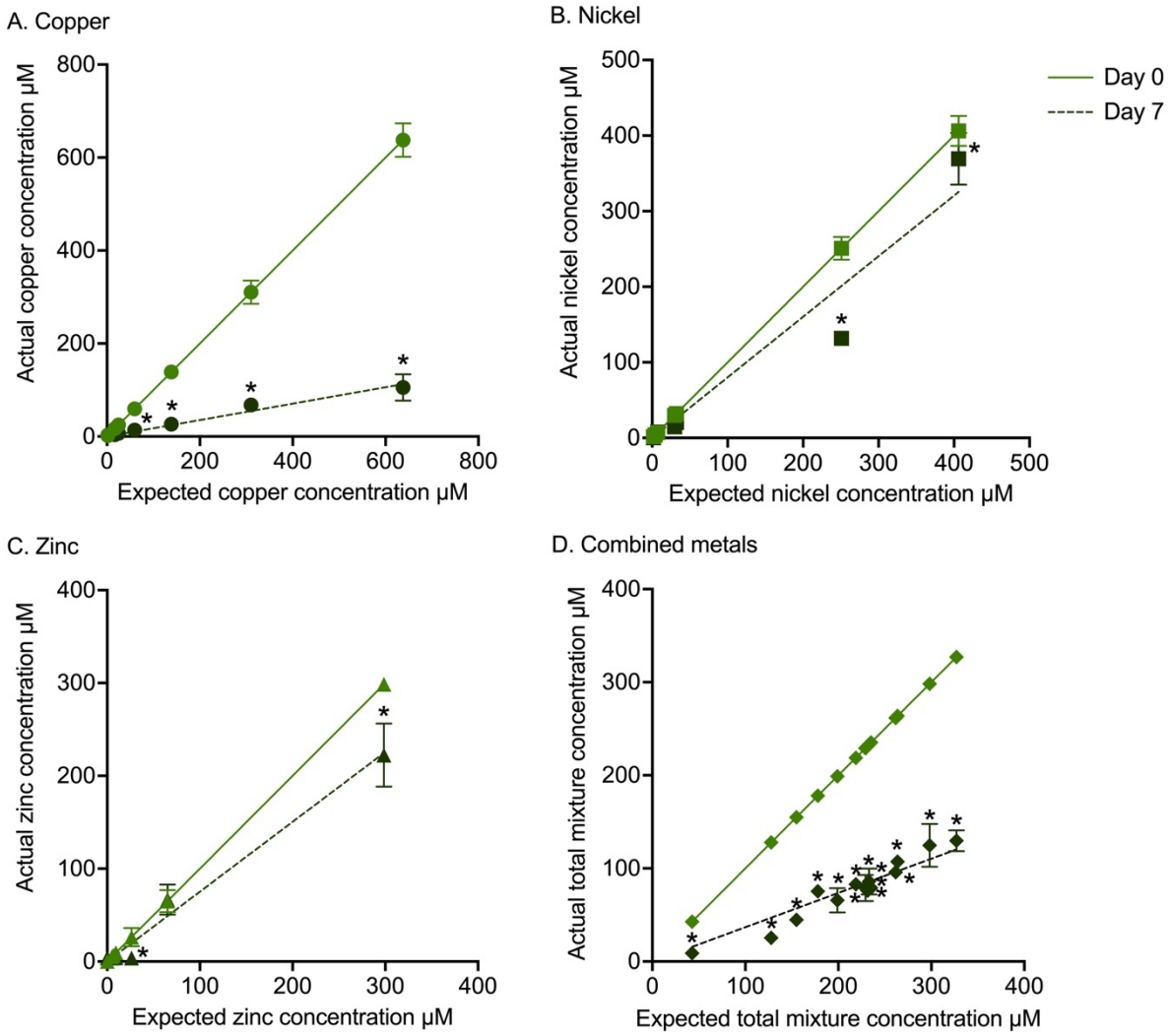

Figure 3.4. Actual concentrations (µM) measured at the beginning (day 0 – solid green line) and at the end (day 7 – dotted green line) of (A) copper, (B) nickel, (C) zinc, and (D) combined metals concentrations compared to the expected concentrations. * Indicates a significant difference between the actual concentration measured at day 0 and day 7 (Sidak's multiple comparisons test, $P < 0.05$).

Table 3.3. Mixed effects model statistical outputs for measured concentrations for *Tetraselmis suecica* on day zero and day seven to single metals, and two-way ANOVA statistical outputs for combined metals. * Indicates significant P-values.

Metal	**Time**	**Concentration**	**Time x Concentration**
Copper	<0.0001*	<0.0001*	<0.0001*
Nickel	<0.0001*	<0.0001*	<0.0001*
Zinc	<0.0001*	<0.0001*	0.0021*
Combined	<0.0001*	<0.0001*	<0.0001*

3.3.2 Single metal growth

T. suecica growth was most impacted by zinc, followed by nickel and copper (Figure 3.5) when comparing EC_{50} values; however, high copper concentrations had the greatest percentage growth inhibition of 17.7% when compared to the controls (Figure 3.6). Growth was significantly influenced by copper, with concentrations above 60 µM being significantly different to the controls (Figure 3.5A). The effect of copper was also significantly influenced by time and the interaction of time (Table 3.4). Copper had a significant negative correlation between both growth rate and percentage growth inhibition and copper concentration (Pearson correlation, P = 0.015).

For nickel, the impact on growth was also significantly influenced by concentration, time, and their interaction (Table 3.4). At day 7 of the exposure, growth for treatments exposed to concentrations greater than 30 µM were significantly different to the controls (Figure 3.5B). Growth parameters showed a significant concentration dependent correlation (Pearson correlation, P = 0.026).

Zinc was the most toxic metal to *T. suecica* growth (Figure 3.5C and Table 3.4). Five of the six tested concentrations were significantly different to the controls, with concentration identified as a significant factor. Following the same trends as copper and nickel, zinc influenced growth because of significant concentration, time and the interaction of concentration and time factors. At low zinc concentrations, growth rates were lower and percentage growth inhibition was higher relative to copper and nickel (Figure 3.6). Zinc did not have a significant correlation between concentration and growth rates or percentage inhibition (Pearson correlation, P = 0.18).

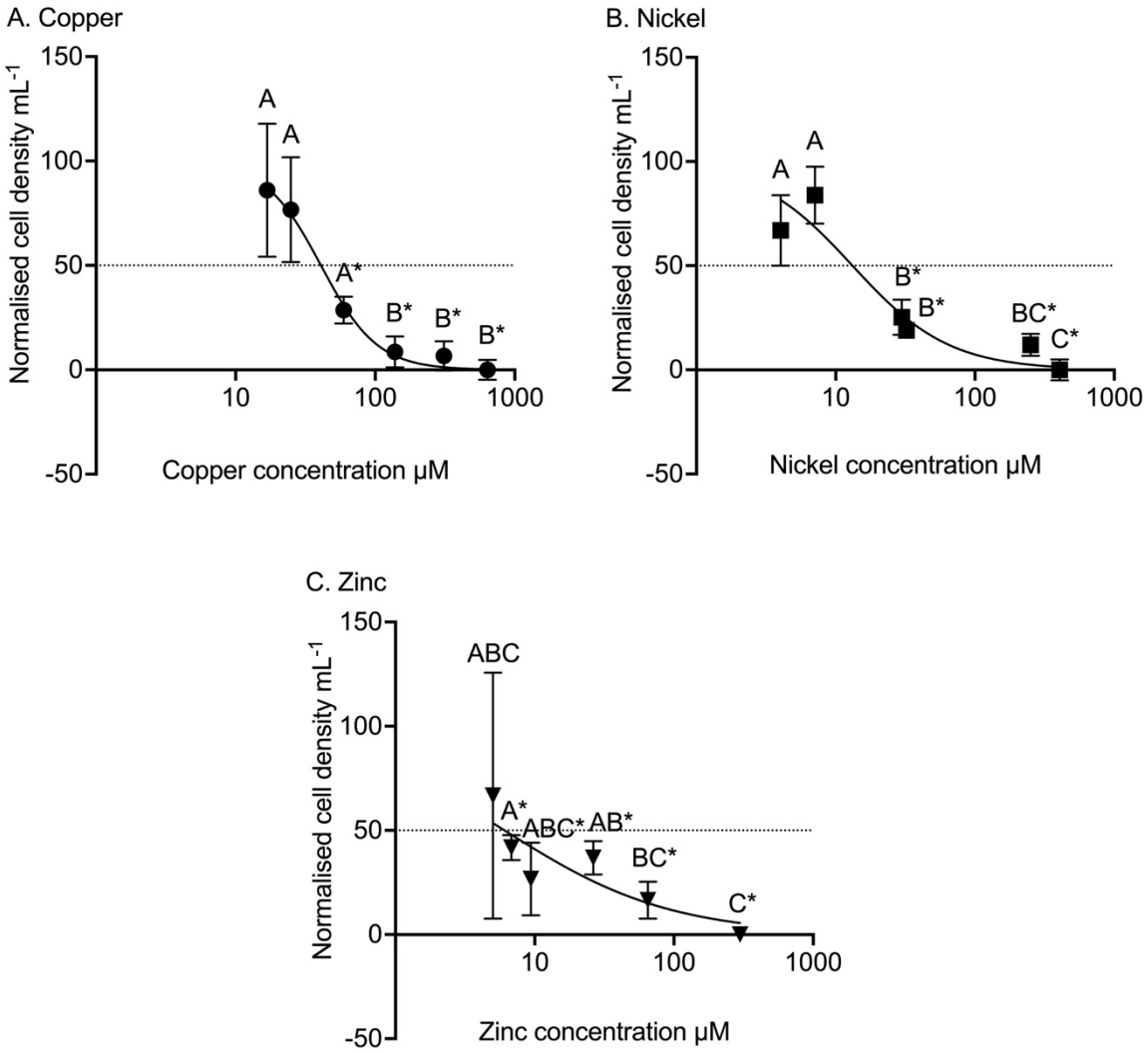

Figure 3.5. Concentration response curves for *Tetraselmis suecica* cell density mL^{-1} (normalised) following singular expose to (A) copper, (B), nickel and (C) zinc after seven days from one independent study. The dotted line shows the EC_{50} for each metal. Letters represent significant differences between concentrations of each metal and * indicates significant differences to the controls (Tukey post-hoc tests, $P < 0.05$).

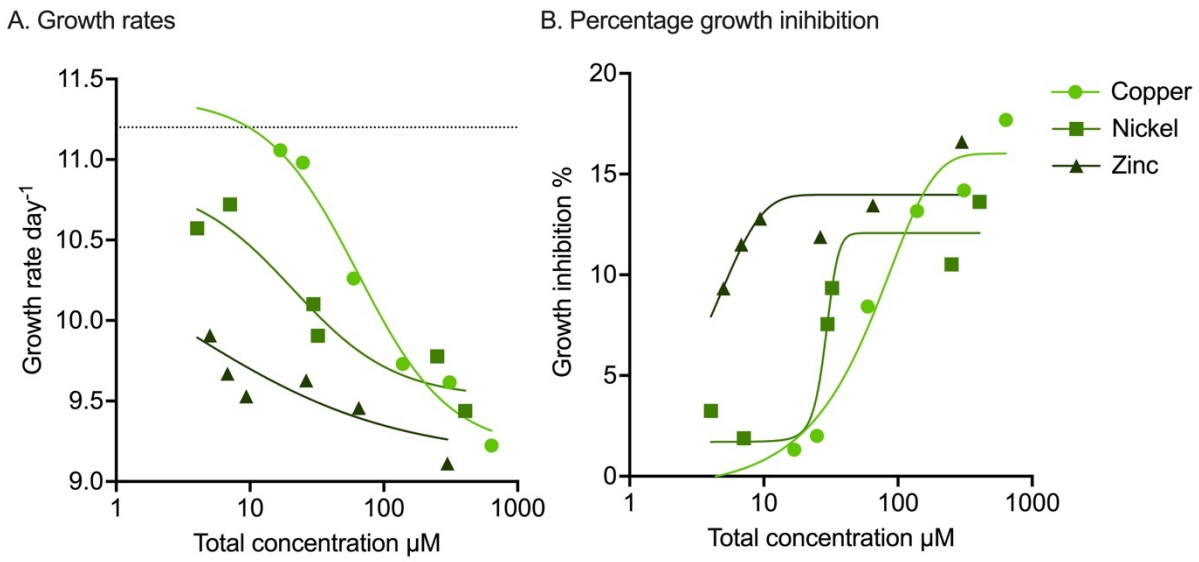

Figure 3.6. Growth rates (day^{-1}) and percentage growth inhibition of *Tetraselmis suecica* over seven days when exposed to copper (circles), nickel (squares), and zinc (triangles).

Table 3.4. Dose response curve statistics for *Tetraselmis suecica* growth after exposure to copper, nickel, zinc, and combined metals (total concentration µM) over seven days. Non-linear regressions produced EC_{50} values (µM) and R^2 values for each metal and time point. The no observed effect concentration (NOEC) and lowest observed effect concentration (LOEC) were calculated from the two-way ANOVA statistical output at days one and seven. * Indicates significant P-values from two-way ANOVA statistics, including whether there was a statistical difference for time, concentration (Conc.) and an interaction between time and concentration (Time x Conc.).

Metal	**Time (days)**	**EC_{50} µM**	**NOEC µM**	**LOEC µM**	**R^2**	**Two-way ANOVA Time**	**Two-way ANOVA Conc.**	**Two-way ANOVA Time x Conc.**
Copper	1	126.80	138.65	310.60	0.01	<0.0001*	<0.0001*	<0.0001*
	7	40.87	24.84	59.52	0.83			
Nickel	1	N/A	406.20	406.20	0.10	<0.0001*	<0.0001*	<0.0001*
	7	13.19	7.10	29.79	0.82			
Zinc	1	8.40	26.31	65.08	0.07	<0.0001*	<0.0001*	0.0021*
	7	6.07	5.01	6.79	0.35			
Combined	1	N/A	N/A	N/A	N/A	<0.0001*	<0.0001*	<0.0001*
	7	N/A	N/A	N/A	N/A			

3.3.3 Growth from combined metal exposure

Cell density was measured during exposures to the three-component metal mixtures, and growth rate and percentage growth inhibition were calculated afterwards using the same equations from the single metal study. All three datasets (cell density, growth rate and percentage growth inhibition) were used in the DSD to determine whether the same main effect drivers were identified.

For *T. suecica* cell density, all three metals within the three-metal mixture were identified as significant main effect drivers from the definitive screening (Figure 3.7). No pairs of metals were identified as being significant from the definitive screening ($P > 0.05$) on cell density, although the copper pairs (copper and nickel, and copper and zinc) were found to be significant from the least squares model ($P = 0.012$ and $P = 0.032$ respectively) (Figure 3.8). The nickel and zinc pair was not significant ($P = 0.25$). The copper and nickel, and copper and zinc pairs were likely significant due to copper, according to the prediction profiler for the least squares model. However, the interaction profiles from the least squares model showed non-linearity between all the pairs of metals within the three-metal mixture, suggesting that the effect of each metal on cell density altered as other metals within the mixtures changed their concentration.

Growth rate and percentage growth inhibition definitive screening outcomes were different to cell density. Copper was the only significant main effect driver for growth rates and percentage growth inhibition from the definitive screening ($P = 0.0059$), with no pairs of metals being significant in the three-metal mixture (Figure 3.7). As only one metal was determined to be a significant main effect driver and no interactions were found between metal pairs within the mixtures, a least squares model could not be run as it requires at least two factors. Instead, copper concentrations were used to plot the mixture effects on two axes for growth rate and growth inhibition (Figure 3.9A and 3.9B). Overall, all three definitive screenings found that copper was the significant main effect driver for the three-metal mixture.

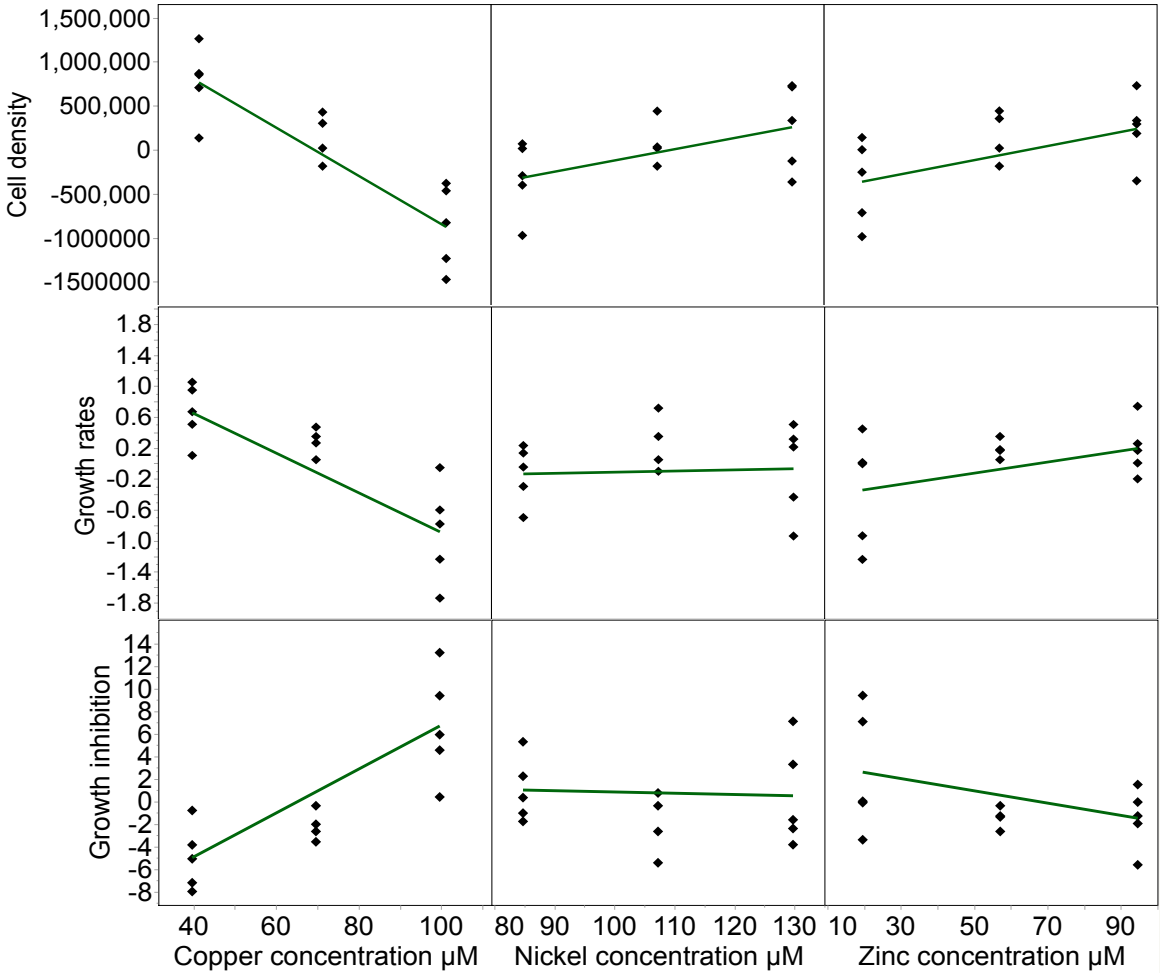

Figure 3.7. Linear regressions of the relationship between mixture factors and cell density, growth rates and percentage growth inhibition for *Tetraselmis suecica* after seven days of mixture exposure. Copper, nickel, and zinc were the three factors within the mixtures. Each diamond represents one mixture solution (14 in total) and is shown three times, once per metal, to show the concentration of each metal within the mixtures.

A. Copper and zinc

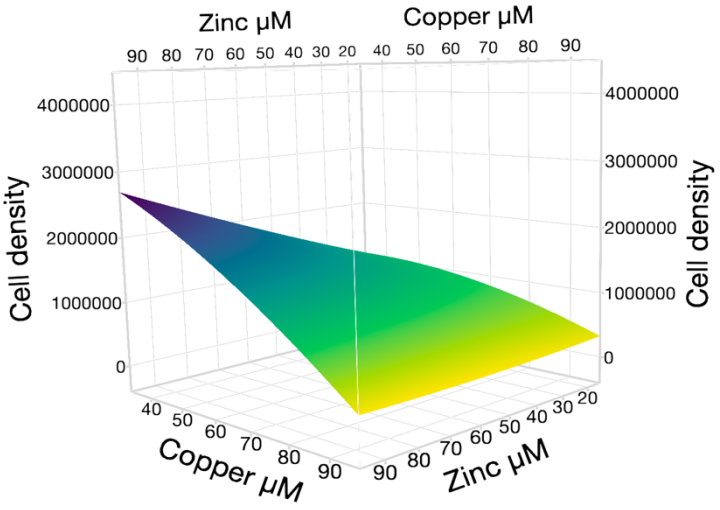

B. Copper and nickel

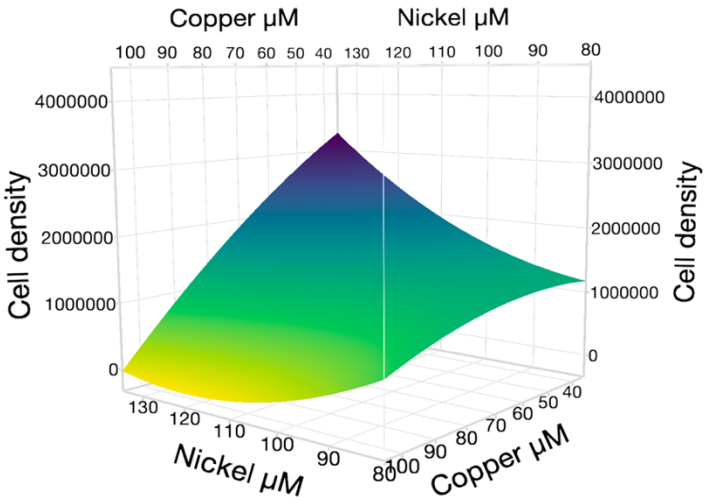

C. Nickel and zinc

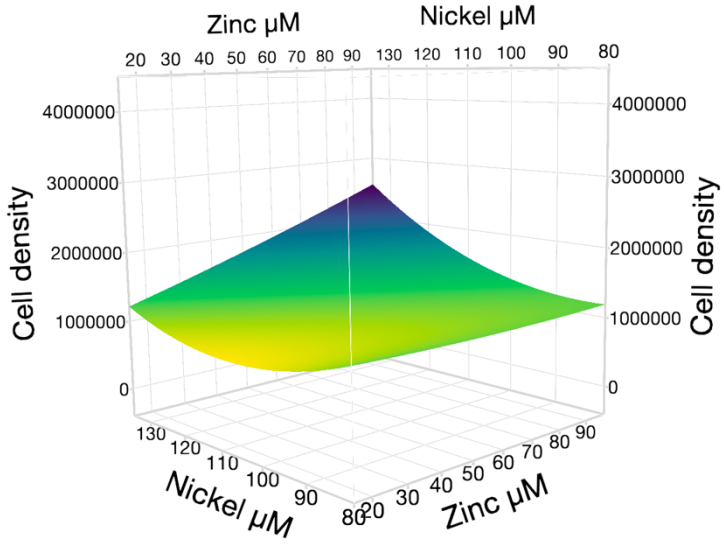

Figure 3.8. Response surface profile for *Tetraselmis suecica* cell density after exposure to three-metal combined solutions containing copper, nickel, and zinc for seven days. Each sub-figure shows data for two metals from the three-metal mixture. (A) copper and zinc, (B) copper and nickel, and (C) nickel and zinc.

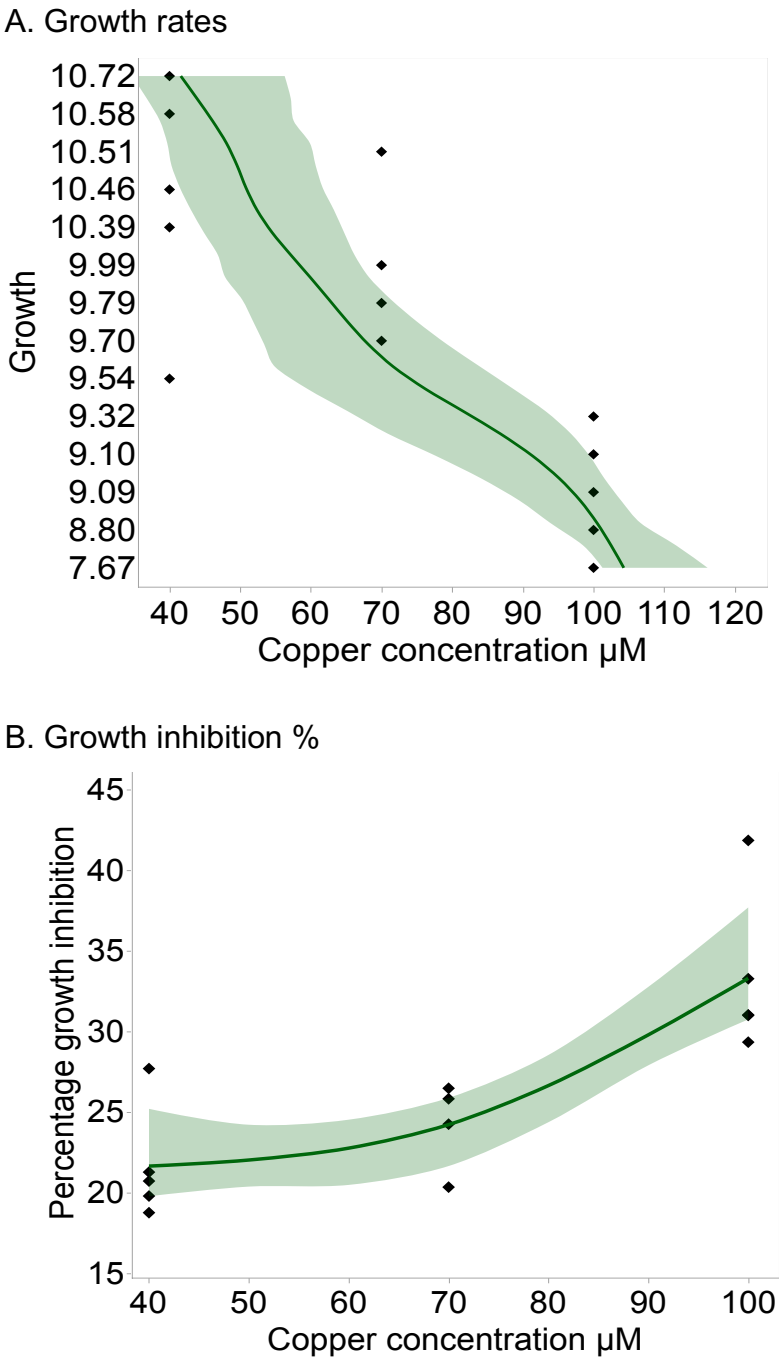

Figure 3.9. Mixture effects on (A) growth rates day^{-1} and (B) percentage growth inhibition. As copper is the main effect driver, it is shown instead of total mixture concentration. Each diamond represents one mixture solution (14 in total) that contains different concentrations of copper, nickel, and zinc. The dark green line shows the least squares model, and the lighter green area represents the confidence limits.

3.3.4 Reactive oxygen species formation

ROS fluorescence was measured for each metal singularly using a cellular probe. Copper exposure resulted in the most ROS formation when compared to controls after seven days of exposure, with a concentration dependent curve (Figure 3.10A). Using a one-way ANOVA, copper had a significant influence on ROS formation ($P < 0.0001$). The highest two concentrations were significantly different from the curve. There was a significant positive correlation between copper concentration and ROS formation (Pearson correlation, $P = 0.0072$). Nickel also had a concentration dependent increase of ROS formation (Figure 3.10B), with a significant positive correlation (Pearson correlation, $P = 0.0008$). Nickel concentration had a significant impact on ROS formation ($P < 0.001$), with concentrations greater than 250 µM being significantly different to the controls. For zinc, only the highest two concentrations resulted in significant increases in ROS formation (Figure 3.10C), in addition to zinc concentration being a significant factor ($P < 0.001$). There was a significant positive correlation between increasing concentration and ROS formation (Pearson correlation, $P = 0.0022$).

Using the DSD approach the formation of cellular ROS was measured in the 15 combined metal solutions. The definitive screening fit showed that both copper and nickel were significant main effect drivers for ROS formation ($P = 0.0197$ and $P = 0.0211$ respectively). The fit least squares model used copper and nickel, as these were the main risk drivers, but the model fit was limited for copper and nickel (Figure 3.11). Furthermore, ROS formation did not have a significant correlation with total combined metal concentration (Pearson correlation, $P = 0.11$), showing the higher total concentration was not causing the increased ROS, but rather the main effect driver concentrations within these mixtures (Figure 3.10D). When compared to the single metal exposures, the measured ROS formation was lower for the combined metal exposures, suggesting an antagonistic interaction.

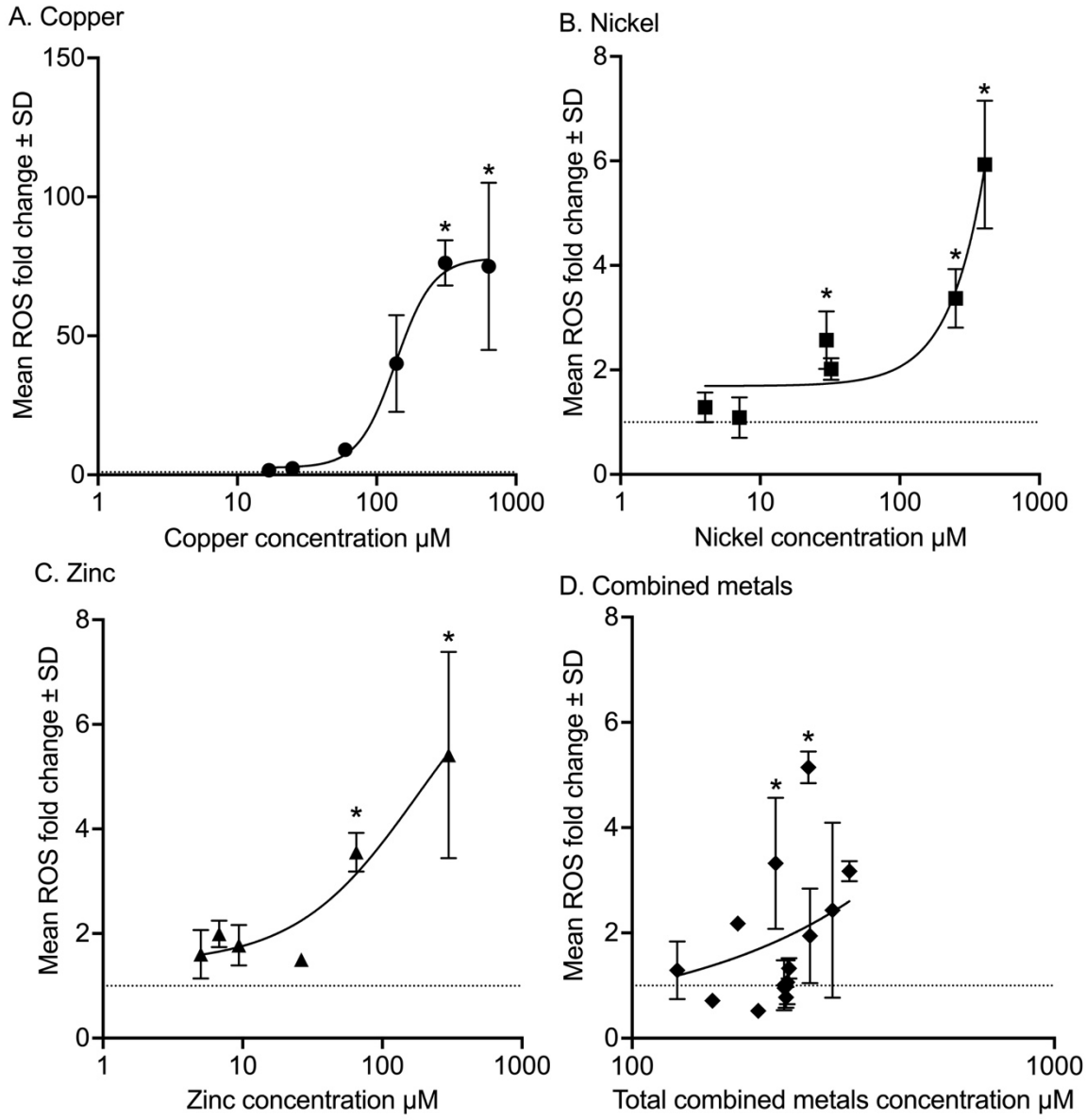

Figure 3.10. Mean reactive oxygen species (ROS) formation ± standard deviation (SD) for (A) copper, (B) nickel, (C) zinc and (D) combined metals. * Indicates metal concentrations that are significantly different to the control (Tukey's post hoc test, $P < 0.05$). The dotted line represents the control.

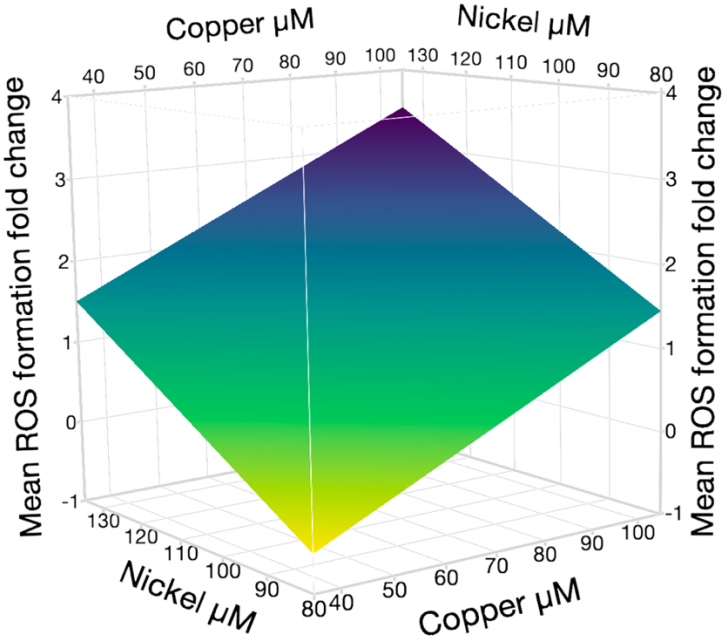

Figure 3.11. Response surface profile for reactive oxygen species (ROS) formation in *Tetraselmis suecica* after exposure to three-metal combined solutions containing copper, nickel, and zinc for seven days.

3.3.5 Dark acclimated fluorescence parameters for single metals

In the dark acclimated state, *T. suecica* exposed to copper had a significant decrease in F_v/F_m fluorescence at 310 µM (Figure 3.12A). Similarly, nickel had a concentration dependent decrease in F_v/F_m with increasing concentration, with 406 µM being significantly different to the controls (Figure 3.12B). However, zinc did not cause a significant decrease at any concentration tested (Figure 3.12C).

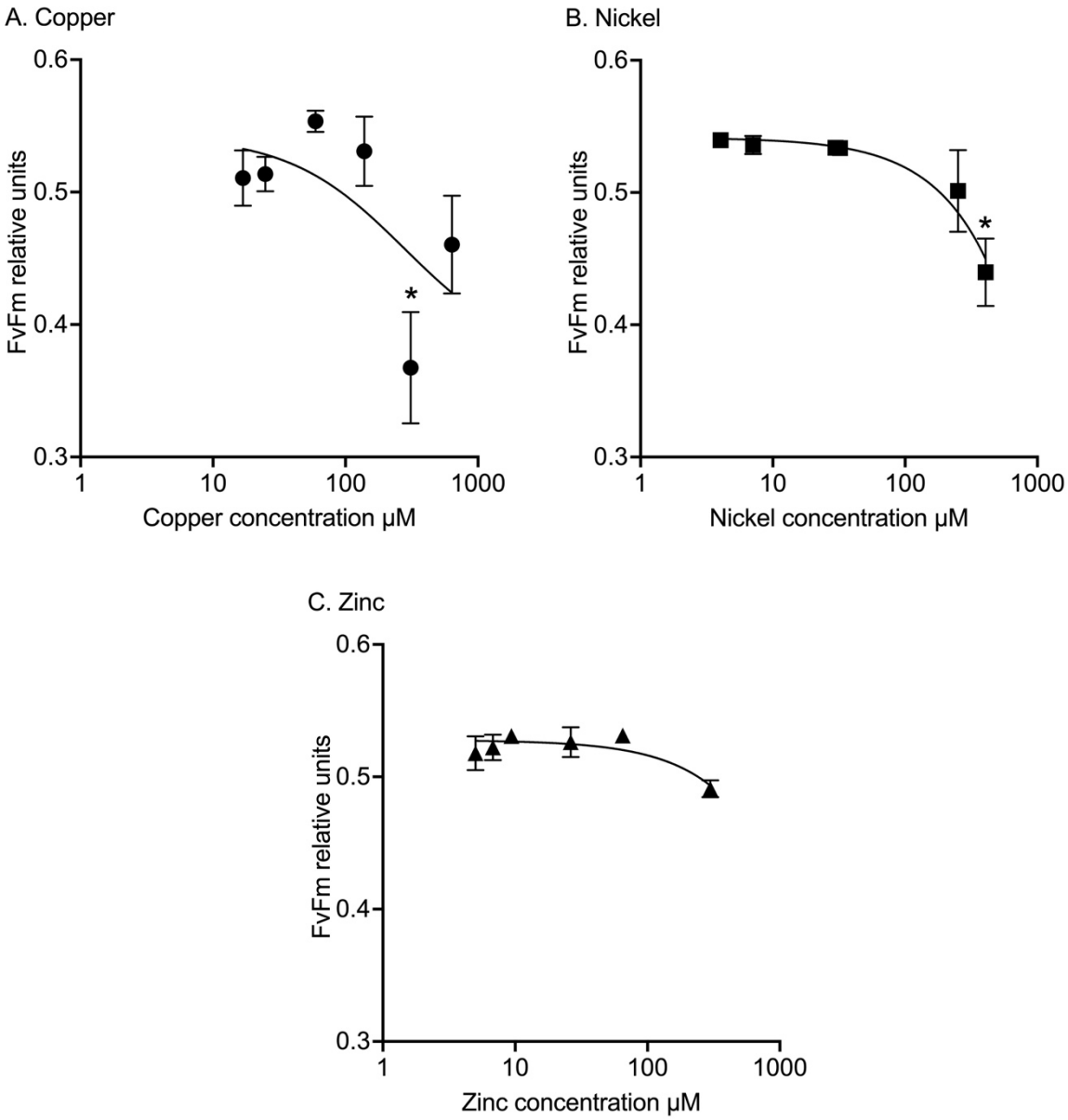

Figure 3.12. F_v/F_m fluorescence of *Tetraselmis suecica* in the dark acclimated state exposed to (A) copper, (B) nickel, and (C) zinc for seven days. Mean ± standard deviation from five replicates per concentration. * Indicates metal concentrations that were significantly different to the control (Tukey's post hoc test, $P < 0.05$).

3.3.6 Light acclimated fluorescence parameters for single metals

In the light acclimated state, *T. suecica* exposed to copper for seven days had an increased relative fluorescence yield at low copper concentrations (up to 140 µM) and a decreased relative fluorescence yield at higher concentrations when compared to the controls (Figure 3.13A). For all concentrations, the relative fluorescence yield slightly decreased with increasing PAR. While for the effective PSII quantum yield (YII) there was a decrease with increasing PAR for all concentrations, including the controls (Figure 3.13B). This copper concentration dependent response for YII was

present at all PAR values tested. At 640 µM, the starting YII relative value was 0.2 lower than the controls and reached 0.0 by 112 PAR mM m^{-2} s^{-1}. These YII responses suggest that non-photochemical processes had been activated. The non-photochemical quenching (NPQ) measured alongside YII showed an increase with increasing PAR and concentration, except for 640 µM (Figure 3.13C). These responses complement each other, with similar inverse trends and relative units measured. In agreement, the coefficient of non-chemical quenching (qN) showed an activation, with a steeper hill slope at lower PAR values and reaching greater relative units than NPQ (Figure 3.13D). At the highest PAR values, the qN was copper concentration dependent, with controls having the lowest qN. The coefficient of photochemical quenching (qP) had an inverse trend to qN, with a decrease in relative units with increasing PAR and copper concentration (Figure 3.13E). Furthermore, exposure to copper resulted in an altered ETR process for *T. suecica* (Figure 3.13F). At 310 and 640 µM, there was a bi-phasic response, with increasing ETRs until 337 PAR mM m^{-2} s^{-1} and 57 PAR mM m^{-2} s^{-1} respectively, before decreasing ETR with further PAR.

These responses to fluorescence parameters after light acclimation show that copper exposure did impact parameters related to PSII and the overall photosynthetic ability in a concentration dependent manner. For all parameters, PAR values, copper concentrations and the interaction between PAR and copper concentration were significant factors influencing responses ($P < 0.0001$*). Significant differences between specific concentrations, determined using the Dunnett's multiple comparisons, were not included in figure 3.13 as the interaction between the two factors was significant for all parameters. This meant that the multiple comparisons could be easily misinterpreted, in addition to making the figures too cluttered and hard to distinguish between concentrations. This was the case for nickel and zinc data as well.

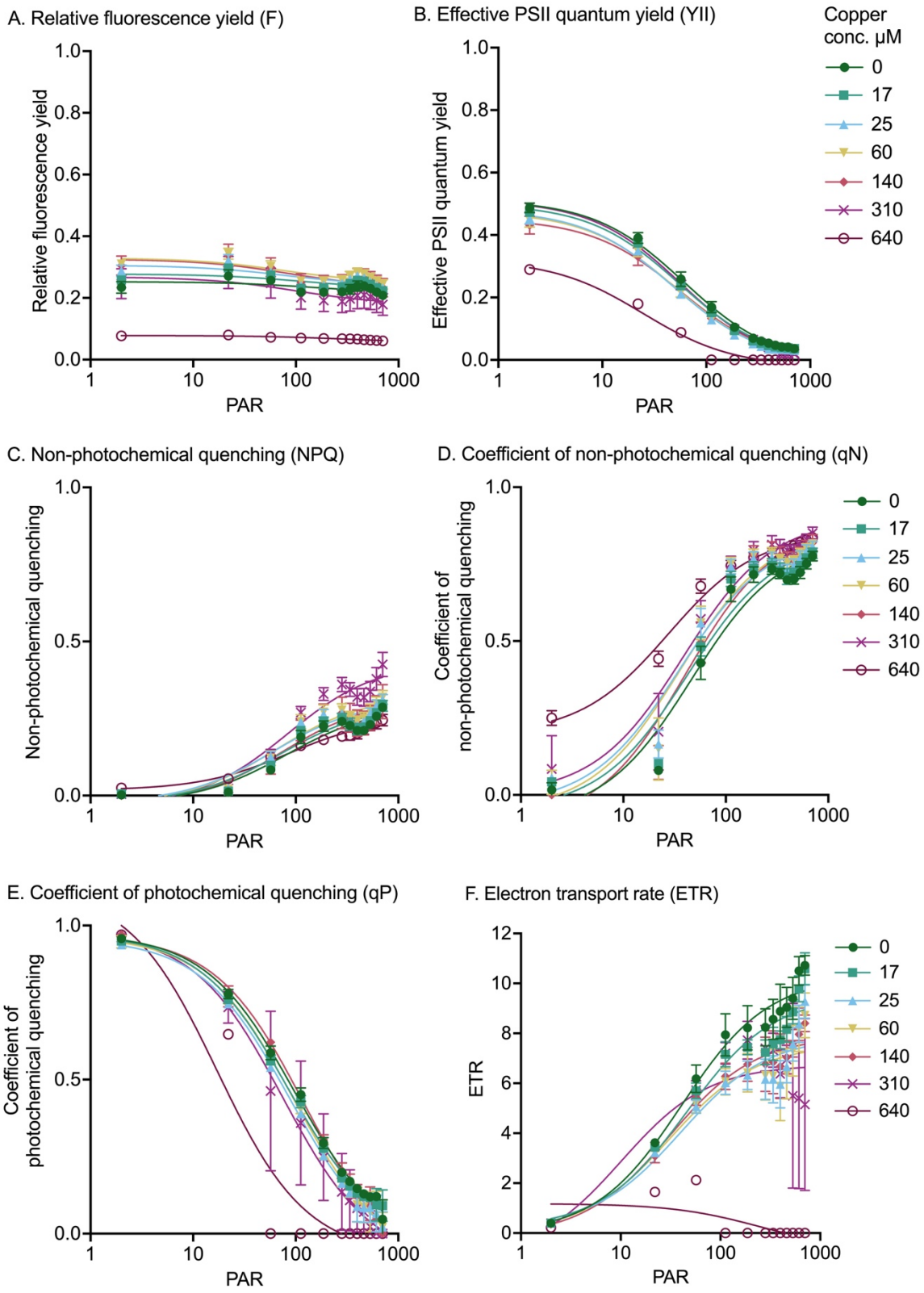

Figure 3.13. Fluorescence parameters of *Tetraselmis suecica* in the light acclimated state exposed to copper for seven days. (A) Relative fluorescence yield, (B) effective photosystem II quantum yield, (C) non-photochemical quenching, (D) coefficient of non-photochemical quenching, and (E) coefficient of photochemical quenching, and (F) electron transport rate (ETR). Mean responses ± standard deviation from five replicates per concentration (conc.). Photosynthetically active radiation (PAR) units are mM m^{-2} s^{-1}.

Similarly to the copper responses, nickel exposed *T. suecica* showed changes in light acclimated fluorescent parameters with increasing PAR. All parameters were significantly impacted by nickel concentration, PAR and the interaction between concentration and PAR ($P < 0.0001$*). The relative fluorescence yield remained consistent at low PAR values but decreased at higher PAR values for all nickel concentrations and the controls (Figure 3.14A). For the YII, there was a nickel concentration dependency shown, with increasing nickel concentrations having lower relative units (Figure 3.14B). In addition, the relative units decreased with increasing PAR for all nickel concentrations, reaching zero at 283 PAR mM m^{-2} s^{-1} for all concentrations. As seen for copper, the nickel exposed algal cells also triggered the non-photochemical process. For NPQ, there was an increase in relative units with increasing nickel concentration and PAR (Figure 3.14C). This was replicated for qN, with controls and low nickel exposed cells having lower relative units when compared to higher nickel exposed cells (Figure 3.14D). However, this was only at PAR values greater than 23 mM m^{-2} s^{-1}, as at the lowest PAR value the controls and low nickel concentrations had higher qN values than higher nickel concentrations. As expected, there was an inverse trend with photo-chemical quenching, with qP relative units decreasing with increasing concentration at each PAR value and with increasing PAR values (Figure 3.14E). Finally, ETR was negatively impacted by nickel, with a decrease in ETR at all concentrations above 113 PAR mM m^{-2} s^{-1} (Figure 3.14F).

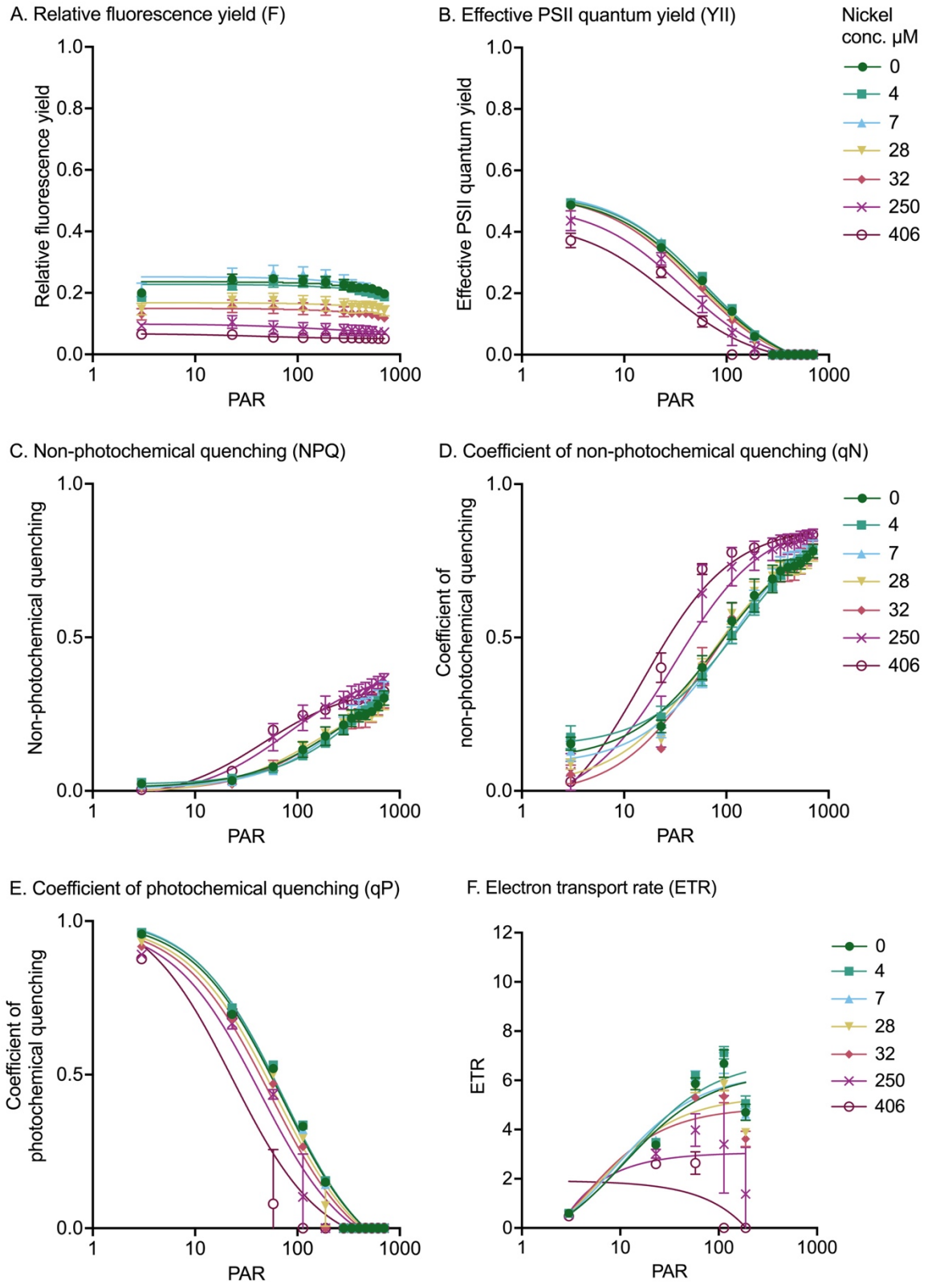

Figure 3.14. Fluorescence parameters of *Tetraselmis suecica* in the light acclimated state exposed to nickel for seven days. (A) Relative fluorescence yield, (B) effective photosystem II quantum yield, (C) non-photochemical quenching, (D) coefficient of non-photochemical quenching and (E) coefficient of photochemical quenching, and (F) electron transport rate (ETR). Mean response ± standard deviation from five replicates per concentration (conc.). Photosynethically active radiation (PAR) units are mM m^{-2} s^{-1}.

For zinc exposed *T. suecica*, light acclimatised parameters were measured and found to be significantly affected by zinc concentration, PAR values and their interaction ($P < 0.0001$*). Responses from zinc exposure were similar to responses seen after copper and nickel exposures. For example, relative fluorescence yield remained consistent at each concentration until high PAR which resulted in a slight decrease (Figure 3.15A), YII relative units were concentration dependent (Figure 3.15B) and non-photochemical and photochemical parameters showed inverse responses being triggered at similar concentrations and PAR values (Figure 3.15C, 3.15D and 3.15E). However, at 300 µM the qN relative units were lower than the controls at high PAR. The effect on the ETR was most prominent at the highest zinc concentration; however, there was a decrease in all ETRs measured above 113 PAR mM m^{-2} s^{-1} (Figure 3.15.F). For ETR, the concentration range being shorter means that some responses seen by the highest copper and nickel concentrations to ETR have been missed.

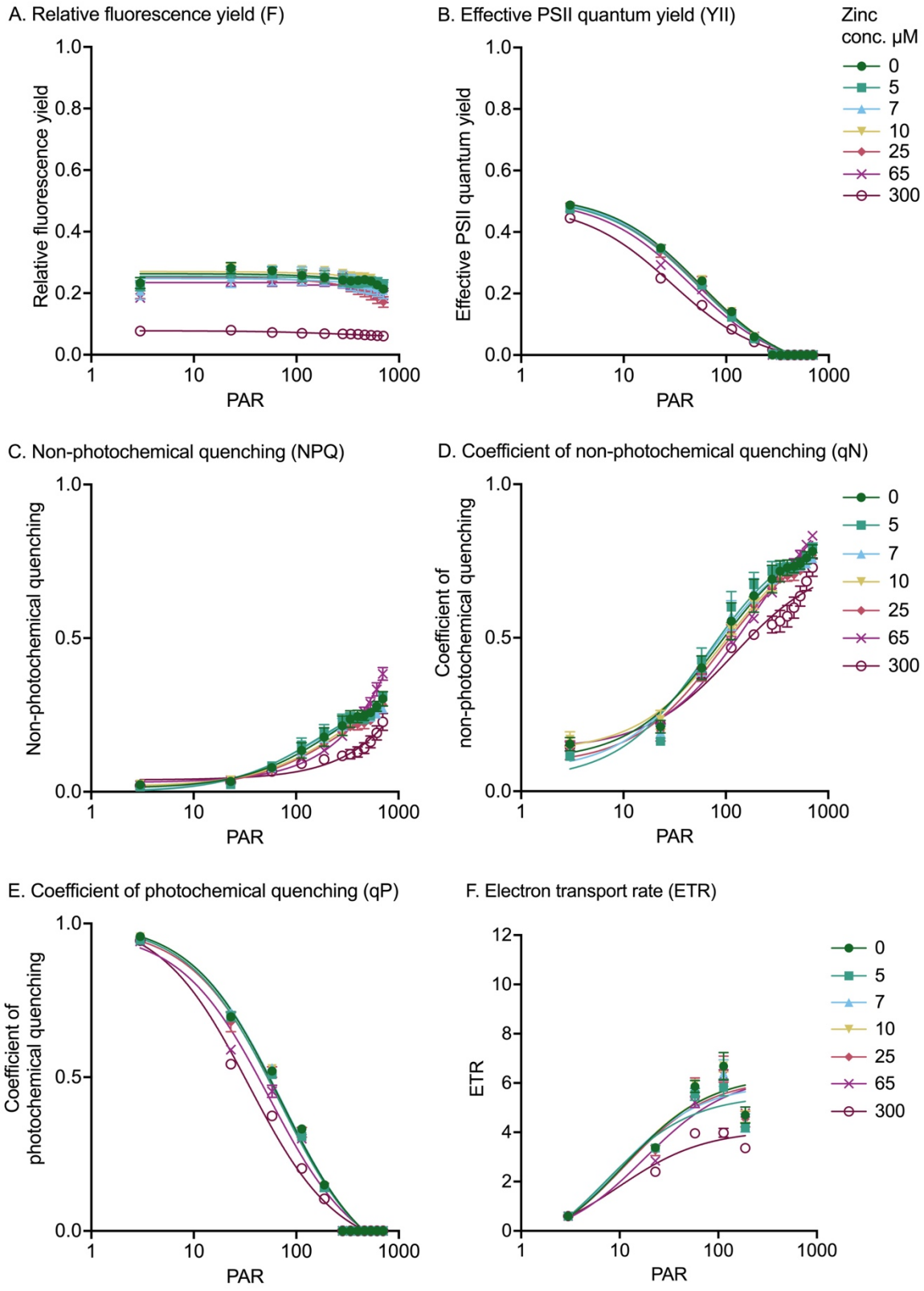

Figure 3.15. Fluorescence parameters of *Tetraselmis suecica* in the light acclimated state exposed to zinc for seven days. (A) Relative fluorescence yield, (B) effective photosystem II quantum yield, (C) non-photochemical quenching, (D) coefficient of non-photochemical quenching and (E) coefficient of photochemical quenching, and (F) electron transport rate (ETR). Mean response ± standard deviation from five replicates per concentration (conc.). Photosynethically active radiation (PAR) units are mM m^{-2} s^{-1}.

3.3.7 Dark acclimated fluorescence parameters for combined metals

In the dark acclimated state, F_v/F_m fluorescence was measured after seven days of exposure to three-metal mixture solutions. Copper was the only metal that was a significant main effect driver from the definitive screening fit, with a P-value of 0.023 (Figure 3.16), and there were no further interactions.

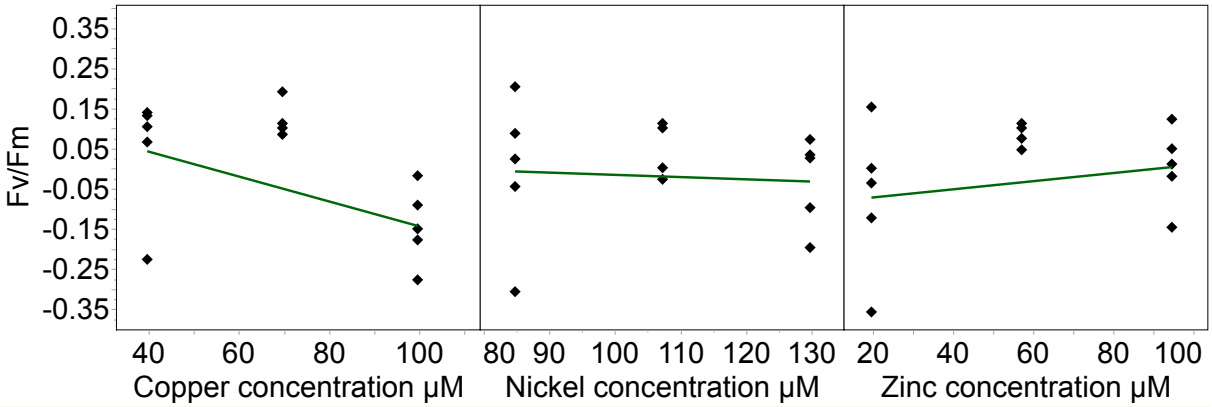

Figure 3.16. Linear regressions of the relationship between mixture factors and F_v/F_m for *Tetraselmis suecica* after seven days of mixture exposure. Copper, nickel, and zinc were the three factors within the mixtures. Each diamond represents one mixture solution (14 in total) and is shown three times, once per metal, to show the concentration of each metal within the mixtures.

3.3.8 Light acclimated fluorescence parameters for combined metals

To investigate the toxicological impact of the three-metal mixtures on *T. suecica* photosynthetic performance, qP, qN and NPQ parameters were measured, in addition to determining the effects on YII and ETR. To achieve this, 81 PAR level was selected to compare the effects between the different mixtures. The three parameters related to non-photochemical and photochemical quenching, qN, NPQ and qP found that copper was the only significant main effect driver within the mixtures (P = 0.013, P = 0.002 and P = 0.044 respectively) and there were no interactions between the three metals (Figure 3.17).

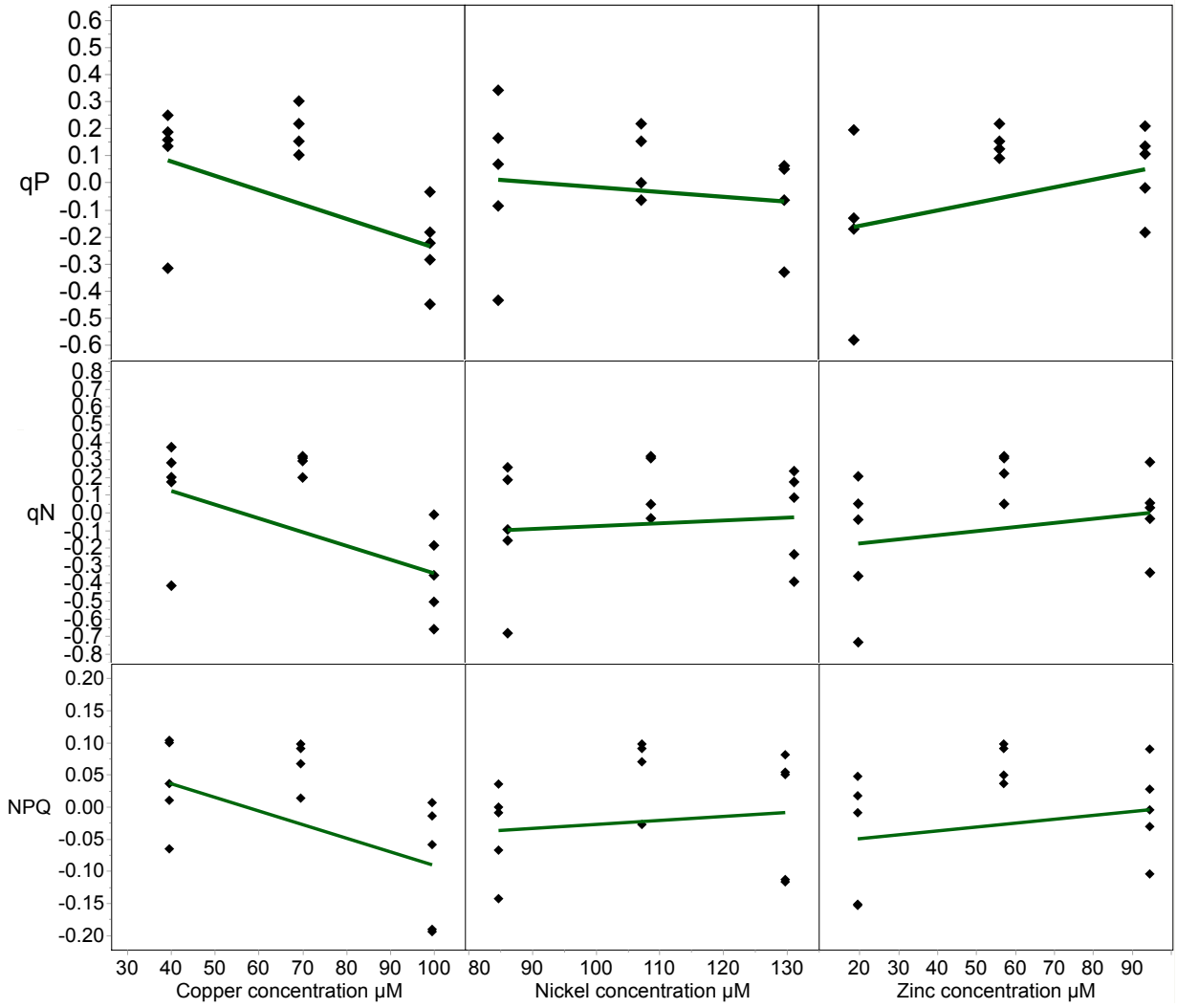

Figure 3.17. Linear regressions of the relationship between mixture factors and qP, qN and NPQ for *Tetraselmis suecica* after seven days of mixture exposure. Copper, nickel, and zinc were the three factors within the mixtures. Each diamond represents one mixture solution (14 in total) and is shown three times, once per metal, to show the concentration of each metal within the mixtures.

For YII, there were no main effects identified (copper P = 0.0597, zinc P = 0.2032 and nickel P = 0.3513) but there was a significant interaction between copper and nickel of 0.0477 according to the definitive fit. Furthermore, the least squares model found that copper was a significant main effect driver in the mixture (P = 0.0161) as well as the interaction between copper and nickel (P = 0.0311) and copper and zinc (P = 0.0359) (Figure 3.18). Similarly, ETR had no significant main risk driver identified from the definitive fit (copper P = 0.06, zinc P = 0.21 and nickel P = 0.35) and no interactions between the metal pairs within the mixtures were significant. The least squares model did find copper to be significant (P = 0.016), with significant interactions between copper and nickel (P = 0.032) and copper and zinc (P = 0.037) (Figure 3.19).

A. Copper and nickel

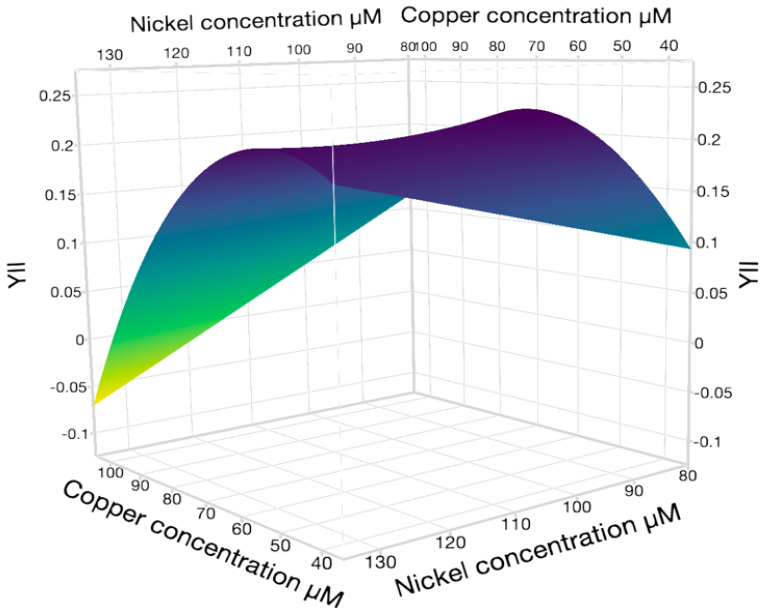

B. Copper and zinc

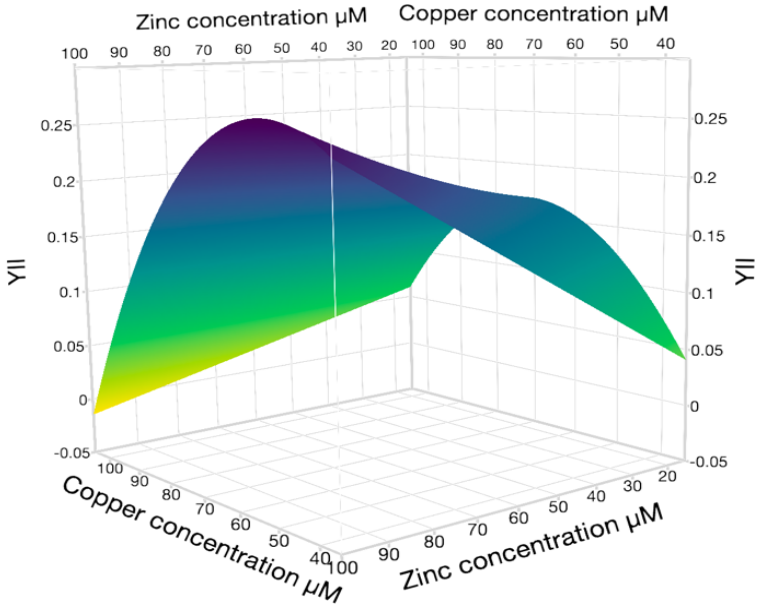

Figure 3.18. Response surface profile for effective photosystem II quantum yield (YII) in *Tetraselmis suecica* after exposure to three-metal combined solutions containing copper, nickel, and zinc for seven days. (A) Copper and nickel and (B) copper and zinc are presented as they had a significant interaction within the three-metal mixtures.

A. Copper and nickel

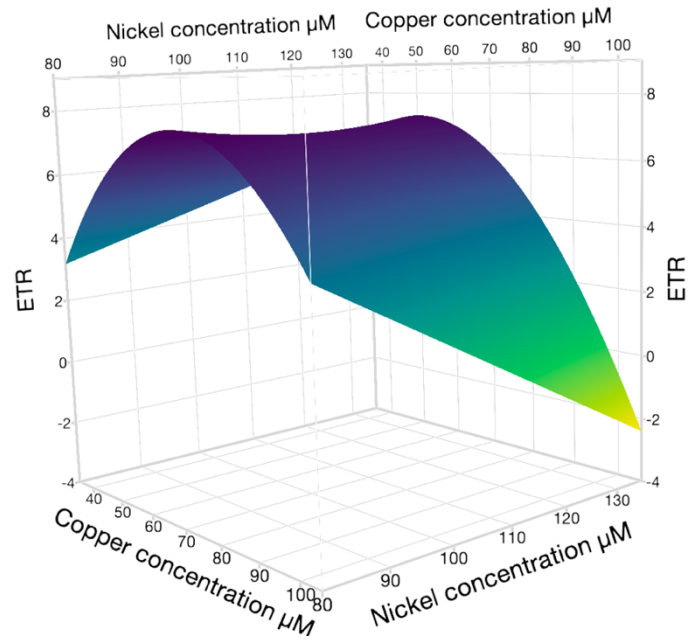

B. Copper and zinc

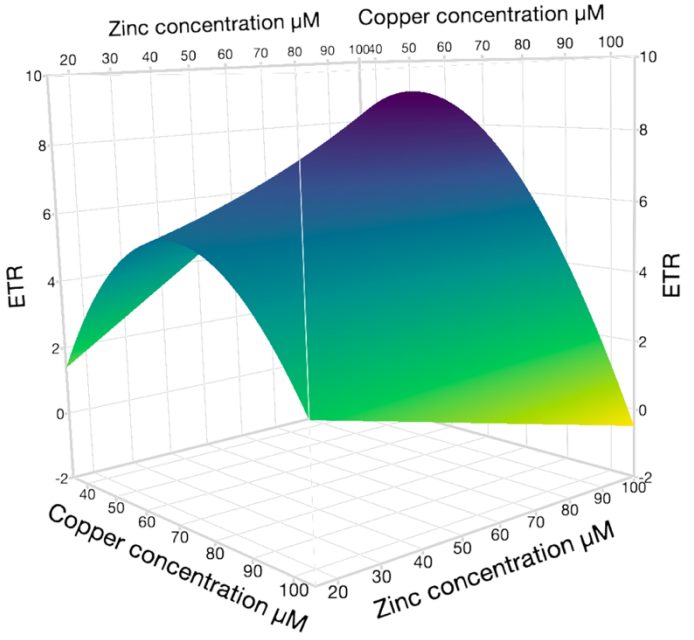

Figure 3.19. Response surface profile for electron transport rate (ETR) in *Tetraselmis suecica* after exposure to three-metal combined solutions containing copper, nickel, and zinc for seven days. (A) Copper and nickel and (B) copper and zinc are presented as they had a significant interaction within the three-metal mixtures.

3.3.9 Principal component analysis

For copper, the two principal components (PC1 and PC2) explained 89.99% of total variance (Figure 3.20A). The active variables qN and NPQ had their trends seen best on PC2, whereas the other six variables were best shown on PC1. Neither qN nor NPQ had any significant correlations with other variables (Table 3.5). All the significant correlations between variables after copper exposure were positive correlations, for example growth inhibition and ROS that are tightly clustered and YII and ETR that had the highest correlation of 1. Growth inhibition, ROS formation and qN were present between the two highest concentrations, whereas qP, YII and NPQ were more closely associated with lower copper concentrations. Interestingly, ETR was placed with the lower copper concentrations, although when looking at the change in ETR its trends were similar to qN.

The total variance for nickel was higher than copper, with PC1 and PC2 representing 97.41% (Figure 3.20B). All the active variables could be best shown from PC1, resulting with two main clusters in opposing directions from the centre, with significant negative correlations between the clusters (Table 3.6). Growth inhibition, ROS formation, NPQ and qN were significantly positively correlated, in the direction of high nickel concentrations. Whereas F, ETR, qP and YII were significantly positively correlated in the direction of low nickel concentrations. These clusters align with the trends seen for each variable with increasing nickel concentration. With F, ETR, qP and YII opposite to growth inhibition, it suggests that these parameters are responsible for growth inhibition from nickel exposure.

With a total variance of 92.04% explained by the two principal components following seven days of zinc exposure, variables separated into three distinct clusters (Figure 3.20C). As seen for copper and nickel, zinc also had growth inhibition and ROS closely clustered, although for zinc this was not a significant correlation (Table 3.7). While growth inhibition was not significantly correlated to any variables, ROS had a significant negative correlation with all the PAM parameters. This suggests that increases in ROS formation reduces important photosynthetic parameters, particularly YII and ETR. Furthermore, the significant positive correlation between YII and qP, which was closely clustered for all three metals, suggests a change from photochemical quenching to non-photochemical quenching occurred.

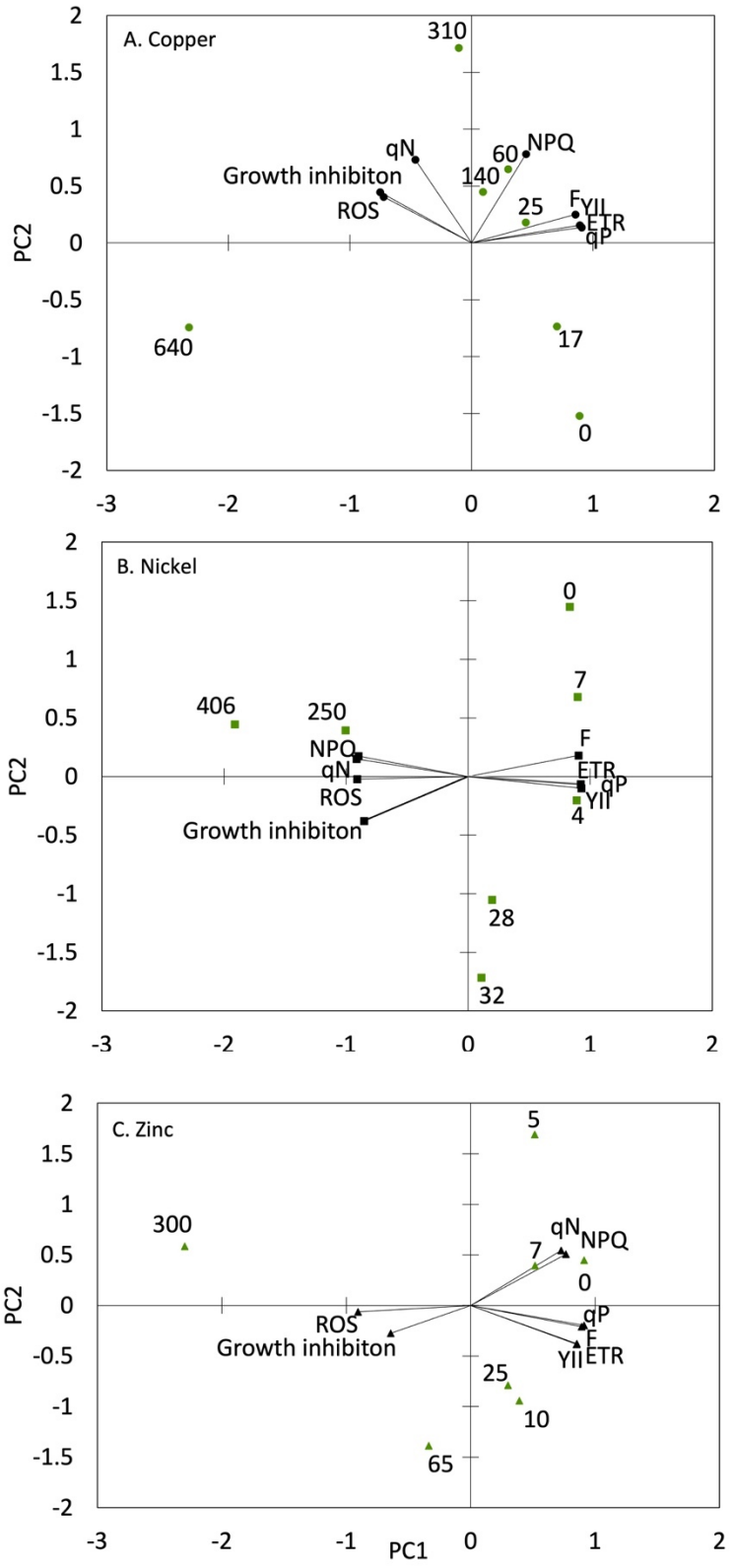

Figure 3.20. Principal component analysis (PCA) of responses in *Tetraselmis suecica* exposed to (A) copper (circles), (B) nickel (squares) and (C) zinc (triangles) after seven days at 113 PAR mM m^{-2} s^{-1}. Active variables are the measured effect responses (black shapes) and active observations are metal concentrations (green shapes).

Table 3.5. Pearson correlation matrix obtained from effect endpoints measured in *Tetraselmis suecica* after seven days of copper exposure. * Values indicate significant differences. Growth inhibition (Growth inh.), reactive oxygen species (ROS), relative fluorescence yield (F), effective PSII quantum yield (YII), coefficient of non-photochemical quenching (qN), coefficient of photochemical quenching (qP), non-photochemical quenching (NPQ) and electron transport rate (ETR).

Variables	Growth inh.	ROS	F	YII	qN	qP	NPQ	ETR
Growth inh.	1	0.921*	-0.581	-0.640	0.691	-0.648	-0.068	-0.639
ROS	0.921*	1	-0.677	-0.553	0.551	-0.662	-0.033	-0.553
F	-0.581	-0.677	1	0.863*	-0.170	0.959*	0.611	0.864*
YII	-0.640	-0.553	0.863*	1	-0.435	0.958*	0.591	1.000*
qN	0.691	0.551	-0.170	-0.435	1	-0.387	0.436	-0.435
qP	-0.648	-0.662	0.959*	0.958*	-0.387	1	0.535	0.959*
NPQ	-0.068	-0.033	0.611	0.591	0.436	0.535	1	0.590
ETR	-0.639	-0.553	0.864*	1.000*	-0.435	0.959*	0.590	1

Table 3.6. Pearson correlation matrix obtained from effect endpoints measured in *Tetraselmis suecica* after seven days of nickel exposure. * Values indicate significant differences. Growth inhibition (Growth inh.), reactive oxygen species (ROS), relative fluorescence yield (F), effective PSII quantum yield (YII), coefficient of non-photochemical quenching (qN), coefficient of photochemical quenching (qP), non-photochemical quenching (NPQ) and electron transport rate (ETR).

Variables	Growth inh.	ROS	F	YII	qN	qP	NPQ	ETR
Growth inh.	1	0.890*	-0.960*	-0.867*	0.829*	-0.864*	0.809*	-0.865*
ROS	0.890*	1	-0.915*	-0.979*	0.927*	-0.953*	0.896*	-0.979*
F	-0.960*	-0.915*	1	0.916*	-0.935*	0.930*	-0.922*	0.915*
YII	-0.867*	-0.979*	0.916*	1	-0.953*	0.983*	-0.928*	1.000*
qN	0.829*	0.927*	-0.935*	-0.953*	1	-0.980*	0.995*	-0.953*
qP	-0.864*	-0.953*	0.930*	0.983*	-0.980*	1	-0.972*	0.982*
NPQ	0.809*	0.896*	-0.922*	-0.928*	0.995*	-0.972*	1	-0.927*
ETR	-0.865*	-0.979*	0.915*	1.000*	-0.953*	0.982*	-0.927*	1

Table 3.7. Pearson correlation matrix obtained from effect endpoints measured in *Tetraselmis suecica* after seven days of zinc exposure. * Values indicate significant differences. Growth inhibition (Growth inh.), reactive oxygen species (ROS), relative fluorescence yield (F), effective PSII quantum yield (YII), coefficient of non-photochemical quenching (qN), coefficient of photochemical quenching (qP), non-photochemical quenching (NPQ) and electron transport rate (ETR).

Variables	Growth inh.	ROS	F	YII	qN	qP	NPQ	ETR
Growth inh.	1	0.705	-0.488	-0.519	-0.557	-0.578	-0.605	-0.515
ROS	0.705	1	-0.889*	-0.851*	-0.781*	-0.924*	-0.806*	-0.850*
F	-0.488	-0.889*	1	0.958*	0.645	0.980*	0.691	0.957*
YII	-0.519	-0.851*	0.958*	1	0.473	0.978*	0.528	1.000*
qN	-0.557	-0.781*	0.645	0.473	1	0.647	0.995*	0.468
qP	-0.578	-0.924*	0.980*	0.978*	0.647	1	0.692	0.976
NPQ	-0.605	-0.806*	0.691	0.528	0.995*	0.692	1	0.523
ETR	-0.515	-0.850*	0.957*	1.000*	0.468	0.976*	0.523	1

3.4 Discussion

Metal uptake and toxicity has been well-documented in marine microalgae, with well-characterised modes of action and toxicity; although metal mixtures and their interactions are still being understood. This chapter aimed to improve understanding of toxicity mechanisms for copper-nickel-zinc mixtures on *Tetraselmis suecica* by assessing photosynthesis and ROS formation. Using fluorescence endpoints measured in this chapter and previously published effects of metals on microalgae, a data- and literature-informed tentative toxicity pathway network for exposure to copper, nickel and zinc was proposed (Figure 3.21). In figure 3.21, the effects are organised following metal uptake causing an initial molecular event (ROS formation) to an adverse outcome (growth inhibition). Organising effect data enables the derivation of a toxicity pathway to better characterise how adverse outcomes happen, specifically when understanding the mechanistic toxicity from a mixture.

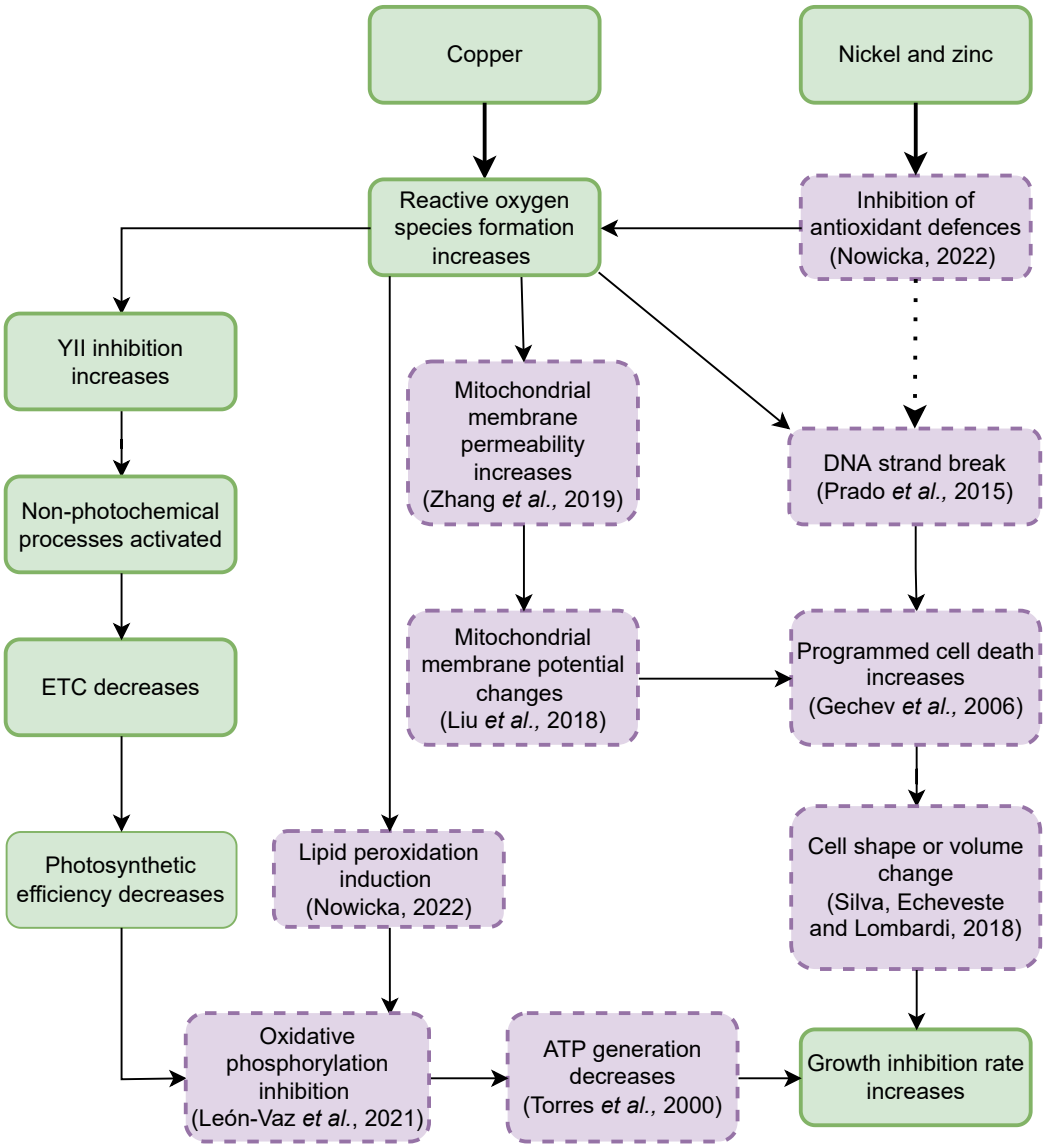

Figure 3.21. Tentative toxicity pathway network for the exposure of copper, nickel, and zinc to the marine microalgae *Tetraselmis suecica*. The molecular initiating event is reactive oxygen species formation, and a series of key events are proposed that lead to growth inhibition. The green boxes (solid edges) are measured endpoints from this chapter and the purple boxes (dotted edges) are informed steps from published literature for microalgae species exposed to metals (Torres *et al.*, 2000; Gechev *et al.*, 2006; Prado *et al.*, 2015; Liu *et al.*, 2018; Silva, Echeveste and Lombardi, 2018; Zhang *et al.*, 2019; León-Vaz *et al.*, 2021; Nowicka, 2022). Dotted lines represent points in the pathway where there are other steps occurring that do not fit into the scope of this pathway.

Figure 3.21 indicates how the metals could be causing toxicity following exposure and uptake. These metals can be taken up and sequestered in the cell wall or inside the cell to immobilse the metals, causing metal concentrations in the media to decrease (Wang *et al.*, 2021). All metal concentrations decreased over the seven-day period, with significantly different mixture concentrations at every concentration assayed. It is important to measure the metal concentrations at the end of an

experiment to quantify concentration changes. The combined metal concentrations changed more than the single metals, indicating that metal interactions are occuring either within the medium or at the uptake sites. Competitive interactions between copper and zinc were found in another study using *T. suecica* (Kumar and Shin, 2017). In Kumar and Shin (2017), the relationship between copper and zinc concentrations was complex, with low copper concentrations increasing extracellular zinc uptake, yet zinc uptake decreased when copper concentrations were increased. This suggests that both metals are competing at the same uptake site(s), with zinc being competitively inhibited by copper; although the highest copper concentrations did allow increased intracellularly zinc uptake. Similar findings were reported by Franklin *et al.* (2002b), as copper inhibited zinc uptake from copper and zinc mixtures. According to Expósito *et al.* (2017), the essential metal transporters of copper and zinc can be used by nickel and other non-essential metals to enter the cell. This adds more competition to the same uptake site(s).

Metal fractionation or speciation analysis could have been conducted to better understand if any interactions were occuring in the exposure solutions by detecting any shifts in metal fractions or species when metals interact. As reported in Franklin *et al.* (2002a), toxicity reduced following copper depletion. Further, cell burden data could provide information on intracellular and extracellular uptake. These interactions would increase the understanding of the toxicity pathway presented in figure 3.21 (Gillmore *et al.*, 2016).

Copper was found to be the main ROS generating metal, both as a single metal and within the three-metal mixtures. As shown in figure 3.21, copper is the only metal capable of directly causing ROS formation. This pattern remained when copper was a component of a mixture, suggesting that ROS generation following mixture exposure is driven by the copper in the mixture rather than by the mixture as a whole. However, the mixture ROS measurements were lower than single copper measurements. Copper is well established as a ROS generating metal. For example, Melegari *et al.* (2013) observed a near 200% relative increase in reactive species in *Chlamydomonas reinhardtii* in response to 100 mg L^{-1} of copper oxide in light and dark exposure conditions. For nickel, ROS production was 37 times higher than the controls in *Chlorella vulgaris* after a four-day exposure to 10 mg L^{-1} of nickel nanoparticles (Oukarroum *et al.*, 2017). Zinc at 100 mg L^{-1} did not generate ROS in *C. reinhardtii* (Gunawan *et al.*, 2013), but did so in *Chlorella vulgaris* when in a

mixture with mercury (Ajitha *et al.*, 2021) albeit at lower levels than the combined value of both metals. Overall, ROS formation is an important mode of action for combined metal toxicity by creating an oxidative imbalance that triggers further effects.

Increased ROS in the chloroplasts can cause partial or total photoinhibition, as shown by an increase in YII inhibition. There were similar trends in chlorophyll fluorescence parameters for copper, nickel, and mixtures, suggesting that the light harvesting capacity of PSII was downregulated during metal exposure, except for nickel. Zinc exposure did not affect F_v/F_m, indicating that the alga's PSII photosynthetic capacity was impacted by copper and nickel yet remained intact for nickel. Similarly to copper and nickel, chromium exposure to *Scenedesmus obliquus* observed a decline in F_v/F_m values after two days (Khalida *et al.*, 2012). Unlike these F_v/F_m responses, zinc did decrease YII. Photoinhibition means that the natural cycle of rapid repair is lost, wherein D1 proteins are repaired throughout light exposure and allow reaction centres to be activated (Holzinger and Karsten, 2013). The physiological significance of photoinhibition is that photosynthetic capacity is reduced.

In addition, a reduction in YII triggered an increase in non-photochemical quenching processes (qN and NPQ) for all single metals. This trend was not seen for the mixtures, with qN and NPQ slightly increasing with increasing zinc and nickel concentration. Surprisingly, copper decreased non-photochemical quenching processes. As NPQ represents energy not being used in primary photochemistry, an increase shows that metal exposure stimulated the algae to dissipate excess light energy as heat. This is an evolved mechanism to protect the photosynthetic apparatus from oxidative damage (Niyogi, 1999). Therefore, the decrease measured when only taking copper into account from the three-metal mixtures suggests that the algae cannot dissipate the excess light energy. Exposure of *C. reinhardtii* to single copper produced a biphasic response with increased NPQ at low concentrations (between 1 – 1.5 µg L^{-1} log concentration) but decreasing at higher concentrations (above 1.5 µg L^{-1} log concentration) after four days (Juneau, El Berdey and Popovic, 2002). This suggests that *C. reinhardtii* can only dissipate energy up to a certain threshold concentration. However, there was a concentration dependent increase in NPQ in *Selenastrum capricornutum* from the same study, supporting the *T. suecica* copper responses in this chapter.

The parameter qP relates to the approximate amount of open PSII reaction centres. In this chapter, the number of open PSII reaction centres decreased as PAR increased for all single metals and mixtures. The literature provided similar evidence to these measured responses. Juneau, El Berdey and Popovic (2002) found *C. reinhardtii* and *S. capricornutum* had similar concentration dependent decreases in qP. In contrast, lead exposure in *Chlorella* sp. and *Scenedesmus* sp. did not significantly impact the proportion of open PSII reaction centres (Dao and Beardall, 2016).

ETR indicates the electron flow rate through the photosynthetic electron transport chain. There were increases in ETR for all metals except for the highest copper and nickel concentrations. Copper and zinc exposed algae continued to obtain ETR values similar to controls, with only the two highest concentrations experiencing a decreased rate. However, most of the nickel concentrations resulted in lower ETR values and the mixtures showed a biphasic response. Overall, the disruption of metals in the electron transport chain seems limited to higher metal concentrations. In *Monoraphidium convolutum*, a short two-hour chromium exposure observed a significant increase in ETR and YII when concentrations were above 1 mg L^{-1}, yet ETR and YII decreased when exposed for longer (two to three days) (Takami *et al.*, 2012). Following 1ppm and 10ppm chromium exposure, *S. obliquus* noted a decrease in Fv'/Fm', which is a measurement that indicates electron transfer between PSII and PSI and showed impaired electron transfer.

Zinc had the greatest impact on cell density, followed by nickel, then copper. Despite having the highest EC_{50} value for cell density, copper had the highest growth inhibition percentages when compared to the controls. In this chapter, cell density, growth rates and percentage growth inhibition were calculated to determine whether there were differences in metal sensitivity. Copper and zinc (both essential metals) were the more toxic to *T. suecica* compared to nickel (non-essential). Microalgae, like other organisms, have evolved to select essential metals and exclude non-essential metals, at the same time as keeping essential metal ion homeostasis (Perales-Vela, Peña-Castro and Cañizares-Villanueva, 2006; Cobbett and Goldsbrough, 2002). One feature of their evolutionary mechanisms uses polymeric materials to scavenge essential metals (Rath, 2011). This could help to explain why essential metals are more toxic than non-essential metals if they are scavenging essential metals in an anthropogenically contaminated environment.

Further, copper was the only metal that was a significant main effect driver within the mixtures for cell density, growth rate and percentage growth inhibition. This is a shift in sensitivity from single exposure to mixture exposure for cell density, but growth rates and growth inhibition remained most impacted by copper. Similar growth rate patterns were noted for *Nitzschia closterium* and *Chlorella* sp., with both exhibiting greater sensitivity for copper than zinc (Johnson *et al.*, 2007). Kumar and Shin (2017) also measured multiple growth parameters in *T. suecica*, reporting that copper was the most sensitive to growth rate, cell division day^{-1} and cell density, rather than zinc or iron. However, there was no effect on growth inhibition when *T. suecica* was exposed to 100 mg L^{-1} of zinc nanoparticles (Castro-Bugallo *et al.*, 2014), although both *Phaeodactylum tricornutum* and *Alexandrium minutum* experienced 80% growth inhibition. Franklin *et al.* (2002b) found that mixtures of copper and zinc had antagonistic interactions on growth in *Chlorella* sp., but that a mixture of copper and cadmium had synergistic interactions because of high copper bound to the cell wall. These responses suggest that copper is an important metal in these binary mixtures, with copper having control over the interactions occurring.

Often growth inhibition is reported as being proportional to the extracellular metal concentration; however, Kumar and Shin (2017) reported that both intracellular and extracellular copper exposures were proportional to growth inhibition for *T. suecica* as internal copper was causing toxicity. This was supported by Franklin *et al.* (2002b), who found that 60% (of a 10 mg L^{-1} copper exposure) was measured intracellularly and 40% extracellularly in *Chlorella* sp., concluding that the proportion of copper that was bound to the cell wall corresponded to copper uptake and toxicity. However, in the same study, zinc toxicity was related to extracellular concentration only. To summarise, the growth parameters inferred that *T. suecica* is unable to effectively respond to and handle stress from increasing concentrations of copper, nickel, and zinc.

The DSD concentrations were based on nominal single concentrations, which resulted in a good range of copper and zinc concentrations in the mixture design. However, nickel had a limited concentration range in the mixture design, including only relatively high concentrations which may have impacted outcomes; more responses might have been shown if the least forcing nickel concentrations were lower. The DSD approach provided information about interactions occurring in multiple parts of the algal cell and along multiple steps of the toxicity pathway. The

combined use of this mixture design and PAM fluorometry enabled much data to be collected whilst identifying main effect drivers and interactions when present in multiple PSII parameters. The use of DSD for the mixture design was successful at evaluating effects of combined metal exposure in *T. suecica*. This suggests that *T. suecica* is a good candidate for further cumulative hazard assessments. Further, the DSD approach can be used to suggest where future research should be focused on the identified main effect drivers and interactions to better inform risk assessments. In this case, the interactions between copper and nickel, and copper and zinc were identified as significant and should be better understood at the mechanistic level.

3.5 Conclusion

The responses observed in this chapter were in line with known MoA for copper, nickel, and zinc. Metal concentration changes highlighted the ability of microalgae to be flexible within a changing environment, exerting some degree of control on uptake mechanisms. However, metal interactions in the exposure solutions or at the uptake sites could be occurring and may be responsible for limiting mixture toxicity in some cases, for example between copper and zinc. Metal exposure did affect photochemistry in algal photosynthesis, with copper having the greatest impact. The molecular initiating event used was ROS formation, which increased for all metals and mixtures, suggesting a similar MoA is retained when these metals are combined; although the mixtures seemed to be interacting in an antagonistic manner when compared to the single ROS responses. Increased non-photochemical quenching highlights a potential protective mechanism to avoid oxidative damage by dissipating excess light as waste heat. However, this was not the same for the mixtures, with a similar non-photochemical quenching regardless of mixture concentration suggesting more oxidative damage than single exposures. The consequential algae growth inhibition and therefore adverse effects at the population level showed that algae are very sensitive to essential metals. Further information is required to fully characterise toxicity; however, the developed toolbox allowed the toxicity responses to be organised into a tentative toxicity pathway. The responses of fluorometer parameters showed the complexity of understanding how metal exposure impacts PSII and photosynthesis capacity, and that more targeted endpoints related to PSII and PSI are required to fully capture the toxicity pathway. Finally, the lack of mixture studies including these targeted endpoints for comparisons highlights the data gap in the current literature.

Chapter 4. Effects of single trace metals on *Tisbe battagliai*

4.1 Introduction

Metals are among the most well studied contaminants in marine and aquatic environments (Macken *et al.*, 2009; Tchounwou *et al.*, 2012). Although naturally occurring in the Earth's crust, most metal contamination results from anthropogenic activities. With rising metal inputs from ever increasing coastal economic and industrial development (increasing terrestrial run-off), the risk of metals to coastal ecosystems and food webs is also rising (Pan and Wang, 2012; Jeong *et al.*, 2019). Once metals have entered the environment, they are environmentally persistent and may bioaccumulate along food webs (Tao *et al.*, 2021; Ali, Khan and Ilahi, 2019a). While low concentrations of many metals are essential for the survival, growth, and reproduction of all living organisms, they become toxic when present at higher concentrations. Both copper and zinc are required for the functioning of enzyme activities in crustaceans, such as copepods, with copper being largely involved in metabolism after being converted into oxidised and reduced states as catalytic cofactors (Nogueira, Lombardi and Nogueira, 2012). According to Rainbow and Luoma (2011) estimations of concentrations of zinc and copper required for enzyme activities are 35 µg/g and 15.2 µg/g dry body weight respectively for crustaceans.

Metal toxicity in seawater is influenced by metal speciation – the distribution of an element amongst physico-chemical species in a system – and fractionation, which impacts their uptake, bioavailability, and biological effects (Olaniran, Balgobind and Pillay, 2013; Magalhaes *et al.*, 2015). Understanding the distribution of metals amongst size fractions provides necessary information for fate, bioavailability and, in turn, biological effects (Town and Filella, 2002). Commonly, most hazard and exposure assessments are categorised into different research areas and between research organisations. Soil, sediment, freshwater, and marine risk assessments are usually carried out independently of each other. Additionally, exposure and effect assessments are conducted individually within these areas, often by different research disciplines (e.g., chemistry, biology or ecotoxicology) with different scientific terminology and places to communicate their findings (Tan *et al.*, 2018). As chemical effects are heavily influenced and depend on exposure factors, this separation leaves many gaps in our understanding of toxicity. Therefore, collecting fractionation data

alongside biological responses can help understand metal toxicity, as well as to inform interpretations of possible interactions with other environmental stressors (i.e., other metals and chemicals) or fluctuating environmental factors (i.e., salinity, pH, and temperature). Whilst a lot is known about metals as general marine contaminants and their mechanisms of toxicity, the sensitivity of these responses within copepods are less known. Therefore, this chapter focuses on toxicity characterisation of metals in the copepod *Tisbe battagliai* to help fulfil this knowledge gap.

4.1.1 Metal exposure in coastal environments

Metals in seawater can exist in dissolved and particulate phases (Macken *et al.*, 2009). The dissolved phase consists of the colloidal fraction and low molecular mass fraction (LMM). Thus, metals can be present as particles, colloids and LMM fractions in seawater; particles are most often larger than 0.45 µm, while colloid exists in the size fraction of 1kDa – 0.45 µm and LMM fraction smaller than 1 kDa (Salbu, 2009).

Coastal environments have complex metal exposure due to the meeting and mixing of seawater with estuarine and/or freshwater. Estuarine environments are typically characterised by the low ionic strength freshwater mixing with high ionic strength seawater (Mosley and Liss, 2019). Freshwater transports particles and colloids into estuarine and coastal waters, which then experience increased aggregation due to the presence of higher ionic strength seawater. This results in high sedimentation of particles and associated metals in estuaries and coastal environments. However, metals associated with colloids and particles transported in freshwater can be remobilised in estuaries or coastal waters due to ion exchange processes, which increases the free metal ion concentration (Teien, Standring and Salbu, 2006). Additionally, the high pH and concentration of carbonates in the seawater can influence metal speciation and fractionation. This means that metal concentrations are usually highest in sediments in coastal environments (Tao *et al.*, 2021). However, there is an equilibrium between the sediments and seawater, which can be disrupted and cause metals to partition back into the seawater (Tao *et al.*, 2021; Ali, Khan and Ilahi, 2019a).

Metals associated with marine organisms can be present on the surface by adsorption or taken up internally within cells (body burden). Uptake of metals is often using an active uptake pathway for essential metals, for example ion channels into

cells. For fish, the gills are an important tissue for ion regulation and mitochondria rich cells actively uptake ions from the passing water, including metals (Evans, 1987). Additionally, metal uptake can occur via the diet, with metals associated with algae able to be bioaccumulated. Therefore, the positively charged LMM fraction is considered to be the most bioavailable metal fraction to organisms (Gagnon and Vigneault, 2013). However, the impact of different metal fractions on bioavailability is disputed in the literature (Town and Filella, 2002). For copepods, the uptake of trace metals can occur via adsorption onto their exoskeleton (positively charged metal ions are attracted to negatively charged surface) and absorption via their permeable surfaces used in respiration for small fractions, and larger particles can be ingested via their feeding mechanisms – e.g., filter and suspension feeding (Wang and Fisher, 1999; Kadiene *et al.*, 2019; Rainbow, 2018a). Which fractions are assumed to be driving toxicity and observed effects has been widely discussed in the literature, concluding that for most aquatic organisms the LMM fraction is bioavailable and responsible for the effects.

4.1.2 Metal toxicity

Metal-induced responses in aquatic organisms include: (1) exposure effects such as reactive oxygen species (ROS) generation, (2) detoxification responses including antioxidant enzymes and antioxidant production, (3) toxicity responses – the induction of oxidative stress, DNA damage and repair and apoptosis, and (4) adverse effects at the individual level with mortality, impaired reproduction and development, and growth. Toxicity pathways can be induced by trace metals capacity for catalysing oxidative reactions, resulting in ROS production causing oxidative stress (Barata *et al.*, 2005). A well-established metal-induced pathway has been previously published, beginning with reactive oxygen species (ROS) generation (Balali-Mood *et al.*, 2021; Rhee *et al.*, 2013a; Jeong *et al.*, 2019), leading to oxidative DNA damage (Pavlaki *et al.*, 2016b; Goswami *et al.*, 2014) and apoptosis (Morcillo, Esteban and Cuesta, 2016; Tollefsen *et al.*, 2017), resulting in reduced survival (Diz *et al.*, 2009; Sunda, Tester and Huntsman, 1987; Kadiene *et al.*, 2017).

Trace metals such copper and iron can facilitate the Haber-Weiss and Fenton reactions, which converts a superoxide anion to a highly reactive hydroxyl radical. If radicals cannot be removed or the production process inhibited, the antioxidant balance in the cell will be disrupted and overwhelmed with radicals, leading to

oxidative stress and cellular damage (Valavanidis *et al.*, 2006). Such cellular insults can be captured by looking at relative gene expression changes using real time qPCR, changes in enzyme activity and by measuring ROS production in the cell (cellular probes are broken down by ROS into a fluorescent product that can be measured). For this chapter, both real time qPCR and ROS production were chosen as tools to measure oxidative stress. Without sufficient defence and removal systems in place, ROS generated from metals exposure can attack DNA, lipids, and proteins, commonly resulting in apoptosis and genotoxicity. Apoptosis can cause cell shrinkage resulting in DNA fragmentation and the formation of apoptotic bodies with condensed DNA (Buttino *et al.*, 2011). The apoptotic cell and organelles within can be functional, although negatively impacted, and often leading to adverse outcomes at the individual level. Apoptosis can be measured directly using a TUNEL assay, or effects can be predicted by looking at related genes, both of which were measured in this chapter. Alongside direct and indirect apoptosis measurements, ROS-induced DNA damage can be measured in multiple direct and indirect ways, including the presence of 8-oxo-dG products and relevant gene expression changes over time, and changing concentrations. When oxidative modifications of DNA occur, the 8-oxo-dG product is the most representative product of these modifications.

Following on from chapter 2.1.2, antioxidant and DNA repair proteins are vital in the defence and repair of ROS, DNA damage and cellular death. The gene catalase (CAT) encodes for an endogenous antioxidant enzyme that scavenges hydrogen peroxide, breaking it down into oxygen and water, whereas GPX2 reduces lipid hydroperoxides into alcohols (Zhuang *et al.*, 2017; Song *et al.*, 2020a), thus neutralising the negative effects of ROS. For DNA repair proteins, RAD50 codes for double strand break repair, while RAD23 is more specific to UV excision repair (Song *et al.*, 2020a). The ATM serine/threonine kinase gene can also aid in DNA damage repair and ROS regulation, alongside controlling cell cycles and division rates (Venkataraman, White and Roberts, 2022). Further, genes for glucocorticoid receptors (GR) are signalling pathway genes, which can be involved in gene expression and can help regulate many cellular processes including cell metabolism and apoptosis (Bailey *et al.*, 2017). Other genes related to apoptosis include CASP3, which encodes for cysteine proteases that has a central role in the execution of apoptosis when calpain triggers the mitochondrial dependent caspase pathway (Wei *et al.*, 2022), and the gene BAX encodes for apoptosis regulation, potentially having

a central role in the bridging of active caspase with the mitochondria, influencing mitochondrial permeability and caspase-9 activation (Miguel *et al.*, 2007).

4.1.3 Aims and objectives

Following on from Chapter 3, toxicity characterisation is missing for many marine and aquatic copepods. Therefore, the two main aims of this chapter are: (1) to complete a toxicity characterisation for copper, nickel, and zinc to the marine copepod *T. battagliai*, focusing on the most established metal-induced toxicity pathway at different levels of biological organisation; and (2) to measure metal fractions to better inform bioavailability.

T. battagliai is used as a model species, as it is a well-documented species in metal ecotoxicological studies and is a recommended acute toxicity standard species in the ISO 14669 (ISO, 1999), yet the mechanistic understanding of metal toxicity is missing. This temperate harpacticoid copepod inhabits shallow coastal environments and lives at the sediment-seawater interface, meaning that both coastal seawater and sediment could be possible exposure routes (Battaglia and Volkmann-Rocco, 1973; Drira *et al.*, 2018). Further, *T. battagliai* with its relatively short life cycle is easy to culture and use in laboratory experiments, requiring minimal space and equipment.

4.2 Materials and Methods

4.2.1 Tisbe battagliai *cultures*

Tisbe battagliai stock cultures obtained from Guernsey Sea Farms (Guernsey, UK) were maintained in line with international standard protocol (ISO, 1999) in filtered (0.22 µm Durapore® filters, Merck, Germany) artificial seawater (ASW) (Tropic Marin Pro Reef Salt) at 19 ± 1 °C, 30 ± 1 ppt salinity (ATC refractometer), pH 8.2 ± 0.2 (SevenExcellence™, Mettler Toledo, OH), under a 16h light: 8h dark photoperiod. The cultures were fed *ad libidum* with a mixed diet of *Isochrysis galbana* and *Tetraselmis suecica* (1:3). Newly gravid females (14 ± 2 days old) and juveniles (6 ± 2 days old) were used in survival tests, and only gravid females were used in all other tests, with five replicates where possible (minimum triplicate). Each replicate contained five individuals in 5mL of exposure medium. All experiments were conducted up to 48 hours, with data collected after 12, 24 and 48 hours depending on the assay. Six and 14 days before juveniles and adults were needed for experiments, stock *T. battagliai* cultures were filtered through a series of meshes to

separate adults (180 – 250 µm), juveniles (100 – 180 µm) and nauplii (40 – 100 µm) that had been released within the previous 24 hours. These nauplii were cultured in a separate beaker to other stock cultures and were used after six or 14 days.

In this study, copper chloride ($CuCl_2$, 99% Sigma-Aldrich, CAS number 7447-39-4), nickel chloride ($NiCl_2$, ≤98% Sigma-Aldrich, CAS number 7791-20-0) and zinc chloride ($ZnCl_2$, ≤98% Fisher Scientific, CAS number 7646-85-7) were used. Chlorides were chosen as the exposure media was ASW, to ensure that another element was not being added to the experiment. Metal stock solutions were made up prior to the experiments in ASW at 30 ppt and stored for up to two weeks in glass Duran® bottles at 4°C. The stock concentrations were 0.05 mM for copper, 0.5 mM for nickel and 0.05 mM for zinc. ASW to be used in experiments was aerated for 24 hours to oxygenate prior to adding metals. Working metal concentrations were made up in ASW 24 hours before the experiment. Range finding tests were conducted first and aimed to cover survival responses from no effect to 100% mortality to produce a concentration response curve for survival after exposure to each metal. Capturing the full range of mortality is important to be able to plot this curve and calculate lethal concentrations (LC_x) values from the slope values. Concentrations within these ranges were used for all biological assays (Table 4.1) and are shown in each assays sub-heading.

Table 4.1. Effects toolbox developed for 14-day old gravid *Tisbe battagliai* exposed to metals. OCED = Organisation for Economic Co-operation and Development.

Category	Method	Endpoint	Sampling
Whole-organism toxicity test	Standard OECD toxicity tests	Survival, reproduction	In situ
Metal analysis	Inductively Coupled Plasma Mass Spectrometry (ICP-MS)	Total metal concentration	In situ
	Metal fractionation	Metal fraction concentrations	In situ
Targeted assay	Real time qPCR	Biomarker gene expression	RNAlater→-80 °C
	H_2DCFDA assay	Cellular ROS formation	In situ
	TUNEL assay	Apoptosis	In situ
	8-oxo-dG assay	Oxidative DNA damage	Flash freeze→-20 °C

Water samples were taken at the beginning (0 hour) and end of each survival experiment (48 hours) to determine total metal concentration. Samples for nickel and zinc survival exposures were measured on an 8900-triple quadrupole inductive coupled plasma mass spectrometry (ICP-MS) (Agilent, Santa Clara, CA, USA) at the isotope lab at the Norwegian University of Life Sciences (NMBU) by fellow MixRisk PhD Candidate Emil Jarosz. Samples for copper were analysed twice, at first by NMBU but there were issues with the concentrations; therefore, the copper exposure was conducted again, and new samples from a survival experiment were measured at Newcastle University by Dr Shannon Flynn. Analysis at Newcastle University was performed using an Agilent 7500 ICP-MS, with a micromist nebuliser, a cooled double concentric spray chamber and nickel cones. Throughout analysis drift was monitored and corrected for using a 100 ppb indium solution that used a T-junction inline internal standard kit to add indium into each sample. Helium gas in a collision gas reaction cell was used to remove polyatomic interferences.

4.2.2 Characterisation of metal fractionation

One litre of each test solution (30 ppt ASW) for each metal was made and left for 24 hours before water fractionation was conducted, without *T. battagliai* individuals. The three test solutions chosen were 0.21, 0.91 and 1.54 µM for copper, 1.89, 3.78 and

5.74 µM for zinc and 10.06, 38.71 and 67.07 µM for nickel. Four different types of samples (described below) were taken in triplicate and were prepared and measured following the same procedure using an Inductively Coupled Plasma Mass Spectrometry (ICP-MS); (1) unfiltered sample (total concentration), (2) 0.45 µM filtered sample (excludes particles), (3) <10kDa filtered sample using a hollow fibre ultrafilter filter of 10 kDa (excludes colloids), and (4) ion exchange column with Chelex resin (binds ions).

To determine total metal concentration, samples were taken by pipetting 1 mL of the 1 L test solution into 15 mL Sarstedt tubes. For particle exclusion, 7 mL of the test solution was taken using a new 15 mL syringe before filtered using a 0.45 µM filter attached to the syringe. The first 2 mL of the test solution was pushed through to wash the filter membrane and the remaining 5 mL was filtered through and collected. One millilitre was added to an individual 15 mL Sarstedt tube per replicate for particle analysis. Once the samples were analysed by ICP-MS, the concentration of particles analysed was calculated based on the measured concentration in unfiltered sample subtracted from the 0.45 µm filtered fraction, using the following equation:

$$Particle\ concentration = total\ unfiltered\ concentration - 0.45\ \mu m\ filtered\ concentration$$

For the exclusion of small colloids, a hollow fibre filter with a 10kDa Microza Hollow-Fibre Ultrafiltration Modules (130 mm, polysulfone membrane, Pall Corporation, USA) was used. The ultrafilter was cleaned before and after the filtration of solutions containing different metals, using 0.01 M NaOH, EDTA solution (3 g L^{-1}), 0.01 M HNO_3 and Milli-Q® water for 30 minutes each. A peristaltic pump forced the water at 0.6 L min^{-1}. Each test solution was pumped through the ultrafilter, with the first ~300 mL discarded and the remaining ~700 mL recirculated through the filter system for 10 minutes. One hundred millilitres of ultrafiltered test solution were collected containing molecules no larger than 10 kDa (~5 nm). One millilitre of ultrafiltrate was added to one 15 mL Sarstedt tube for LMM sample analysis. The LMM fraction concentration is equal to the <10kDa hollow fibre concentration. The colloidal fraction was calculated by subtracting the concentration in the LMM fraction from the concentration in the 0.45 µM filtered, with the following equation:

$$Colloid\ concentration = 0.45\ \mu m\ filtered\ concentration - < 10\ kDa\ hollow\ fibre\ concentration$$

The remaining 97 mL of the hollow fibre filtered test solution was filtered through an ion exchange column filled with Chelex® 100 resin to retain charged species (50-100 mesh, sodium form, Bio-Rad Laboratories Inc., USA). Before use, the resin was cleaned with 50 mL of Milli-Q® water and 50 mL of uncontaminated ASW. Afterwards, 70 mL of solution was pumped through the column and triplicate 1 mL samples were collected into 15 mL Sarstedt tubes. The Chelex resin retains any positively charged LMM metal species; therefore, the eluate from the Chelex resin should contain not reactive and non-positively charged species. Blank samples of ASW without any metals added were taken before each metal solution was pumped through the hollow fibre and ion exchange column to account for any metal presence from these systems or already in the seawater.

The sample preparation before ICP-MS analysis included adding 1 mL ultrapure nitric acid (70%), diluting samples to 10 mL with ultrapure water (Milli-Q®) and adding 200 µL of 100 µg L^{-1} rhodium and indium as internal standards was added to each sample tube. Samples were analysed on an 8900-triple quadrupole ICP-MS at the isotope lab at NMBU by Emil Jarosz. Analysed certified reference materials (CRM) indicated good accuracy for all analyses conducted by ICP-MS (NIST SRM 1640a and RTC QCI-3034-1, Sigma-Aldrich, Germany).

4.2.3 Acute toxicity test - Survival

Survival of gravid females and juveniles was determined using a copepod immobility assay (ISO, 1999). Immobility was defined as no swimming movement following a single contact event with a pipette tip and no movement after 10 seconds. For the gravid female survival tests, the measured concentrations used were 0.14, 0.17, 0.34, 0.78, 1.00, 1.22, 1.92, 4.60 and 6.65 µM for copper, 0.36, 0.62, 1.44, 2.79, 5.50 and 8.06 µM for zinc and 1.87, 3.82, 18.53, 41.15, 58.83 and 78.21 µM for nickel. For the juvenile survival tests, the measured concentrations used were 0.06, 0.12, 0.29, 0.45, 0.59, 0.73, 0.88, 1.03, 1.17, 1.50, 1.77, 2.36 and 2.93 µM for copper, 0.10, 0.18, 0.37, 0.70, 1.80, 3.70, 7.30 and 11.0 µM for zinc and 0.21, 0.42, 2.10, 4.21, 8.42, 21.04, 31.55, 42.09 and 63.13 µM for nickel.

4.2.4 Reactive Oxygen Species formation

Intracellular ROS formation was determined in situ following metal exposure using the probe 2'7'-dichlorodihydrofluorescein diacetate (H_2DCFDA, Invitrogen, Molecular

Probes Inc., Eugene, OR, USA), originally described for aquatic copepods by Xie *et al.* (2007). As seen in chapter 3.2.7, H_2DCFDA is cleaved by the enzyme esterase and oxidised by ROS, resulting with a fluorescent product DCF (Rhee *et al.*, 2013a). To optimise this assay for *T. battagliai*, the probe concentration was reduced, and the probe incubation and uptake time was increased to consider the cuticle and higher complexity of an individual copepod compared to an algal cell culture. Additionally, the volume of ASW in each well was reduced from 180 µL to 45 µL to ensure the individual copepod was at the base of the well, as fluorescence measurements were taken from the bottom of the plate.

The measured concentrations used were 0.14, 0.78, 1.22, 1.92 and 4.60 µM for copper exposure, 0.2, 0.36, 0.62, 2.79 and 5.50 µM for zinc exposure and 0.15, 1.87, 3.82, 18.33 and 41.15 µM for nickel exposure. A stock solution of H_2DCFDA (5 mM) was diluted to a working solution of 5 µM in ASW in darkness, of which 5 µL was added to 45 µL of ASW in each well, with a final concentration of 0.5 µM. A surviving individual copepod per replicate was sampled after 24 and 48 hours of exposure, washed with ASW and pipetted into a black, clear bottom 96-well microplate (Corning Costar). The samples were immediately analysed using a Fluostar Optima plate reader (BMG Labtech, Ortenberg, Germany) at emission wavelength 535 nm and excitation wavelength 485 nm over two hours, to allow the probe to be taken up (probe uptake times were determined in a preliminary experiment). The microplate was covered in aluminium foil to protect from light between measurements. In addition to exposed samples, the background natural fluorescence of ASW containing the same concentration of probe and only ASW were measured. The relative fluorescence for each irradiance at each time point was expressed as fold change normalised to the control. Each replicate was normalised to individual copepod length (as a proxy for biomass), measured under an inverted fluorescence DMi8 microscope (Leica, Wetzlar, Germany) (x40 mag).

4.2.5 DNA extraction

Twenty gravid female *T. battagliai* were pooled per replicate and frozen immediately in liquid nitrogen and stored at -20 °C until DNA extraction. The measured concentrations used were 0.78, 1.22, 1.92, 4.60 and 6.65 µM for copper exposure, 2.79, 3.60, 5.50, 7.30 and 8.06 µM for zinc exposure and 3.82, 18.33, 41.15, 58.83 and 78.21 µM for nickel exposure. Total DNA was isolated using the Quick-DNA™

Tissue/Insect Microprep Kit (Zymo Research Corporation, Irvine, CA, USA) according to the manufacturer's protocol with some adaptions. During the first step, the number of beads in the ZR BashingBead™ Lysis Tube were reduced to 10 beads and the volume of BashingBead™ Buffer added to these tubes was reduced to 250 µL to account for the low starting material of 20 individuals (copepod tissue). After the bead bashing steps, 200 µL of supernatant was added to the Zymo-Spin III-F Filter and centrifuged for one minute at 8,000 x *g*. Six hundred microlitres of Genomic Lysis Buffer was added to the filtrate in the collection tube and mixed well. Beta-mercaptoethanol was not added to the Genomic Lysis Buffer due to an unsuitable chemical fume cupboard within which to perform DNA extractions. The remaining steps were followed according to the manufacturer's protocol, eluting the DNA from the column matrix using 20 µL of DNA Elution Buffer via centrifugation at 10,000 x *g*. The eluted DNA was frozen at -20 °C until further downstream analysis.

4.2.6 Oxidative DNA damage quantification

Oxidative DNA damage was quantified using the EpiQuik™ 8-oxo-dG DNA Damage Quantification Direct Kit (Fluorometric) (Epigentek Group Inc., Farmingdale, NY, USA) according to the manufacturer's protocol with only a little method development required. 8-oxo-dG (8-hydroxy-2'deoxyguanosine) is an oxidised derivative of deoxyguanosine (from the C8 of the imidazole ring of deoxyguanosine (dG)), generated from ROS in cellular DNA (Giorgio *et al.*, 2020). This assay binds extracted DNA to a 96-well plate, with a high affinity for DNA. Each well is incubated with capture and detection antibodies specific for 8-oxo-dG. Following this, the signal is enhanced to be quantified fluorometrically using a fluorescence plate reader. This kit was chosen as it is one of the fastest 8-oxo-dG detection kits available, when compared to liquid chromatography mass spectrometry approaches. Additionally, the starting amount of DNA was low, which was useful when pooling individuals to be able to extract enough DNA from *T. battagliai*, due to their small size.

Isolated gravid female DNA was diluted to 50 ng per replicate and added to individual wells. 50 ng of DNA is lower than the recommended manufacturer's protocol and was reduced because of a low DNA yield from samples and had previously been trialled with *Daphnia magna* (Song *et al.*, 2020b). A single point negative control and a five-point positive control standard curve were added to individual wells. The plate was covered using a plate seal and incubated at 37 °C for 90 minutes to bind the controls

and DNA samples to the wells. The binding solution was removed, and each well was washed three times using diluted Wash Buffer. The Wash Buffer was diluted from a 10 times concentrated solution on the day of analysis, along with all antibodies and solutions used throughout. After DNA binding, 8-oxo-dG DNA capture steps were followed from the manufacturers protocol. Fifty microlitres of diluted Capture Antibody (1:100 of Capture Antibody to diluted Wash Buffer) was added to each well, covered and incubated at room temperature for an hour. The antibody was removed from each well and washed three times with diluted Wash Buffer. Fifty microlitres of diluted Detection Antibody (1:1000 of Detection Antibody to diluted Wash Buffer) was added to each well, covered and incubated at room temperature for 30 minutes. The antibody was removed from each well and washed four times with diluted Wash Buffer. Fifty microlitres of diluted Enhancer Solution (1:5000 of Enhancer Solution to diluted Wash Buffer) was added to each well, covered and incubated at room temperature for 30 minutes. The solution was removed, and each well was washed five times using diluted Wash Buffer. To detect the fluorescence signal, 50 µL of Fluorescence Development Solution was added to each well and incubated at room temperature for four minutes and covered using aluminium foil to protect the samples from light. After four minutes, the solution turned pink if in the presence of sufficient 8-oxo-dG products. Using a TECAN Spark 20m fluorescence microplate reader (TECAN, Männedorf, Switzerland) the plate was measured after two minutes at excitation 530 nm and emission 590 nm. Data were presented as fold change compared to the controls for each metal, as the known concentration of 8-oxo-dG standards did not produce a reliable standard curve to calculate absolute concentrations of 8-oxo-dG damage in experimental samples.

4.2.7 Apoptosis

Apoptotic cellular death for gravid females were conducted using the In Situ Cell Death Detection Kit Fluorescein (Roche, Basel, Switzerland) following 24 hours of single metal exposure. One of the central aspects of apoptosis is DNA degradation. DNA cleavage can form nicks (single- and double-stranded DNA breaks) or oligonucleosomic fragments that can be detected by labelling the free radical 3'OH termini with fluorescent markers dUTP (Rhee *et al.*, 2013a; Buttino *et al.*, 2011). This can be achieved during an enzymatic reaction, known as terminal deoxynucleotidyl transferase (TdT), which catalyses the polymerisation of nucleotides to the free radical 3'OH end of DNA (Buttino *et al.*, 2011). These nicks can then be fluorescently

quantified using a fluorescence plate reader. This kit was chosen as it is regularly used and referenced in other ecotoxicology studies with marine copepods and provided a quick, straight forward method with only a few steps to conduct. This assay underwent over two and a half years of method development to try to produce an intact individual method that could be photographed using a fluorescence microscope, however this was not successful. Another kit was used at first (DeadEnd™ Fluorometric TUNEL System, Promega, Wisconsin, US), before changing to the Roche kit that had been successfully used at NIVA's ecotoxicology labs using *D. magna* samples. Instead, a method was produced using homogenised samples and the fluorescence was read by a fluorescent microplate reader. Problems also occurred when establishing reliable positive and negative controls, therefore for this reason the data could not be absolutely quantified and is instead presented as fold change data.

The measured concentrations used for this assay were 0.78, 1.22, 1.92, 4.60 and 6.65 µM for copper exposure, 2.79, 3.60, 5.50, 7.30 and 8.06 µM for zinc exposure and 3.82, 18.33, 41.15, 58.83 and 78.21 µM for nickel exposure. One individual copepod was used per replicate and placed into a black, clear bottom 96-microplate well (Corning CoStar). Each individual copepod was homogenised using a homogenising stick that was turned twice whilst in the well. Positive and negative controls were added to the plate. Positive controls were homogenised individuals that underwent DNA digestion using 1 mg mL^{-1} DNase 1. After 10 minutes of digestion at 37 °C the reaction was stopped using 75 °C and ice treatment for 10 minutes each. This was repeated twice and then the solution was removed leaving the individual copepod in the well. TUNEL dye, containing 45 µL of the label solution and 5 µL of the enzyme solution, was added to each experimental sample and positive control well (50 µL) in darkness and the plate was incubated at 37 °C for 90 minutes. The negative control was one individual copepod exposed to only the label solution (50 µL) and was replicated five times. The TUNEL fluorescence was measured using a TECAN Spark 20m fluorescence microplate reader immediately at excitation 450 – 500 nm and emission 515 – 565 nm. The data were expressed as fold changes compared to the control for each metal.

4.2.8 RNA extraction

Twenty *T. battagliai* were pooled for each replicated time point (12 and 24 hours) for copper chloride experiments only in RNALater and stored at 4 °C overnight, then at -80 °C until RNA extraction. The measured copper concentrations were 0.14, 1.22, 4.60 and 6.65 µM, alongside a control. On the day of total RNA extraction, each sample was defrosted on ice for 10 minutes, and transferred onto a Whatman 105 filter (Cytiva Life Sciences, Marlborough, MA, USA) to absorb excess RNALater. Using ethanol (70% v/v) cleaned tweezers, each sample was carefully transferred into ZR BashingBead lysis tubes containing 400 µL RNA lysis buffer. The tweezers were ethanol cleaned between samples. Total RNA was isolated using the ZR Tissue and Insect RNA MicroPrep kit (Zymo Research Corporation, Irvine, CA, USA) according to the manufacturer's protocol from step two, with some adaptions. For step one, the ZR BashingBead lysis tubes were placed into a Precellys 24 tissue homogeniser (Bertin Instruments, Montigny-le-Bretonneux, France) (three cycles per second for two minutes with a 30 second break) and homogenised twice, with a five-minute interval between samples to protect against heat damage. In-Column DNase I digestion was carried out as an additional step between steps seven and eight. Finally, 15 µL of DNase/RNase free water was used to elute the RNA. The eluted RNA was stored at -80 °C until required. RNA purity (260/280 > 1.8, 260/230 > 1.9) was checked by pipetting 1 µL of eluted RNA onto a Nanodrop ND-1000 and RNA integrity measured using a Bio-analyser (Agilent Technologies, Santa Clara, CA, USA) looking for well-defined peaks with flat baselines.

4.2.9 Quantitative real-time qPCR analysis

Transcriptional analysis by quantitative real-time reverse-transcription polymerase chain reaction (RT-qPCR) was performed on samples collected after 12 and 24 hours of copper exposure. Original RNA samples were diluted to a concentration of 200 ng with nuclease-free water to a final volume of 20 µL. The same nuclease-free water was used for all samples throughout the analysis. The diluted RNA samples were vortexed for five seconds and 16 µL of each diluted RNA sample was transferred to a skirted 96-well PCR plate on ice and 4 µL of cDNA mix was added. A thin film was added to the plate and rolled to ensure it was airtight. The plate was placed in a MasterCycler gradient, with an incubation time of 60 minutes. Meanwhile, the remaining diluted RNA was pooled to make no reverse transcriptase (NRT) control samples. The no template control (NTC) contained only water. Afterwards,

cDNA samples were diluted from 40 ng to 0.2 ng mL^{-1} to create a source plate of 200 µL per well of diluted cDNA. A cDNA sample (2.5 µL) was added to 197.5 µL of nuclease-free water to create enough diluted cDNA to analyse 20 genes. An additional 2 µL of cDNA was taken from each sample and combined to make standards. The original cDNA plate was sealed using a film and roller and kept at -20 °C and the new diluted source plate was kept on ice. NRT and NTC control samples were added to the cDNA source plate.

Primer working solutions were prepared fresh on the day of analysis (3.2 mM) by combining forward primer stock and reverse primer stock to nuclease-free water. This was repeated for all 20 gene primers. Four genes could be analysed at once for all samples at both time points using a 384-sample plate and CFX384 PCR instrument (Bio-Rad Laboratories, Hercules, CA, USA). Following this, 925 µL Sybr Green Fastmix was added to each primer working solution. Fifteen microlitres of the mastermix solution was added to the 384-sample plate, alongside 5 µL cDNA sample and covered. The 384-sample plate was placed in a CFX384 PCR instrument. The sample volume was set to 20 µL and the total run took two hours 33 minutes to complete six cycles, repeating cycle one to five 39 times (cycle one = three minutes at 95 °C, cycle two = 20 seconds at 95 °C, cycle three temperature was edited to the specific primers being used (see Table 4.2), cycle four = 30 seconds at 72 °C, cycle five = three minutes at 95 °C, cycle six = 30 seconds at 65 °C and finished at 95 °C).

Table 4.2. Real time quantitative PCR primer genes for *Tisbe battagliai* and pre-determined annealing temperatures for cycle three.

Gene ID	**Gene name**	**Gene symbol**	**Function**	**Annealing temperature**
Tb_CL6143.Contig1	Elongation factor 1-delta	EEF1D	Reference gene	51.6
Tb_CL3883.Contig4	Glycerol-3-phosphate dehydrogenase	GDPH	Reference gene	51.6
Tb_CL6318.Contig2	28s ribosomal protein mitochondrial	MRPS28	Reference gene	53.8
Tb_CL10504.Contig1	Tata-box-binding protein	TBP	Reference gene	60.0
Tb_Unigene23526	Catalase	CAT	Antioxidant	51.6

Tb_CL6525.Contig2	Glutathione reductase	GR	Antioxidant	50.3
Tb_Unigene20920	Glutathione peroxidase 2	GPX2	Antioxidant	60.0
Tb_CL900.Contig1	Nucleotide excision repair factor RAD23	RAD23	DNA excision repair	53.8
Tb_Unigene29749	DNA repair protein complementing xp-g cells	ERCC5	DNA excision repair	60.0
Tb_CL4393.Contig1	Serine-protein kinase ATM	ATM	DNA double-strand break sensor	53.8
Tb_CL6594.Contig1	DNA repair protein RAD50	RAD50	DNA double-strand break repair	51.6
Tb_CL4178.Contig2	Apoptosis regulator	BAX	Apoptosis positive regulator	50.3
Tb_CL2937.Contig1	Caspase-3	CASP3	Apoptosis executor	50.3
Tb_CL4927.Contig1	Peptidyl-prolyl cis-trans isomerase-like	PPIF	Mitochondrial permeability transition pore	60.0
Tb_Unigene23451	ADP ATP translocase 1	SLC25A4	Mitochondrial permeability transition pore	60.0
Tb_Unigene20048	Succinate dehydrogenase	SDHB	Mitochondrial ETC Complex II	60.0
Tb_Unigene24973	H+ transporting ATP synthase gamma subunit	ATP5C1	Mitochondrial ETC Complex V	50.3
Tb_CL110.Contig1	Na+ K+ ATPase alpha-subunit 1	ATP1A1	Osmo/ion regulation	60.0
Tb_CL8968.Contig1	Aromatic-l-amino-acid decarboxylase	DDC	Pigmentation	60.0
Tb_Unigene23211	Histamine H1 receptor	HRH1	Phototactic behaviour	53.8

4.2.10 Statistical analysis

A linear regression for metal fractionation data and concentration response curves for survival after treatment were created using GraphPad Prism 8 (GraphPad Software Inc., CA, USA). A non-linear regression allowed EC_{50} values to be calculated after 24 and 48 hours for adults and juveniles exposed to each metal. All statistical analyses were conducted using GraphPad Prism 8. All data were checked for normality using the Kolmogorov-Smirnov normality test, log_{10} transformed and normalised if necessary. Data conforming to normality were further analysed using a one-way or two-way analysis of variance (ANOVA). Tukey's HSD Post Hoc tests were used to determine significant differences between concentrations and time points ($P < 0.05$). Principal component analysis and Pearson correlation coefficient were conducted as described in Chapter 3.2.10.

4.3 Results

4.3.1 Exposure characteristics

Physicochemical exposure media parameters remained within the expected ranges. At a salinity of 30 ppt and after 24-hour aeration, the pH was 8.23 ± 0.2. These remained consistent during the 48-hour experiments.

4.3.2 Metal fractionation

Copper and zinc were present in all measured size fractions of particles, colloids and LMM that were concentration dependent (Figure 4.1A and 4.1B), whereas LMM dominated for nickel (Figure 4.1C). For nickel and zinc, LMM had the highest contribution among tested fractions and had a significant positive correlation with total metal concentration for nickel and close to significant for zinc ($P = 0.06$, Pearson correlation co-efficient). Copper was present in the exposure media mainly in the dissolved phase as colloid and LMM fractions, both positively correlated to total metal concentration, which was close to significant for colloids ($P = 0.057$). However, with increasing total concentration of copper, the percentage of LMM decreased (Table 4.3). Zinc had a relatively consistent LMM percentage contribution with increasing total concentration (Table 4.3), yet a concentration dependent increase is shown in Figure 4.1B. Meanwhile, the correlation between total concentration and colloid concentration was significantly negative. Nickel had the highest LMM fraction percentage across the three tested concentrations, with 98% and 97% at medium

and high concentrated solutions (Table 4.3). Nickel particles remained consistently low, between 1 and 2% over the concentration range.

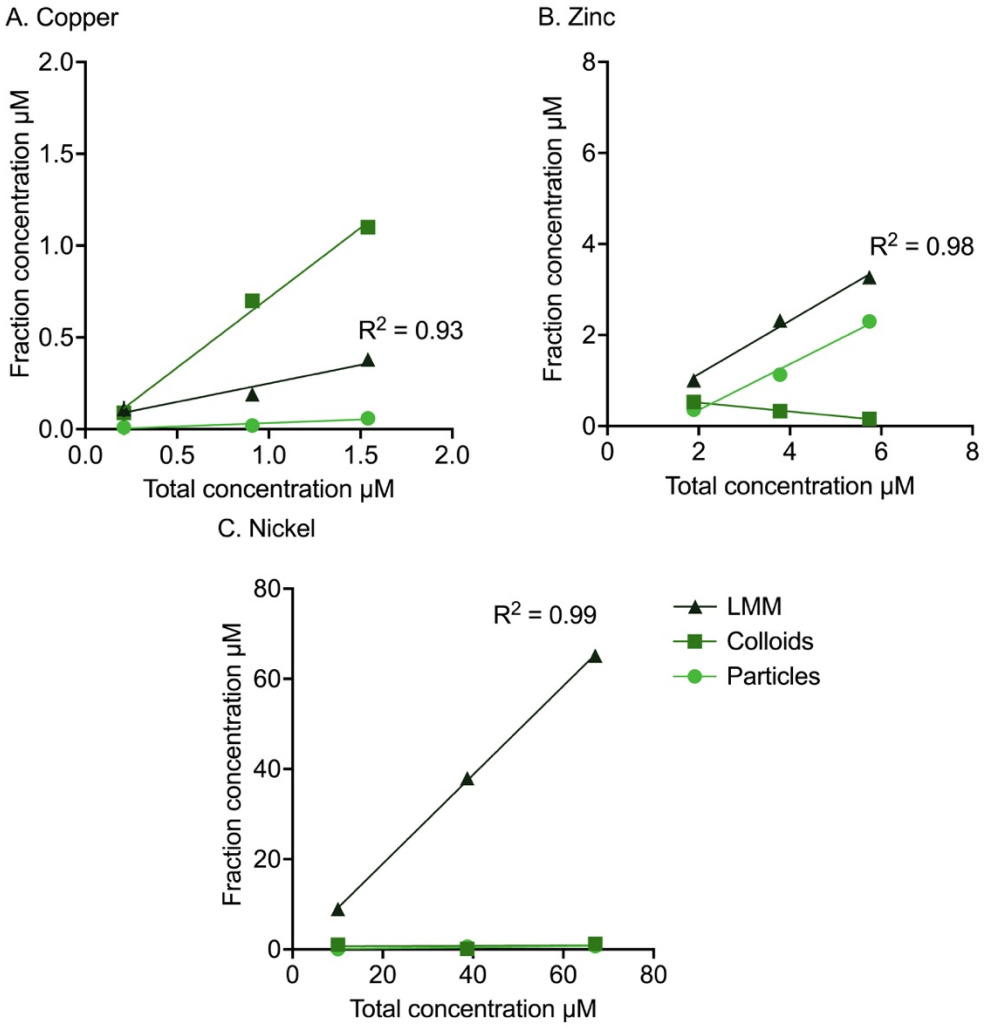

Figure 4.1. Mean metal size fractions (± standard deviation) of single metal exposure solutions of (A) copper, (B) zinc and (C) nickel in 30 ppt artificial seawater at three different concentrations (n = 3) at the beginning of the experiment (0 hour). Three size fractions – particles, colloids, and low molecular mass (LMM). R^2 values are shown for each metal LMM linear regression.

Table 4.3. Percentages of each fraction (particles, colloids, and low molecular mass (LMM)) of copper, nickel, and zinc in three single concentration solutions at 0 hours.

Metal	Total concentration µM	Particles %	Colloids %	LMM %
Copper	0.21	3.59	44.31	52.10
	0.91	1.96	77.34	20.70
	1.54	4.03	71.45	24.52
Nickel	10.06	0.56	10.51	88.93
	38.71	1.62	0.29	98.09
	67.07	1.02	1.86	97.12
Zinc	1.89	18.77	28.02	53.22
	3.78	29.93	8.72	61.34
	5.74	40.14	2.83	57.03

4.3.3 Survival

For both gravid females (Figure 4.2) and juveniles (Figure 4.3), copper had the greatest impact of the three trace metals on survival after 24 and 48 hours, followed by zinc and nickel. Juveniles had a higher sensitivity to copper, nickel and zinc compared to the adults. Time, concentration and the interaction between time and concentration were significant factors impacting survival for gravid females and juveniles after exposure to copper, nickel, and zinc, except for juveniles exposed to nickel that found the interaction between time and concentration was not significant (Table 4.4). As seen in table 4.4, similar patterns were found for both life stages regarding which factors were having a significant impact on survival and which metals had the lowest EC_{50} values.

When displaying the measured gravid female survival with only the contribution of LMM concentration to the overall concentration, the curves for nickel and zinc were similar to the total concentration curves (Figure 4.2). This is because of the large LMM contribution to the total concentration for these two metals. For copper, however, there is a shift along the x-axis, as the LMM contribution to total concentration is lower.

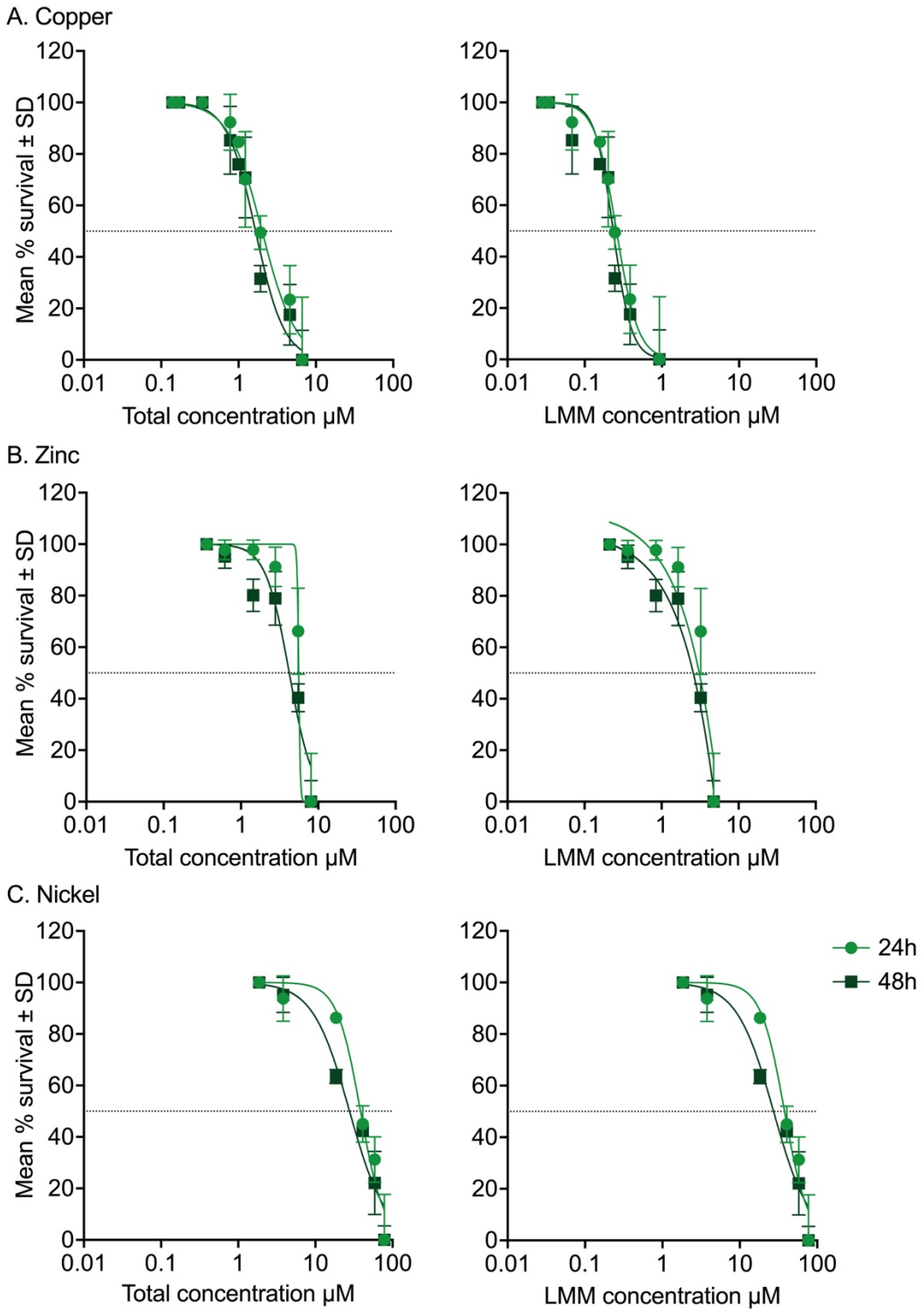

Figure 4.2. Mean survival percentage (± standard deviation) of 14-day old gravid female *Tisbe battagliai* exposed for 24 and 48 hours to (A) copper, (B) zinc and (C) nickel. Each metal is shown with total concentrations on the left and low molecular mass (LMM) concentrations on the right. Only a total metal exposure was conducted, and samples were taken for three concentrations to measure LMM concentration. These three samples were used to calculate the LMM concentrations for the whole curve. This was achieved by using the simple linear regression slope in figure 4.1 for LMM concentrations. In each total concentration experiment, there were five replicates. Non-linear regressions were used to calculate EC_{50} values at 24 and 48 hours. The dotted line at 50% on the y-axis shows the EC_{50} values.

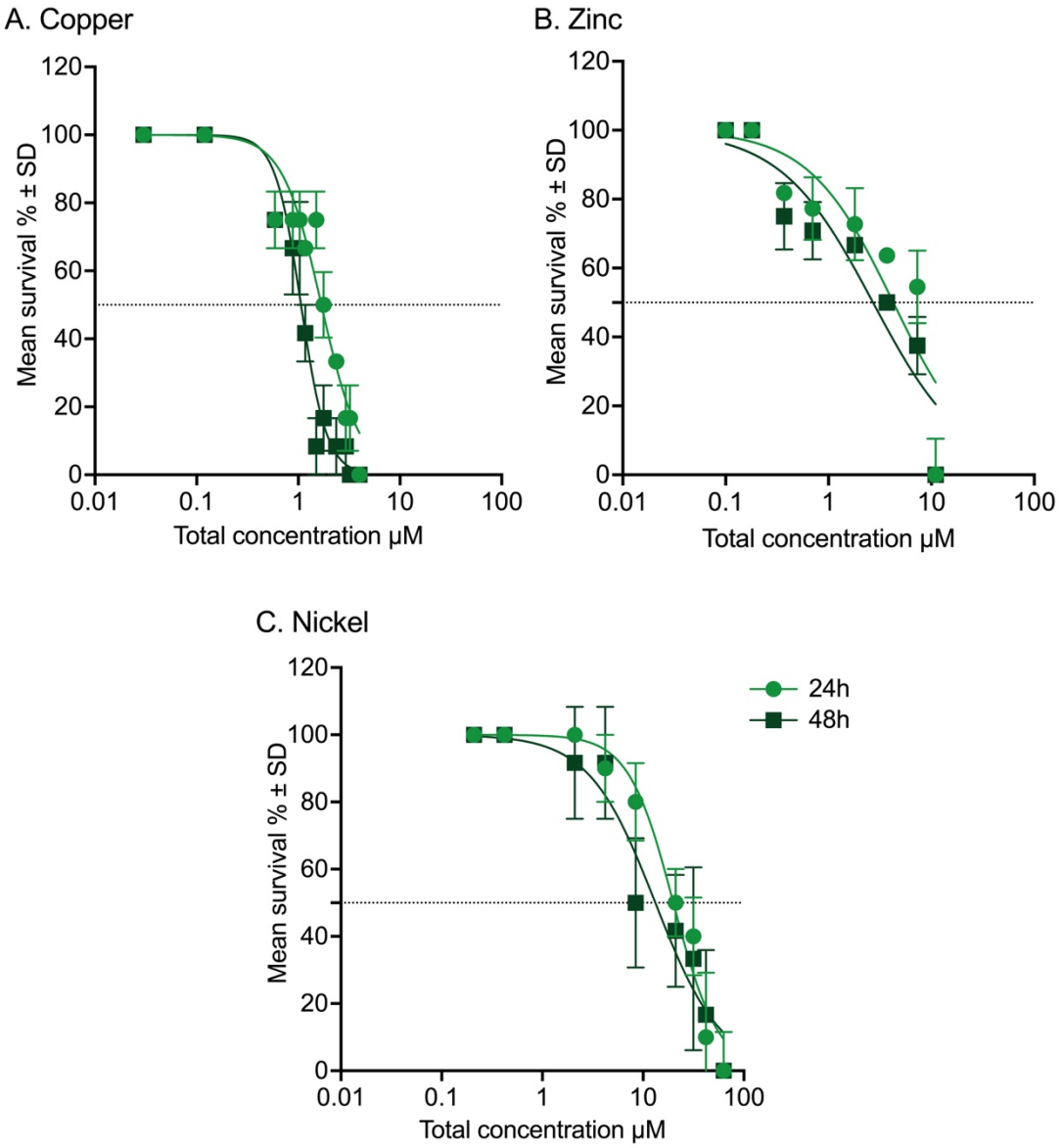

Figure 4.3. Mean survival percentage (± standard deviation) of six-day old juvenile *Tisbe battagliai* exposed for 24 and 48 hours (n = 4) to (A) copper, (B) zinc and (C) nickel. Nominal concentrations are presented, with non-linear regressions used to calculate EC_{50} values at 24 and 48 hours. The dotted line at 50% on the y-axis shows the EC_{50} values.

Table 4.4. Dose response curve statistics for gravid female adult and juvenile *Tisbe battagliai* survival after exposure to copper (Cu), nickel (Ni), and zinc (Zn) (total concentration µM) at 24 and 48 hours (h). Non-linear regressions produced EC_{50} values (µM) and R^2 values for each metal exposed per life stage and time point (e.g., gravid female exposed to copper at 24 hours). No observed effect concentration (NOEC) and low observed effect concentration (LOEC) were calculated from the two-way ANOVA statistical output for each curve. * Indicates significant P-values from two-way ANOVA statistics, including whether there is a statistical difference for time, concentration (Conc.) and an interaction between time and concentration (Time x Conc.).

Life stage	Metal	Time (h)	EC_{50} µM	NOEC µM	LOEC µM	R^2	Two-way ANOVA Time	Two-way ANOVA Conc.	Two-way ANOVA Time x Conc.
Gravid female	Cu	24	2.01	1.22	1.92	0.91	<0.0001*	<0.0001*	<0.0001*
		48	1.66	1.00	1.22	0.94			
	Zn	24	6.62	2.79	5.5	0.93	<0.0001*	<0.0001*	0.0022*
		48	4.52	0.62	1.44	0.92			
	Ni	24	38.42	18.53	41.15	0.94	0.0007*	<0.0001*	0.0338*
		48	27.70	3.82	18.53	0.95			
Juvenile	Cu	24	1.69	1.50	1.77	0.65	<0.0001*	<0.0001*	<0.0001*
		48	1.03	1.03	1.17	0.71			
	Zn	24	4.26	0.18	0.37	0.73	<0.0001*	<0.0001*	0.0068*
		48	2.71	0.18	0.37	0.83			
	Ni	24	19.95	8.42	21.04	0.79	0.0012*	<0.0001*	0.182
		48	13.22	4.2	8.42	0.83			

4.3.4 Reactive oxygen species production

Cellular ROS production was measured fluorescently over 48 hours and showed a concentration-dependent increase for copper after 24 hours, for nickel and zinc after 48 hours (Figure 4.4). For copper, the highest ROS measured was 9.75-fold higher than the control at 1.2 µM after 24 hours (Figure 4.4A). All concentrations had a significant reduction in ROS formation after 48 hours when compared to 24 hours (Table 4.5). Concentration was another significant factor for copper ROS formation (Table 4.5). For zinc, there was a small but significant increase in ROS formation with concentration at 24 hours, except for 5.5 µM that had lower ROS than the controls

(Figure 4.4B). This pattern changes to an inverted u response after 48 hours, with ROS increasing up to 0.62 μM and then decreasing at the highest two concentrations (Figure 4.4B). Time was also a significant factor for ROS formation, with the interaction between time and concentration influencing the ROS production shown. For nickel, there was a small but not significant increase in ROS formation after 24 hours (Figure 4.4C). After 48 hours, there was a strong and significant concentration dependent increase and reached the highest measured ROS value out of all three metals (13-fold increase at 18.33 μM). Additionally, time was a significant factor affecting ROS production, with significant differences between the two time points for all three measured nickel concentrations. For nickel, both time and concentration were most likely driving the ROS formation pattern shown (Table 4.5).

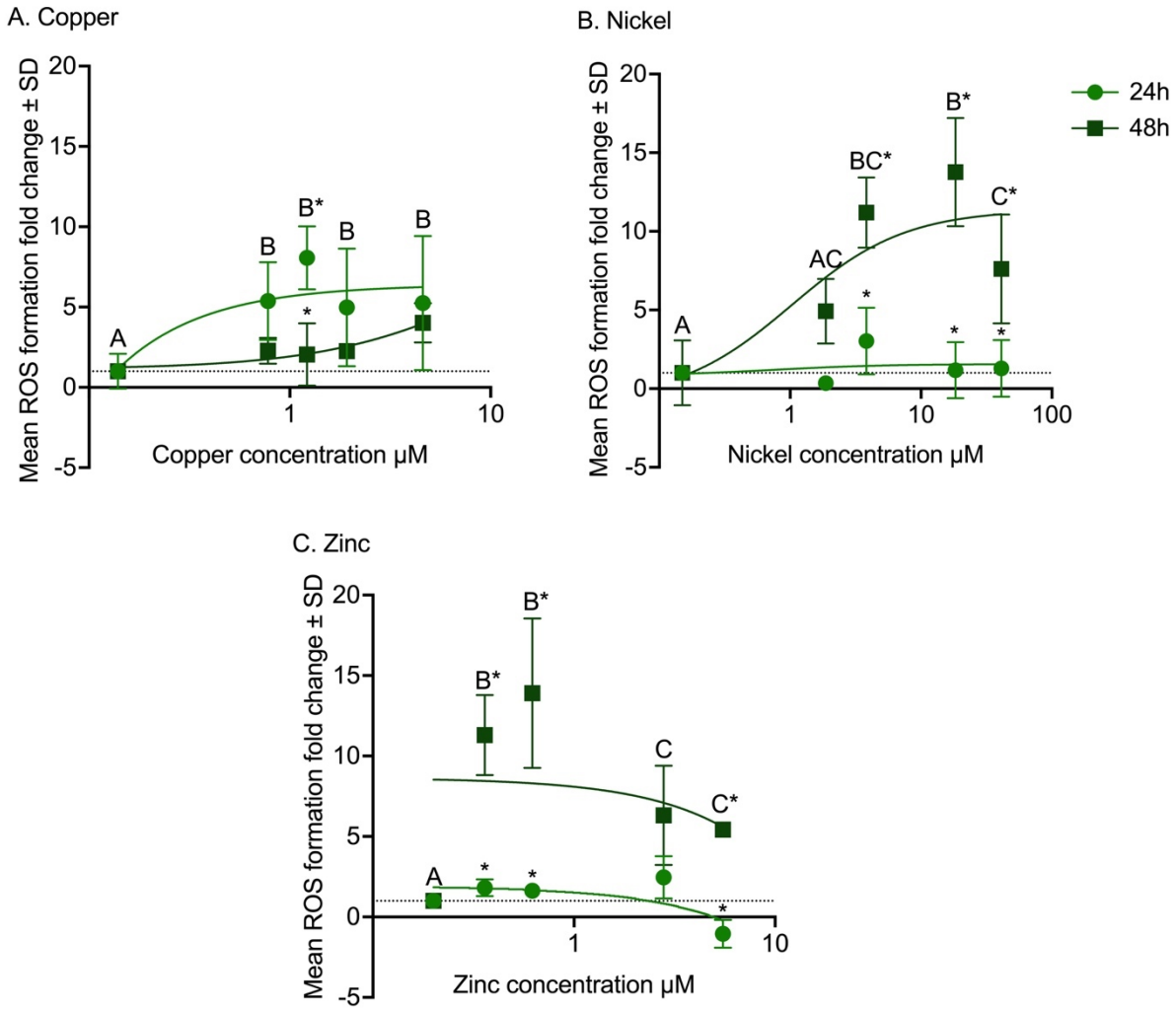

Figure 4.4. Mean fold change (± standard deviation) of reactive oxygen species (ROS) formation in 14-day old gravid females *Tisbe battagliai* (n = 4) exposed to (A) copper, (B) nickel and (C) zinc for 24 and 48 hours. A non-linear regression was added at each time point. Letters indicates significant differences between concentrations within the time point and * indicates that the concentration is significantly different between the two time points (Tukey Post-Hoc, $P < 0.05$).

Table 4.5. Two-way ANOVA statistical outputs for cellular reactive oxygen species formation following exposure to total concentrations of copper, nickel, and zinc for 24 and 48 hours. * Indicates significant P-values.

Metal	**Time**	**Concentration**	**Time * Concentration**
Copper	0.0018*	0.0004*	0.14
Zinc	<0.0001*	<0.0001*	0.0002*
Nickel	<0.0001*	<0.0001*	0.0013*

4.3.5 Oxidative DNA damage

ROS-mediated oxidative damage was quantified by measuring 8-oxo-dG products produced in extracted DNA samples after 24 hours of metal exposure (Figure 4.5). Copper data exhibited no change in 8-oxo-dG produced with increasing concentration (One-way ANOVA, $P > 0.05$), until the highest concentration, which increased 1.6-fold higher than the controls albeit not significantly (Figure 4.5A). However, four of the five zinc concentrations showed a decrease in 8-oxo-dG produced, except for the highest concentration that was 1.5-fold higher than the control but was also not significantly different (One-way ANOVA, $P > 0.05$; Figure 4.5B). The only significant difference was seen for the highest concentration of nickel (78 μM; Tukey Post-Hoc, $P = 0.0145$), although all nickel concentrations showed between 1.8- to 2.2-fold increase in 8-oxo-dG (Figure 4.5C). The highest 8-oxo-dG produced occurred at a nickel concentration of 41 μM.

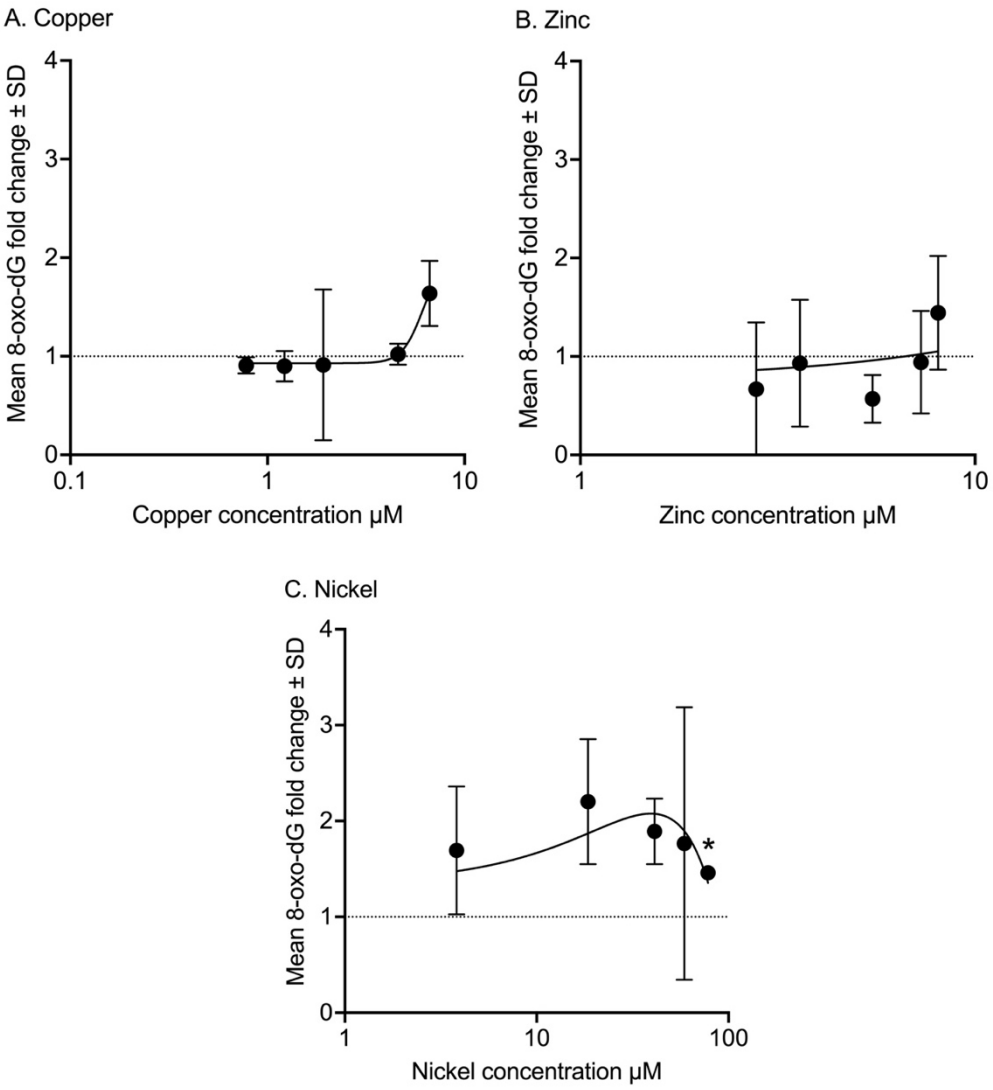

Figure 4.5. Mean relative fold change of 8-oxo-dG DNA damage ± standard deviation (SD) after 24 hours of (A) copper, (B) zinc and (C) nickel exposure to 14-day old gravid female *Tisbe battagliai*. For each concentration, n = 3 pooled samples. The dotted line shows the control sample for each metal (= one relatively). A non-linear regression was added for each metal. * Indicates a significant difference from the control for that metal (Tukey Post-Hoc, $P < 0.05$).

4.3.6 Apoptosis

Following a two-way ANOVA, copper, nickel, and zinc were significant factors for apoptosis ($P = 0.0032$), as well as concentration ($P < 0.0001$). Copper replicates observed a concentration dependent increase in apoptosis after 24 hours of exposure with the two highest concentrations of 4.6 and 6.65 µM were significantly different to the controls (Figure 4.6A). Similarly, zinc exhibited a concentration dependent increase in apoptosis, but only the highest concentration of 8.06 µM was significantly different to the controls (Figure 4.6B). In contrast to copper and zinc, nickel had statistically similar apoptotic responses for all concentrations (Pearson

correlation, P = 0.15), but the highest concentration of 78.21 µM was significantly different to the controls (Figure 4.6C).

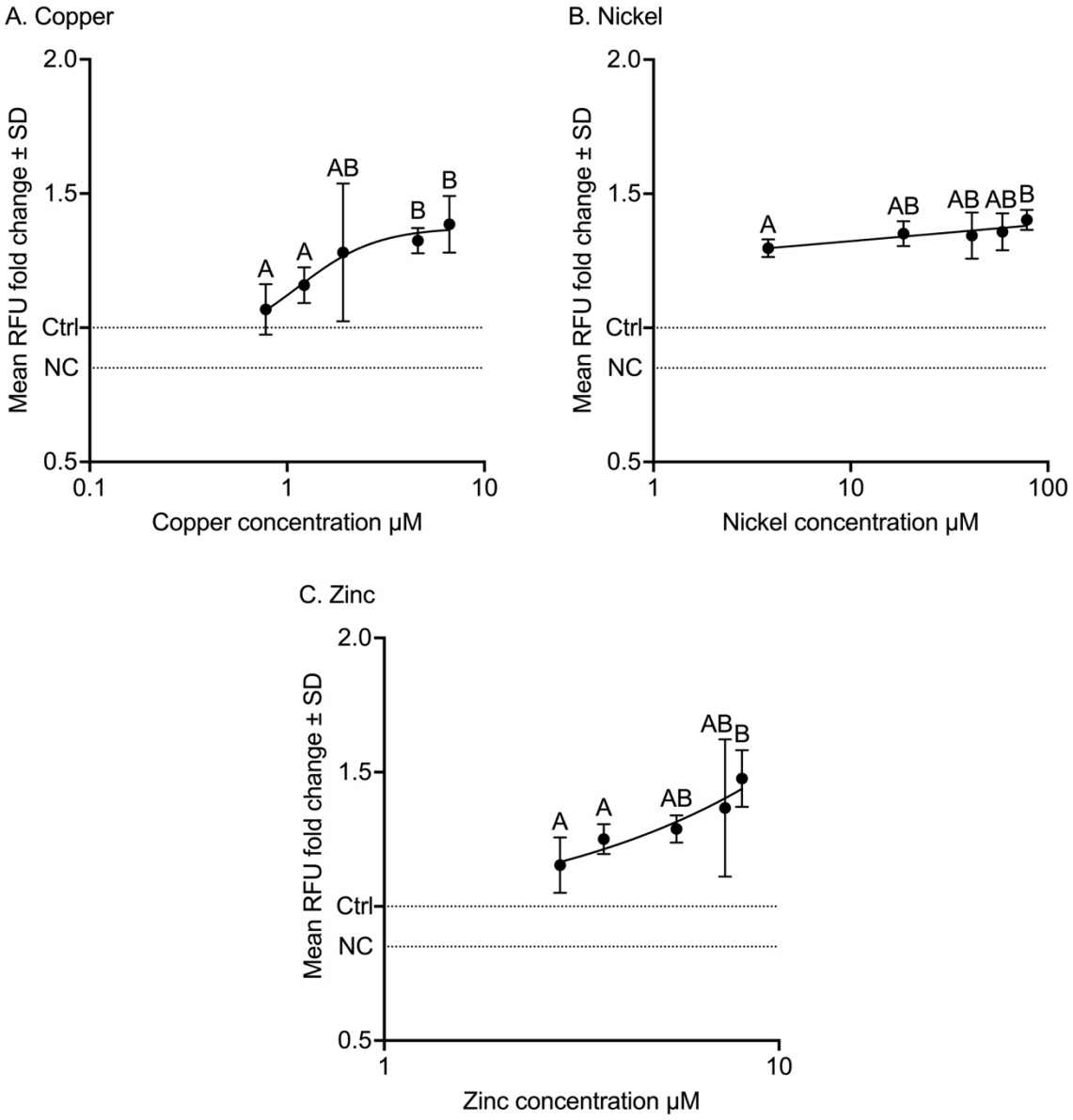

Figure 4.6. Relative fluorescence units (RFU) of TUNEL dye in *Tisbe battagliai* following exposure of (A) copper, (B) nickel and (C) zinc for 24 hours. The Ctrl line on the y-axis represents the control value (one RFU) and NC shows the negative control RFU. A non-linear regression was added for each metal. Letters indicates a significant difference from the control for that metal (Tukey Post-Hoc, P < 0.05).

4.3.7 Gene expression

The antioxidant gene GR exhibited a significant concentration dependent increase over 12 hours, but this was not continued after 24 hours (Figure 4.7). The only factor influencing GR regulation was concentration (Table 4.6). On the contrary, CAT experienced down regulation at all copper concentrations, after 12 and 24 hours (Figure 4.7) and was significantly impacted by time and concentration as separate factors (Table 4.6). For GPX2, there were different responses at each time point, with 12 hours causing upregulation that was similar across all concentrations and 24 hours observing down regulation (Figure 4.7). Concentration was the only non-significant factor influencing GPX2 regulation (Table 4.6).

DNA damage repair genes were significantly upregulated after 12 hours, with a concentration dependent increase (Figure 4.7A). After 24 hours of exposure, RAD23 and ATM were downregulated from 12 hours and had a similar expression to the control (0.14 µM) (Figure 4.7B). However, at 4.6 µM RAD50 expression was the highest, with a 3.75-fold increase. However, gene expression decreased to a similar level as controls at 6.65 µM (1.2-fold regulation). RAD23 was the only related gene to repairing DNA damage that had time as a significant factor (Table 4.6). Both RAD23 and RAD50 were significantly impacted by concentration and the interaction of time and concentration.

For genes related to apoptosis regulation, CASP3 was downregulated at the lowest copper concentration after 12 hours, but with an increase in concentration the gene was upregulated (Figure 4.7A). After 24 hours, there was little change in regulation when compared to the controls (Figure 4.7B). Both time and the interactions between time and concentration were significant factors for CASP3 (Table 4.6). Instead, BAX exhibited higher up regulation after both time points, with a 2.11-fold increase after 12 hours of exposure to 6.65 µM (Figure 4.7A). Although this upregulation reduced after 24 hours, 4.60 µM observed similar upregulation at both time points. Concentration was the only significant factor for BAX (Table 4.6).

Table 4.6. Mixed effects model statistical outputs for relative gene expression after 12 and 24 hours of copper exposure. * Indicates significant P-values.

Gene	Time	Concentration	Time * Concentration
CAT	0.0096*	<0.0001*	0.1636
GR	0.20	0.0029*	0.1881
GPX2	0.0003*	0.4066	0.0313*
RAD50	0.13	<0.0001*	0.0005*
RAD23	0.0047*	0.0004*	0.0004*
ATM	0.087	0.057	0.17
CASP3	0.0317*	0.2348	0.023*
BAX	0.076	0.0007*	0.066

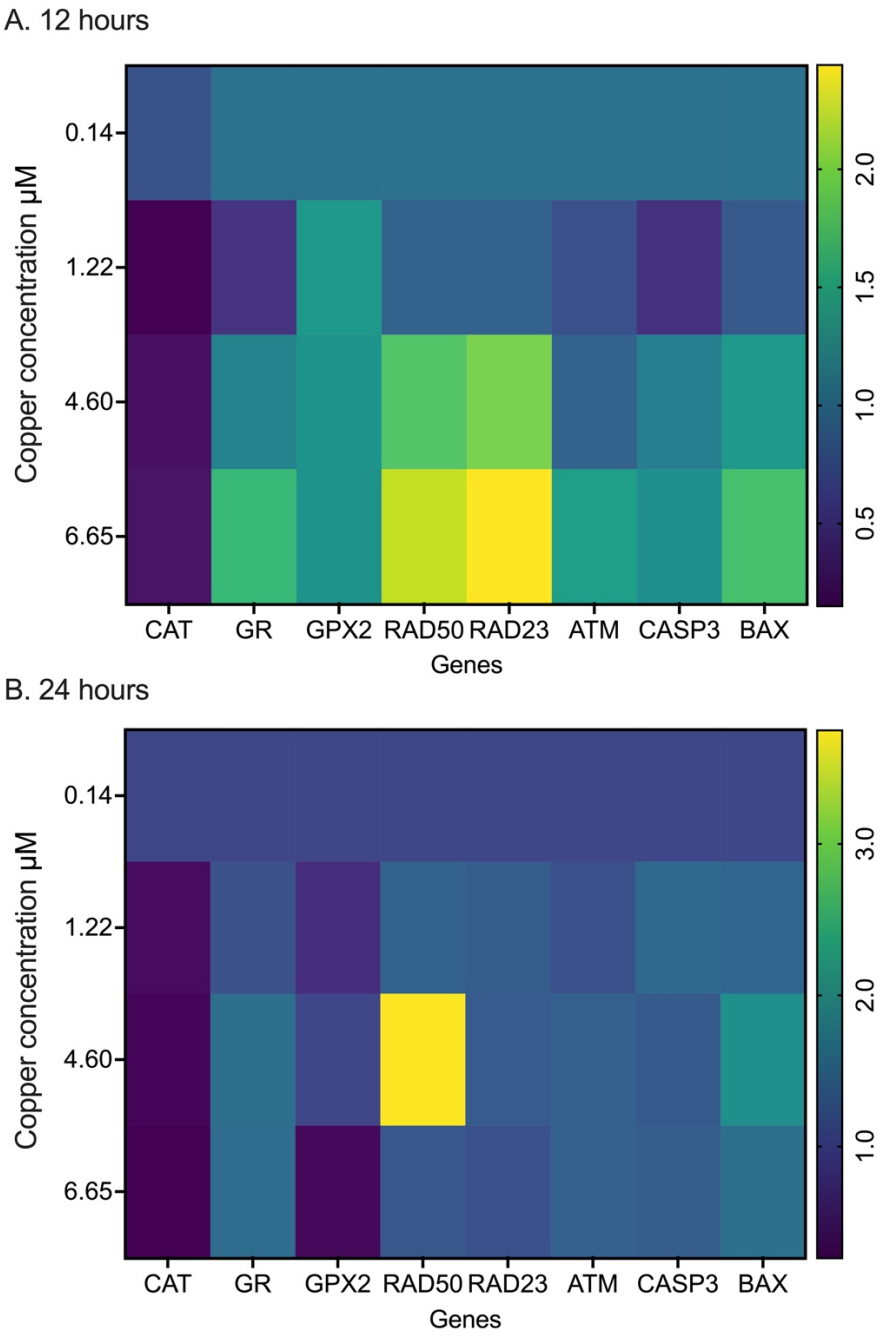

Figure 4.7. Heat map of mean relative expression of eight genes of interest for *Tisbe battagliai* following (A) 12-hour and (B) 24-hour exposure to copper (0.14, 1.22, 4.60 and 6.65 µM). CAT = catalase, GR = glucocorticoid receptor and GPX2 = antioxidant, RAD50 = DNA double stand break repair, RAD 23 = UV excision repair, ATM = ATM serine/threonine kinase, CASP3 = apoptosis executer and BAX = apoptosis regulator.

4.3.8 Principal component analysis

For copper the two principal components (PC1 and PC2) explained 82.17% of total variance (Figure 4.8A). Most of the active variables were best shown on PC1, for example survival, ROS, apoptosis, and the genes CAT, GR, RAD23, ATM, CASP3

and BAX. The other variables 8-oxo-dG, GPX2 and RAD50 observed their trends best on PC2. As shown in figure 4.8A, there was one cluster containing the variables ROS, apoptosis, GR, RAD23, RAD50, ATM, BAX and CASP3, which was closely associated with the higher copper concentrations (Figure 4.8). However, only a few endpoints were significantly correlated, for example GR and ATM and ROS and CASP3 observed positive correlations (Table 4.7). Instead, apoptosis and the CAT gene were shown in opposite directions away from the centre, with a significant negative correlation. This suggests that the down regulation of CAT was related an increase in apoptosis.

The total variance for nickel was higher than copper, with PC1 and PC2 representing 88.56% (Figure 4.8B). 8-oxo-dG and apoptosis were tightly clustered at the higher nickel concentrations and best represented from PC1, but this cluster was not significant (Table 4.8). As well, survival and ROS were best shown on PC2 but were not correlated with each other. There were no significant positive or negative correlations for nickel suggesting that changes in these variables are independent of each other (Table 4.8).

Zinc had the highest total variance of the three metals, with 99.55% explained by the two principal components (Figure 4.8C). All four variables exhibited their trends best on PC1, with survival and apoptosis displayed in opposing directions from the centre due to a significant negative correlation between the two variables. The same trend was seen between the ROS and 8-oxo-dG variables (Table 4.9). These suggest that increases in apoptotic detection leads to reduced survival, but also that increased ROS generation can decrease 8-oxo-dG.

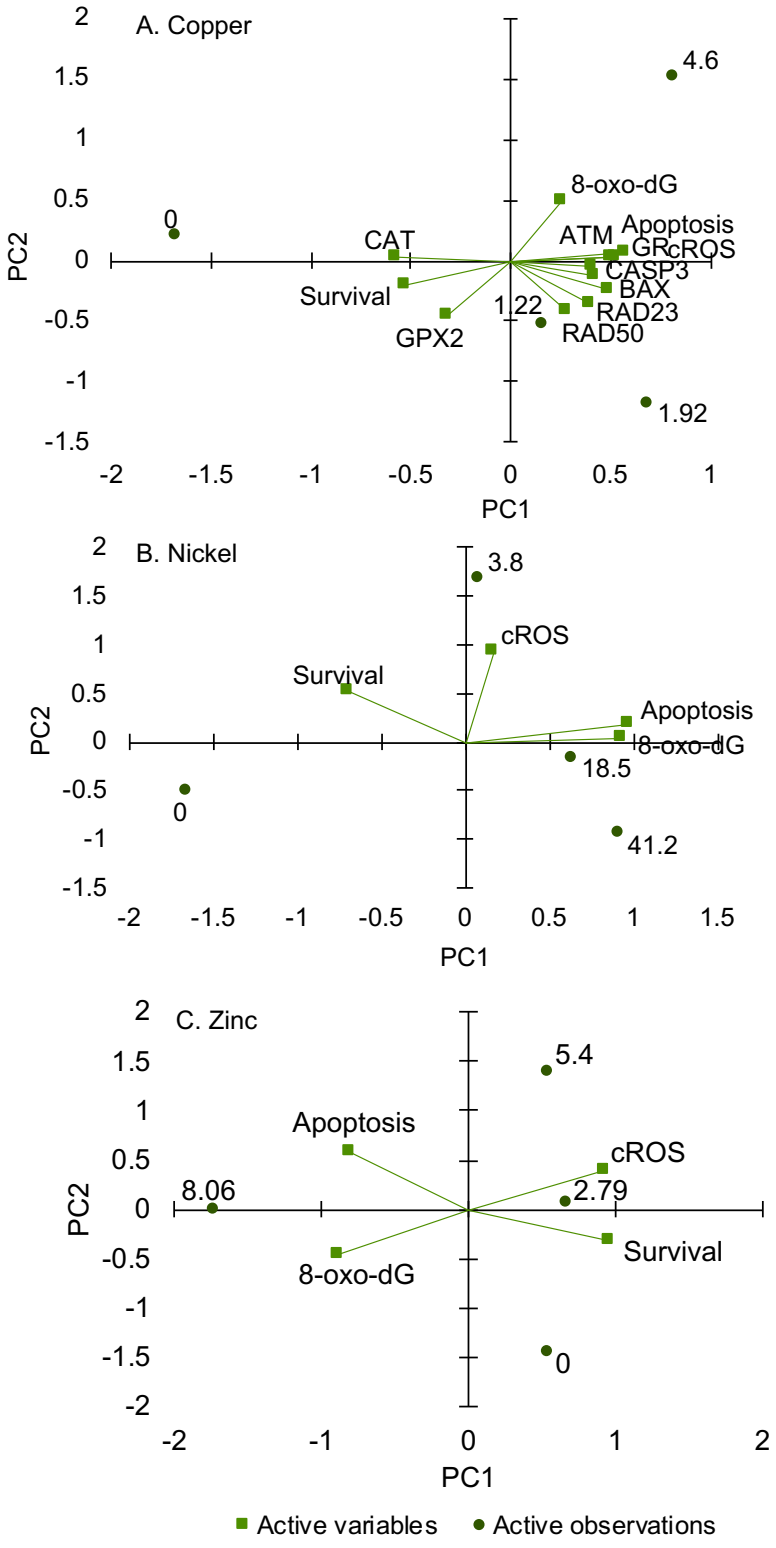

Figure 4.8. Principal component analysis (PCA) of responses in 14-day old gravid female *Tisbe battagliai* exposed to (A) copper, (B) nickel and (C) zinc for 24 hours. Active variables are the measured effect responses (squares) and active observations are metal concentrations (circles). cROS = cellular ROS, RAD23 – UV excision repair gene, RAD50 – double-strand DNA break repair gene, BAX – apoptosis regulator gene, CASP3 – apoptosis executor gene, GR – glucocorticoid receptor gene, GPX2 – antioxidant gene and CAT - catalase.

Table 4.7. Pearson correlation matrix obtained from effect endpoints measured in *Tisbe battagliai* after 24 hours of copper exposure. Bold values indicate significant differences between the two variables. ROS = reactive oxygen species, 8-oxo-dG = oxidative DNA damage, CAT = catalase, GR = glucocorticoid receptor and GPX2 = antioxidant, RAD50 = DNA double stand break repair, RAD23 = UV excision repair, ATM = ATM serine/threonine kinase, CASP3 = apoptosis executer and BAX = apoptosis regulator.

Variables	**Survival**	**cROS**	**Apoptosis**	**8-oxo-dG**	**CAT**	**GR**	**GPX2**	**RAD50**	**RAD23**	**ATM**	**CASP3**	**BAX**
Survival	1	-0.488	-0.936	-0.765	0.871	-0.899	0.726	-0.281	-0.340	-0.928	-0.496	-0.687
cROS	-0.488	1	0.753	-0.006	**-0.817**	0.302	-0.462	0.147	0.892	0.385	0.990	0.472
Apoptosis	-0.936	0.753	1	0.521	-0.987	0.828	-0.654	0.361	0.644	0.877	0.741	0.765
8-oxo-dG	-0.765	-0.006	0.521	1	-0.375	0.563	-0.823	-0.246	-0.310	0.571	0.074	0.120
CAT	0.871	**-0.817**	-0.987	-0.375	1	-0.794	0.552	-0.442	-0.758	-0.845	-0.789	-0.810
GR	-0.899	0.302	0.828	0.563	-0.794	1	-0.357	0.642	0.355	**0.996**	0.254	0.883
GPX2	0.726	-0.462	-0.654	-0.823	0.552	-0.357	1	0.444	-0.052	-0.417	-0.562	-0.037
RAD50	-0.281	0.147	0.361	-0.246	-0.442	0.642	0.444	1	0.526	0.609	0.013	0.876
RAD23	-0.340	0.892	0.644	-0.310	-0.758	0.355	-0.052	0.526	1	0.410	0.819	0.675
ATM	-0.928	0.385	0.877	0.571	-0.845	**0.996**	-0.417	0.609	0.410	1	0.341	0.884
CASP3	-0.496	0.990	0.741	0.074	-0.789	0.254	-0.562	0.013	0.819	0.341	1	0.374
BAX	-0.687	0.472	0.765	0.120	-0.810	0.883	-0.037	0.876	0.675	0.884	0.374	1

Table 4.8. Pearson correlation matrix obtained from effect endpoints measured in *Tisbe battagliai* after 24 hours of nickel exposure. Bold values indicate significant differences between the two variables. ROS = reactive oxygen species and 8-oxo-dG = oxidative DNA damage.

Variables	Survival	cROS	Apoptosis	8-oxo-dG
Survival	1	0.229	-0.556	-0.458
cROS	0.229	1	0.303	0.092
Apoptosis	-0.556	0.303	1	0.953
8-oxo-dG	-0.458	0.092	0.953	1

Table 4.9. Pearson correlation matrix obtained from effect endpoints measured in *Tisbe battagliai* after 24 hours of zinc exposure. Bold values indicate significant differences between the two variables. ROS = reactive oxygen species and 8-oxo-dG = oxidative DNA damage.

Variables	Survival	cROS	Apoptosis	8-oxo-dG
Survival	**1**	0.742	**-0.950**	-0.710
cROS	0.742	**1**	-0.517	**-0.984**
Apoptosis	**-0.950**	-0.517	**1**	0.460
8-oxo-dG	-0.710	**-0.984**	0.460	**1**

4.4 Discussion

This chapter assessed the biological effects of copper, nickel, and zinc exposure on *T. battagliai* by measuring effects at different levels of biological organisation. Alongside toxicity measurements, metal fractionation was determined to understand whether the total concentration of the metal was present as one fraction or multiple fractions, and the impact this has on toxicity. Copper, nickel, and zinc are some of the most studied trace metals in effect studies, due to their worldwide contamination and natural presence in all marine environments; however, integrated effects and exposure assessments are less common.

For the exposure solutions used in this chapter, all three metals were present as mostly LMM and colloidal fractions, with the addition of particles for zinc. As nickel is dominating as ions in the exposure solutions, the toxicity observed is because of this fraction. Interestingly, nickel had high bioavailability but the lowest toxicity of the three metals, but the opposite was true for copper, as it was mainly present as colloids yet is the most toxic metal of the three, causing the greatest impact on

survival. This suggests that copper toxicity is not only resulting from ions being up taken by *T. battagliai*. Evidence of metal particles being up taken has been reported by the freshwater Cladophora *Daphnia magna* (Byrnes, 2021) and by *T. battagliai* (Jarosz *et al.*, 2022). According to Byrnes (2021), uranium particles were present in the intestinal trait of *D. magna*. Furthermore, Villagran *et al.* (2019) found that copepods *Acartia tonsa* and *Eurytemora americana* could be accumulating six metals from the particulate phase, including copper, nickel, and zinc. The reasons are likely due to feeding habits of invertebrates, including filtering, and gathering particles from surrounding media that could result in higher exposure to metal suspended particles. In short, this could act as a route of exposure for passive uptake of higher molecular weight fractions (Salbu, 2015). For this reason, total concentration was used for effect endpoints in this chapter as the larger and suspended fractions of metal present could not be excluded from potentially causing toxicity.

Moreover, the same trends and significant differences were found when using either total concentration or LMM concentration for survival and measured biological endpoints, with the only difference being a shift of responses along the concentration x-axis due to lower LMM concentrations for copper and zinc. This shift does reveal that total concentration is more toxic for copper and zinc, as is expected with large contributions from colloids and particles respectively. However, without data on body burden concentrations for *T. battagliai* or exposing each metal fraction individually, which fractions are contributing to the measured effects cannot be determined. Therefore, only survival data were shown with LMM concentration to illustrate the similar curves and shift in x-axis, as there are some limitations with these data. For example, the exposure solutions for copper and zinc contained a mixture of fractions, therefore presenting the effects data as total concentration is more representative. Additionally, if only LMM concentration was taken for copper and zinc and used for their effects data, the effects from the LMM concentration would be exaggerated and seem more toxic than the effects measured from a filtered copper or zinc solution containing only metals as ions.

Exceptions from the assumed bioavailability from metal ions for marine organisms were noted as early as Campbell (1995). In Fisher *et al.* (2000) they used total dissolved metal concentrations (< 0.2 µm) because of the uncertainties around metal complexes and their bioavailability. Their first order bioenergetic-based kinetic model, which considered both dissolved and particulate metal fractions, showed that under

most environmental conditions marine zooplankton can up take around 20% of dissolved zinc. The fractions belonging in the dissolved phase have had conflict in the literature, with the dissolved phase being defined as any fraction that is attained via filtration on a membrane pore size of 0.22 – 0.45 μm (Gagnon and Vigneault, 2013). These pore sizes separate large particles, but colloids remain in the dissolved fraction. According to Hargreaves *et al.* (2017) the colloidal fraction is separate, existing between 1kDa – 0.45 μM and dissolved is < 1kDa. However, not all dissolved metals will be able to be up taken in the same way depending on their charge. Colloids, for example, might not be charged and are more likely to be up taken via ingestion as small particles in the water column. Furthermore, high proportions of copper in the colloid fraction have been reported in the literature, according to Hargreaves *et al.* (2017) around 52% in wastewater and zinc in the particulate fraction accounted for 32%. These percentages are similar to the exposure solutions in this present chapter, making these findings relevant for wider scenarios.

Characterising an organism's toxicity to a stressor can be complex; therefore, organising the measured effects into a toxicity pathway can help with interpretation (Figure 4.9). As ROS is a known mode of action (MoA) for trace metals, the ROS data from this thesis supports this well-accepted MoA. However, the data from this study does not show any change in oxidative DNA damage measured using the 8-oxo-dG kit, for either copper, nickel, or zinc. For this reason, the DNA damage box is purple as these data did not follow the metal toxicity pathway. Following this, changes in apoptosis were directly measured and the pathway ends with decreased survival. The data shows significantly increased ROS and apoptosis, but as the only measurement of DNA damage was 8-oxo-dG products in this chapter, this part of the pathway cannot be fully completed. One reason for this could be that the DNA assay was not sensitive, as it did not have the ability to discriminate any differences between control and experimental samples.

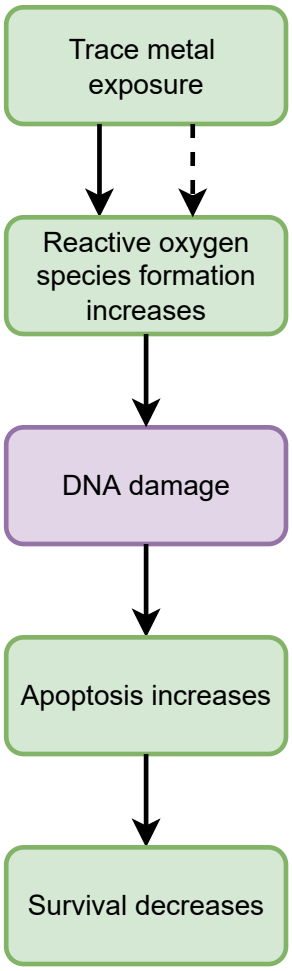

Figure 4.9. A data-orientated toxicity pathway for the short-term trace metal exposure in *Tisbe battagliai*. The solid arrow represents direct ROS generation (e.g., copper) and the dotted arrow represents indirect ROS generation (e.g., nickel and zinc). The purple box represents experimental data that did not show any change in measured DNA damage.

The exposure toxicity showed by increased ROS formation was seen after 24 hours of copper exposure, but longer for nickel and zinc. Changes at gene level happen quicker than molecular biomarker changes to stress, shown by increased oxidative stress related genes being up regulation after 12 hours. Most genes were not upregulated after 24 hours, suggesting that responses to toxicity had occurred and were no longer needed. This could explain the decreased ROS for copper at 48 hours. As copper is a known ROS inducing metal, this could be why ROS formation occurs quicker than the other two metals, which cannot directly generate ROS but cause oxidative stress by interrupting enzyme activities. Both nickel and zinc had greater ROS formation after 48 hours, potentially as they impact ROS production via an indirect route. In the marine copepod *Tigriopus japonicus*, 24 hours of high copper exposure lead to a significant 2.3-fold increase in ROS at 2 mg L^{-1} when compared to

the controls (Rhee *et al.*, 2013a). Another study on the same species found that after 96 hours of copper exposure, ROS significantly increased by 2.8-fold at 10 µg L^{-1} and 2.5-fold at 100 µg L^{-1} (Kim *et al.*, 2014a). In that study, lower concentrations over a long period were used, which resulted in higher ROS formation. In the present chapter, the copper concentrations were between 20 – 600 µg L^{-1}, where after 24 hours of exposure detected ROS was greater than at similar concentrations measured at 96 hours in *T. japonicus*, a similar sized marine copepod. This suggests that *T. battagliai* is more sensitive to copper than *T. japonicus*. In the same study by Kim *et al.* (2014a), zinc did not generate ROS in *T. japonicus* after four days of exposure at 50 and 250 µg L^{-1}. This is contrary to this Chapter's finding with zinc inducing ROS at low concentrations. In addition, the same response of no ROS generation was found in *T. japonicus* to nickel exposure (Wang and Wang, 2010), which also is contrary to this Chapter as nickel generated the highest ROS measured. Although nickel did not cause ROS production in *T. japonicus*, this could be explained by well-functioning enzymatic responses, as GST, GPx and GSH were all increased in the same study. This could suggest that *T. battagliai* could not respond to increasing nickel concentrations in the same way.

Copper-mediated ROS formation can lead to DNA damage, shown by genes related to DNA repair being upregulated (Figure 4.9). One of these genes, RAD50, is an important gene for DNA double strand repair and was responding to DNA-induced stress. Though, measured oxidative DNA damage showed only a slight increase in 8-oxo-dG products. These 8-oxo-dG results do not compliment the observed ROS formation for copper, but also nickel and zinc, as although no gene expression was measured for these two metals, they both had high ROS formation and low 8-oxo-dG. This is surprising as high ROS exposure leads to oxidative modifications of DNA and the 8-oxo-dG product is the most representative product of these modifications. This could be a limitation of sampling timings for nickel and zinc, as an increase in ROS formation was not observed until 48 hours, whilst the 8-oxo-dG DNA damage was sampled for after 24 hours. Additional sampling points at 48 or 72 hours might have provided better information for nickel and zinc, as the 24-hour response might suggest underrepresenting oxidative DNA damage. Yet, during the same 24-hour exposure, there was mortality measured for all three metals. Normally DNA damage would be measured before mortality is observed. This provides further reasoning that the assay was not sensitive for the species and using another, more sensitive assay,

such as the comet assay, could have revealed the DNA damage present. Three other marine copepod species (*Acartia tonsa*, *Temora longicornis* and *Tigriopus brevicornis*) also did not have copper-induced DNA strand breaks when exposed to concentrations up to 60 µg L^{-1} over 72 hours (Sahlmann *et al.*, 2019). In contrast, three marine zooplankton species sensitivity to copper was reported; *Paracalanus parvus* < *Oithona rigida* < *Euterpina acutifrons*, with *E. acutifrons* having up to 60% of DNA damage from a copper, nickel and zinc contaminated site (Goswami *et al.*, 2014).

For copper, the gene BAX had a significant concentration-dependent increase over 24 hours, suggesting that apoptosis regulation was required for the individuals exposed to higher concentrations. However, CASP3 remained relatively similar to the controls at both time points. The measured apoptosis supports the response seen from the BAX gene, in addition to changes in apoptosis correlating with impacted survival (Figure 4.9). Apoptosis was directly measured for *T. japonicus*, although only at one copper concentration of two mg L^{-1} (Rhee *et al.*, 2013a). There was a significant 2.3-fold increase in positive TUNEL cells present when compared to the controls after 24 hours. This result compliments the present findings.

Copper had the greatest effect on survival, followed by zinc and nickel for both juveniles and gravid females, with juveniles being more sensitive than the gravid females. The wider implications of this increased sensitivity at an earlier life stage means that populations in contaminated environments may have fewer individuals reaching sexually mature adult ages, impacting on population growth. *T. battagliai* juveniles have shown high sensitivity to copper, with EC_{50} values of 0.19 mg L^{-1} after 24 hours and 0.08 mg L^{-1} after 48 hours (Macken *et al.*, 2009). Diz *et al.* (2009) found *T. battagliai* nauplii to have a similar 48-hour LC_{50} value of 0.0831 mg L^{-1} and gravid females to be less sensitive (0.256 mg L^{-1}), complementing this chapter's findings. In addition, this order of metal toxicity has been widely reported in the literature. *Tisbe holothuriae* was most affected by copper, zinc, cadmium and nickel (Verriopoulos and Dimas, 1988) and, according to Abel (1997), copper followed by zinc and nickel decrease in toxicity for most aquatic organisms.

4.5 Conclusion

In characterising a toxicity pathway for single trace metals, this Chapter contributes additional information on metal effects at multiple biological levels for a marine copepod. Although metals are a well-studied group of contaminants in coastal environments, there are data gaps for many important invertebrate species including copepods. At the adverse outcome level, two life stages were investigated to find that juveniles are more sensitive to trace metals than adults. Furthermore, the bioavailability of different metal fractions is questioned for copepods as although copper had the lowest LMM concentration, it also exhibited the greatest toxicity, and the opposite was true for nickel. Therefore, further research is needed on the bioavailability of different metal fractions, to determine how they impact toxicity. The integrated hazard assessment applied in this Chapter provides a good understanding of single metal toxicity, which could be applied to a combined metal exposure.

Chapter 5. Effects of combined trace metals on *Tisbe battagliai*

5.1 Introduction

The European Union produced 78.8 million tonnes of chemicals classified as hazardous to the environment in 2020 (Eurostat, 2020), frequently contaminating coastal environments with untreated waste and chemicals, mostly originating from land-based sources (industrial and domestic) (Pan and Wang, 2012). Marine organisms are exposed to many of these as complex mixtures (Pitombeira de Figuerêdo *et al.*, 2016). It is essential to understand the complexity of mixtures and their adverse outcomes on marine life of regulatory importance as the focus of risk assessment shifts from single stressors and their adverse outcomes, to combined stressors (Tan *et al.*, 2018). Mixtures can be more toxic than their individual components, even when the individual components are present at concentrations where the single exposure would show no observed effect (NOEC) (Beyer *et al.*, 2014). This increased toxicity is due to non-interaction effects (e.g., additive) or synergistic interactions between interacting components. An additive effect occurs when the mixture toxicity equals the addition of the individual component's toxicity, while a synergistic effect multiplies the individual component's toxicity (Rodea-Palomares *et al.*, 2015). The third option for a mixture is being less toxic than expected, having antagonistic interactions between components. It is therefore important to understand the change in impact that metals can have when in a mixture.

There are several levels of interactions occurring within mixtures: firstly, in the exposure phase between the metals, secondly with active or passive uptake (toxicokinetics), and thirdly with the biological targets and downstream effects (toxicodynamics). Interactions between metals, occurring at biological uptake sites, are the result of similar physical and chemical properties, affecting metal accumulation and, in turn, metal toxicity (Kamunde and MacPhail, 2011). The mechanisms of metal interactions are complex and disputed in the literature. For example, copper and zinc belong to the same metal group, with comparable ionic radii and binding affinity to organic macromolecules, suggesting that competitive interactions would occur in a mixture; however, both metals have competitive and non-competitive effects at uptake sites when combined (Kamunde and MacPhail,

2011). This could be explained by a change in metal fractionation and other interactions occurring in the exposure medium (abiotic factors) (Teien, Standring and Salbu, 2006; Caporale and Violante, 2016; Simonsen *et al.*, 2019). Metals can be present as ions (low molecular mass - LMM), colloids or particles. A change from LMM to colloid could therefore impact the metals interactions and how the fraction is taken up (accumulated in) by the organism. Additionally, the presence of another metal or chemical can increase the uptake of necessary trace metals by facilitated up take, leading to increased body burdens. As metal fractionation and interactions are fundamental to evaluating potential mixture toxicity, both fractionation and toxicity can be determined in an integrated exposure and effects study. Commonly, exposure and effects are determined separately; however, toxicity cannot be fully characterised without both being measured simultaneously.

Metals in a complex mixture contribute to combined effects and can be modelled via concentration addition (CA) and independent action (IA) (Petersen and Tollefsen, 2011). CA assumes that all stressors in the mixture affect the same target to cause the adverse outcome, i.e., the stressors have a similar mode of action (MoA). IA leads to the same outcome but each stressor in the mixture impacts a different target, assuming different MoAs (Beyer *et al.*, 2014). The CA model was first introduced by Loewe and Muischnek (1926) and was followed by the IA model in 1939 (Bliss, 1939). These models are a reference for additive effects; therefore, deviations from these models can be recognised as synergistic or antagonistic effects (Petersen, Heiaas and Tollefsen, 2014). In risk assessments, the use of the CA model has been more common as it is more conservative than IA and often a good approximation for mixtures; however, this can result in incorrect mixture toxicity estimations as only non-interactions are assumed, and in turn misinform hazard assessments and chemical management (Deruytter *et al.*, 2017). Using these models, the combined effects of metals could be additive (Yoo *et al.*, 2021; Damasceno *et al.*, 2017), synergistic (Yoo *et al.*, 2021; Deruytter *et al.*, 2017) and antagonistic (Deruytter *et al.*, 2017; Damasceno *et al.*, 2017) in marine organisms.

In this Chapter, *Tisbe battagliai* is studied using a cumulative hazard assessment with three-metal mixtures comprising copper, nickel, and zinc. Each metal mixture contained different ratios of each metal (different concentrations), following a previously established metal-induced toxicity pathway in Chapter 4. This pathway initiates with reactive oxygen species (ROS) formation, leading to oxidative DNA

damage and apoptotic cellular damage, impacting on survival. This integrated assessment is achieved using Definitive Screening Design (DSD) - an iteration of the Design of Experiments statistical approach previously used in Chapter 3. In short, a DSD approach reduces the number of experimental runs required to characterise toxicity by using mixture solutions that contain different ratios of each component to understand the highest toxicity (i.e., most forcing) and lowest toxicity (i.e., least forcing) observed in the design space (Jones and Nachtsheim, 2011). With the addition of centre points into the design, the curvature of the line can be determined, to produce response surface profiles for well-fitting data.

5.2 Materials and Methods

5.2.1 Tisbe battagliai cultures

Stock and experimental conditions for *T. battagliai* were conducted under the same conditions as described in Chapter 4.2.1.

5.2.2 Exposure set up and combined metal models

This combined metal study used the same three metals as the single metal study (Chapter 4.2.2). Metal stock solutions were made in an identical way and stored under the same conditions as described in Chapter 4. Single metal concentration dose response curves and LC_x values were used to select concentrations for each metal within the mixture, following the DSD (Chapter 3.2.3). Briefly, this DSD approach used fourteen runs (mixture solutions), with each run (exposure solution) containing all three metals at different concentrations. The design uses the least forcing (lower concentration; single metal LC_{20} value), the centre point (mid concentration; approximately the single metal LC_{50} value) and the most forcing values (higher concentration; single metal LC_{80} value) for each three metals to design mixture solutions using different concentrations of each metal simultaneously. Solution four and eleven contain the same concentrations of each metal, to add centre points into the design to check the curvature of the line. Controls were added to each block (solution 15). This was conducted in triplicate as a minimum and separately for juvenile (Tables 5.1) and gravid female (Table 5.2) *T. battagliai* as they have different LC_x values.

Mean results were inputted into JMP Pro 15.2.0 (SAS Institute, NC, USA) and firstly a definitive screening was fitted to the data to identify main effect drivers (a single

metal driving the mixture effects) and second order effect estimates (whether the metal pairs – copper and nickel, copper and zinc and copper and nickel – within the three-metal mixture are causing the mixture effects). Depending on the outcome of the definitive screening, a standard least squares combined model was then ran to produce prediction profilers, surface profilers and interaction plots (Jones and Nachtsheim, 2011).

Table 5.1. Definitive screening mixture design for juvenile *Tisbe battagliai* and total concentrations (µM) of copper, nickel, and zinc added to each run (solution). For each metal, the mixture design, with minus (-) indicating least forcing, zero (0) indicating centre point, plus (+) indicating most forcing and the concentration used is shown. Actual concentrations measured on an ICP-MS are displayed.

Run	**Block**	**Copper concentration µM**		**Nickel concentration µM**		**Zinc concentration µM**	
1	1	-	1.06	-	3.05	-	1.48
2	1	-	1.06	+	15.50	0	3.71
3	1	0	2.37	-	3.05	-	1.48
4	1	0	2.37	0	9.58	0	3.71
5	1	0	2.37	+	15.50	+	5.52
6	1	+	3.61	-	3.05	0	3.71
7	1	+	3.61	+	15.50	+	5.52
8	2	-	1.06	-	3.05	+	5.52
9	2	-	1.06	0	9.58	+	5.52
10	2	-	1.06	+	15.50	-	1.48
11	2	0	2.37	0	9.58	0	3.71
12	2	+	3.61	-	3.05	+	5.52
13	2	+	3.61	0	9.58	-	1.48
14	2	+	3.61	+	15.50	-	1.48
Control	1 & 2	Control	0.00	Control	0.00	Control	0.00

Table 5.2. Definitive screening mixture design for gravid female *Tisbe battagliai* and total concentrations (µM) of copper, nickel, and zinc added to each run (solution). For each metal, the mixture design, with minus (-) indicating least forcing, zero (0) indicating centre point, plus (+) indicating most forcing and the concentration µM used is shown. Actual concentrations measured on an ICP-MS are displayed.

Run	Block	Copper concentration µM		Nickel concentration µM		Zinc concentration µM	
1	1	-	0.6	-	11.08	-	2.99
2	1	-	0.6	+	68.63	0	5.48
3	1	0	1.28	-	11.04	-	2.99
4	1	0	1.28	0	39.64	0	5.48
5	1	0	1.28	+	68.63	+	9.53
6	1	+	2.19	-	11.08	0	5.48
7	1	+	2.19	+	68.63	+	9.53
8	2	-	0.6	-	11.08	+	9.53
9	2	-	0.6	0	39.64	+	9.53
10	2	-	0.25	+	68.63	-	2.99
11	2	0	1.28	0	39.64	0	5.48
12	2	+	2.19	-	11.08	+	9.53
13	2	+	2.19	0	39.64	-	2.99
14	2	+	2.19	+	68.63	-	2.99
Control	1 & 2	Control	0.00	Control	0.00	Control	0.00

5.2.3 Characterisation of metal fractionation

Water fractionation was conducted prior to the start of the gravid female *T. battagliai* experiments. This was to determine the bioavailability of the metal ions when in a combined solution. This was conducted following the same water fractionation protocol detailed in Chapter 4.2.2, with a few adaptations. One litre of each combined metals solution in 30 ppt artificial seawater (ASW) was made and left to rest at room temperature (19°C) and in darkness for 24 hours before water fractionation was conducted. The hollow fibre was cleaned between each sample as there were multiple metals in each solution and blank samples were taken after each clean to check for any remaining metal residue. Metals were present in solutions as particles, colloids, and LMM fractions. The ICP-MS analysis was only performed for the exposure solutions at the beginning of experiments.

5.2.4 Predicted mixture responses

Concentration addition (CA) and independent action (IA) models were conducted for juveniles and gravid females in Microsoft Excel (version 16.56). Single survival data for each metal were used to calculate predicted survival. All single metal data were

normalised (0 – 100) and a sigmoidal dose response with a variable slope and constraints (minimum zero and maximum 100) were used to fit the data.

For the CA model, the sigmoidal dose response slope, EC_{50}, and maximum and minimum values from each metal were used. Equation 1 was used to calculate the predicted effect from the total mixture concentration of the three metals, where $EC_{x(mix)}$ = the predicted total concentration of the mixture that gives X% effect, p_i = the relative fraction of the component *i* in the mixture, and EC_{x_i} = the concentration of component *i* provoking a certain effect (x) when applied alone.

$$\mathrm{ECx}_{(\mathrm{mix})} = \left(\sum_{\mathrm{i}-1}^{\mathrm{n}} \frac{\mathrm{p_i}}{\mathrm{ECx_i}}\right)^{-1} \quad \text{-- (Eq 5.1)}$$

For IA, the same single metal sigmoidal dose response data were used, and effects were given as a percentage of the controls as given in Equation 2, where E_{mix} = the effect of the mixture of n components, and E_i = the effect of substance *i* when applied alone.

$$\mathrm{E_{Mix}} = 1 - \prod_{\mathrm{i}=1}^{\mathrm{n}}(1 - \mathrm{E_i}) \quad \text{-- (Eq 5.2)}$$

For the mixture design, the EC_{50} level was chosen to calculate the equi-effective concentration ratios, ensuring that all metals were contributing to the mixture effect rather than one metal being solely responsible for the predicted effects. These mixture data for CA and IA predictions were imported into GraphPad Prism 9 (GraphPad Software Inc., California, USA) and a non-linear regression performed to calculate EC_{50} values for each CA and IA model after 24 and 48 hours of exposure. Afterwards, CA and IA models for each mixture solution conducted in the DSD were produced (14 solutions in total for each life stage, using the original concentrations for juveniles), using the same metal ratios and concentrations to allow direct predicted and measured data comparisons. Parameters from the regression were used to quantify the predictive accuracy of each model using the model deviation ratio (MDR) that is calculated by dividing the predicted toxicity by the observed toxicity. These MDR values were used to determine whether the mixture was antagonistic (< 0.5), additive (≥ 0.5 and > 2) or synergistic (≥ 2).

5.2.5 Acute toxicity test – survival

For both juveniles and gravid females, survival was defined using an immobility assay (Chapter 4.2.2) after 24 and 48 hours of exposure to combined metal solutions. The individual is recorded as being alive if they respond by moving after being gently prodded with a pipette tip within 10 seconds.

5.2.6 Reactive oxygen species formation

Cellular reactive oxygen species (ROS) formation was determined *in vivo* following combined metal experiments using the probe 2'7'-dichlorodihydrofluorescein diacetate (H_2DCFDA, Invitrogen, Molecular Probes Inc., Eugene, OR). This was conducted following the same methodology described in Chapter 4.2.1. Briefly, a final concentration of H_2DCFDA of 0.5 µM was exposed to each alive gravid female replicate for two hours. Fluorescence was measured using a VICTOR^3™ plate reader (PerkinElmer, MA) at emission wavelength 535 nm and excitation wavelength 485 nm and data were normalised to individual gravid female length.

5.2.7 DNA extraction

Twenty gravid female *T. battagliai* were pooled per replicate following 24-hours of exposure to each mixture solution. These samples were frozen and extracted following the same procedure detailed in Chapter 4.2.6. In brief, the Quick-DNA™ Tissue/Insect Microprep Kit (Zymo Research Corporation, Irvine, CA, USA) was used with reductions in the starting material and starting volumes. Once eluted, the extracted DNA was frozen at -20 °C until the oxidative DNA damage assay was conducted.

5.2.8 Oxidative DNA damage quantification

Oxidative DNA damage was quantified in the isolated DNA using the EpiQuik™ 8-oxo-dG DNA Damage Quantification Direct Kit (Fluorometric) (Epigentek Group Inc., Farmingdale, NY, USA). The same protocol as described in Chapter 4.2.7 was followed, starting with 50 ng of DNA and ending with fluorescence signal detection of sufficient 8-oxo-dG products using a TECAN Spark 20m fluorescence microplate reader. The standard curve was generated using known concentrations of 8-oxo-dG (ng) standards that were provided by the manufacturers in the kit. As the 8-oxo-dG damage concentration is known in these standards (for example 50 ng), the relative fluorescence units measured from the fluorescence plate reader for the standards

were plotted, and a line of best fit added (Figure 5.1). Using the slope value from this standard curve allowed absolute quantification of 8-oxo-dG DNA damage in experimental samples, rather than presenting the data as fold change from the controls, as presented in Chapter 4. Absolute quantification was calculated using sample relative fluorescence units (RFU) and standard curve slope (Figure 5.1):

$$8-\mathrm{OHdG\ (ng)} = \frac{(\mathrm{Sample\ RFU} - \mathrm{NC\ RFU})}{\mathrm{Slope}}$$

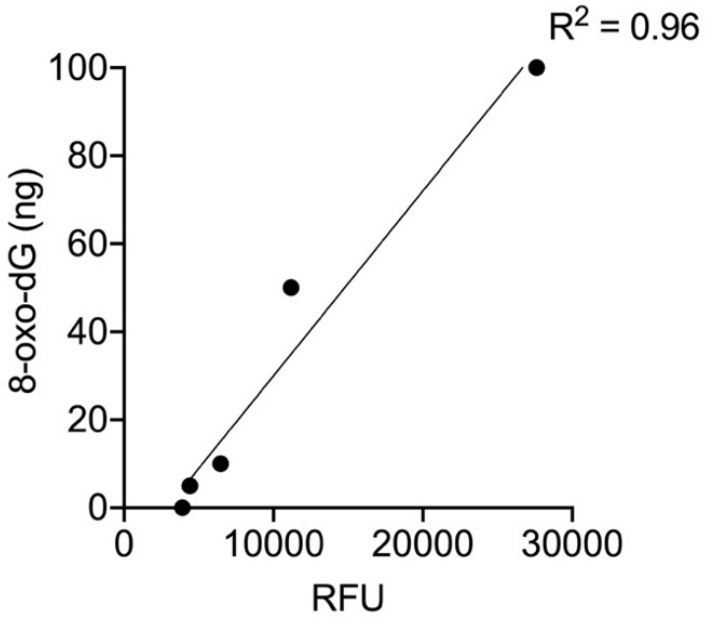

Figure 5.1. Standard curve for 8-oxo-dG DNA damage quantification. A simple linear regression was fitted to calculate the slope value and produce a R^2 value based on goodness of fit.

5.2.9 Apoptosis

The In Situ Cell Death Detection Kit Fluorescein (Roche, Basel, Switzerland) was used to measure apoptotic cellular death in gravid individual females following 24-hours of combined metal exposure (see Chapter 4.2.8 for details). In short, an individual gravid female was homogenised and exposed to the TUNEL dye at 37 °C for 90 minutes. The TUNEL fluorescence was measured immediately at excitation 450 – 500 nm and emission 515 – 565 nm using a TECAN Spark 20m fluorescence microplate reader.

5.2.10 Statistical analysis

A simple linear regression was fitted to the metal fractionation data. Additionally, CA and IA responses were log_{10} transformed and normalised to be used a non-linear regression was used to calculate LC_{50} values after 24 and 48 hours. All statistical analyses were conducted using GraphPad Prism 8.

To analyse the combined metals data, the measured responses for each endpoint were imported into JMP Pro 15.2 (SAS Institute, Cary, North Carolina, USA) and the definitive screening was fitted to the data. This provides main effect, and second order effect estimates and accompanying P-values. The least squares model is fitted to the data, and surface profiler and interaction plots were produced. Data were also analysed in GraphPad Prism 9 (GraphPad Software Inc., California, USA) to perform Pearson correlation coefficients using the total mixture solution concentration. This was calculated by adding all three metal concentrations together to gain a total mixture concentration.

5.3 Results

5.3.1 Exposure characteristics

Elemental composition of the artificial seawater showed expected concentrations as reported by manufacturer at the salinity used in all experiments (30 ppt) (Jarosz *et al.*, 2022). The physiochemical parameters remained within their expected ranges in accordance with the mixture study protocol designed for MixRisk studies with *T. battagliai*, with a salinity of 30 ppt, temperature of 19.0 ± 1^{o}C and pH of 8.1 ± 0.2.

5.3.2 Metal fractionation characteristics

Nickel and zinc were dominated by the LMM fraction (Figures 5.2B and 5.2C), with nickel having an absence of colloids and particles in most of the mixture solutions (Table 5.3). The LMM fraction contributed least to copper exposure, with copper being mostly present in the colloidal form (Figure 5.2A). This was consistent across all three copper concentrations used in the mixtures (colloids were 43.52 – 80.62%) and all three fractions showed significant positive correlations with total concentration (Pearson correlation coefficient r, $P < 0.05$). Only LMM had a significant positive correlation with total concentration for nickel, whereas both colloidal and particulate fraction concentrations had a significant negative correlation. For zinc, only colloids and LMM had a significant positive correlation.

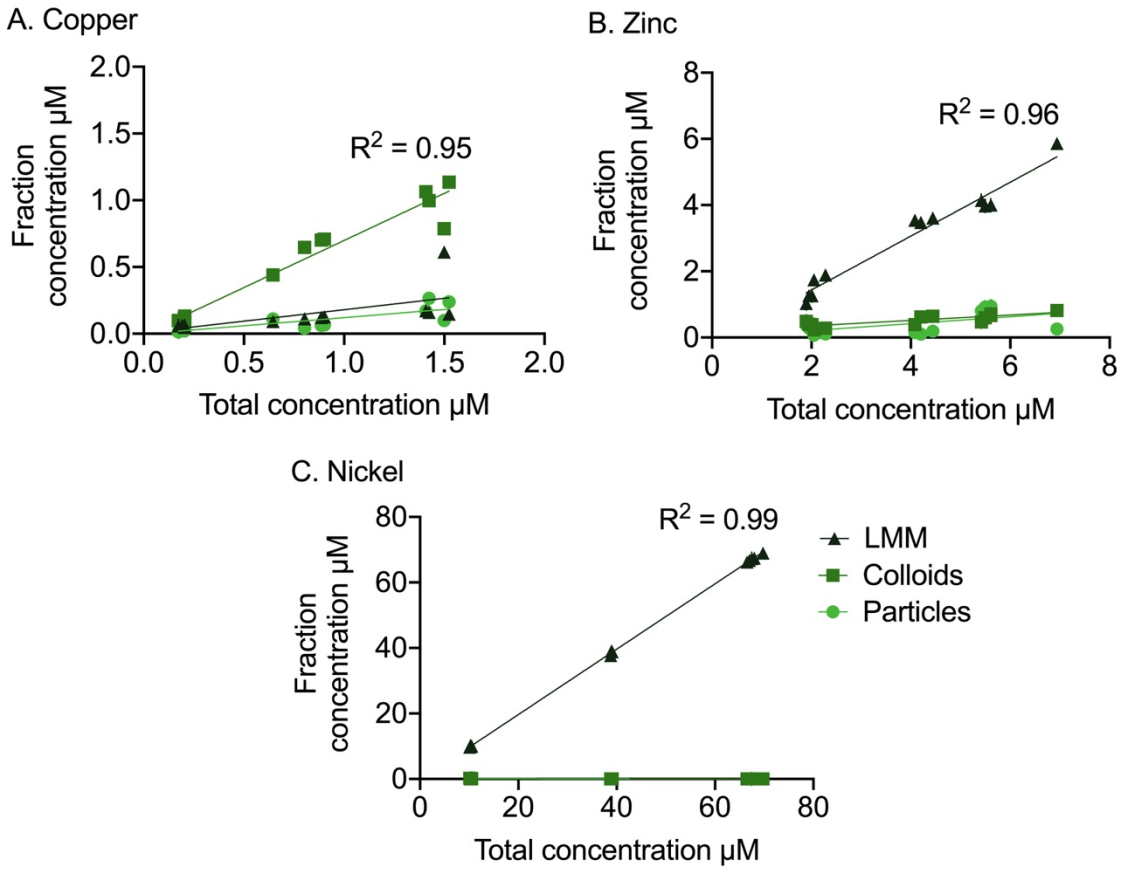

Figure 5.2. Metal fractionation of 13 combined metal solutions exposed to gravid female *Tisbe battagliai*, containing varying concentrations of: (A) copper, (B) zinc, and (C) nickel in 30 ppt artificial seawater (0.22 µm filtered). As solutions 4 and 11 are the same, data were collected for one solution. The water samples represent the combined solutions at the beginning of the combined experiments (0 hour). All samples were measured on an ICP-MS and a simple linear regression was fitted for each fraction for each metal, with R^2 values reported for the main fraction present.

Table 5.3. Percentages of each fraction (particles, colloids, and low molecular mass (LMM)) of copper, nickel, and zinc when combined in different concentration ratios in 14 solutions. Solution (Sol.) 4 and 11 are the same solution (centre points).

	Copper			**Nickel**			**Zinc**		
Sol.	Particles %	Colloids %	LMM %	Particles %	Colloids %	LMM %	Particles %	Colloids %	LMM %
1	8.83	57.35	33.82	2.45	1.69	95.86	3.47	11.39	85.15
2	9.80	58.33	31.88	0.00	0.00	99.16	4.34	14.50	81.16
3	7.35	78.62	14.03	3.57	1.08	95.34	4.67	12.44	82.89
4 / 11	5.36	80.62	14.02	0.00	0.00	100.4	2.42	14.86	82.73
5	7.01	79.14	13.85	0.00	0.00	99.62	3.65	11.81	84.54
6	6.63	52.49	40.88	0.00	0.00	100	3.60	9.57	86.83
7	17.27	68.29	14.45	0.00	0.00	99.75	16.71	10.90	72.39
8	12.10	64.74	23.17	1.63	2.19	96.18	16.00	12.66	71.34
9	24.19	48.91	26.90	0.00	0.00	97.21	16.82	11.84	71.34
10	24.35	43.52	32.13	0.00	0.00	99.57	19.97	25.80	54.22
12	12.15	75.56	12.29	2.20	0.11	97.69	14.79	8.71	76.50
13	15.76	74.59	9.65	0.00	0.00	99.27	14.58	20.65	64.77
14	18.63	70.03	11.34	0.00	0.00	98.86	17.68	19.32	63.01

5.3.3 Predicted survival

Predicted mixtures using CA and IA modelling of copper, nickel, and zinc had a predicted greater effect on juvenile survival than gravid female survival (Figure 5.3). As expected, the predicted curves shifted left along the x-axis for both life stages after 48 hours when compared to 24 hours. CA predictions for juveniles had a 24-hour EC_{50} value of 8.409 µM and 48-hour EC_{50} value of 5.466 µM. These were higher than IA predicted values of 10.03 µM and 6.014 µM respectively. For gravid females, CA had a greater predicted mortality with a 24-hour EC_{50} value of 18.09 µM and 48-hour EC_{50} value of 16.73 µM when compared to the IA mixture values of 32.09 µM and 23.32 µM respectively. Predicted mixture designs for 24-hour juvenile data indicate that zinc is the main driver at low mixture concentrations and nickel is the main driver at high mixture concentrations. At 48 hours, zinc remains the predicted main driver at low mixture concentrations, but copper is the main driver at high mixture concentrations. For gravid females, 24- and 48-hour design indicates

that copper is the main driver at low mixture concentrations. For high mixture concentrations, nickel is the main driver at 24 hours and zinc at 48 hours.

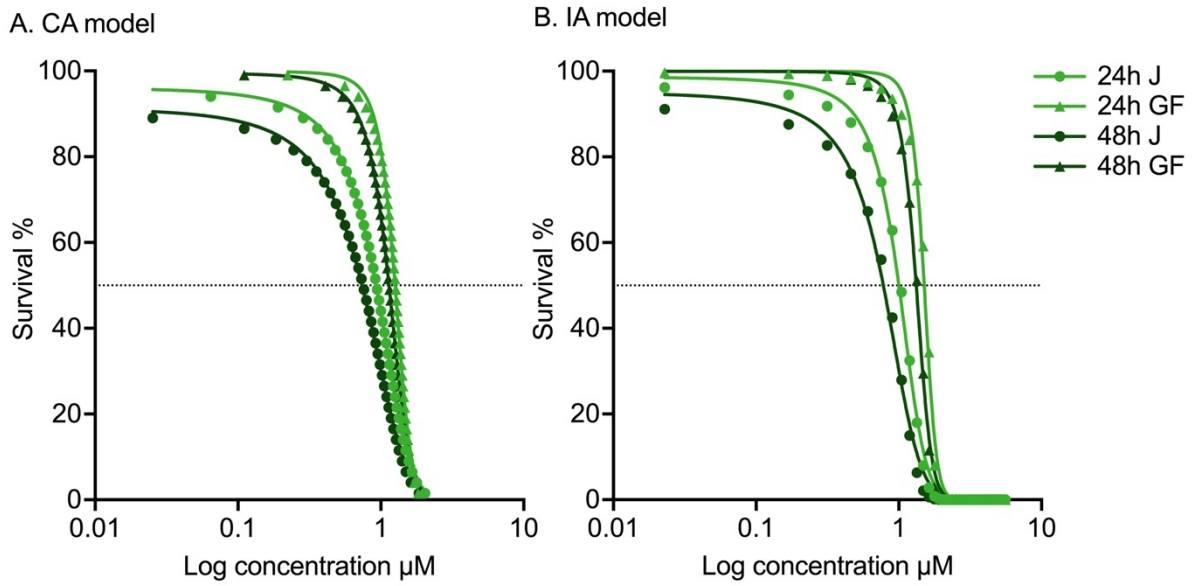

Figure 5.3. Concentration addition (CA) and independent action (IA) response curves for survival predictions for combined copper, nickel, and zinc exposure to juvenile (J) and gravid female (GF) *Tisbe battagliai* for 24- and 48-hour exposures.

Most of the mixture solutions exposed to the juvenile individuals were well predicted by IA at both time points (Figure 5.4). Measured data overlapped better with IA predictions than CA predictions, particularly at 24 hours, indicating different MoA for the metals in the mixtures. At 48 hours, the seven mixture solutions with surviving individuals were similarly predicted by both models as nearly all the MDR values were within a factor of two (Table 5.4). Most of these mixtures were additive and antagonistic, with only one MDR value greater than two, suggesting synergistic interactions in mixture ten as the only one at 24 hours exposure. Interestingly, all the solutions at 24 hours with MDR values below 0.5 (i.e., indicating antagonism) for both models contained the lowest nickel concentrations, but all the possible copper and zinc concentrations. At 48 hours, these solutions caused either total mortality (solutions six and twelve, MDR value cannot be calculated) or both models predicted higher than 0.5 for the MDR values (solutions one and three). This indicates that these mixtures consist of metals displaying a time-dependent effect on juvenile survival.

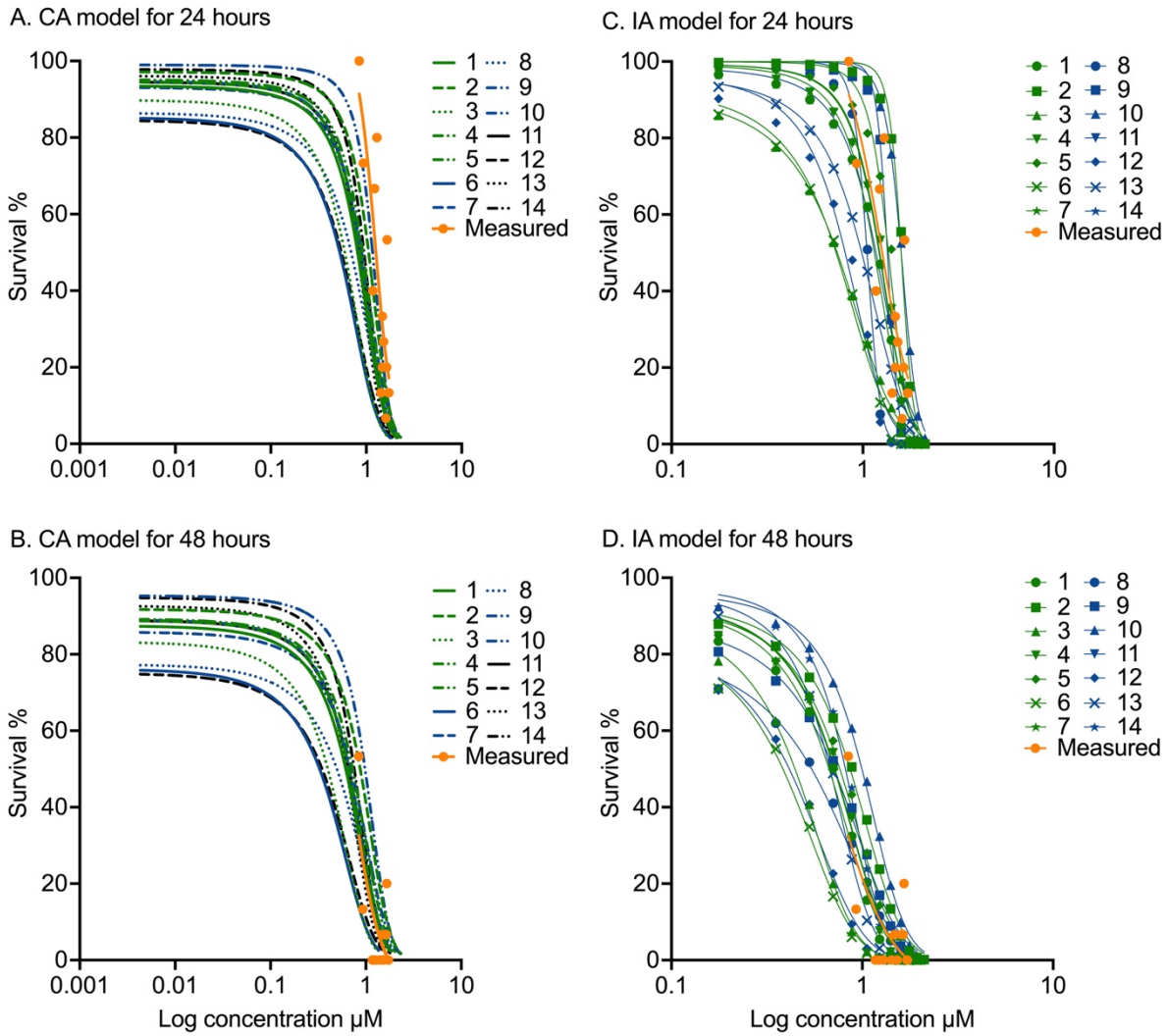

Figure 5.4. Concentration addition (CA) and independent action (IA) response curves for survival predictions for 14 mixture solutions (green lines) exposed to juvenile *Tisbe battagliai* for 24 (A and C) and 48 hours (B and D). Orange lines represent the measured mixture data.

Table 5.4. Model deviation ratios (MDRs) for 14 mixture solutions exposed to juvenile *Tisbe battagliai* for 24 and 48 hours. Yellow values indicate when the MDR values are within a factor of two (additivity), green values indicate antagonism, red values indicate synergy and – indicates that no value could be calculated due to total mortality measured.

Mixture solution	24 hours		48 hours	
	MDR CA	MDR IA	MDR CA	MDR IA
1	0.00	0.02	**0.53**	**0.62**
2	0.23	**0.83**	**0.52**	0.43
3	0.25	0.32	**0.86**	**0.74**
4	0.39	**1.00**	**1.06**	**1.08**
5	**0.62**	**0.85**	-	-
6	0.30	0.46	-	-
7	**0.50**	**0.84**	-	-
8	0.16	**0.59**	-	-
9	**0.53**	**0.81**	-	-
10	**1.71**	2.50	**1.71**	**1.46**
11	**0.63**	**1.13**	**1.06**	**0.80**
12	0.06	0.16	-	-
13	**0.74**	**1.28**	-	-
14	0.45	**0.81**	**0.64**	**0.54**

For gravid females, IA predictions were more comparable to measured data than CA predictions (Figure 5.5). Measured data at both time points showed greater survival than predicted by CA and IA. In support, most mixture solutions showed deviations outside both models greater than a factor of two, leading to lower than 0.5 MDR values and indicating that antagonistic interactions were occurring (Table 5.5). At 48 hours, most of the mixture solutions were better predicted by IA, rather than CA, suggesting additive interactions were occurring due to the chemicals having different MoAs.

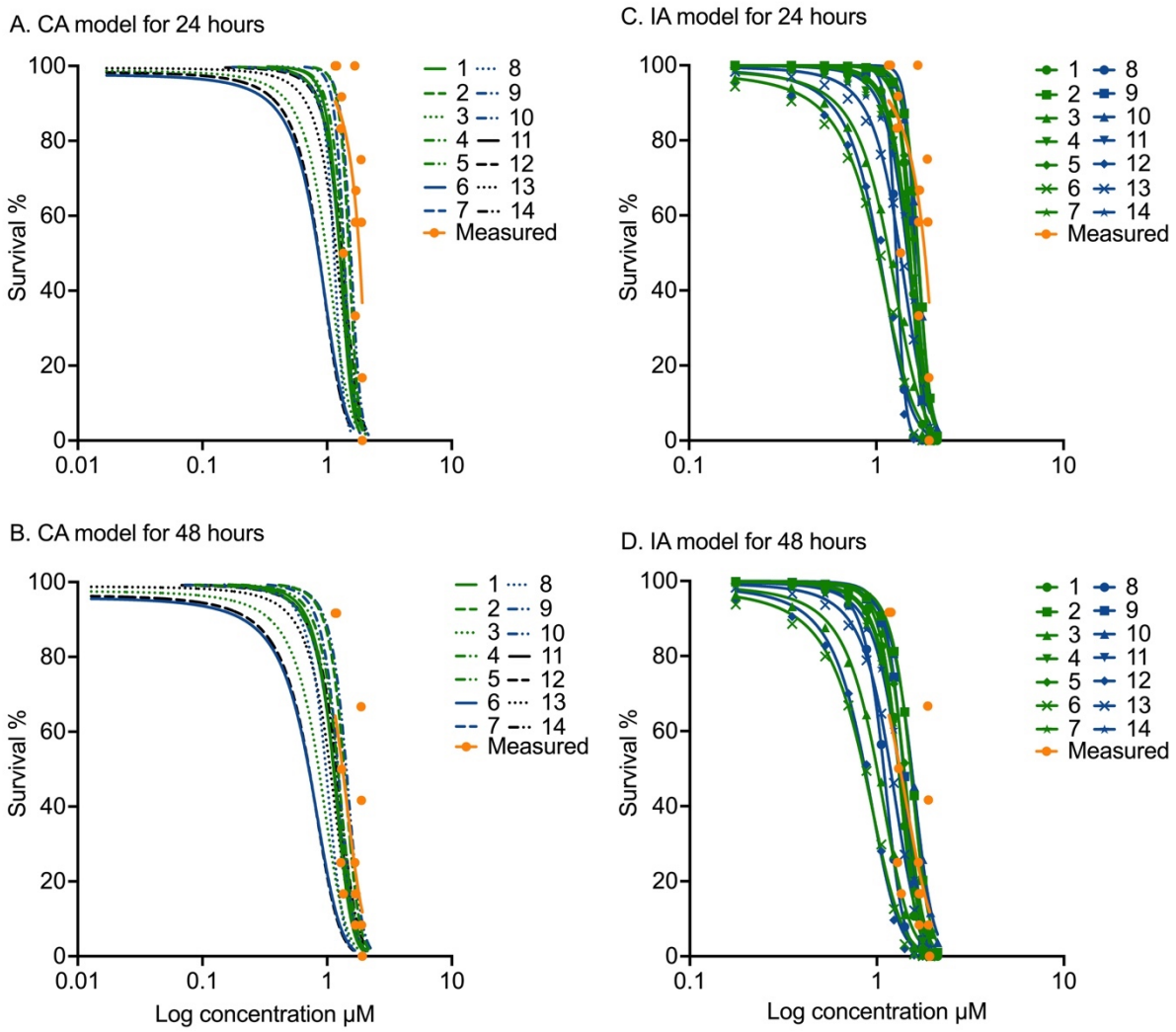

Figure 5.5. Concentration addition (CA) and independent action (IA) concentration response curves for survival predictions for 14 mixture solutions exposed to gravid female *Tisbe battagliai* for 24 (A and C) and 48 hours (B and D). Orange lines represent the measured mixture data.

Table 5.5. Model deviation ratios (MDRs) for 14 mixture solutions exposed to gravid female *Tisbe battagliai* for 24 and 48 hours. Yellow values indicate when the MDR values are within a factor of two (additivity), green values indicate antagonism, and – indicates that no value could be calculated due to total mortality measured.

Mixture solution	24 hours		48 hours	
	MDR CA	MDR IA	MDR CA	MDR IA
1	0.05	0.20	0.32	**0.61**
2	0.37	**0.55**	**0.90**	**1.15**
3	0.01	0.00	0.13	0.19
4	**0.52**	**1.01**	**0.93**	**1.33**
5	**0.51**	**0.75**	-	-
6	0.16	0.21	0.27	0.37
7	-	-	-	-
8	0.36	**0.62**	0.47	**0.60**
9	0.39	**0.70**	**0.65**	**0.82**
10	0.33	0.43	0.25	0.33
11	0.33	**0.57**	**0.63**	**0.83**
12	0.32	0.48	**0.52**	**0.67**
13	0.00	0.00	0.45	**0.57**
14	0.23	0.33	0.24	0.31

5.3.4 Measured survival

For juvenile *T. battagliai*, there was no main effect driver found from the definitive screening after 24 or 48 hours, but nickel was close to being significant at both time points (P = 0.0573 and P = 0.0606 respectively). However, the standard least square combined model estimated that nickel was significant after 24 hours (P = 0.0385).

Within the three-metal mixtures for gravid females, copper, nickel, and zinc were all identified as main effect drivers for reducing survival after 24 hours (P = 0.0254, 0.0029 and 0.0033, respectively) from the definitive screening fit (Figure 5.6), with interactions between copper*zinc and copper*nickel being significant in the combined model (P = 0.0083 and 0.0368, respectively) (Figure 5.7). The interaction between nickel*zinc was close to being significant, with a P-value of 0.0525. Following the 48-hour exposure to the three-metal mixtures, copper, nickel, and zinc were all identified as main effect drivers for survival (P = 0.0349, 0.0187 and 0.0063 respectively) (Figure 5.6). There were no significant interactions between any metal pairs (P > 0.05) (Figure 5.8).

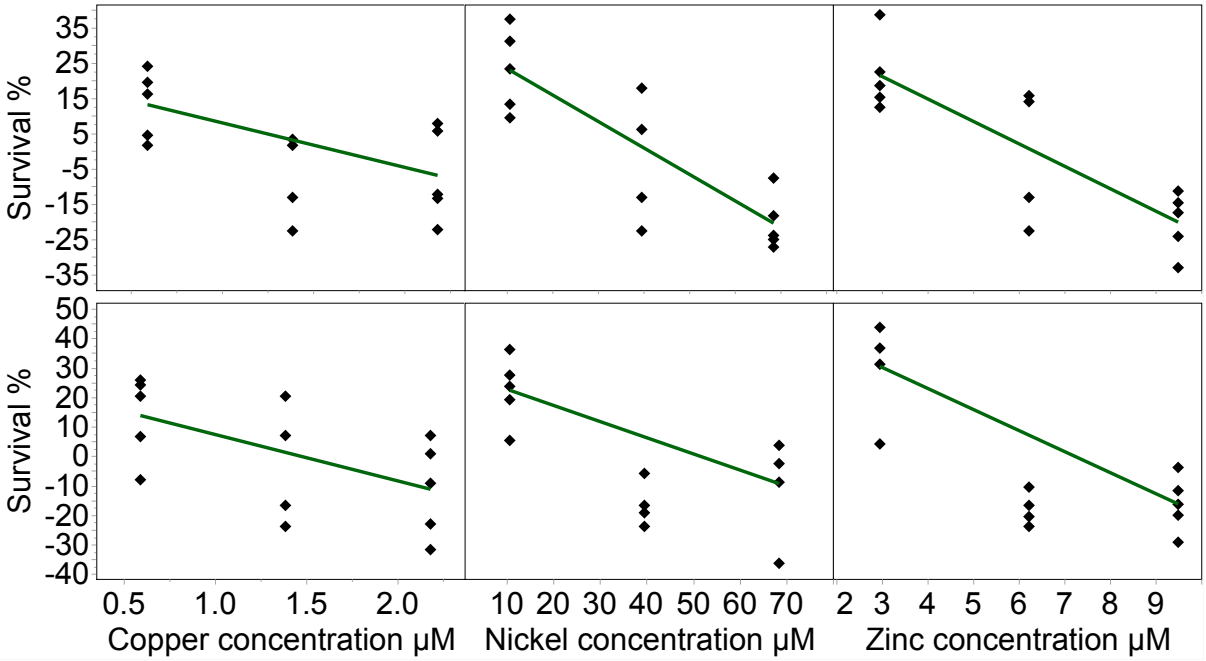

Figure 5.6. Linear regressions of the relationship between mixture factors and percentage survival for 14-day old gravid female *Tisbe battagliai* after 24 hours (top) and 48 hours (bottom) of mixture exposure. Copper, nickel, and zinc were the three factors within the mixtures. Each diamond represents one mixture solution (14 in total) and is shown three times, once per metal, to show the concentration of each metal within the mixtures.

A. Copper and nickel

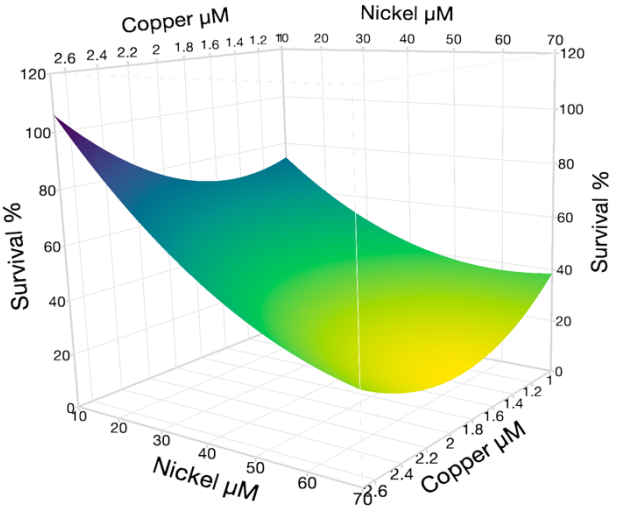

B. Copper and zinc

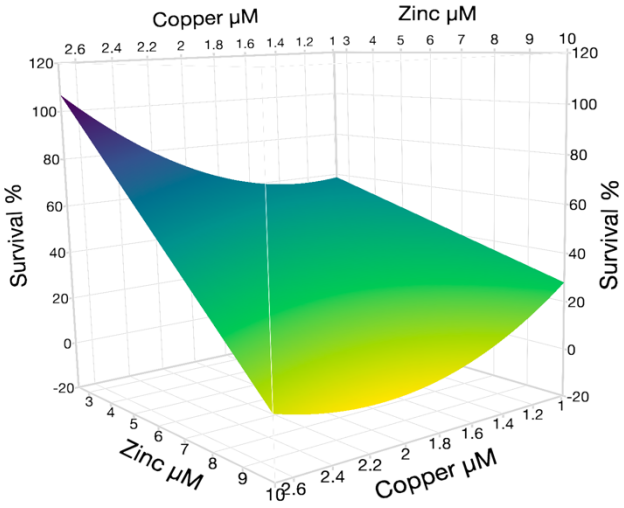

C. Nickel and zinc

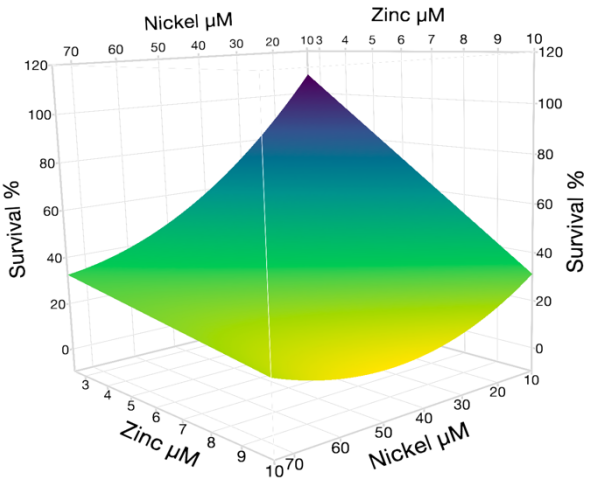

Figure 5.7. Response surface profile for measured gravid female *Tisbe battagliai* survival after 24-hour exposure to three-metal combined solutions containing copper, nickel, and zinc. Each sub-figure shows data for two metals from the three-metal mixture. (A) copper and zinc, (B) copper and nickel and (C) nickel and zinc.

A. Copper and nickel

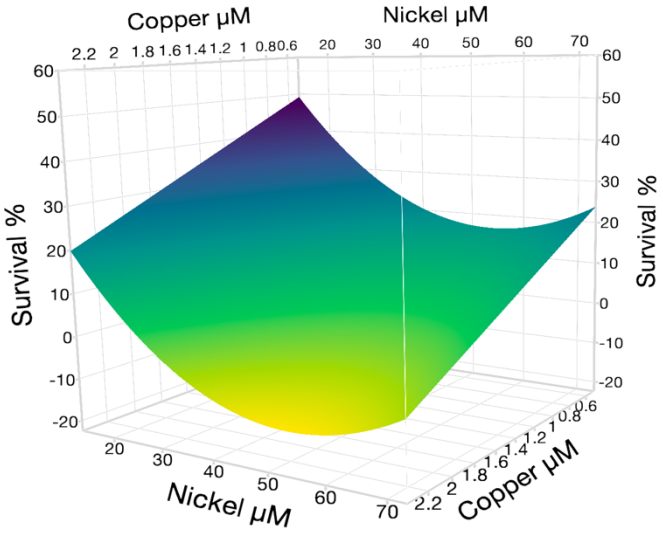

B. Copper and zinc

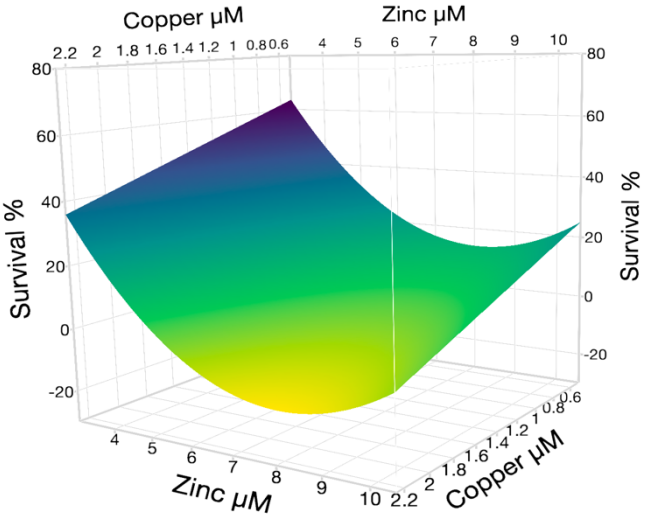

C. Nickel and zinc

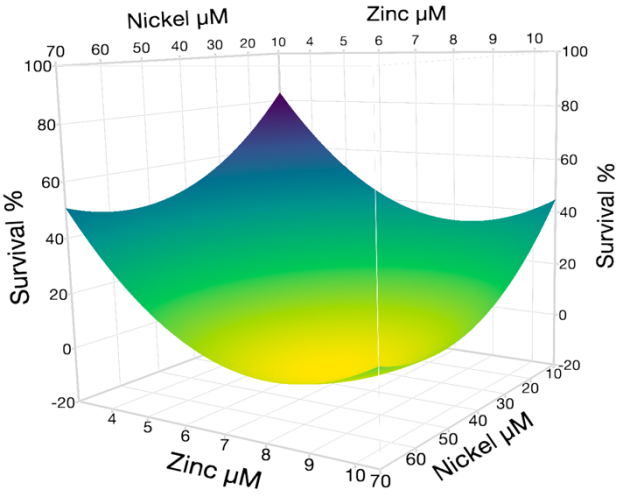

Figure 5.8. Response surface profile for measured gravid female *Tisbe battagliai* survival after 48-hour exposure to three-metal combined solutions containing copper, nickel, and zinc. Each sub-figure shows data for two metals from the three-metal mixture. (A) copper and zinc, (B) copper and nickel and (C) nickel and zinc.

5.3.5 Reactive oxygen species production

There was no main metal driving the mixture effects found for ROS production after 24 hours (nickel P = 0.167, copper P = 0.216 and zinc P = 0.8362). Although there was no correlation between ROS production and total mixture concentration (Pearson correlation analysis, P = 0.644), solutions 8 and 12 did trigger an 8- and 8.6-fold increase in ROS generation.

5.3.6 Oxidative DNA damage

There was no main effect driver found for oxidative DNA damage, though nickel was close to being significant P = 0.0641 (Figure 5.9 and 5.10). The paired effects of copper*nickel, copper*zinc and nickel*zinc within the mixtures were significant, driven by nickel according to the prediction profiles (P < 0.0001). Additionally, the copper*nickel, copper*zinc, and nickel*zinc pairs within the combined three-metal mixture had non-parallel interaction profiles, showing that the effect of each metal on DNA damage changed as other metal concentrations changed.

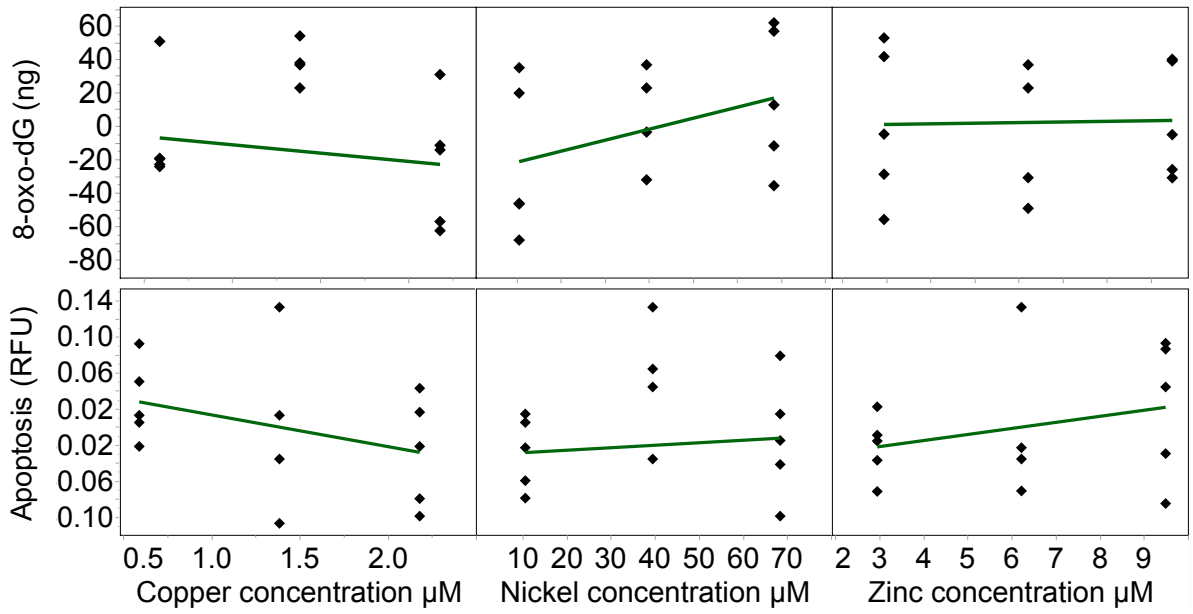

Figure 5.9 Linear regressions of the relationship between mixture factors and 8-oxo-dG DNA damage (top) and apoptosis (relative fluorescence units RFU) (bottom) for *Tisbe battagliai* after 24 hours of mixture exposure. Copper, nickel, and zinc were the three factors within the mixtures. Each diamond represents one mixture solution (14 in total) and is shown three times, once per metal, to show the concentration of each metal within the mixtures.

A. Copper and nickel

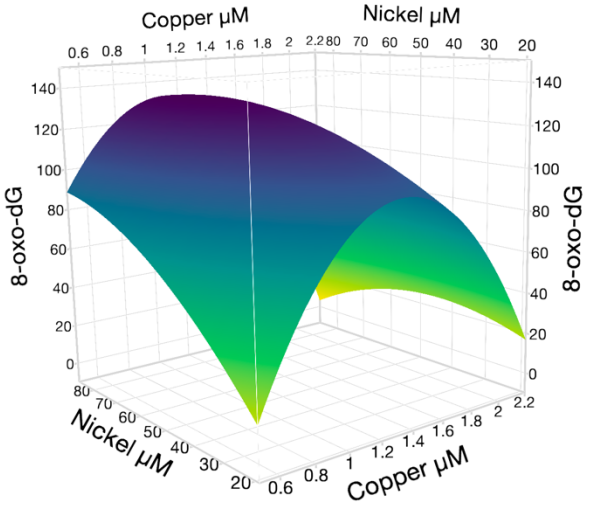

B. Copper and zinc

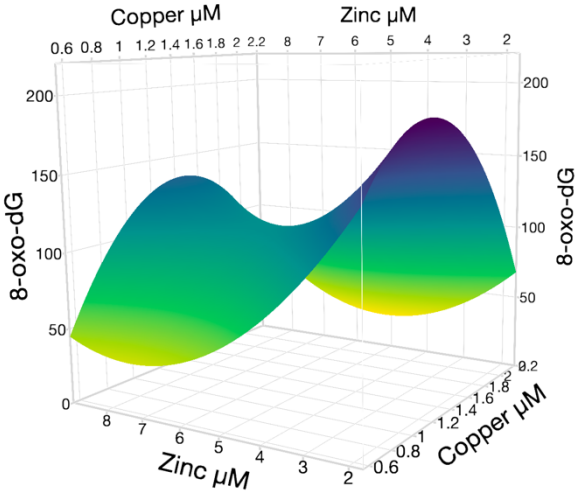

C. Nickel and zinc

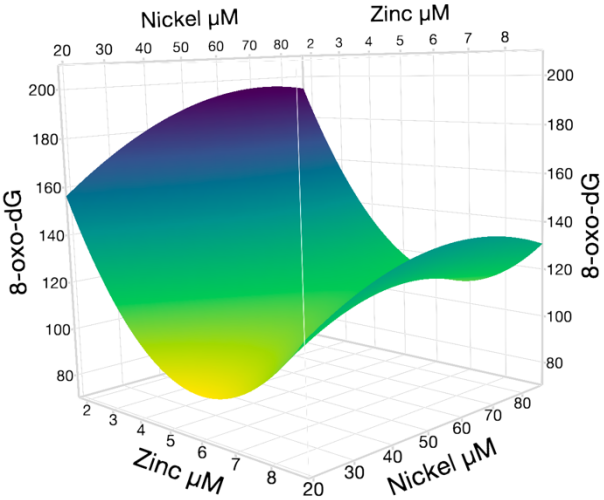

Figure 5.10. Response surface profiles for observed oxidative DNA damage (8-oxo-dG) to gravid female *Tisbe battagliai* after 24-hour exposure to three-metal combined solutions containing copper, nickel, and zinc (14 solutions in total). Each sub-figure shows data for two metals from the three-metal mixture. (A) Copper and zinc, (B) copper and nickel and (C) nickel and zinc.

5.3.7 Apoptosis

There was no main effect driver found for apoptosis within the three-metal mixtures ($P > 0.05$) and no interactions between the metals within the mixtures were identified ($P > 0.05$) (Figure 5.9).

5.4 Discussion

Trace metals studies for marine organisms are limited for cumulative hazard assessments, yet coastal environments are heavily contaminated, and sediments are a main sink for metals (Pirrie *et al.*, 2003). Once concentrations exceed a threshold alongside other chemicals, effects at the individual level occur at multiple levels of biological organisation, threatening the overall population. Combined effect studies for aquatic organisms have been focused on mortality and LC_{50} values, which might not detect all changes caused by the mixtures, as mortality is the final stage of the toxicity pathway (Yoo *et al.*, 2021). Rather, sublethal, cellular and molecular effects can provide more light on the combined effects of mixtures.

In this chapter, effect endpoints following a specific toxicity pathway of interest were measured, alongside metal fractionation and predictive models, with an aim to understand the mixture interactions causing toxicity. Metal fractionation data informs whether there were any interactions occurring in the mixture solution before the metals were taken up by the organism. Comparisons to predictive CA and IA models provide further information about the mixture interactions and whether the toxicity expected was similar, greater, or lesser than additivity predictions using the CA and IA models.

When comparing combined metal solutions to single metal solutions in Chapter 4, the LMM contribution for zinc increased when in the mixture solutions, suggesting that zinc is more bioavailable in the presence of other trace metals (copper and/or nickel). This indicates that an interaction between the metals was occurring before being up taken by *T. battagliai*. Although interactions at the uptake site were not measured in this Chapter, nickel and zinc are known to have a competitive interaction for metal uptake, as both metals interact actively with calcium channels (Nys *et al.*, 2015). In *Daphnia magna* this competitive interaction between nickel and zinc affected the uptake process of each other due to sharing common uptake sites (Komjarova and Blust, 2008). In the same study, copper was the main metal causing interactions with zinc, resulting in copper interfering with zinc uptake and not the opposite direction.

Uptake mechanisms for copper are via the sodium channels, rather than calcium channels, therefore this interference is non-competitive.

Furthermore, as nickel and zinc were present in the mixtures as mostly the LMM fraction that is known to be bioavailable for most species, it is often said to be responsible for any observed toxicity. This dissolved metal form is well documented at impacting on cellular components, specifically DNA and proteins. Data from 8-oxo-dG measurements support this as nickel was close to being a significant main effect driver, and nickel could have been leading the interaction within its pairs. Copper was measured mostly as colloids in these mixtures yet was found to be a main toxicity driver for survival at 24 and 48 hours of exposure and having second order effects in a binary mixture with nickel and zinc on oxidative DNA damage in gravid female *T. battagliai*. These data question whether the typically assumed LMM bioavailability is solely responsible for toxicity in these mixtures and further suggest that the larger sized metal species are contributing as well, as previously discussed in Chapter 4. However, without body burden data no conclusions can be drawn. Toxicity from other fractions were seen in the freshwater rotifer *Brachionus calyciflorus*, as colloids did contribute to trace element toxicity during exposure to field water samples, due to their filter feeding behaviour (Vignati *et al.*, 2005). Following on from Chapter 4, the importance of metal fractionation data was understood, and all mixture solutions were measured. As a change in fractionation for zinc was observed and can be involved in the mixture characterisation. The interactions identified from the DSD models show that an interaction is occurring; however, on their own it is unclear where this interaction is occurring.

Using cellular ROS fluorescent dyes to measure ROS formation in gravid females, there was an increase in some of the mixtures, but these increases were lower than single metal exposures suggesting an antagonistic interaction. These ROS results do not compliment the observed oxidative DNA damage results, as exposure to ROS causes oxidative modifications of DNA and 8-oxo-dG is the most representative product of these modifications. Although a main toxicity driver was not identified for oxidative DNA damage, nickel was close to being significant. However, unlike the oxidative DNA damage data, the ROS data was not a good fit for the standard least squares model, limiting the information available about the interactions. For *D. celebensis*, antioxidant enzyme activity was measured after 48 hours using two total

mixture concentrations of three metals, and both resulted in significantly higher enzyme activity from SOD and GST when compared to controls (Yoo *et al.*, 2021).

IA predicted toxicity was most similar to observed lethality for both juveniles and gravid females over the 48-hour exposure, suggesting that the three metals have different MoAs within the mixtures and act with non-competitive intentions, under given exposure conditions. This is interesting as these metals have similar uptake mechanisms, and all three metals are known to cause ROS generation individually, with ROS formation being a well-established MoA (Brix, Schlekat and Garman, 2017; Kim *et al.*, 2014a).

When compared between predicted and measured survival data for juvenile and gravid female *T. battagliai*, both CA and IA models found the mixture solutions to be mostly additive. This chapter found that the mixture of copper, nickel, and zinc seemed to act similarly to both six-day old and 14-day old *T. battagliai*, except for a time dependent effect only on juvenile survival. A similar finding was observed in the copepod *Eurytemora affinis* that was exposed a mixture of trace metals over three generations and multiple life stages, finding no significant difference between the number of copepodites and gravid females (Das *et al.*, 2020). Both life stages were impacted by the mixture exposure though, as males and non-gravid females had significantly higher survival.

On the contrary to this Chapter's results, most mixtures for marine invertebrate species were determined to be synergistic. For example, the binary mixtures exposed to ovigerous female *Tisbe holothuriae*, where binary pairs of copper and nickel, and nickel and zinc had synergistic interactions after 48 hours exposure (Verriopoulos and Dimas, 1988). Although, the combined effects of copper, cadmium and arsenic have been recently determined as additive in adult *Diaphanosoma celebensis* (Yoo *et al.*, 2021), but the binary pairs of these metals were synergistic. For adult *Artemia* sp., zinc and nickel binary mixtures were additive at a salinity of 35 ppt, but antagonistic effects were noted when the salinity was lowered to 10 ppt (Damasceno *et al.*, 2017). Whereas, for juveniles of the scallop *Argopecten ventricosus* exposed to a three-metal mixture of cadmium, chromium, and lead, with synergistic interactions, while the binary pairs of cadmium and chromium and cadmium and lead were antagonistic, produced from toxic unit analyses (Trombini, Hampel and Blasco, 2016). For *Mytilus edulis* larval development, binary mixtures of copper and nickel

were synergistic and antagonistic depending on whether the nickel concentration was low or high respectively (Deruytter *et al.*, 2017).

T. battagliai is a good candidate for a cumulative hazard assessment (Trombini, Hampel and Blasco, 2016; Macken *et al.*, 2009; Thomas *et al.*, 2003). The DSD approach for gravid female successfully fitted survival between the most forcing and least forcing concentrations, providing main effect and second order effect estimates, that all three metals were impacting survival over the 48-hour exposure. The interactions between copper and both zinc and nickel were significant at 24 hours, whereas a change occurred at 48 hours with data suggesting nickel and zinc have a different type of interaction. Interactions between metals are complex but using this approach - rather than a traditional one factor increasing at a time design - allows both main and second order effects to be determined simultaneously. For juveniles though, after two different concentration ranges were used in the DSD, the data was not a good fit for the approach and no main effect drivers were identified. This suggests that the experimental design was not best suited for the juvenile study. Further development and use of this design of experiments approach for ecotoxicology is therefore still required.

5.5 Conclusion

In this chapter, the interactions within a three-metal mixture were investigated and varied at different levels of biological organisation - for example, all three metals influenced survival for gravid female individuals, and no particular metal influenced toxicity for ROS formation. Comparisons between predictive and measured mixtures found most to be additive and antagonistic for both life stages, with IA models overlapping better with measured lethality. This suggestion of different MoAs was supported by the lack of significant correlations between measured endpoints, potentially meaning that other routes of toxicity are occuring. These varied results highlight the complexity of mixtures and why measuring the effects are important for understanding real environmental scenarios. An integrated exposure and effects approach allowed us to use metal fractionation data and interactions between the three metals from the DSD, to better understand the observed toxicity, within the current understanding of the literature that focuses on adverse outcome rather than targeted bioassays for marine copepods.

Chapter 6. Assembling a toxicity pathway for UVB radiation-induced effects on the marine copepod *Tisbe battagliai*

6.1 Introduction

The Montreal Protocol, with subsequent amendments (Nations, 1987), was a fundamental step towards safeguarding the stratospheric ozone layer, and in turn protecting human and environmental health from penetrating UV radiation (UVR) (Velders *et al.*, 2007; Papanastasiou *et al.*, 2018; United Nations Environment Programme, 2012; Bais *et al.*, 2018; Williamson *et al.*, 2019). UVR comprises three bands of decreasing harmfulness: UVC (200-280 nm), UVB (280-320 nm) and UVA (320-340 nm) (Dahms and Lee, 2010). UVC does not reach the Earth's surface as it is absorbed by oxygen and stratospheric ozone, whereas both UVB and UVA penetrate into the water column (Alves and Agustí, 2020). Ozone depletion, predominant over the Antarctic (Farman, Gardiner and Shanklin, 1985) and periodically over the Arctic (Manney *et al.*, 2011), increases the quantity of UVB reaching the Earth's surface, posing potential short and long-term hazards to biota (Kim *et al.*, 2009; Newsham and Robinson, 2009; Dahms and Lee, 2010). Despite the partial recovery of the stratospheric ozone, UVR is still an ongoing issue, especially for more vulnerable organisms and life stages (Lacuna and Uye, 2000) and where irradiance levels are high (e.g., clear waters, high altitudes and/or shallow waters) (Häder *et al.*, 2007).

UVB causes adverse outcomes for zooplankton under short- (severe effects) and long-term (subtle effects) exposures scenarios (Nazari *et al.*, 2010; Wolinski *et al.*, 2016; Wang *et al.*, 2019; Velders *et al.*, 2007; Stábile *et al.*, 2021; Dahms, Dobretsov and Lee, 2011; Dahms and Lee, 2010; Won *et al.*, 2014). Fitness is compromised by the reallocation of resources away from growth and reproduction towards repair mechanisms, potentially disrupting food web dynamics (Lacuna, 2002).

Coastal waters are more effective than oceanic waters at attenuating UVR (Tedetti and Sempere, 2006), with the 10% irradiance depth ($Z10\%$) of UVB for coastal waters ranging between 0.09-8 m versus 0.3-10.4 m for oceanic waters (Aas and Hojerslev, 2001). Despite this, the responses of benthonic copepods to UVB exposure are particularly pertinent. Unlike their planktonic counterparts they lack the opportunity to undertake extensive diel vertical migrations whereby populations

descend to depth during daylight hours and return to surface waters during darkness. This mass synchronised movement reduces UVR exposure by allowing planktonic copepods to exploit a depth refugium (Williamson *et al.*, 2011).

Tisbe battagliai inhabits shallow tidepools along western European coasts (Drira *et al.*, 2018) preferring to maintain close contact with the substrate (predominantly rocks and seaweeds). The opportunities for UVB attenuation within these habitats are greatly reduced, exposing animals to potentially damaging UVB exposure (Hollmann *et al.*, 2015); for instance, the 10% irradiance depth for DNA damage effective dose [*Z*10% DNA] for coastal waters ranges between 1.5-4.5 m (Tedetti and Sempere, 2006; Browman *et al.*, 2000).

T. battagliai may deploy several protective strategies to reduce UVB damage, including shelter seeking and avoidance behaviours (Dahms, Dobretsov and Lee, 2011), accumulation of UV-protective algae pigments (*T. battagliai* has a semi-transparent body) (Rautio and Korhola, 2002; Hansson, Hylander and Sommaruga, 2007; Hylander and Jephson, 2010), and cellular repair mechanisms (Souza *et al.*, 2012). Studies into the adverse effects of UVB on copepods have included focus on life history parameters, incorporating survival, fecundity and developmental success (Hylander, Grenvald and Ki¯rboe, 2014). Life history modelling has been augmented with numerous biochemical and molecular studies that have partly elucidated some of the modes of action (MoA) of UVB in crustaceans (Tartarotti and Torres, 2009; Souza *et al.*, 2010). Many of these MoA involve production of excessive reactive oxygen species (ROS) (Lu and Wu, 2005), lipid peroxidation, protein oxidation, and oxidative DNA damage (Song *et al.*, 2020b). Downstream events are also well studied, including the altered transcriptional regulation of genes involved in antioxidant defence and DNA repair, induced oxidative stress (Obermuller, Karsten and Abele, 2005; Obermuller, Puntarulo and Abele, 2007), apoptosis (Souza *et al.*, 2012; Hollmann *et al.*, 2016) and modifications to DNA (Rastogi *et al.*, 2010; Cadet, Douki and Ravanat, 2015). UVB absorption by thymine or cytosine can cause a specific type of DNA damage via formation of cyclobutane pyrimidine dimers (CPD) (Kim, Park and Choi, 2009; Kim *et al.*, 2009). DNA strands enter an excited state capable of forming pyrimidine hydrates or cross-links with adjacent pyrimidines (Rastogi *et al.*, 2010). These CPDs may affect the transcription of important genes that are relevant for embryonic and larval development, leading to decreased individual and population survival rates (Dahms and Lee, 2010). Despite extensive

work on these adverse effects, the mechanistic understanding underpinning how these effects are causally linked (e.g., the toxicity pathway) is missing.

Toxicity pathways assemble a sequence of causally linked toxicological events across different levels of biological organisation, spanning the continuum from the first molecular interaction between a stressor and it's biological target (the molecular initiating event, MIE), through a series of key events (KE) leading to the adverse outcomes of concern (OECD, 2018; Villeneuve *et al.*, 2014). Toxicity pathways and adverse outcome pathways (AOPs) are becoming more widely implemented in regulatory toxicology (Tollefsen *et al.*, 2014), with the adverse outcomes being relevant to the regulatory endpoints and assessment of the chemical stressor (Carusi *et al.*, 2018; Sachana, 2019). To date, toxicity pathways have focused on chemical exposure; therefore, the development of non-chemical stressors toxicity pathways (e.g., for UVB) is important to fulfil the framework's capability in environmental risk assessment (Song *et al.*, 2020a). As a crucial step towards this, in this chapter a toxicity pathway was developed for *T. battagliai* co-exposed to UVB and low UVA as the most relevant and biologically damaging UVR for shallow coastal environments.

6.2 Methods

6.2.1 Tisbe battagliai culture

Stock *T. battagliai* cultures were maintained as described in Chapter 4.2.1, with some alterations. The cultures were kept at 19 ± 1°C and in 35 ppt ASW (ATC refractometer), pH 8.2 ± 0.2 (SevenExcellence™, Mettler Toledo, OH), and 8.0 ± 0.5 mg mL^{-1} dissolved oxygen (SevenExcellence™, Mettler Toledo, OH). Newly gravid females (14 ± 2 days old) were used in all tests.

6.2.2 Ultraviolet B radiation exposure

All experiments were conducted in a custom-designed UV incubator (Multitron-Pro, Infors HT, Switzerland) fitted with UVA (UVA 36W/78, Centra Osram, Berlin, Germany) and UVB (PL-L 36W/UVB UV6, Waldmann, Illingen-Schwenningen) tubes, using the same filters and emission spectra as Xie *et al.* (2020). Visible light, UVB and UVA intensities were measured before and after each experiment using a SpectroSense 2+ filter radiometer (Skye Instruments Ltd., Llandrindod Wells, UK). Six- and 12-well plates and 50 mL plastic beakers were used throughout, containing

between 5 and 30 mL of ASW depending on the number of individuals required for specific endpoints.

UVB irradiances were chosen following a 48-hour range-finding test (0.05, 0.1, 0.25, 0.5 and 1.0 W m^{-2}) using an immobility assay following the methodology described in Chapter 4.2.4. In short, immobility is noted when no movement occurs 10 seconds post contact with a pipette tip and assumes mortality has occurred. The nominal exposure irradiances were 0.008 (UVA only control), 0.05, 0.1, 0.2, 0.4 and 0.8 W m^{-2}, with an additional no UVB/UVA control, under standard culture conditions. Exposures were performed using the same conditions as stock cultures for 48 hours although under the following diel cycle: one hour of visible light, 12 hours of visible with UV light, one hour of visible light, and 10 hours of darkness. A pilot test was carried out to identify possible artefacts (changes in temperature, evaporation, salinity, pH) that could confound life-history and molecular endpoints. Exposure variables including pH (SevenExcellence™, Mettler Toledo, OH), dissolved oxygen (SevenExcellence™, Mettler Toledo, OH), temperature (internal probe) and salinity (ATC refractometer) were recorded throughout the experiment. Medium was renewed every 12 – 14 hours to keep the salinity within an acceptable range (± 2 ppt) (ISO, 1999). Using the immobility assay, *T. battagliai* (n = 5) were exposed to UVB for 24 and 48 hours. The effect toolbox for *T. battagliai*, shown in Table 4.1, was used for characterising UVB impacts, including the specifically developed CPD-DNA damage endpoint for this study.

6.2.3 Neonate development

The neonate development assay was modified from the short term development assay from Macken, Lillicrap and Langford (2015). Newly gravid females (14±2 days) carrying their first clutch were individually pipetted into a discrete well of a 12-well multiplate (5 mL of ASW per well) and exposed to UVB for 24 hours. Afterwards, the well plates were maintained under the same conditions as the stock cultures for a further seven days. The reproduction cycle was followed (delay between clutch formation) alongside the number of nauplii hatched from both the first and second clutches. Nauplii development from both clutches was tracked to the first copepodid stage (four days). Clutch 1 was only exposed to UVB whilst in the egg sac carried by the exposed female, i.e., not during oogenesis, whereas clutch 2 was UVB exposed during oogenesis, but not in the egg sac stage. The medium was renewed after the

24-hour UVB exposure and 2 x 10^5 algal cells mL^{-1} (counted on a Beckman Coulter Counter, Beckman Coulter Life Sciences, Indianapolis, IN, USA) were added (Macken, Lillicrap and Langford, 2015). Counts for offspring were carried out on days one, three, four and seven under a dissecting microscope (SMZ745T, Nikon, Tokyo, Japan). The female was isolated into a new well once the second clutch had hatched. Counts of female survival, clutch presence and the number of eggs hatched were taken. Nauplii survival to copepodite stage was calculated after four days to determine whether there was any developmental delay.

6.2.4 Reactive oxygen species formation

Intracellular (ROS) formation was determined in situ following UVB exposure using the probe H_2DCFDA for cellular ROS and dihydrorhodamine 123 (DHR123, Invitrogen, Molecular Probes Inc., Eugene, OR, USA) for mitochondrial ROS. For H_2DCFDA the same method as presented in Chapter 4.2.4 was followed. Briefly, 50 µL of H_2DCFDA (0.5 µM) in ASW was added to each black, clear bottom 96-microplate well (Corning CoStar). For DHR123, the same method was followed as shown for H_2DCFDA. One individual copepod per replicate was added per well containing the probe solution. Fluorescence measurements were taken using a VICTOR^3™ plate reader (PerkinElmer, MA) at emission wavelength 535 nm and excitation wavelength 485 nm for two hours and data were normalised to individual copepod length, measured under an inverted fluorescence IX70 microscope (Olympus Corporation, Tokyo, Japan) (x40 mag).

6.2.5 DNA extraction and cyclobutene pyrimidine dimers quantification

DNA was extracted from pooled *T. battagliai* samples (n = 30) using the Quick-DNA™ Tissue/Insect Microprep Kit (Zymo Research, CA, USA), as previously described in Chapter 4.2.5, with one exception that beta-mercaptoethanol was added to the Genomic Lysis Buffer in a DNase free chemical fume hood. Samples were taken in triplicate after 12, 24 and 48 hours of exposure. DNA concentration was determined using 1 µL of extracted DNA on a Nanodrop ND-1000 (Nanodrop Technologies, Wilminton, DE, USA). DNA was frozen at -80 ^oC until further processing. The CPD formation was quantified colourimetrically using the OxiSelect™ UV-Induced DNA Damage ELISA Kit CPD (Cell Biolabs, Inc., San Diego, CA, USA). The manufacturer's product manual was followed, with changes made to reduce the CPD-DNA concentrations in the standard curve samples to be more

relevant to the lower DNA concentrations in *T. battagliai* samples. All antibody work was carried out in a dark room at ambient temperature (20 °C). At step 12 of the protocol, the reaction was stopped by adding 100 µL of substrate solution to each well after five minutes of incubation. The absorbance at 450 nm was read immediately on a SpectraMax 190 spectrophotometer (Molecular Devices, San Jose, CA, USA) to avoid colour fade over time. The absolute amount of CPD (ng mL^{-1}) was calculated using the slope of the standard curve. For this Chapter, direct DNA damage from UVB exposure was measured (CPD formation), rather than indirect oxidative DNA damage (i.e., 8-oxo-dG damage was measured in Chapter 4 and 5). Specifically, CPD formation was chosen as it is the most frequent damage from UVB radiation, whereas other DNA lesions such as 6-4 photoproducts (6-4 PPs) are predominantly the result of shorter UV wavelengths (i.e., UVC radiation) (Häder, 2022). The ELISA CPD kit is an enzyme immunoassay that can rapidly detect CPD in isolated DNA. Any cells containing CPD damage were probed using an anti-CPD antibody, followed by a HRP conjugated secondary antibody. Any unbound HRP antibody was washed off and a substrate solution was added to each well to react with HRP. This reaction was ended using an acid and then the absorbance was measured as an indirect measurement of CPD detected in the DNA sample.

6.2.6 RNA extraction

Total RNA was isolated from gravid females using the ZR Tissue and Insect RNA MicroPrep kit (Zymo Research Corporation, Irvine, CA, USA) according to the manufacturer's protocol with adaptations, previously described in Chapter 4.2.8. In brief, twenty *T. battagliai* were pooled for each replicated time point (12 and 24 hours), Samples were stored in RNALater at 4 °C overnight, then at -80 °C until RNA extraction. The eluted RNA (15 µL) was stored at -80 °C until downstream analysis. RNA purity (260/280 > 1.98, 260/230 > 1.9) was checked using a Nanodrop ND-1000 (Thermo Fisher Scientific Inc., Waltham, MA) and RNA integrity measured using a Bio-analyser (Agilent Technologies, Santa Clara, CA) looking for defined peaks with stable baselines.

6.2.7 Quantitative real-time qPCR analysis

Transcriptional analysis by real time quantitative polymerase chain reaction (RT qPCR) was carried out on extracted RNA samples that were exposed to UVB for 12 and 24 hours. The same kit and methodology were followed as described in Chapter

4.2.9. In summary, the extracted RNA samples were diluted to 200 ng in 20 µL, 16 µL of which was used to create cDNA samples after 60 minutes incubation. cDNA samples were further diluted to 0.2 ng mL^{-1} and pipetted into the cDNA source plate. Freshly prepared primer working solutions were made (3.2 mM) for 20 genes. Sybr Green Fastmix was added to each primer working solution to make a mastermix solution. Four genes were analysed per 384-sample plate, which was covered before being placed in a CPX384 R-T system PCR instrument (Bio-Rad, Hercules, CA, USA). 20 µL was sampled and the total run took two hours and 33 minutes to complete six cycles, with pre-determined primer annealing temperatures for cycle three. Cycles one to five were repeated 39 times - cycle one = three minutes at 95 °C, cycle two = 20 seconds at 95 °C, cycle four = 30 seconds at 72 °C, cycle five = three minutes at 95 °C, cycle six = 30 seconds at 65 °C and finished at 95 °C.

6.2.8 Statistical analysis

Irradiance-response curves for survival and development data after treatment exposure were created using GraphPad Prism 8 (GraphPad Software, San Diego, USA). All statistical analyses were conducted, and figures created using GraphPad Prism 8. Survival and developmental percentage data were transformed using arcsine and $\log_x$ transformations. A non-linear regression was used to calculate survival $LI_{50,}$ No Observed Effect Irradiance (NOEI) and Lowest Observed Effect Irradiance (LOEI) values after 24 and 48 hours. All data were checked for normality using the Kolmogorov-Smirnov normality test and analysed accordingly with parametric tests, with additional homogeneity of variance, if necessary. Two-way analysis of variance (2W ANOVA) was carried out to determine significant differences between irradiances and time ($P \leq 0.05$), with Tukey's post hoc test to determine differences between irradiances within each timepoint ($P \leq 0.05$). When there were missing data for some replicates, a mixed effect model was used as this can handle missing data better than a 2W ANOVA. ROS, CPD-DNA damage, and gene expression data were normalised to specified time points and expressed as fold changes when suitable. A principal component analysis (PCA) was applied to the full data set to characterise relationships between endpoints using XLSTAT (Addinsoft, Paris, France). Pearson's correlation coefficients were also calculated using XLSTAT as an estimate of the strength of association between the different endpoints ($P \leq 0.05$).

6.3 Results

6.3.1 Exposure quality

The full spectrum of UVA, UVB and visible light tubes were measured during the experimental period (Figure 6.1) and the total exposure dose (kJ m^{-2}) calculated (Table 6.1). The transmittance of UVB was 66.8% for plastic beakers and 59.2% for microplates used throughout this study (7.6% dosimetry difference). Glass measured 0.72% transmittance and was therefore not used. The deviation of irradiance measurements taken at the base of a beaker filled with ASW was 8%. Experimental seawater parameters were measured during and after the experimental period (Table 6.2).

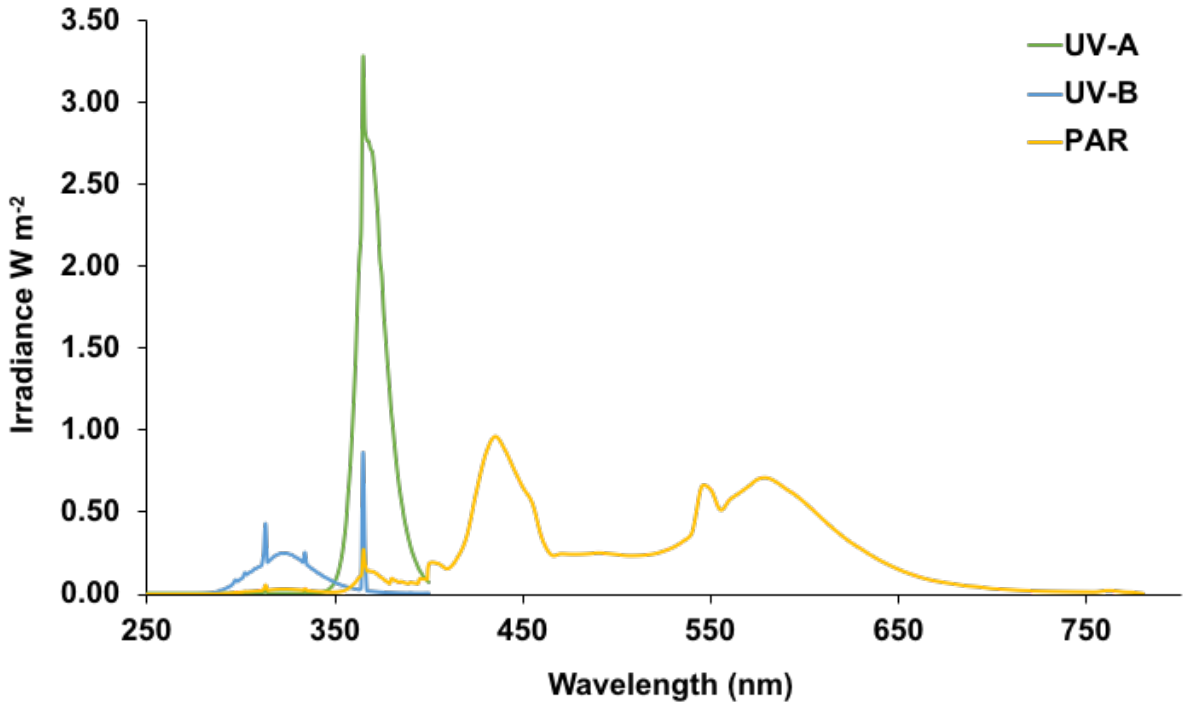

Figure 6.1. Emission spectra of ultraviolet A (UVA – green), ultraviolet B (UVB – blue) and fluorescent tubes (PAR – yellow) in the UV incubator. PAR = photosynthetically active radiation.

Table 6.1. Ultraviolet radiation dosimetry measured at the beginning of each experiment. The total dose of UVB exposure was calculated, taking the periods of darkness and only PAR into account.

Nominal UVB Irradiance W m^{-2}	**Measured UVB irradiance W m^{-2}**	**Measured UVA irradiance**	**24-hour UVB total dose kj m^{-2}**	**48-hour UVB total dose kj m^{-2}**
0	0	3.2	0	0
0.008	0.008 – 0.009	3.105 – 3.2	0.35 – 0.39	0.69 – 0.78
0.05	0.053 – 0.06	3.14 – 3.2	2.29 – 2.59	4.58 – 5.18
0.1	0.09 – 0.12	3.27 – 3.34	3.89 – 5.18	7.78 – 10.37
0.2	0.204 – 0.22	3.25 – 3.6	8.81 – 9.50	17.63 – 19.01
0.4	0.39 – 0.41	3.4 – 3.5	16.85 – 17.71	33.70 – 35.42
0.8	0.81 – 0.85	3.7 – 3.9	34.99 – 36.72	69.98 – 73.44

Table 6.2. Exposure seawater measurements for salinity (ppt) and pH during (24 hours) and after exposure (48 hours) of UVB to gravid female *Tisbe battagliai.*

Nominal UVB Irradiance W m^{-2}	**Salinity 24h**	**pH 24h**	**Salinity 48h**	**pH 48h**
0	35.33 ± 0.58	8.24 ± 0.02	36.33 ± 0.58	8.32 ± 0.03
0.008	35.00 ± 0.00	8.25 ± 0.00	37.67 ± 0.58	8.38 ± 0.01
0.05	35.33 ± 0.58	8.25 ± 0.01	37.33 ± 0.58	8.39 ± 0.01
0.1	36.00 ± 0.00	8.26 ± 0.00	37.00 ± 1.00	8.36 ± 0.01
0.2	36.00 ± 0.00	8.27 ± 0.00	37.33 ± 0.58	8.35 ± 0.02
0.4	35.67 ± 0.58	8.27 ± 0.00	37.33 ± 0.58	8.34 ± 0.01
0.8	36.00 ± 0.00	8.27 ± 0.00	36.67 ± 0.58	8.35 ± 0.02

6.3.2 Survival

After 24 hours of UVB, *T. battagliai* had 70% survival at the highest irradiance tested (1.0 W m^{-2}). However, an irradiance-dependent reduction in survival was observed after 48 hours, with an LI_{50} of 0.37 W m^{-2} (Figure 6.2A; Table 6.3). Both time and irradiance were significant factors affecting survival (Table 6.4).

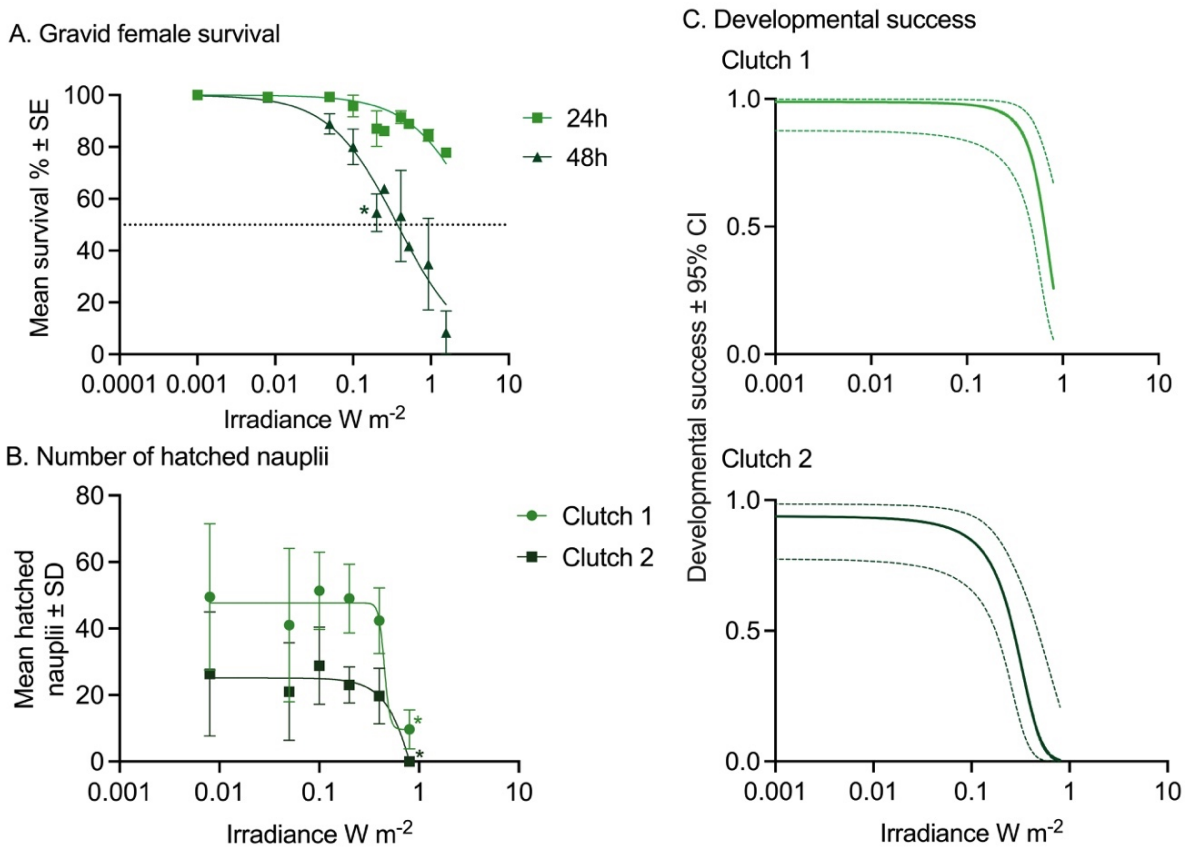

Figure 6.2. The life-history effects of UVB radiation on *Tisbe battagliai* after 24 and 48 hours of exposure. (A) Irradiance response curves for gravid female mean survival ± standard error following 24 and 48 hours of UVB exposure, n = 5. * Denotes the no observed effect irradiance (NOEI) at 48 hours. The dotted line at 50% survival shows the EC_{50} values. (B) The number of hatched nauplii by gravid females post 24-hour exposure to UVB, n = 6. * Denotes the irradiance that is significantly different to the controls and all other tested irradiances (Tukey post hoc test). (C) Developmental success of clutch one and two released by gravid females post 24-hours exposure to UVB, n = 6. The dotted lines represent the confidence limits of the simple logistic regression.

Table 6.3. Irradiance response curve statistics for life-history assays after exposing gravid female *Tisbe battagliai* to 24 and 48 hours of UVB radiation. Lethal irradiance that caused 50% mortality (LI_{50}), no observed effect concentration (NOEC) and low observed effect concentration (LOEC).

Endpoint		**LI_{50} W m^{-2}**	**NOEC W m^{-2}**	**LOEC W m^{-2}**	**R^2**
Gravid female survival	24 hours	4.363	NA	NA	0.48
	48 hours	0.373	0.1	0.2	0.79
Hatched nauplii	Clutch 1	0.448	0.4	0.8	0.49
	Clutch 2	1.326	0.4	0.8	0.43
Developmental success	Clutch 1	0.4	0.05	0.8	0.47
	Clutch 2	0.2	0.05	0.8	0.5

Table 6.4. Two-way ANOVA or mixed effect models (underlined endpoints when this was used instead of an 2W-ANOVA) for all endpoints measured. * Denotes significant P values.

Endpoint	**Source**	**df**	**Sum of squares**	**Mean square**	**F**	**P**
Adult survival	Time Irradiance Interaction	1 9 9	N/A	N/A	89.84 8.804 6.586	<0.0001* <0.0001* 0.0004*
Clutch presence	Time Irradiance Interaction	3 6 18	11.10 4.226 4.155	3.698 0.7044 0.2308	28.24 3.40 1.76	<0.0001* 0.0095* 0.0399*
Clutch one survival	Time Irradiance Interaction	3 6 18	0.7439 9.753 0.1021	0.2480 1.626 0.005675	45.34 8.769 1.038	<0.0001* <0.0001* 0.4257
Clutch two survival	Time Irradiance Interaction	1 5 5	0.2154 2.105 0.04686	0.2154 0.4210 0.009372	5.598 2.434 0.2436	0.0246* 0.0576 0.9398
Clutch development	Clutch Irradiance Interaction	1 6 6	1.190 6.738 0.643	1.190 1.123 0.107	10.87 10.25 0.98	0.0015* <0.0001* 0.4466
Clutch hatched	Clutch Irradiance Interaction	1 6 6	8541 11454 522	8541 1909 87	52.37 11.57 0.53	<0.0001* <0.0001* 0.7810
mtROS	Time Irradiance Interaction	1 6 6	1.454 0.7240 1.682	1.454 0.1207 0.2803	32.31 0.46 6.23	<0.0001* 0.8290 0.0023*

cROS	Time Irradiance Interaction	1 6 6	3.761 17.58 27.29	3.761 2.930 4.548	3.02 1.09 3.65	0.1043 0.4146 0.0215*
CPD-DNA damage	Time Irradiance Interaction	2 6 12	56.28 353.60 314.90	28.14 58.94 26.24	6.89 23.96 6.43	0.0053* <0.0001* <0.0001*
RAD23	Time Irradiance Interaction	1 5 5	N/A	N/A	39.06 6.272 2.009	<0.0001* 0.0002* 0.0950
RAD50	Time Irradiance Interaction	1 5 5	N/A	N/A	1.006 1.532 0.9039	0.3211 0.1987 0.4868
BAX	Time Irradiance Interaction	1 5 5	N/A	N/A	0.06018 3.4320 0.8044	0.8085 0.0176* 0.5587
CASP3	Time Irradiance Interaction	1 5 5	N/A	N/A	0.9822 1.424 0.8491	0.3329 0.2514 0.5306
GR	Time Irradiance Interaction	1 5 5	N/A	N/A	7.572 3.251 1.059	0.0116* 0.0221* 0.4095
GPX2	Time Irradiance Interaction	1 5 5	N/A	N/A	6.613 2.377 0.9724	0.0134* 0.0533 0.4447

6.3.3 Development

Adult survival

Only the 0.8 W m^{-2} treatment resulted in any mortalities (33% after three days and 50% by day seven). There were no mortalities during the 24-hour exposure. There was a significant interaction between UVB irradiance intensity and exposure time with the interaction driven by irradiance rather than time (Table 6.5).

Clutch presence (gravid)

The presence of an egg clutch was recorded on days one, three, four and seven post UVB exposure. Typically, *T. battagliai* releases one clutch every two to three days (Hutchinson *et al.*, 1999). This pattern of clutch presence was only seen for the controls, 0.05 and 0.1 W m^{-2} treatments, having a new clutch on days four and seven. Irradiances higher than 0.1 W m^{-2} had fewer individuals carrying a clutch, showing that clutch presence was affected by UVB irradiance, as determined by 2W-ANOVA (Table 6.5). At the highest tested irradiance 0.8 W m^{-2}, only 20% of

individuals had clutches present on days one, three and four, with the percentage reducing to zero by day seven. Time was also a significant factor on clutch presence (2W-ANOVA) as day one was significantly different to all other days.

Clutch survival

Both clutches yielded similar numbers of hatched nauplii (Figure 6.2B). Irradiance intensity significantly reduced hatching success with the clutches from females exposed to 0.8 W m^{-2} UVB producing significantly fewer nauplii than the other treatments (Table 6.3). For clutch one, both irradiance and time were significant factors contributing to survival (Table 6.4). However, 0.8 W m^{-2} was the only significant irradiance affecting survival (Tukey post hoc, $P < 0.05$), whereas all time points were significantly different (Tukey post hoc, $P < 0.05$). After day one, hatched nauplii from clutch one had a high survival probability across all UVB irradiances except for 0.8 W m^{-2}, which was the only irradiance that significantly differed from the controls and all other tested irradiances (Tukey post hoc, $P < 0.05$). Survival decreased by 70% at 0.8 W m^{-2} after three days and all nauplii were dead after four days. Exposure time was the only significant factor affecting nauplii survival from clutch two, despite the number of surviving nauplii reducing from 0.2 W m^{-2} to 0.4 W m^{-2} (Table 6.4).

Clutch developmental rates

There was a significant reduction in developmental success between clutches one and two and in response to increasing UVB irradiances (Table 6.4). After four days, all clutch one nauplii had developed to the copepodite stage except those exposed to 0.4 and 0.8 W m^{-2} of UVB, with 67% and 33% respectively reaching the first copepodite stage (Figure 6.2C). The 0.8 W m^{-2} exposure was significantly different to the controls and to all other irradiances except for 0.4 W m^{-2}. Clutch two development appeared to be affected by irradiances above 0.05 W m^{-2}, although only the 0.8 W m^{-2} treatment was significantly different from the controls, with no individuals developing to the copepodite stage by day four (Figure 6.2C; Table 6.4).

6.3.4 Oxidative Stress

Cellular reactive oxygen species formation

There was a general irradiance-dependent increase, albeit not statistically significant, in cellular ROS formation with irradiance after 24 hours, with up to a 3.8-fold increase at 0.4 W m^{-2} (Figure 6.3A). However, there was no change in ROS formation at 0.8

W m^{-2} compared to the control (1.4-fold). There were no significant differences between irradiances or time at either 24 or 48 hours; however, there was a significant interaction between irradiance and time (Table 6.4).

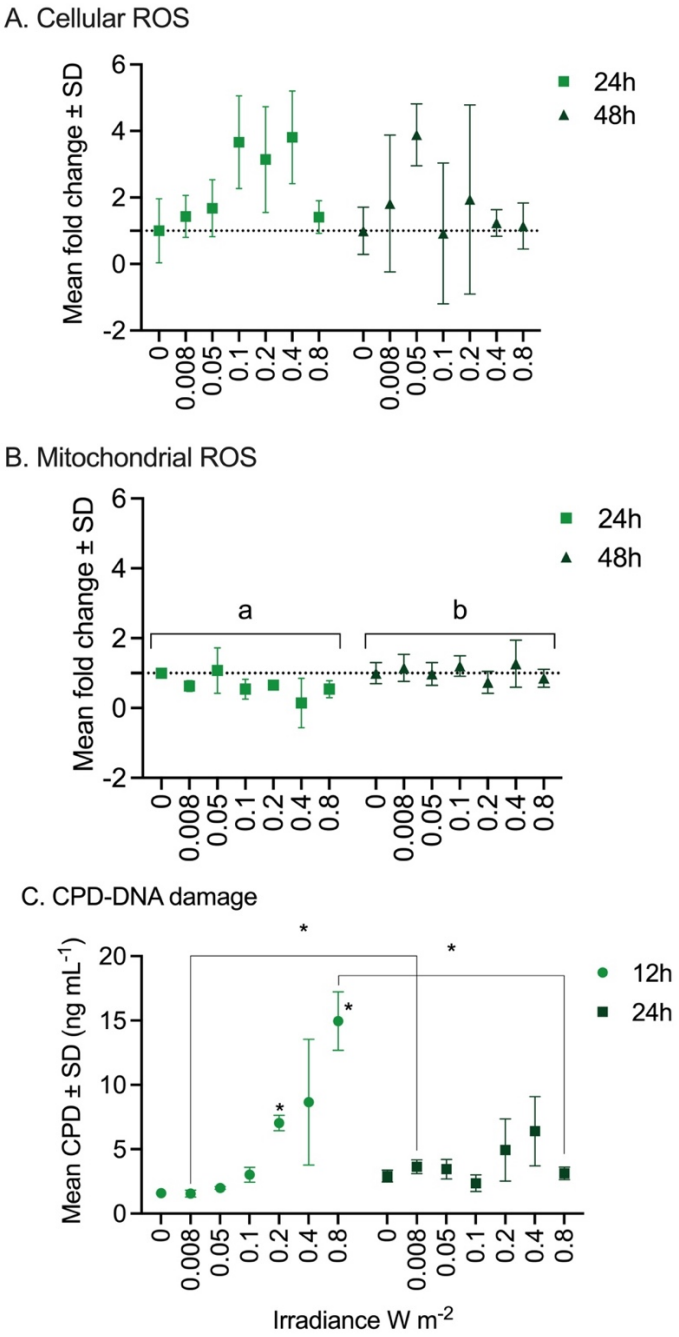

Figure 6.3. Cellular responses of *Tisbe battagliai* after 12, 24 and 48 hours of UVB exposure. (A) Mean fold change of cellular reactive oxygen species (ROS) formation ± standard deviation, n = 5. The dotted line at 1 indicates the control. (B) Mean fold change of mitochondrial ROS formation ± standard deviation, n = 5. Letters denote significant differences between the 24- and 48-hour time points (Tukey post hoc test). The dotted line at 1 indicates the control. (C) Mean cyclobutane pyrimidine dimers (CPD) ng mL^{-1} ± standard deviation, n = 3. * Denotes significant differences between the control and irradiances and between the same irradiance at different time points (Tukey post hoc test).

Mitochondrial reactive oxygen species formation

Mitochondria ROS (mtROS) formation exhibited a decreasing, but non-significant, trend with irradiance after 24 hours (Figure 6.3B) and had returned to levels similar to the controls for all irradiances after 48 hours. Though time did significantly affect mtROS formation (Table 6.4).

Antioxidant gene expression

The relative expression of the anti-oxidation gene glutathione reductase (GR) increased slightly with irradiance at 12 hours, albeit not significantly (Figure 6.4A). Although at 24 hours, there was a small significant increase with irradiance, with 0.2 W m^{-2} having the highest fold increase and was the only irradiance significantly different to the controls (Tukey post hoc, $P < 0.05$). GR regulation was affected by both irradiance level and time (Table 6.4). Glutathione peroxidase 2 (GPX2) did not change expression after 12 hours of exposure, and only slightly increased after 24 hours for the highest two irradiances tested (Figure 6.4B). However, catalase (CAT) had no significant differences after 24 hours.

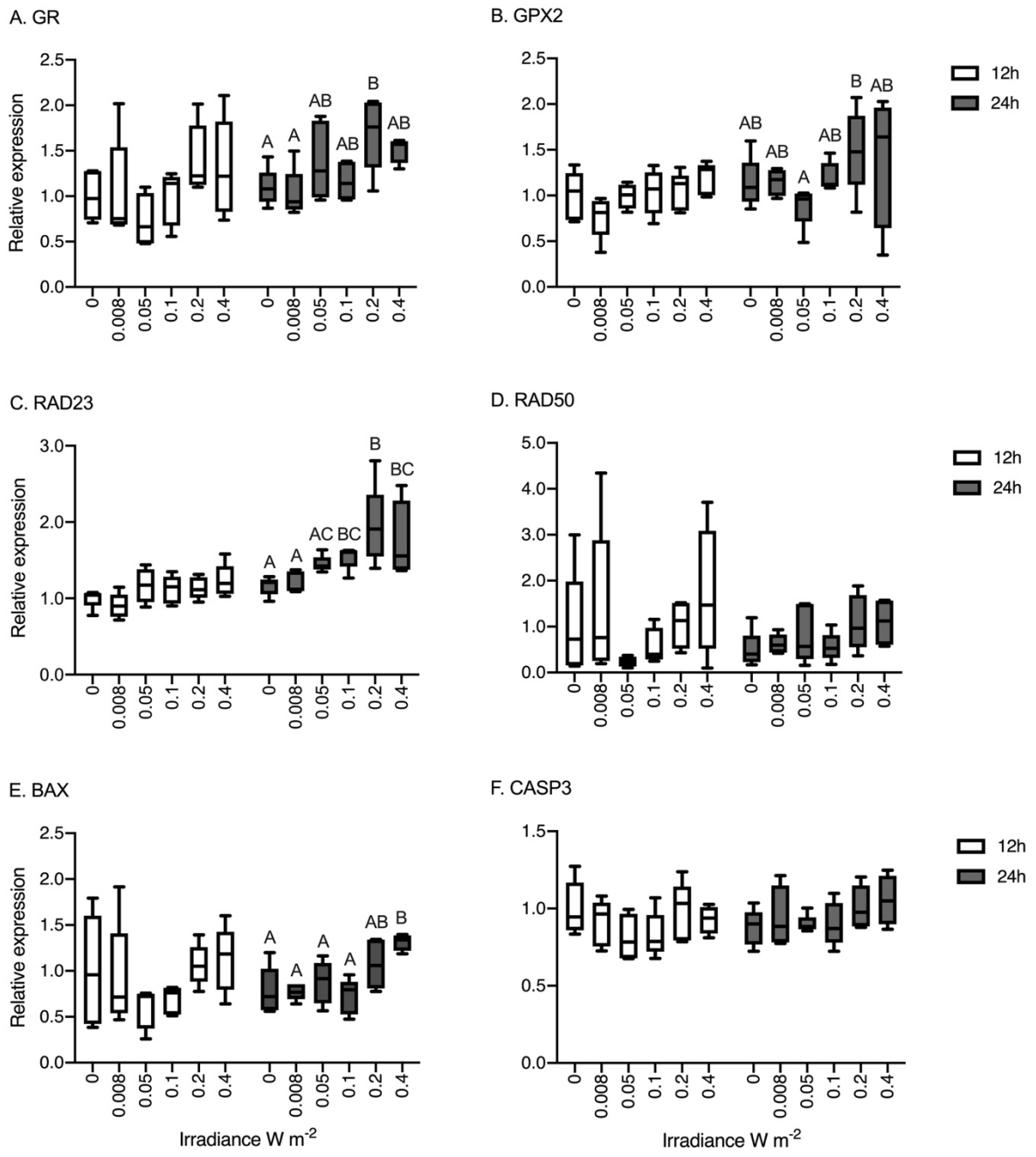

Figure 6.4. Transcriptional responses of *Tisbe battagliai* after 12 and 24 hours of UVB exposure (n = 5). (A) GR = glucocorticoid receptor, (B) GPX2 = catalyses the reduction of hydrogen peroxide by glutathione, (C) RAD23 = UV excision repair, (D) RAD50 = double-strand DNA break repair, (E) BAX = apoptosis regulator and (F) CASP3 = central role in the execution-phase of cell apoptosis. Letters denote significant differences between the control and all irradiances at 24 hours (Tukey post hoc test, $P < 0.05$).

6.3.5 DNA Damage

Cyclobutane pyrimidine dimer (CPD) formation

Increases in CPD-DNA breaks had a strong irradiance-dependent relationship (Figure 6.3C). At 12 hours, there was an irradiance-dependent response in CPD

increase, with a five-fold and a nine-fold median increase at 0.4 W m^{-2} and 0.8 W m^{-2}, respectively. This was not seen at 24 and 48 hours which exhibited a bi-phasic response. Both irradiance and time were significant factors affecting CPD concentration (Table 6.4). Additionally, the interaction of irradiance and time was significant. Over the full period of 48 hours, 0.1 W m^{-2} also remained relatively constant with a mean CPD concentration of 3.02 ng mL^{-1} at 12 hours to 3.50 ng mL^{-1} at 48 hours. The 0.05 and 0.2 W m^{-2} treatments had irradiance response increases over time, although there were no significant differences between time points, while 0.4 W m^{-2} had an irradiance response decrease over time, from 8.66 ng mL^{-1} at 12 hours to 3.65 ng mL^{-1} at 48 hours. The 0.8 W m^{-2} treatment had the highest CPD concentration at 12 hours of 14.96 ng mL^{-1}, which reduced significantly to 3.12 ng mL^{-1} at 24 hours (Tukey post hoc, $P < 0.05$).

DNA excision repair gene expression

The highest upregulation was seen for DNA damage related genes. For RAD23, irradiance and time were significant factors affecting its stress responses to UVB (Table 6.4). RAD23 was significantly upregulated at two irradiances (Tukey post hoc, $P < 0.05$), with a two- and 1.5-fold increase relative to the controls at 0.2 and 0.4 W m^{-2} respectively (Figure 6.4C). For RAD23, both 0.2 and 0.4 W m^{-2} were significantly different between time points. Whereas RAD50 was upregulated 1.7-fold after 12 hours at the highest irradiance tested and downregulated 0.24-fold at the lowest irradiance tested, but these were not significant (Figure 6.4D), and there was little change at 24 hours.

Apoptotic gene expression

The highest irradiance tested (0.4 W m^{-2}) had a significant effect on the upregulation of BAX after 24 hours (Figure 6.4E). Irradiance was the only significant factor affecting relative expression (Table 6.4). However, CASP3 was not significantly upregulated at any irradiance after 12 and 24 hours (Figure 6.4F).

6.3.6 Principal component analysis

The two principal components explained 79.04% of total variance (PC1 and PC2) (Figure 6.5). Adult survival was directly opposite cellular ROS formation and genes GR, GPX2 and RAD23, suggesting that these measured responses after 24 hours of UVB exposure were linked to the observed survival trends. All the measured responses and genes related to oxidative damage, DNA damage and apoptosis were

clustered together, except for mitochondria ROS formation and CAT as they did not vary with increasing irradiance. A Pearson correlation analysis established that increases in the relative expression of BAX and CASP3 apoptosis regulating genes were significantly positively correlated with the increase in CPD-DNA damage (Table 6.5). Adult survival was significantly negatively correlated with genes involved in oxidative stress and RAD23, and negatively correlated with cellular ROS, albeit not significant. Clutch presence was most positively correlated with RAD23.

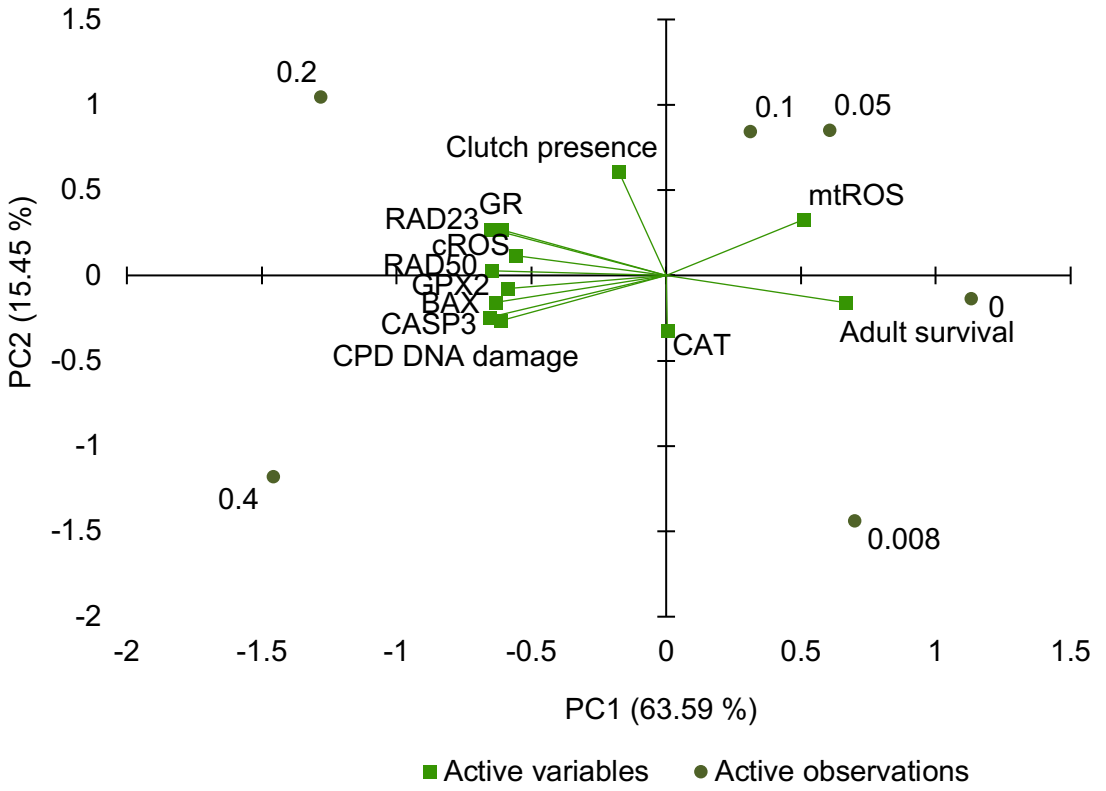

Figure 6.5. Principal component analysis (PCA) of responses in *Tisbe battagliai* exposed to UVB radiation for 24 hours. Active variables are the measured effect responses (green squares) and active observations are irradiances W m^{-2} (dark green circle). cROS – cellular reactive oxygen species, mtROS – mitochondrial reactive oxygen species, RAD23 – UV excision repair gene, RAD50 – double-strand DNA break repair gene, BAX – apoptosis regulator gene, CASP3 – apoptosis executor gene, GR – glucocorticoid receptor gene, GPX2 – antioxidant gene and CAT - catalase.

Table 6.5. Pearson correlation matrix obtained from effect endpoints measured in *Tisbe battagliai* after 24 hours of UVB radiation exposure. Bold values indicate significant differences.

Variables	Adult survival	Clutch presence	RAD23	RAD50	BAX	CASP3	GR	GPX2	CAT	cROS	mtROS	CPD DNA damage
Adult survival	**1**	-0.495	**-0.952**	-0.802	-0.713	-0.798	**-0.846**	**-0.889**	-0.025	-0.791	0.606	-0.674
Clutch presence	-0.495	**1**	0.586	0.157	-0.134	-0.064	0.425	0.202	-0.014	0.494	0.058	-0.236
RAD23	**-0.952**	0.586	**1**	**0.859**	0.720	0.724	**0.932**	0.714	-0.121	0.807	-0.500	0.644
RAD50	-0.802	0.157	**0.859**	**1**	**0.913**	**0.871**	**0.933**	0.596	-0.154	0.561	-0.473	**0.897**
BAX	-0.713	-0.134	0.720	**0.913**	**1**	**0.901**	0.788	0.649	-0.223	0.566	-0.627	**0.974**
CASP3	-0.798	-0.064	0.724	**0.871**	**0.901**	**1**	0.695	0.801	0.197	0.615	-0.779	**0.950**
GR	**-0.846**	0.425	**0.932**	**0.933**	0.788	0.695	**1**	0.571	-0.345	0.575	-0.284	0.714
GPX2	**-0.889**	0.202	0.714	0.596	0.649	0.801	0.571	**1**	0.185	0.680	-0.730	0.657
CAT	-0.025	-0.014	-0.121	-0.154	-0.223	0.197	-0.345	0.185	1	0.112	-0.428	-0.049
cROS	-0.791	0.494	0.807	0.561	0.566	0.615	0.575	0.680	0.112	**1**	-0.793	0.477
mtROS	0.606	0.058	-0.500	-0.473	-0.627	-0.779	-0.284	-0.730	-0.428	-0.793	**1**	-0.651
CPD DNA damage	-0.674	-0.236	0.644	**0.897**	**0.974**	**0.950**	0.714	0.657	-0.049	0.477	-0.651	**1**

6.4 Discussion

This chapter proposes a toxicity pathway addressing the biological effects of UVB exposure on *Tisbe battagliai*, an ecologically important intertidal benthic copepod, and taken here as representative of mobile meiozoobenthic communities. The adverse effects of UVB on marine copepods are well-studied; however, the causality between modes of action and adverse effects has not yet been fully established. Toxicity pathway development was enabled by detailed characterisation of changes to molecular and cellular biomarkers belonging to KE along one main toxicological pathway.

Determining an integrated understanding of an organism's exposure to UV is not straightforward, and even less so for aquatic and marine species. However, the evidence presented here suggests that UVB exposure triggers an irradiance-dependent toxicity pathway in *T. battagliai*. This pathway was conceptualised by assembling responses encompassing different levels of biological organisation (Figure 6.6), with ROS and CPD formation considered as the main molecular initiating events, inducing a series of complex key events leading to adverse outcomes. However, other possible routes to toxicity exist that were not included in this study, for illustration, see the toxicity pathway assembled for UVB effects in *D. magna* by Song *et al.* (2020b).

Oxidative stress and fitness are inversely proportional in copepods (Barreto and Burton, 2013; Han *et al.*, 2014; Halsband *et al.*, 2021). In this study, ROS-mediated oxidative stress was induced at 24 hours and was linked with consequential DNA damage. A similar response was observed in *Tigriopus japonicus*, exhibiting a near two-fold increase in intracellular ROS after 24-hours dose of 12 kJ m^{-2} UVB – approximately 0.14 W m^{-2} (Kim *et al.*, 2015).

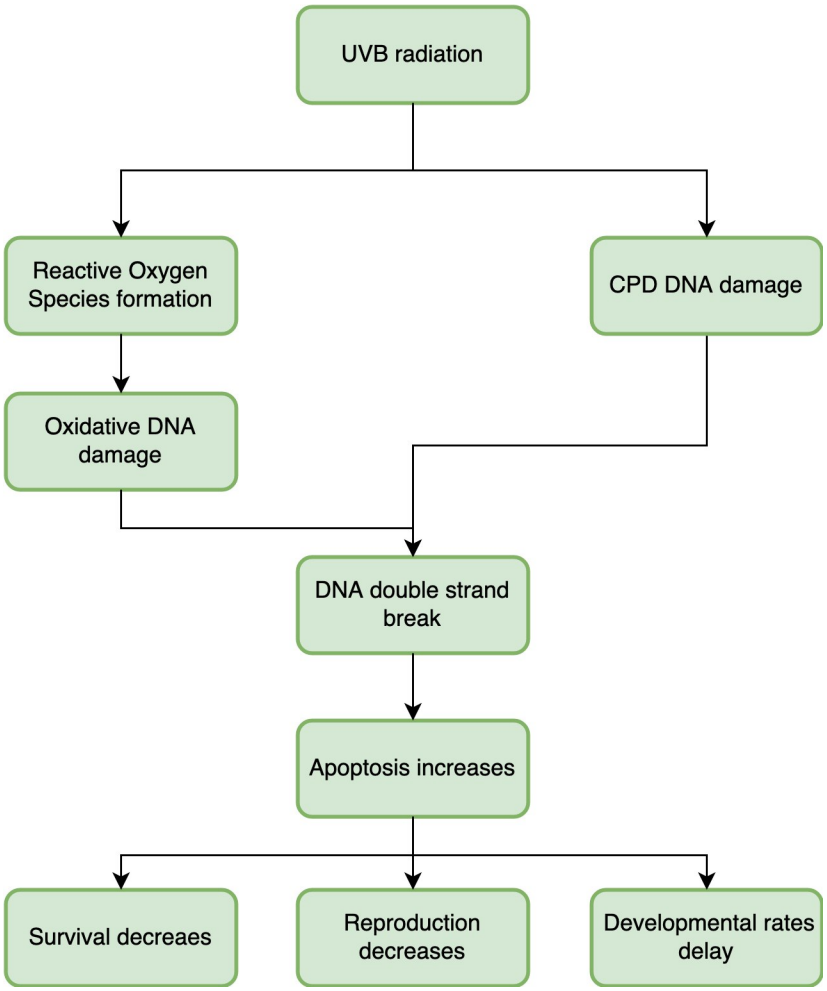

Figure 6.6. A putative toxicity pathway for the short-term ultraviolet B (UVB) radiation exposure in *Tisbe battagliai*. The direction of the arrow indicates the trend in the measured endpoint.

This study used two different ROS probes, which detected different ROS formation in this present study. Possible explanations could be attributed to the forms of ROS able to be detected. H_2DCFDA is able to detect many ROS including hydrogen peroxide, hydroxyl radicals, hydroperoxides, and peroxynitrite. DHR123 can provide information on nonsuperoxide ROS in the mitochondria, preferably hydrogen peroxide and peroxynitrite, but not superoxide (Cho and Hwang, 2011). Additionally, DHR123 has been found to produce a large background fluorescence in the absence of ROS in samples (Soh, 2006). However, this probe has produced similar results to the H_2DCFDA probe in other studies, including with UVB exposure to *Daphnia magna* (Song *et al.*, 2020b). Furthermore, the ROS and RNA samples were taken following a 10-hour period of darkness. Cells can manage ROS accumulation and ROS-induced stress if afforded time to recover (Obermuller, 2006); the period of darkness provided just such a potential recovery window. Swift acting endogenous

enzymatic defences could constrain ROS accumulation (Das and Roychoudhury, 2014; Kim, Park and Choi, 2009; Souza *et al.*, 2012). For instance, caspase-3 increased two-fold after one hour and glutathione S-transferase (GST) increased 2.5-fold after two hours of cumulative UVR doses in adult *Eudiaptomus gracilis* (Souza *et al.*, 2012). GST activity changes could be a suitable sign of UVB induced ROS formation and management (Souza *et al.*, 2012). Although enzyme activity was not measured directly in the present study, the extent of gene transcription does provide valuable insight. The upregulation of GR after 24 hours would account for the decreased ROS detected at 0.1-0.4 W m^{-2} after 48 hours and 0.8 W m^{-2} throughout the experiment. This pattern is not universally reflected in the crustacean literature, for example, Won and co-workers described that *Paracyclopina nana* experienced dose dependent UV-induced ROS production and oxidative stress-mediated cellular damage, inferring that the mechanisms for ROS production and removal were unbalanced (Won *et al.*, 2014).

In addition to oxidative stress, UVB exposure can directly damage DNA by inducing the formation of DNA photoproducts (DNA lesions) such as cyclobutane pyrimidine dimers (CPD) that may lead to apoptotic cell death. Apoptosis eliminates damaged cells to protect the whole organism from genomic instability and mutations (Elmore, 2007), yet unchecked apoptosis is a major contributor to organ failure and mortality in crustaceans (Hollmann *et al.*, 2016; Menze *et al.*, 2010a). High levels of CPD DNA lesions were present at all irradiances after 12 hours. Further, RAD23, a DNA nucleotide excision repair gene specific to UVB-induced damage was significantly upregulated at the two highest irradiances, indicative that DNA photoproduct formation is a main cytotoxicity route for *T. battagliai*. Although not measured directly, genes involved with apoptotic signalling pathways were significantly upregulated, but only at high UVB irradiances. Although, CASP3 plays a critical role in the execution-phase of apoptosis in some crustaceans (Miguel *et al.*, 2007; Hollmann *et al.*, 2016), its importance in copepods is ambiguous (Romano *et al.*, 2003; Shi *et al.*, 2017). Direct apoptosis measurements for *D. magna* showed significant increases in apoptosis following 0.1 and 0.2 W m^{-2} exposures after 2 days (Song *et al.*, 2020b) and *Macrobrachium olfersii* embryos had significantly increased numbers of apoptotic cells after 12 hours of 5.58 kJ m^{-2} UVB exposure (~ 0.065 W m^{-2}), in addition to increased BAX and CASP3 activity (Schramm *et al.*, 2017).

Given the propensity for UVB to damage biological macromolecules, including DNA and lipids, the efficient operation of molecular and cellular repair mechanisms are vital for zooplankton survival (Stábile *et al.*, 2021); however, they incur a metabolic cost. This additional energy requirement could be fulfilled by reallocating energy from somatic growth and reproduction (Wolinski *et al.*, 2020; Stábile *et al.*, 2021). Short-term reproduction was measured by counting clutches and the number of hatched nauplii, then observing their survival. Our results showed that UVB caused short-term reproductive problems, including delayed development for the first two clutches, particularly in the second clutch even at low irradiances. This has been seen in other marine copepods, for example, *Tigriopus californicus* produced fewer clutches with no hatched nauplii when exposed to irradiances above 0.5 W m^{-2} for one and three hours (Heine *et al.*, 2019).

T. battagliai's reproductive strategy enables them to store sperm, meaning they can produce multiple clutches from a single mating (Hutchinson *et al.*, 1999). However, this can increase the vulnerability of the stored sperm to environmental stressors (Fitzer *et al.*, 2012). If the paternal DNA is damaged by UVB this may lead to reproductive impairment that could have population level impacts. Similar impacts on reproductive success have been seen in the marine copepods *Calanus finmarchicus* (Rodriguez *et al.*, 2000) and *Paracyclopina nana* (Won *et al.*, 2014) and the marine cladoceran *Daphniopsis tibetana* (Wang *et al.*, 2019). According to Lacuna and Uye (2000), eggs were more susceptible to UVB than other life stages of the brackish copepod *Sinocalanus tenellus*. This higher sensitivity may explain why once hatched, naupliar mortality was high, with clutch one having increased mortality over the seven-day monitoring period. There was an irradiance dependant decrease in survival for clutch two, albeit not significant.

Adverse life history effects were detected at irradiances of 0.2 W m^{-2} and above, which is commensurate with the upper range of ground level summer irradiances in the UK (DEFRA, 2020). Developmental delays were determined by the number of individuals that moulted to the first copepodite stage by day 4. Even though the second clutch in this study was not directly exposed to UVB, there were more life-history effects, with developmental delays seen after all irradiances when compared with clutch one; potentially a reproductive impact of high CPD related DNA damage in the gravid female. This highlights the importance of investigating more than a single clutch, as clutch two was more impacted from UVB damage than clutch one.

Tigriopus japonicus also experiences irradiance dependent developmental delay, taking six to eight days to reach the copepodite stage (Puthumana *et al.*, 2017). Furthermore, copepods including the Harpacticoida have been reported to experience dormancy (diapause) when under environmental stress, thus conserving energy (Dahms, 1995). Diapause can be triggered by abiotic factors including photoperiod and chemical cues (Coull and Dudley, 1976; Dahms, 1995). Protection from UVR has been reported from the coating of resting eggs in some copepod species (Fryer, 1996), further suggesting the ability to select for development delay when faced with environmental stress.

Survival was somewhat reduced after 24 hours, however by 48 hours the mortalities were high suggesting a delay between ROS formation and death. Such delay is unsurprising as a time lag is expected between ROS formation, oxidative DNA damage and death; likely modulated by the transcription of genes related to oxidative damage repair. Such an interpretation is supported by the correlation biplot, although the mtROS data did not fit this pattern and antioxidant genes such as CAT, which code for the protein to break down hydrogen peroxide before it can be converted into ROS, and GPX2, which catalyses the reduction of hydrogen peroxide by glutathione, were not induced at any irradiance tested.

To appropriately contextualise the interpretation of these data it must be recognised that the exposure intertidal organisms such as *T. battagliai* to UVR varies in time and space, ranging from the macroscale (e.g., proximity to ozone-depleted high latitudes) to the microscale (e.g., the extent of shading within the local environment), from strong seasonal signals characteristic of temperate and polar latitudes, to the extremes of night versus day, and even throughout daylight hours (solar azimuth and weather fluctuations). Temporal variation is further complicated by tidal cycles, which directly affect water column depth and, by extrapolation, the extent of UVR attenuation (Santas, Kousoulaki and Häder, 1997). For example, in the southern North Sea UVB does not penetrate beyond one metre, with a mean attenuation coefficient of 3.5 for 305nm during summer months (Dring *et al.*, 2001). However, intertidal organisms are exposed to damaging UV irradiances during tidal emersion, thus providing the evolutionary driver towards behavioural and physiological adaptation.

Other local features also exert strong controls over UVR exposure, including the concentration of dissolved and particulate compounds in the water, as well as biotic and behavioural responses such as the accumulation of UV-protecting chemicals (Hylander and Jephson, 2010), burrowing or shelter-seeking behaviours, and the extent to which the organism partitions its foraging between diurnal and nocturnal phases (Hicks, 1986; Armonies, 1989; Miner, Morgan and Hoffman, 2000; Leech and Williamson, 2000). While not all of these can be considered in a laboratory study, natural daylight cycles and UV exposure were mimicked alongside environmentally relevant UVB dose-rates. The copepods used in the present study were not acclimatised or pre-exposed to UVB, therefore the sudden exposure to UVB may make them more susceptible to stress compared to field collected or pre-acclimated organisms (Kim, Park and Choi, 2009; Kim *et al.*, 2009).

6.5 Conclusion

The effects assessment of UVB radiation carried out on *T. battagliai* included multiple levels of biological organisation to understand possible effects and outcomes. The targeted biomarkers suggest a toxicity pathway mediated by DNA damage and terminating in loss of reproductive fitness and mortality at UVB irradiances above 0.2 W m^{-2} after 48 hours. Toxicity pathway development is the first step to full toxicological effects quantification, particularly if the AOP framework is to be fully implemented into all aspects of ecological risk assessment – which would be a rarity for non-chemical stressors such as UVB. Developing toxicity pathways for both chemical and non-chemical stressors will greatly enhance our understanding of toxicity mechanisms in marine copepods.

Chapter 7. Synthesis

In this thesis, hazard assessments were conducted for two lower trophic marine organisms, *Tetraselmis suecica* and *Tisbe battagliai*. A summary of the thesis' findings is presented to compare species sensitivity to single and combined metals. Following this, a holistic approach to metal toxicity characterisation is presented, by integrating aspects of exposure and hazard assessments. To respond to the needs of an ever-changing environment, non-chemical stressors must be introduced into hazard assessments. In turn, this can better inform environmental risk assessment, especially amid a climate crisis. To conclude, a review of the contribution that this thesis has made towards hazard and risk assessment within the scope of the MixRisk project is presented.

7.1 Species sensitivity for copper, nickel, and zinc

From the single metals, copper was most toxic to *Tisbe* survival but had the least impact on *Tetraselmis* growth, suggesting differing modes of action between the species. Reactive oxygen species (ROS)—which is known to be copper induced—was measured for both species, with *Tetraselmis* having the highest ROS levels. The 24-hour LC_{50} for gravid female *Tisbe* was over 60-fold lower than the 24-hour EC_{50} value for *Tetraselmis*, suggesting that food web impacts would be most felt at the primary consumer level. In contrast, the 24-hour EC_{50} and LC_{50} zinc exposure values were similar for both species (*Tetraselmis* 8.40 and *Tisbe* 6.62 µM). Although not directly comparable in time, the seven-day nickel EC_{50} value for *Tetraselmis* was over two-fold lower than the 48-hour LC_{50} value for gravid female *Tisbe*.

The systematic review (Chapter two) found that bioaccumulation via trophic transfer was an avenue of toxicity for some copepods, indicating that there are additional exposure routes for *Tisbe* that were not characterised in this thesis. If taken to a larger scale – for example using a mesocosm experiment set up to mimic field conditions – then these additional exposure routes should be included. An interesting experimental set up would include multiple species exposure, where both microalgae and copepods are exposed to metals via contaminated water and sediment. This could facilitate a better understanding of how multiple species can be impacted by anthropogenic chemical stressors.

7.2 Cumulative hazard assessments for trace metals

Chapters 3 and 5 examined more realistic environmental scenarios involving exposure to mixtures of metals. All three metals contributed to the overall mixture toxicity for both species, although under mixture conditions copper was identified as the main effect driver for *Tetraselmis* growth in contrast with the single metals outcome. This change in metal influence suggests that interactions are occurring within the exposure solutions, at the uptake site, or once inside the cells. The mixture outcome was more consistent for *Tisbe* survival with all three metals identified as significant main effect drivers.

Definitive screening design (DSD) enabled the identification of metals that were acting as main effect drivers, as well identifying metals interactions. Copper-nickel-zinc mixtures exhibited significant interactions; however, as uptake measurements or body burden concentrations were not recorded it is difficult to specify where these interactions were occurring i.e., at the uptake site (toxicokinetic) or within the organism (toxicodynamic).

To understand whether there were any interactions within the exposure solutions, and if so, how they might impact bioavailability and toxicity, metal fractionation analysis was included in Chapters 4 and 5 alongside effect measurements. Metal fractionation was measured in single and combined metal solutions (seawater) for *Tisbe*, showing a shift in zinc fractions when present with copper and/or nickel. Low molecular mass fraction concentrations increased from single zinc solutions to copper-nickel-zinc solutions, suggesting interactions were occurring in the seawater before being taken up by the organism. When metal interactions occur within the exposure pathway they can contribute to increased toxicity in the effects pathway, as many metals rely on other metals to be up taken; for example, non-essential metals can be up taken alongside essential metals or by hijacking ion pumps for essential metals and creating competitive uptake (Martinez-Finley *et al.*, 2012). Further interactions may have occurred at the uptake site or once inside the organism. Information on these exposure interactions would have provided greater clarity on mixture interactions for marine copepods and would have further helped characterise toxicity and mixture mode of actions. Introducing these into common practice for cumulative hazard assessments for chemical stressors would foster a more holistic understanding of toxicity.

Overall, these main findings suggest that metal mixtures will impact microalgae and copepods even at low concentrations, with all three metals able to contribute to overall mixture toxicity rather than a single metal dominating within the mixture. This adds an additional level of complexity to the management of chemical mixtures in coastal environments, as interactions need to be considered for the most sensitive species even when individual stressors are at low concentrations. Despite this, comparisons between predicted and measured *Tisbe* survival found mostly additive outcomes and antagonistic interactions. As regulatory mixture assessments tend to use additive prediction models as a worst-case scenario (Kienzler *et al.*, 2014), this will lead to adequate management, whereas synergistic interactions could lead to inadequate management. Though as mentioned by Fong, Bittick and Fong (2018), management of one stressor from the synergistic mixture could accelerate community recovery, as the net effect on the community will be reduced. Further information on cumulative toxicity mechanisms are needed to successfully implement management of combined stressors, rather than only adverse outcomes, as effects of some chemicals will not be detected as mortality is the final outcome of all toxicity effects (Yoo *et al.*, 2021). The use of molecular effects alongside adverse outcomes can be important when dealing with low environmental concentrations as molecular effects can be modulated following low mixture exposure.

7.3 Cumulative hazard assessments for chemical and non-chemical stressors

As previously discussed, hazard assessments have historically focused on chemical stressors. However, when considering real-life mixture scenarios, multiple stressor types (including non-chemical stressors) are likely to be interacting. Including non-chemical stressors in cumulative hazard assessments therefore represents an important step forward in developing a fit-for-purpose assessment, and to facilitate greater applicability from laboratory studies to field studies. As shown in Chapters 4 and 6, some effects resulting from trace metals and UVB radiation involved in similar toxicity oxidative stress pathways. These responses could be compared to individual stressor responses and predictive models used to determine whether interactions are additive, antagonistic, or synergistic.

Drawing on the toxicity characterised in this thesis and using published literature, a conceptual diagram was developed to show a possible real-life scenario (Figure 7.1). This figure highlights the complexity of developing hazard assessments that can

handle realistic stressor combinations and interactions for multiple species. As shown in Chapter 2, exposure route and concentration can heavily influence stressor toxicity; as such, the figure includes three possible exposure routes – water, dietary, and sediment exposure. Here, sediment is featured as an exposure route that is of particular importance for species that exist at the sediment-seawater interface.

Although this depicts a complex web of interactions, this remains a simplistic approach to understanding and characterising real-life scenarios in a coastal setting. As the focus was on coastal species and environments, there will also be interactions occurring between the atmosphere and sediment in the intertidal zone. In figure 7.1, this interaction is highlighted using overlapping circles; however, the main interactions are likely occurring between the seawater and atmosphere, and the seawater and sediment. Considering interactions between these compartments will become more important as climate change continues. A changing climate will introduce additional physical stressors such as marine heat waves. Developing a more robust understanding of the impact/interactions of non-chemical stressors on the toxicity of chemical stressors should be a growing research priority. For example, the toxicity of polycyclic aromatic hydrocarbons increases when exposed to UV radiation (Häder *et al.*, 2015).

Chemical stressors are very likely to be heavily influenced climate change in the Arctic, which is experiencing rapidly increasing temperatures, thinning sea ice cover and, in spring 2020, unprecedented UV radiation increases which doubled UV indices for some locations (Neale *et al.*, 2021), posing an existential threat to many species of polar microalgae and copepods (Serreze and Meier, 2019). Melting sea ice also provides a significant source of metals to the surrounding seawater, including copper, nickel and zinc (Tovar-Sánchez *et al.*, 2010). This could lead to these organisms experiencing higher irradiances and increased metal concentrations. Furthermore, common predictions used by climate models group areas together and make assumptions about interactions and how organisms will respond. This can miss important variations and sensitivities at a local level and reinforces the importance of experimentally verifying mixture scenarios.

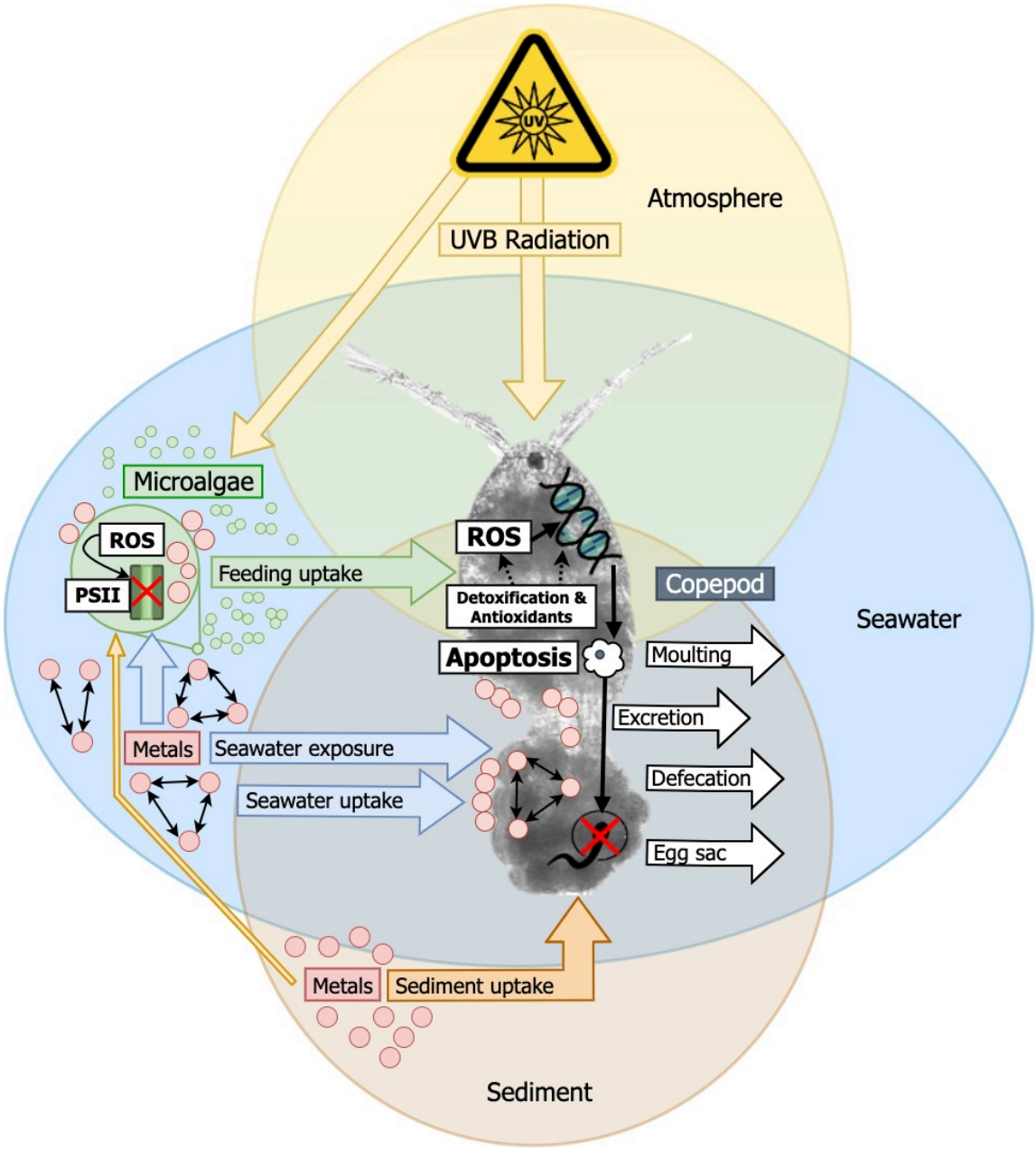

Figure 7.1. A conceptual diagram of multiple interactions occurring in the coastal environment for *Tisbe battagliai* and *Tetraselmis suecica* (green circles in the seawater). The overlaid coloured circles represent different interacting parts of the environment (blue = seawater, yellow = atmosphere and brown = sediment) and how these intersect with *T. battagliai* and *T. suecica*. Each part of the environment is providing a chemical (metals) or non-chemical stressor (UVB radiation). For the metals (red circles), the possible uptake mechanisms are labelled using large arrows pointing towards the copepod or microalgae. For the microalgae, the arrow for metal up take from sediment is narrower, as this is likely not the main up take route. For the copepod, uptake from seawater can occur by absorption or adsorption. The large arrows pointing away from the copepod represent possible removal mechanisms for metals. The thin black arrows are showing the direction of internal stress, with reactive oxygen species (ROS), DNA damage, apoptosis and reproductive and development impacts occurring inside the copepod. The thin dotted arrows suggest possible routes for detoxification and antioxidant activity. For the microalgae, ROS formation and photosystem II (PSII) efficiency inhibition impacts are shown after metal exposure.

Although this thesis has characterised combined metal toxicity within two lower trophic species along a potential pathway, it has not been possible to evaluate how non-chemical stressors may modify these. There remains a vast gap in our understanding of the interactions between chemical and non-chemical stressors, as studies have not traditionally focused on this. Utilising the data from this thesis, figure 7.2 shows which aspects of the toxicity pathway have been characterised and where data gaps exist. The main gaps include understanding how uptake and exposure affect toxicity and how multiple simultaneous routes of exposure affect toxicity. Further research to address these gaps can help to better characterise the uptake, exposure, and response mechanisms of lower trophic species.

The DSD mixture design used in this thesis was a successful tool for multi stressor studies. Although this thesis focused on a chemical mixture, the ability to add non-chemical stressors to this mixture design is unlike most used approaches in ecotoxicology. One of these approaches is the biotic ligand model (BLM). BLM is a mechanistic approach used in aquatic ecotoxicology to determine metal toxicity in the natural environment (Niyogi and Wood, 2004). BLM uses chemical speciation and toxicological data to predict the toxicity of metals using an equilibrium geochemical speciation model, a metal-organic model and a toxicological model, assuming that metal toxicity is proportional to the fraction of metal bound to the biotic ligand or within the target organism (Smith, Balistrieri and Todd, 2015). This approach is specific for metals that benefits from its ability to incorporate metal bioavailability with metal toxicity, originally developed for individual metals. The development of this model to include multiple metals has been achieved, with Wang *et al.* (2020) using extended BLMs for binary metals that include competition between magnesium and metal ions. However, this approach is limited to how far it can be extended to include other chemical stressors outside of metals and would not be able to include non-chemical stressors. This highlights how important a flexible model that can be used for any stressor type is as a tool to improve mixture toxicity predictions. The DSD design is a novel approach to mixture toxicity for aquatic ecotoxicology, which could be further implemented for up to 20 stressors in a mixture scenario. This is vital for characterising toxicity and understanding how the toxicity of non-stressors are being altered in a changing climate.

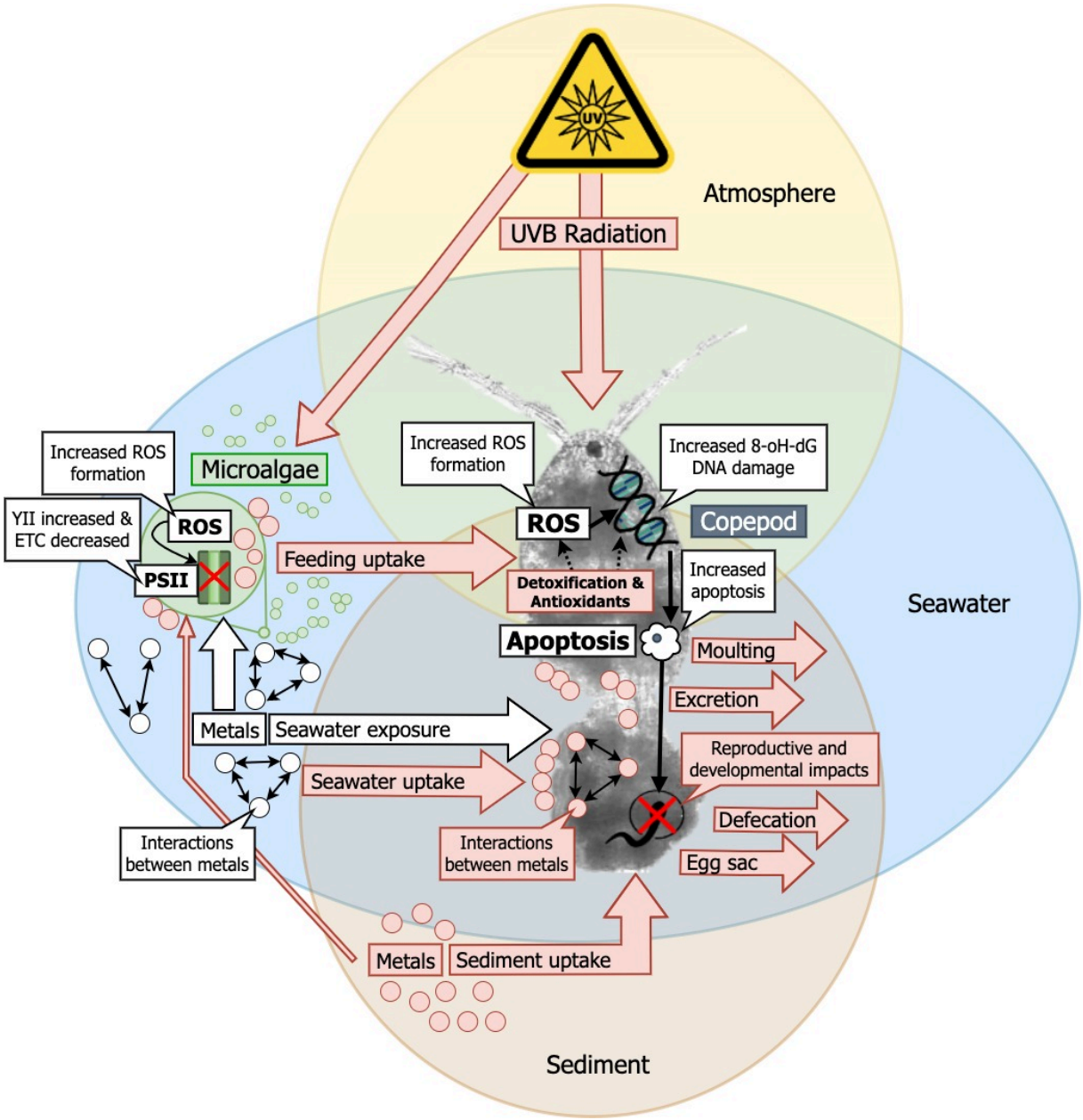

Figure 7.2. A data populated conceptual diagram of multiple interactions occurring in the coastal environment for *Tisbe battagliai* and *Tetraselmis suecica*. The boxes and arrows in white represent exposures, interactions and endpoints that were measured in a combined stressor experiment in this thesis. The red boxes and arrows indicate the data gaps in this complex web of combined stressors and multiple species that were not directly measured in this thesis.

7.4 The future of cumulative hazard assessments

DEFRA has predicted potential risks to marine species, habitats and fisheries from higher temperatures, increased ocean acidification and invasive species by 2050. This could be disastrous for marine environments and the industries that depend on them (predicted to cost tens of millions GBP per annum) (DEFRA, 2022). According to Forzieri *et al.* (2016), cumulative hazard assessment involving climate hazards

poses two main challenges: (1) how to compare hazards that often have different processes and outcomes, and (2) that interactions between hazards can trigger cascading effects. The use of standardised approaches can help when comparing hazards; however, most of this research is focused on chemical stressors, rather than non-chemical and physical stressors that will become more potent or more frequent in the climate crisis. The second issue can be included in the design of hazard assessments, for example using toxicity pathways. The role of adverse outcome pathways (AOPs) in cumulative hazard assessments helps organise effects and understand interactions that trigger an effect at the next level of biological organisation. The use of AOPs can support a holistic approach to hazard assessment, which includes effects that are triggered by hazards (Gill and Malamud, 2014).

7.5 Conclusion

The MixRisk project aimed to develop and evaluate tools for a holistic approach to risk assessment of complex chemical and non-chemical mixtures assessments. This was achieved using computational tools to estimate risk and experimentally to verify risk predictions and evaluate predictive models for chemical and non-chemical stressors – concentration addition (CA) and independent action (IA) models. Within this thesis, combined toxicity assessments were conducted for metals identified as high-risk in a marine environment. The use of a statistical design of experiments approach to tackle experimental mixtures in a laboratory setting provided a tool to determine mixture interactions that could be compared to predicted interactions (CA and IA), yet were quicker, cheaper, and used fewer resources than more traditional approaches. By using an integrated ecotoxicological approach that organises effects at different biological levels, this thesis characterised a stressor-specific toxicity pathway from exposure to adverse outcome and identified key areas of research for the future of hazard assessment in the marine environment.

References

Aas, E. and Hojerslev, N. (2001) 'Attenuation of ultraviolet irradiance in North European coastal waters', *Oceanologia,* 43(2), pp. 139-139.

Abel, P. D. (1997) 'Water pollution biology', *Journal of the Marine Biological Association of the United Kingdom,* 77(3), pp. 917-917.

Ajitha, V., Sreevidya, C. P., Sarasan, M., Park, J. C., Mohandas, A., Singh, I. S. B., Puthumana, J. and Lee, J.-S. (2021) 'Effects of zinc and mercury on ROS-mediated oxidative stress-induced physiological impairments and antioxidant responses in the microalga *Chlorella vulgaris*', *Environmental Science and Pollution Research,* 28(25), pp. 32475-32492.

Ali, H. and Khan, E. (2019) 'Trophic transfer, bioaccumulation, and biomagnification of non-essential hazardous heavy metals and metalloids in food chains/webs—concepts and implications for wildlife and human health', *Human and Ecological Risk Assessment: An International Journal,* 25(6), pp. 1353-1376.

Ali, H., Khan, E. and Ilahi, I. (2019a) 'Environmental Chemistry and Ecotoxicology of Hazardous Heavy Metals: Environmental Persistence, Toxicity, and Bioaccumulation', *Journal of Chemistry*.

Ali, H., Khan, E. and Ilahi, I. (2019b) 'Environmental chemistry and ecotoxicology of hazardous heavy metals: environmental persistence, toxicity, and bioaccumulation', *Journal of Chemistry,* 2019, pp. 1 - 15.

Alves, R. N. and Agustí, S. (2020) 'Effect of ultraviolet radiation (UVR) on the life stages of fish', *Reviews in Fish Biology and Fisheries,* 30(2), pp. 335-372.

Ameri, M., Baron-Sola, A., Khavari-Nejad, R. A., Soltani, N., Najafi, F., Bagheri, A., Martinez, F. and Hernández, L. E. (2020) 'Aluminium triggers oxidative stress and antioxidant response in the microalgae *Scenedesmus* sp.', *Journal of Plant Physiology,* 246-247, pp. 1 - 30.

Arifin, Z., Puspitasari, R. and Miyazaki, N. (2012) 'Heavy metal contamination in Indonesian coastal marine ecosystems: A historical perspective', *Coastal Marine Science,* 35(1), pp. 277 - 233.

Armonies, W. (1989) 'Meiofaunal emergence from intertidal sediment measured in the field: significant contribution to nocturnal planktonic biomass in shallow waters', *Helgoländer Meeresuntersuchungen,* 43(1), pp. 29-43.

Bailey, A., De Wit, P., Thor, P., Browman, H. I., Bjelland, R., Shema, S., Fields, D. M., Runge, J. A., Thompson, C. and Hop, H. (2017) 'Regulation of gene expression is associated with tolerance of the Arctic copepod *Calanus glacialis* to CO2-acidified sea water', *Ecology and Evolution,* 7(18), pp. 7145-7160.

Bais, A. F., Lucas, R. M., Bornman, J. F., Williamson, C. E., Sulzberger, B., Austin, A. T., Wilson, S. R., Andrady, A. L., Bernhard, G., McKenzie, R. L., Aucamp, P. J., Madronich, S., Neale, R. E., Yazar, S., Young, A. R., de Gruijl, F. R., Norval, M., Takizawa, Y., Barnes, P. W., Robson, T. M., Robinson, S. A., Ballaré, C. L., Flint, S. D., Neale, P. J., Hylander, S., Rose, K. C., Wängberg, S. Å., Häder, D. P., Worrest, R. C., Zepp, R. G., Paul, N. D., Cory, R. M., Solomon, K. R., Longstreth, J., Pandey, K. K., Redhwi, H. H., Torikai, A. and Heikkilä, A. M. (2018) 'Environmental effects of ozone depletion, UV radiation and interactions with climate change: UNEP Environmental Effects Assessment Panel, update 2017', *Photochemical & photobiological sciences : Official journal of the European Photochemistry Association and the European Society for Photobiology,* 17(2), pp. 127-179.

Balaji, S., Kalaivani, T., Sushma, B., Pillai, C. V., Shalini, M. and Rajasekaran, C. (2016) 'Characterization of sorption sites and differential stress response of microalgae isolates against tannery effluents from ranipet industrial area—An application towards phycoremediation', *International Journal of Phytoremediation,* 18(8), pp. 747-753.

Balali-Mood, M., Naseri, K., Tahergorabi, Z., Khazdair, M. R. and Sadeghi, M. (2021) 'Toxic mechanisms of five heavy metals: mercury, lead, chromium, cadmium, and arsenic', *Frontiers in Pharmacology,* 12(227), pp. 1 - 19.

Balls, P. W. (1985) 'Copper, lead and cadmium in coastal waters of the western North Sea', *Marine Chemistry,* 15(4), pp. 363-378.

Banks, A. M., Whitfield, C. J., Brown, S. R., Fulton, D. A., Goodchild, S. A., Grant, C., Love, J., Lendrem, D. W., Fieldsend, J. E. and Howard, T. P. (2022) 'Key reaction components affect the kinetics and performance robustness of cell-free protein synthesis reactions', *Computational and Structural Biotechnology Journal,* 20, pp. 218-229.
Barata, C., Lekumberri, I., Vila-Escalé, M., Prat, N. and Porte, C. (2005) 'Trace metal concentration, antioxidant enzyme activities and susceptibility to oxidative stress in the tricoptera larvae *Hydropsyche exocellata* from the Llobregat river basin (NE Spain)', *Aquatic Toxicology,* 74(1), pp. 3-19.
Barka, S., Pavillon, J. F. and Amiard, J.-C. (2001) 'Influence of different essential and non-essential metals on MTLP levels in the Copepod *Tigriopus brevicornis*', *Comparative biochemistry and physiology. Toxicology & pharmacology : CBP,* 128(4), pp. 479-93.
Barreto, F. S. and Burton, R. S. (2013) 'Elevated oxidative damage is correlated with reduced fitness in interpopulation hybrids of a marine copepod', *Proceedings of the Royal Society B: Biological Sciences,* 280(1767), pp. 1-6.
Battaglia, B. and Volkmann-Rocco, B. (1973) 'Geographic and reproductive isolation in the marine Harpacticoid Copepod *Tisbe*', *Marine Biology,* 19(2), pp. 156-160.
Bengtsson, B.-E. (1978) 'Use of a harpacticoid copepod in toxicity tests', *Marine Pollution Bulletin,* 9(9), pp. 238-241.
Beyer, J., Petersen, K., Song, Y., Ruus, A., Grung, M., Bakke, T. and Tollefsen, K. E. (2014) 'Environmental risk assessment of combined effects in aquatic ecotoxicology: A discussion paper', *Pollutant Responses in Marine Organismsî (PRIMO17),* 96, pp. 81-91.
Bielmyer, G. K., Grosell, M. and Brix, K. V. (2006) 'Toxicity of silver, zinc, copper, and nickel to the Copepod *Acartia tonsa* Exposed via a phytoplankton diet', *Environmental Science & Technology,* 40(6), pp. 2063-2068.
Blaxter, J. H., Douglas, B., Tyler, P. A. and Mauchline, J. (1998) *Advances in marine biology, the biology of calanoid copepod.* Cambridge, MA: Academic Press.
Bliss, C. I. (1939) 'The toxicity of poisons applied jointly', *Annals of Applied Biology,* 26(3), pp. 585-615.
Boissonnot, L., Niehoff, B., Hagen, W., Søreide, J. E. and Graeve, M. (2016) 'Lipid turnover reflects life-cycle strategies of small-sized Arctic copepods', *Journal of Plankton Research,* 38(6), pp. 1420-1432.
Bopp, S. K., Abicht, H. K. and Knauer, K. (2008) 'Copper-induced oxidative stress in rainbow trout gill cells', *Aquatic Toxicology,* 86(2), pp. 197-204.
Briffa, J., Sinagra, E. and Blundell, R. (2020) 'Heavy metal pollution in the environment and their toxicological effects on humans', *Heliyon,* 6(9), pp. 1 - 26.
Brix, K. V., Schlekat, C. E. and Garman, E. R. (2017) 'The mechanisms of nickel toxicity in aquatic environments: An adverse outcome pathway analysis', *Environmental Toxicology and Chemistry,* 36(5), pp. 1128-1137.
Browman, H., Rodriguez, A., BÈland, F., Cullen, J., Davis, R., Kouwenberg, J., Kuhn, P., McArthur, B., Runge, J. and St-Pierre, J.-F. (2000) 'Impact of ultraviolet radiation on marine crustacean zooplankton and ichthyoplankton: A synthesis of results from the estuary and Gulf of St. Lawrence, Canada', *Marine Ecology Progress Series,* 199, pp. 293-311.
Buttino, I., Hwang, J. S., Sun, C. K., Hsieh, C. T., Liu, T. M., Pellegrini, D., Ianora, A., Sartori, D., Romano, G., Cheng, S. H. and Miralto, A. (2011) 'Apoptosis to predict copepod mortality: state of the art and future perspectives', *Hydrobiologia,* 666(1), pp. 257-264.
Byrnes, I. T. B. (2021) *Characterization of radioactive particle exposure using micro and nano-focused X-ray techniques.* PhD thesis, Norwegian University of Life Sciences, Ås, Norway.
Cadet, J., Douki, T. and Ravanat, J.-L. (2015) 'Oxidatively generated damage to cellular DNA by UVB and UVA radiation', *Photochemistry and Photobiology,* 91(1), pp. 140-155.
Campana, O., Simpson, S. L., Spadaro, D. A. and Blasco, J. (2012) 'Sub-lethal effects of copper to benthic invertebrates explained by sediment properties and dietary exposure', *Environmental Science & Technology,* 46(12), pp. 6835-6842.
Campbell, P. G. C. (1995) 'A critique of the free-ion activity model.', in Tessier, A. and Turner, D.R. (eds.) *Metal Speciation and Bioavailability in Aquatic Systems*. Chichester, UK: John WIley and Sons, pp. 45 - 102.

Caporale, A. G. and Violante, A. (2016) 'Chemical processes affecting the mobility of heavy metals and metalloids in soil environments', *Current Pollution Reports,* 2(1), pp. 15-27.
Caramujo, M.-J., De Carvalho, C. C. C. R., Silva, S. J. and Carman, K. R. (2012) 'Dietary carotenoids regulate astaxanthin content of copepods and modulate their susceptibility to UV light and copper toxicity', *Marine Drugs,* 10(5), pp. 998 - 1018.
Cardwell, R. D., DeForest, D. K., Brix, K. V. and Adams, W. J. (2013) 'Do Cd, Cu, Ni, Pb, and Zn biomagnify in aquatic ecosystems?', in Whitacre, D.M. (ed.) *Reviews of Environmental Contamination and Toxicology Volume 226*. New York, NY: Springer New York, pp. 101-122.
Carusi, A., Davies, M. R., De Grandis, G., Escher, B. I., Hodges, G., Leung, K. M. Y., Whelan, M., Willett, C. and Ankley, G. T. (2018) 'Harvesting the promise of AOPs: An assessment and recommendations', *Science of The Total Environment,* 628-629, pp. 1542-1556.
Castro-Bugallo, A., González-Fernández, Á., Guisande, C. and Barreiro, A. (2014) 'Comparative responses to metal oxide nanoparticles in marine phytoplankton', *Archives of Environmental Contamination and Toxicology,* 67(4), pp. 483-493.
Cedergreen, N. (2014) 'Quantifying synergy: a systematic review of mixture toxicity studies within environmental toxicology', *PLOS ONE,* 9(5), pp. e96580.
Ceschin, S., Bellini, A. and Scalici, M. (2021) 'Aquatic plants and ecotoxicological assessment in freshwater ecosystems: a review', *Environmental Science and Pollution Research,* 28(5), pp. 4975-4988.
Chaitanya, R. K., Shashank, K. and Sridevi, P. (2016) 'Oxidative stress in invertebrate systems', in Ahmed, R. (ed.) *Free Radicals and Diseases*. London, UK: IntechOpen.
Cho, S. and Hwang, E. S. (2011) 'Chapter 7 - Fluorescence-based detection and quantification of features of cellular senescence', in Darzynkiewicz, Z., Holden, E., Orfao, A., Telford, W. and Wlodkowic, D. (eds.) *Methods in Cell Biology*: Academic Press, pp. 149-188.
Christopher, K. (2007) 'Marine insurance in Britain and America, 1720-1844: a comparative institutional analysis', *The Journal of Economic History,* 67(2), pp. 379-409.
Cid, A., Herrero, C., Torres, E. and Abalde, J. (1995) 'Copper toxicity on the marine microalga *Phaeodactylum tricornutum*: effects on photosynthesis and related parameters', *Aquatic Toxicology,* 31(2), pp. 165-174.
Cobbett, C. and Goldsbrough, P. (2002) 'Phytochelatins and metallothioneins: roles in heavy metal detoxification and homeostasis', *Annual Review of Plant Biology,* 53(1), pp. 159-182.
Committee, E. S., More, S. J., Bampidis, V., Benford, D., Bennekou, S. H., Bragard, C., Halldorsson, T. I., Hernández-Jerez, A. F., Koutsoumanis, K., Naegeli, H., Schlatter, J. R., Silano, V., Nielsen, S. S., Schrenk, D., Turck, D., Younes, M., Benfenati, E., Castle, L., Cedergreen, N., Hardy, A., Laskowski, R., Leblanc, J. C., Kortenkamp, A., Ragas, A., Posthuma, L., Svendsen, C., Solecki, R., Testai, E., Dujardin, B., Kass, G. E. N., Manini, P., Jeddi, M. Z., Dorne, J.-L. C. M. and Hogstrand, C. (2019) 'Guidance on harmonised methodologies for human health, animal health and ecological risk assessment of combined exposure to multiple chemicals', *EFSA Journal,* 17(3), pp. 1 - 77.
Coull, B. C. and Dudley, B. W. (1976) 'Delayed naupliar development of meiobenthic copepods', *The Biological Bulletin,* 150(1), pp. 38-46.
Dahms, H.-U. (1995) 'Dormancy in the Copepoda — an overview', *Hydrobiologia,* 306(3), pp. 199-211.
Dahms, H.-U., Dobretsov, S. and Lee, J.-S. (2011) 'Effects of UV radiation on marine ectotherms in polar regions', *Comparative Biochemistry and Physiology Part C: Toxicology & Pharmacology,* 153(4), pp. 363-371.
Dahms, H.-U. and Lee, J.-S. (2010) 'UV radiation in marine ectotherms: molecular effects and responses', *Aquatic Toxicology,* 97(1), pp. 3-14.
Damasceno, É. P., de Figuerêdo, L. P., Pimentel, M. F., Loureiro, S. and Costa-Lotufo, L. V. (2017) 'Prediction of toxicity of zinc and nickel mixtures to *Artemia* sp. at various salinities: from additivity to antagonism', *Ecotoxicology and Environmental Safety,* 142, pp. 322-329.
Danouche, M., El Ghachtouli, N. and El Arroussi, H. (2021) 'Phycoremediation mechanisms of heavy metals using living green microalgae: physicochemical and molecular approaches for enhancing selectivity and removal capacity', *Heliyon,* 7(2021), pp. 1 - 11.
Dao, L. H. T. and Beardall, J. (2016) 'Effects of lead on two green microalgae *Chlorella* and *Scenedesmus*: photosystem II activity and heterogeneity', *Algal Research,* 16, pp. 150-159.

Das, K. and Roychoudhury, A. (2014) 'Reactive oxygen species (ROS) and response of antioxidants as ROS-scavengers during environmental stress in plants', *Frontiers in Environmental Science,* 2, pp. 53.
Das, S., Ouddane, B., Hwang, J.-S. and Souissi, S. (2020) 'Intergenerational effects of resuspended sediment and trace metal mixtures on life cycle traits of a pelagic copepod', *Environmental Pollution,* 267, pp. 1 - 12.
Dayras, P., Bialais, C., Ouddane, B., Lee, J. S. and Souissi, S. (2020) 'Effects of different routes of exposure to metals on bioaccumulation and population growth of the cyclopoid copepod *Paracyclopina nana*', *Chemosphere,* 248(2020), pp. 1 - 13.
Debelius, B., Forja, J. M., DelValls, Á. and Lubián, L. M. (2009) 'Toxicity and bioaccumulation of copper and lead in five marine microalgae', *Ecotoxicology and Environmental Safety,* 72(5), pp. 1503-1513.
DEFRA (2020) 'UV radiation data for Reading University monitoring site'. Available at: https://uk-air.defra.gov.uk/data/uv-data (Accessed: 2020/04/28/).
DEFRA (2022) *UK Climate Change Risk Assessment.* London, UK: Department for Environment, Food & Rural Affairs (ISBN 978-1-5286-3136-5).
Deruytter, D., Baert, J. M., Nevejan, N., De Schamphelaere, K. A. C. and Janssen, C. R. (2017) 'Mixture toxicity in the marine environment: Model development and evidence for synergism at environmental concentrations', *Environ Toxicol Chem,* 36(12), pp. 3471-3479.
Diz, F. R., Araújo, C. V. M., Moreno-Garrido, I., Hampel, M. and Blasco, J. (2009) 'Short-term toxicity tests on the harpacticoid copepod *Tisbe battagliai*: Lethal and reproductive endpoints', *Ecotoxicology and Environmental Safety,* 72(7), pp. 1881-1886.
Djebbi, E., Bonnet, D., Pringault, O., Tlili, K. and Yahia, M. N. D. (2021) 'Effects of nickel oxide nanoparticles on survival, reproduction, and oxidative stress biomarkers in the marine calanoid copepod *Centropages ponticus* under short-term exposure', *Environ Sci Pollut Res Int,* 28(17), pp. 21978-21990.
Dring, M. J., Wagner, A., Franklin, L. A., Kuhlenkamp, R. and L¸ning, K. (2001) 'Seasonal and diurnal variations in ultraviolet-B and ultraviolet-A irradiances at and below the sea surface at Helgoland (North Sea) over a 6-year period', *Helgoland Marine Research,* 55(1), pp. 3-11.
Drira, Z., Kmiha-Megdiche, S., Sahnoun, H., Pagano, M., Tedetti, M. and Ayadi, H. (2018) 'Water quality affects the structure of copepod assemblages along the Sfax southern coast (Tunisia, southern Mediterranean Sea)', *Marine and Freshwater Research,* 69(2), pp. 220-231.
Dubrez, L., Causse, S., Borges Bonan, N., Dumétier, B. and Garrido, C. (2020) 'Heat-shock proteins: chaperoning DNA repair', *Oncogene,* 39(3), pp. 516-529.
Duffus, J. H. (2002) '"Heavy metals" a meaningless term? (IUPAC Technical Report)', *Pure and Applied Chemistry,* 74(5), pp. 793-807.
Elmore, S. (2007) 'Apoptosis: a review of programmed cell death', *Toxicologic Pathology,* 35(4), pp. 495-516.
Ensibi, C. and Daly Yahia, M. N. (2017) 'Toxicity assessment of cadmium chloride on planktonic copepods *Centropages ponticus* using biochemical markers', *Toxicology Reports,* 4(2017), pp. 83-88.
Eurostat (2020) 'Chemicals production and consumption statistics'. Available at: https://ec.europa.eu/eurostat/statistics-explained/index.php?title=Chemicals_production_and_consumption_statistics (Accessed: 22nd March 2022).
Evans, D. H. (1987) 'The fish gill: site of action and model for toxic effects of environmental pollutants', *Environmental Health Perspectives,* 71, pp. 47-58.
Expósito, N., Carafa, R., Kumar, V., Sierra, J., Schuhmacher, M. and Papiol, G. G. (2021) 'Performance of *Chlorella Vulgaris* exposed to heavy metal mixtures: linking measured endpoints and mechanisms', *International Journal of Environmental Research and Public Health,* 18(3), pp. 1 - 19.
Expósito, N., Kumar, V., Sierra, J., Schuhmacher, M. and Giménez Papiol, G. (2017) 'Performance of *Raphidocelis subcapitata* exposed to heavy metal mixtures', *Science of The Total Environment,* 601-602, pp. 865-873.

Farland, W. H. (1992) 'The U.S. Environmental Protection Agency's risk assessment guidelines: current status and future directions', *Toxicology and Industrial Health,* 8(3), pp. 205-212.
Farman, J. C., Gardiner, B. G. and Shanklin, J. D. (1985) 'Large losses of total ozone in Antarctica reveal seasonal ClOx/NOx interaction', *Nature,* 315(6016), pp. 207-210.
Felix, C., Ubando, A., Madrazo, C., Sutanto, S., Tran-Nguyen, P. L., Go, A. W., Ju, Y.-H., Culaba, A., Chang, J.-S. and Chen, W.-H. (2019) 'Investigation of direct biodiesel production from wet microalgae using definitive screening design', *Innovative Solutions for Energy Transitions,* 158(2019), pp. 1149-1154.
Filimonova, V., Gonçalves, F., Marques, J. C., De Troch, M. and Gonçalves, A. M. (2016) 'Biochemical and toxicological effects of organic (herbicide Primextra(®) Gold TZ) and inorganic (copper) compounds on zooplankton and phytoplankton species', *Aquat Toxicol,* 177(2016), pp. 33-43.
Fisher, N. S., Stupakoff, I., Sañudo-Wilhelmy, S., Wang, W.-X., Teyssié, J.-L., Fowler, S. W. and Crusius, J. (2000) 'Trace metals in marine copepods: a field test of a bioaccumulation model coupled to laboratory uptake kinetics data', *Marine Ecology Progress Series,* 194, pp. 211-218.
Fitzer, S. C., Bishop, J. D. D., Caldwell, G. S., Clare, A. S., Upstill-Goddard, R. C. and Bentley, M. G. (2012) 'Visualisation of the copepod female reproductive system using confocal laser scanning microscopy and two-photon microscopy', *Journal of Crustacean Biology,* 32(5), pp. 685-692.
Flora, S. J. S., Mittal, M. and Mehta, A. (2008) 'Heavy metal induced oxidative stress & its possible reversal by chelation therapy', *Indian Journal of Medical Research,* 128(4), pp. 501 - 523.
Fong, C. R., Bittick, S. J. and Fong, P. (2018) 'Simultaneous synergist, antagonistic and additive interactions between multiple local stressors all degrade algal turf communities on coral reefs', *Journal of Ecology,* 106(4), pp. 1390-1400.
Forget, J., Beliaeff, B. and Bocquené, G. (2003) 'Acetylcholinesterase activity in copepods (*Tigriopus brevicornis*) from the Vilaine River estuary, France, as a biomarker of neurotoxic contaminants', *Aquat Toxicol,* 62(3), pp. 195-204.
Forzieri, G., Feyen, L., Russo, S., Vousdoukas, M., Alfieri, L., Outten, S., Migliavacca, M., Bianchi, A., Rojas, R. and Cid, A. (2016) 'Multi-hazard assessment in Europe under climate change', *Climatic Change,* 137(1), pp. 105-119.
Foyer, C. H. (2018) 'Reactive oxygen species, oxidative signaling and the regulation of photosynthesis', *Environmental and experimental botany,* 154, pp. 134-142.
Franklin, N. M., Stauber, J. L., Apte, S. C. and Lim, R. P. (2002a) 'Effect of initial cell density on the bioavailability and toxicity of copper in microalgal bioassays', *Environmental Toxicology and Chemistry,* 21(4), pp. 742-751.
Franklin, N. M., Stauber, J. L., Lim, R. P. and Petocz, P. (2002b) 'Toxicity of metal mixtures to a tropical freshwater alga (*Chlorella* sp.): The effect of interactions between copper, cadmium, and zinc on metal cell binding and uptake', *Environmental Toxicology and Chemistry,* 21(11), pp. 2412-2422.
Fryer, G. (1996) 'Diapause, a potent force in the evolution of freshwater crustaceans', *Hydrobiologia,* 320(1), pp. 1-14.
Gagnon, C. and Vigneault, B. (2013) 'Metal speciation in aquatic ecotoxicology', in Férard, J.-F. and Blaise, C. (eds.) *Encyclopedia of Aquatic Ecotoxicology*. Dordrecht: Springer Netherlands, pp. 687-698.
Gaudet, C. L., Milne, D. A., Wong, M. P. and Nason, T. G. E. (1995) 'A framework for ecological risk assesessment at contaminated sites in Canada', *Human and Ecological Risk Assessment: An International Journal,* 1(3), pp. 207-230.
Gechev, T. S., Van Breusegem, F., Stone, J. M., Denev, I. and Laloi, C. (2006) 'Reactive oxygen species as signals that modulate plant stress responses and programmed cell death', *BioEssays,* 28(11), pp. 1091-1101.
Gee, J. M. (1989) 'An ecological and economic review of meiofauna as food for fish', *Zoological Journal of the Linnean Society,* 96(3), pp. 243-261.
George, E. N. K. and Orrenius, S. (1999) 'Calcium Signaling and Cytotoxicity', *Environmental Health Perspectives,* 107, pp. 25-35.

Gill, J. C. and Malamud, B. D. (2014) 'Reviewing and visualizing the interactions of natural hazards', *Reviews of Geophysics,* 52(4), pp. 680-722.
Gillmore, M. L., Golding, L. A., Angel, B. M., Adams, M. S. and Jolley, D. F. (2016) 'Toxicity of dissolved and precipitated aluminium to marine diatoms', *Aquatic Toxicology,* 174, pp. 82-91.
Giorgio, M., Dellino, G. I., Gambino, V., Roda, N. and Pelicci, P. G. (2020) 'On the epigenetic role of guanosine oxidation', *Redox Biology,* 29, pp. 101398.
Gissi, F., Stauber, J. L., Binet, M. T., Trenfield, M. A., Van Dam, J. W. and Jolley, D. F. (2018) 'Assessing the chronic toxicity of nickel to a tropical marine gastropod and two crustaceans', *Ecotoxicol Environ Saf,* 159, pp. 284-292.
Gomes, T. n., Xie, L., Brede, D., Lind, O.-C., Solhaug, K. A. r., Salbu, B. and Tollefsen, K. E. (2017) 'Sensitivity of the green algae Chlamydomonas reinhardtii to gamma radiation: Photosynthetic performance and ROS formation', *Aquatic Toxicology,* 183, pp. 1-10.
Goswami, P., Thirunavukkarasu, S., Godhantaraman, N. and Munuswamy, N. (2014) 'Monitoring of genotoxicity in marine zooplankton induced by toxic metals in Ennore estuary, Southeast coast of India', *Marine Pollution Bulletin,* 88(1), pp. 70-80.
Griffitt, R. J., Luo, J., Gao, J., Bonzongo, J.-C. and Barber, D. S. (2008) 'Effects of particle composition and species on toxicity of metallic nanomaterials in aquatic organisms', *Environmental Toxicology and Chemistry,* 27(9), pp. 1972-1978.
Guanzon, N. G., Nakahara, H. and Yoshida, Y. (1994) 'Inhibitory effects of heavy metals on growth and photosynthesis of three freshwater microalgae', *Fisheries science,* 60(4), pp. 379-384.
Guillard, R. R. L. and Ryther, J. H. (1962) 'Studies of marine planktonic diatoms I. *Cyclotella nana* Hustedt, and *Detonula confervacea* (Cleve)', *Gran. Canadian Journal of Microbiology,* 8(2), pp. 229 - 240.
Gunawan, C., Sirimanoonphan, A., Teoh, W. Y., Marquis, C. P. and Amal, R. (2013) 'Submicron and nano formulations of titanium dioxide and zinc oxide stimulate unique cellular toxicological responses in the green microalga *Chlamydomonas reinhardtii*', *Journal of Hazardous Materials,* 260, pp. 984-992.
Gutierrez, M. F., Gagneten, A. M. and Paggi, J. C. (2010) 'Copper and chromium alter life cycle variables and the equiproportional development of the freshwater copepod *Notodiaptomus conifer* (SARS)', *Water, Air, & Soil Pollution,* 213(1), pp. 275-286.
Häder, D.-P. (2022) 'Solar UV-B and Primary Producers in Aquatic Ecosystems', in Kataria, S. and Singh, V.P. (eds.) *UV-B Radiation and Crop Growth*. Singapore: Springer Nature Singapore, pp. 71-92.
Häder, D.-P., Williamson, C. E., Wängberg, S.-Å., Rautio, M., Rose, K. C., Gao, K., Helbling, E. W., Sinha, R. P. and Worrest, R. (2015) 'Effects of UV radiation on aquatic ecosystems and interactions with other environmental factors', *Photochemical & Photobiological Sciences,* 14(1), pp. 108-126.
Häder, D. P., Kumar, H. D., Smith, R. C. and Worrest, R. C. (2007) 'Effects of solar UV radiation on aquatic ecosystems and interactions with climate change', *Photochemical & Photobiological Sciences,* 6(3), pp. 267-285.
Hagopian-Schlekat, T., Chandler, G. T. and Shaw, T. J. (2001) 'Acute toxicity of five sediment-associated metals, individually and in a mixture, to the estuarine meiobenthic harpacticoid copepod *Amphiascus tenuiremis*', *Marine Environmental Research,* 51(3), pp. 247-264.
Hakimzadeh, R. and Bradley, B. P. (1990) 'The heat shock response in the copepod *Eurytemora affinis* (POPPE)', *Journal of Thermal Biology,* 15(1), pp. 67-77.
Hall, L. W., Ziegenfuss, M. C., Anderson, R. D. and Lewis, B. L. (1995) 'The effect of salinity on the acute toxicity of total and free cadmium to a Chesapeake Bay copepod and fish', *Marine Pollution Bulletin,* 30(6), pp. 376-384.
Halsband, C., Dix, M. F., Sperre, K. H. and Reinardy, H. C. (2021) 'Reduced pH increases mortality and genotoxicity in an Arctic coastal copepod, *Acartia longiremis*', *Aquatic Toxicology,* 239, pp. 1 - 4.
Han, J., Won, E.-J., Lee, B.-Y., Hwang, U.-K., Kim, I.-C., Yim, J. H., Leung, K. M. Y., Lee, Y. S. and Lee, J.-S. (2014) 'Gamma rays induce DNA damage and oxidative stress associated

with impaired growth and reproduction in the copepod *Tigriopus japonicus*', *Aquatic Toxicology,* 152, pp. 264-272.
Hansson, L.-A., Hylander, S. and Sommaruga, R. (2007) 'Escape from UV threats in zooplankton: A cocktail of behavior and protective pigmentation', *Ecology,* 88(8), pp. 1932-1939.
Hargreaves, A. J., Vale, P., Whelan, J., Constantino, C., Dotro, G., Campo, P. and Cartmell, E. (2017) 'Distribution of trace metals (Cu, Pb, Ni, Zn) between particulate, colloidal and truly dissolved fractions in wastewater treatment', *Chemosphere,* 175, pp. 239-246.
Heavisides, E., Rouger, C., Reichel, F. A., Ulrich, C., Wenzel-Storjohann, A., Sebens, S. and Tasdemir, D. (2018) 'Seasonal variations in the metabolome and bioactivity profile of *Fucus vesiculosus* extracted by an optimised, pressurised liquid extraction protocol', *Marine Drugs,* 16(12), pp. 1 - 28.
Heine, K. B., Powers, M. J., Kallenberg, C., Tucker, V. L. and Hood, W. R. (2019) 'Ultraviolet irradiation increases size of the first clutch but decreases longevity in a marine copepod', *Ecology and evolution,* 9(17), pp. 9759-9767.
Heuschele, J., Lode, T., Konestabo, H. S., Titelman, J., Andersen, T. and Borgå, K. (2022) 'Drivers of copper sensitivity in copepods: A meta-analysis of LC50s', *Ecotoxicology and Environmental Safety,* 242, pp. 113907.
Hicks, G. (1986) 'Distribution and behaviour of meiofaunal copepods inside and outside seagrass beds', *Marine ecology progress series. Oldendorf,* 31(2), pp. 159-170.
Hollmann, G., Ferreira, G. d. J., Geihs, M. r. A., Vargas, M. A., Nery, L. E. M., Leit„o, l., Linden, R. and Allodi, S. (2015) 'Antioxidant activity stimulated by ultraviolet radiation in the nervous system of a crustacean', *Aquatic Toxicology,* 160, pp. 151-162.
Hollmann, G., Linden, R., Giangrande, A. and Allodi, S. (2016) 'Increased p53 and decreased p21 accompany apoptosis induced by ultraviolet radiation in the nervous system of a crustacean', *Aquatic Toxicology,* 173, pp. 1-8.
Holzinger, A. and Karsten, U. (2013) 'Desiccation stress and tolerance in green algae: consequences for ultrastructure, physiological and molecular mechanisms', *Frontiers in Plant Science,* 4, pp. 1 - 18.
Hope, B. K. (2006) 'An examination of ecological risk assessment and management practices', *Environment International,* 32(8), pp. 983-995.
Hsiao, S.-H. and Fang, T.-H. (2013) 'Trace metal contents in male, non-ovigerous and ovigerous females, and the egg sacs of the marine copepod, *Euchaeta concinna* Dana, 1849 (Copepoda, Euchaetidae), collected from the southern East China Sea', *Crustaceana,* 86(11), pp. 1410-1424.
Hu, G., Zhang, B., Zhou, P., Hou, Y., Jia, H., Liu, Y., Gan, L., Zhang, H., Mao, Y. and Fang, J. (2019) 'Depletion of protein thiols and the accumulation of oxidized thioredoxin in Parkinsonism disclosed by a red-emitting and environment-sensitive probe', *Journal of Materials Chemistry B,* 7(16), pp. 2696-2702.
Hundie, K. B. and Akuma, D. A. (2022) 'Optimization of biodiesel production parameters from *Prosopis julifera* seed using definitive screening design', *Heliyon,* 8(2), pp. 1 - 10.
Hussain, F., Eom, H., Ali Toor, U., Lee, C. S. and Oh, S.-E. (2021) 'Rapid assessment of heavy metal-induced toxicity in water using micro-algal bioassay based on photosynthetic oxygen evolution', *Environmental Engineering Research,* 26(6), pp. 1 - 10.
Hutchinson, T. H., Pounds, N. A., Hampel, M. and Williams, T. D. (1999) 'Impact of natural and synthetic steroids on the survival, development and reproduction of marine copepods (*Tisbe battagliai*)', *Science of The Total Environment,* 233(1), pp. 167-179.
Hwang, D. S., Lee, K. W., Han, J., Park, H. G., Lee, J., Lee, Y. M. and Lee, J. S. (2010) 'Molecular characterization and expression of vitellogenin (Vg) genes from the cyclopoid copepod, *Paracyclopina nana* exposed to heavy metals', *Comp Biochem Physiol C Toxicol Pharmacol,* 151(3), pp. 360-8.
Hylander, S., Grenvald, J. C. and Ki¯rboe, T. (2014) 'Fitness costs and benefits of ultraviolet radiation exposure in marine pelagic copepods', *Functional Ecology,* 28(1), pp. 149-158.
Hylander, S. and Jephson, T. (2010) 'UV protective compounds transferred from a marine dinoflagellate to its copepod predator', *Journal of Experimental Marine Biology and Ecology,* 389(1-2), pp. 38-44.

Irigoien, X., Head, R. N., Harris, R. P., Cummings, D., Harbour, D. and Meyer-Harms, B. (2000) 'Feeding selectivity and egg production of *Calanus helgolandicus* in the English Channel', *Limnology and Oceanography,* 45(1), pp. 44-54.
Author (1999)*: Water quality - Determination of acute lethal toxicity to marine copepods (Copepoda, Crustacea)*: International Organisation for Standardisation. Available at: https://www.iso.org/standard/25162.html.
Jahan, K., Mosto, P., Mattson, C., Frey, E. and Derchak, L. (2004) 'Metal uptake by algae', in Popov, V., Itoh, H., Brebbia, C.A. and Kungolos, S. (eds.) *Waste management and the environment II*. Southampton, UK: WIT Press, pp. 223 - 232.
Jaishankar, M., Tseten, T., Anbalagan, N., Mathew, B. B. and Beeregowda, K. N. (2014) 'Toxicity, mechanism and health effects of some heavy metals', *Interdisciplinary toxicology,* 7(2), pp. 60-72.
Jankovic, A., Chaudhary, G. and Goia, F. (2021) 'Designing the design of experiments (DOE) – An investigation on the influence of different factorial designs on the characterization of complex systems', *Energy and Buildings,* 250(2021), pp. 1 - 17.
Jara-Marini, M. E., Soto-Jiménez, M. F. and Páez-Osuna, F. (2009) 'Trophic relationships and transference of cadmium, copper, lead and zinc in a subtropical coastal lagoon food web from SE Gulf of California', *Chemosphere,* 77(10), pp. 1366-1373.
Jarosz, E., Eastabrook, C. L., Byrnes, I. T. B., Lind, O., Skipperud, L., Wolf, R., Tollefsen, K. E. and Teien, H.-C. 2022. Effect of salinity on speciation, uptake and toxicity in marine copepod *Tisbe battagliai* exposed to Al, Cu, Zn and Ni.
Jarvis, T. A., Miller, R. J., Lenihan, H. S. and Bielmyer, G. K. (2013) 'Toxicity of ZnO nanoparticles to the copepod *Acartia tonsa*, exposed through a phytoplankton diet', *Environ Toxicol Chem,* 32(6), pp. 1264-9.
Jeong, C.-B., Lee, Y. H., Park, J. C., Kang, H.-M., Hagiwara, A. and Lee, J.-S. (2019) 'Effects of metal-polluted seawater on life parameters and the induction of oxidative stress in the marine rotifer *Brachionus koreanus* and the marine copepod *Tigriopus japonicus*', *Comparative Biochemistry and Physiology Part C: Toxicology & Pharmacology,* 225(2019), pp. 1 - 7.
Johnson, H. L., Stauber, J. L., Adams, M. S. and Jolley, D. F. (2007) 'Copper and zinc tolerance of two tropical microalgae after copper acclimation', *Environmental Toxicology,* 22(3), pp. 234-244.
Jones, B. and Nachtsheim, C. J. (2011) 'A class of three-level designs for definitive screening in the presence of second-order effects', *Journal of Quality Technology,* 43(1), pp. 1-15.
Jones, R. and Henderson, E. W. (1987) 'The dynamics of energy transfer in marine food chains', *South African Journal of Marine Science,* 5(1), pp. 447-465.
Juneau, P., El Berdey, A. and Popovic, R. (2002) 'PAM fluorometry in the determination of the sensitivity of *Chlorella vulgaris*, *Selenastrum capricornutum*, and *Chlamydomonas reinhardtii* to copper', *Archives of Environmental Contamination and Toxicology,* 42(2), pp. 155-164.
Jung, M.-Y. and Lee, Y.-M. (2012) 'Expression profiles of heat shock protein gene families in the monogonont rotifer *Brachionus koreanus* — exposed to copper and cadmium', *Toxicology and Environmental Health Sciences,* 4(4), pp. 235-242.
Kadiene, E. U., Bialais, C., Ouddane, B., Hwang, J.-S. and Souissi, S. (2017) 'Differences in lethal response between male and female calanoid copepods and life cycle traits to cadmium toxicity', *Ecotoxicology,* 26(9), pp. 1227-1239.
Kadiene, E. U., Ouddane, B., Hwang, J.-S. and Souissi, S. (2019) 'Bioaccumulation of metals in calanoid copepods by oral intake', *Scientific Reports,* 9(1), pp. 9492.
Kamunde, C. and MacPhail, R. (2011) 'Metal–metal interactions of dietary cadmium, copper and zinc in rainbow trout, *Oncorhynchus mykiss*', *Ecotoxicology and Environmental Safety,* 74(4), pp. 658-667.
Khalida, Z., Youcef, A., Zitouni, B., Mohammed, Z. and Radovan, P. (2012) 'Use of chlorophyll fluorescence to evaluate the effect of chromium on activity photosystem II at the alga *Scenedesmus obliquus*', *Int J Res Rev Appl Sci,* 12(2), pp. 304-314.
Ki, J. S., Raisuddin, S., Lee, K. W., Hwang, D. S., Han, J., Rhee, J. S., Kim, I. C., Park, H. G., Ryu, J. C. and Lee, J. S. (2009) 'Gene expression profiling of copper-induced responses

in the intertidal copepod *Tigriopus japonicus* using a 6K oligochip microarray', *Aquat Toxicol,* 93(4), pp. 177-87.
Kienzler, A., Berggren, E., Bessems, J., Bopp, S., Linden, S. V. d. and Worth, A., reports, J.s.a.p. (2014) *Assessment of mixtures - review of regulatory requirements and guidance.* Luxembourg: Publications Office of the European Union.
Kim, B.-M., Rhee, J.-S., Jeong, C.-B., Seo, J. S., Park, G. S., Lee, Y.-M. and Lee, J.-S. (2014a) 'Heavy metals induce oxidative stress and trigger oxidative stress-mediated heat shock protein (hsp) modulation in the intertidal copepod *Tigriopus japonicus*', *Comparative Biochemistry and Physiology Part C: Toxicology & Pharmacology,* 166(2014), pp. 65-74.
Kim, B.-M., Rhee, J.-S., Lee, K.-W., Kim, M.-J., Shin, K.-H., Lee, S.-J., Lee, Y.-M. and Lee, J.-S. (2015) 'UV-B radiation-induced oxidative stress and p38 signaling pathway involvement in the benthic copepod *Tigriopus japonicus*', *Comparative Biochemistry and Physiology Part C: Toxicology & Pharmacology,* 167, pp. 15-23.
Kim, B. M., Rhee, J. S., Jeong, C. B., Seo, J. S., Park, G. S., Lee, Y. M. and Lee, J. S. (2014b) 'Heavy metals induce oxidative stress and trigger oxidative stress-mediated heat shock protein (hsp) modulation in the intertidal copepod Tigriopus japonicus', *Comp Biochem Physiol C Toxicol Pharmacol,* 166(2014), pp. 65-74.
Kim, J., Lee, M., Oh, S., Ku, J.-L., Kim, K.-H. and Choi, K. (2009) 'Acclimation to ultraviolet irradiation affects UV-B sensitivity of *Daphnia magna t*o several environmental toxicants', *Chemosphere,* 77(11), pp. 1600-1608.
Kim, J., Park, Y. and Choi, K. (2009) 'Phototoxicity and oxidative stress responses in *Daphnia magna* under exposure to sulfathiazole and environmental level ultraviolet B irradiation', *Aquatic Toxicology,* 91(1), pp. 87-94.
Klimisch, H. J., Andreae, M. and Tillmann, U. (1997) 'A systematic approach for evaluating the quality of experimental toxicological and ecotoxicological data', *Regulatory Toxicology and Pharmacology,* 25(1), pp. 1-5.
Knauert, S. and Knauer, K. (2008) 'The role of Reactive Oxygen Species in copper toxicity to two freshwater green algae', *Journal of Phycology,* 44(2), pp. 311-319.
Komjarova, I. and Blust, R. (2008) 'Multi-metal interactions between Cd, Cu, Ni, Pb and Zn in water flea *Daphnia magna*, a stable isotope experiment', *Aquatic Toxicology,* 90(2), pp. 138-144.
Kozlowsky-Suzuki, B., Koski, M., Hallberg, E., Wallén, R. and Carlsson, P. (2009) 'Glutathione transferase activity and oocyte development in copepods exposed to toxic phytoplankton', *Harmful Algae,* 8(3), pp. 395-406.
Kumar, K. and Shin, K.-H. (2017) 'Effect of copper on marine microalga *Tetraselmis suecica* and its influence on intra- and extracellular iron and zinc content', *Korean Journal of Ecology and Environment,* 50(1), pp. 16-28.
Kumar, K. S., Dahms, H. U., Lee, J. S., Kim, H. C., Lee, W. C. and Shin, K. H. (2014) 'Algal photosynthetic responses to toxic metals and herbicides assessed by chlorophyll a fluorescence', *Ecotoxicol Environ Saf,* 104, pp. 51-71.
Lacuna, D. G. (2002) 'Survey of ultraviolet radiation-absorbing mycosporine-like amino acids in adult females of planktonic copepods', *Annals of Tropical Research,* 24(2), pp. 1-22.
Lacuna, D. G. and Uye, S.-i. (2000) 'Effect of UVB radiation on the survival, feeding, and egg production of the brackish-water copepod, Sinocalanus tenellus, with notes on photoreactivation', *Hydrobiologia,* 434(1), pp. 73-79.
Lauer, M. M. and Bianchini, A. (2010) 'Chronic copper toxicity in the estuarine copepod *Acartia tonsa* at different salinities', *Environ Toxicol Chem,* 29(10), pp. 2297-303.
Lauritano, C., Procaccini, G. and Ianora, A. (2012) 'Gene expression patterns and stress response in marine copepods', *Marine Environmental Research,* 76, pp. 22-31.
Lee, K.-W., Hwang, D.-S., Rhee, J.-S., Ki, J.-S., Park, H. G., Ryu, J.-C., Raisuddin, S. and Lee, J.-S. (2008) 'Molecular cloning, phylogenetic analysis and developmental expression of a vitellogenin (Vg) gene from the intertidal copepod *Tigriopus japonicus*', *Comparative Biochemistry and Physiology Part B: Biochemistry and Molecular Biology,* 150(4), pp. 395-402.
Lee, Y.-M., Lee, K.-W., Park, H., Park, H. G., Raisuddin, S., Ahn, I.-Y. and Lee, J.-S. (2007) 'Sequence, biochemical characteristics and expression of a novel Sigma-class of glutathione

S-transferase from the intertidal copepod, *Tigriopus japonicus* with a possible role in antioxidant defense', *Chemosphere,* 69(6), pp. 893-902.
Leech, D. M. and Williamson, C. E. (2000) 'Is tolerance to UV radiation in zooplankton related to body size, taxon, or lake transparency?', *Ecological Applications,* 10(5), pp. 1530-1540.
León-Vaz, A., Romero, L. C., Gotor, C., León, R. and Vigara, J. (2021) 'Effect of cadmium in the microalga *Chlorella sorokiniana*: A proteomic study', *Ecotoxicology and Environmental Safety,* 207, pp. 111301.
Lewis, A. S., Sax, S. N., Wason, S. C. and Campleman, S. L. (2011) 'Non-chemical stressors and cumulative risk assessment: an overview of current initiatives and potential air pollutant interactions', *International Journal of Environmental Research and Public Health,* 8(6), pp. 2020 - 2073.
Li, H., Shi, L., Wang, D. and Wang, M. (2015) 'Impacts of mercury exposure on life history traits of *Tigriopus japonicus*: Multigeneration effects and recovery from pollution', *Aquat Toxicol,* 166, pp. 42-9.
Liberati, A., Altman, D. G., Tetzlaff, J., Mulrow, C., Gøtzsche, P. C., Ioannidis, J. P. A., Clarke, M., Devereaux, P. J., Kleijnen, J. and Moher, D. (2009) 'The PRISMA statement for reporting systematic reviews and meta-analyses of studies that evaluate health care interventions: explanation and elaboration', *PLOS Medicine,* 6(7), pp. 1 - 28.
Liu, Y., Wang, S., Wang, Z., Ye, N., Fang, H. and Wang, D. (2018) 'TiO2, SiO2 and ZrO2 Nanoparticles Synergistically Provoke Cellular Oxidative Damage in Freshwater Microalgae', *Nanomaterials*, 8(2). DOI: 10.3390/nano8020095.
Lode, T., Heuschele, J., Andersen, T., Titelman, J., Hylland, K. and Borgå, K. (2020) 'Contrasting effects of predation risk and copper on copepod respiration rates', *Environmental Toxicology and Chemistry,* 39(9), pp. 1765-1773.
Lode, T., Heuschele, J., Andersen, T., Titelman, J., Hylland, K. and Borgå, K. (2021) 'Density-dependent metabolic costs of copper exposure in a coastal copepod', *Environ Toxicol Chem,* 40(9), pp. 2538-2546.
Loewe, S. t. and Muischnek, H. (1926) 'Über kombinationswirkungen', *Naunyn-Schmiedebergs Archiv für experimentelle Pathologie und Pharmakologie,* 114(5-6), pp. 313-326.
Lu, X. Y. and Wu, R. S. S. (2005) 'Ultraviolet damages sperm mitochondrial function and membrane integrity in the sea urchin *Anthocidaris crassispina*', *Ecotoxicology and Environmental Safety,* 61(1), pp. 53-59.
Macken, A., Giltrap, M., Ryall, K., Foley, B., McGovern, E., McHugh, B. and Davoren, M. (2009) 'A test battery approach to the ecotoxicological evaluation of cadmium and copper employing a battery of marine bioassays', *Ecotoxicology,* 18(4), pp. 470-480.
Macken, A., Lillicrap, A. and Langford, K. (2015) 'Benzoylurea pesticides used as veterinary medicines in aquaculture: Risks and developmental effects on nontarget crustaceans', *Environmental Toxicology and Chemistry,* 34(7), pp. 1533-1542.
Magalhaes, D., Marques, M., Baptista, D. and Buss, D. (2015) 'Metal bioavailability and toxicity in freshwaters', *Environmental Chemistry Letters,* 13.
Manney, G. L., Santee, M. L., Rex, M., Livesey, N. J., Pitts, M. C., Veefkind, P., Nash, E. R., Wohltmann, I., Lehmann, R., Froidevaux, L., Poole, L. R., Schoeberl, M. R., Haffner, D. P., Davies, J., Dorokhov, V., Gernandt, H., Johnson, B., Kivi, R., Kyrˆ, E., Larsen, N., Levelt, P. F., Makshtas, A., McElroy, C. T., Nakajima, H., Parrondo, M. C., Tarasick, D. W., von der Gathen, P., Walker, K. A. and Zinoviev, N. S. (2011) 'Unprecedented Arctic ozone loss in 2011', *Nature,* 478(7370), pp. 469-475.
Martinez-Finley, E. J., Chakraborty, S., Fretham, S. J. B. and Aschner, M. (2012) 'Cellular transport and homeostasis of essential and nonessential metals', *Metallomics : integrated biometal science,* 4(7), pp. 593-605.
Medina, M., Barata, C., Telfer, T. and Baird, D. (2002) 'Age- and sex-related variation in sensitivity to the pyrenoid cypermetrin in the marine copepod *Acartia tonsa* Dana', *Archives of environmental contamination and toxicology,* 42(1), pp. 17-22.
Melegari, S. P., Perreault, F., Costa, R. H. R., Popovic, R. and Matias, W. G. (2013) 'Evaluation of toxicity and oxidative stress induced by copper oxide nanoparticles in the green alga *Chlamydomonas reinhardtii*', *Aquatic Toxicology,* 142-143, pp. 431-440.

Menze, M. A., Fortner, G., Nag, S. and Hand, S. C. (2010a) 'Mechanisms of apoptosis in Crustacea: what conditions induce versus suppress cell death?', *Apoptosis,* 15(3), pp. 293-312.
Menze, M. A., Fortner, G., Nag, S. and Hand, S. C. (2010b) 'Mechanisms of apoptosis in Crustacea: What conditions induce versus suppress cell death?', *Apoptosis : an international journal on programmed cell death,* 15(3), pp. 293-312.
Middag, R., de Baar, H. J. W., Bruland, K. W. and van Heuven, S. M. A. C. (2020) 'The Distribution of Nickel in the West-Atlantic Ocean, Its Relationship With Phosphate and a Comparison to Cadmium and Zinc', *Frontiers in Marine Science,* 7.
Miguel, N. C. d. O., Wajsenzon, I. J. I. R., Takiya, C. M., de Andrade, L. R., Tortelote, G. G., Einicker-Lamas, M. and Allodi, S. (2007) 'Catalase, Bax and p53 expression in the visual system of the crab *Ucides cordatus* following exposure to ultraviolet radiation', *Cell and Tissue Research,* 329(1), pp. 159-168.
Miliou, H., Verriopoulos, G., Maroulis, D., Bouloukos, D. and Moraitou-apostolopoulou, M. (2000) 'Influence of life-history adaptations on the fidelity of laboratory bioassays for the impact of heavy metals (Co2+ and Cr6+) on tolerance and population dynamics of *Tisbe holothuriae*', *Marine Pollution Bulletin,* 40(4), pp. 352-359.
Miner, B. G., Morgan, S. G. and Hoffman, J. R. (2000) 'Postlarval chromatophores as an adaptation to ultraviolet radiation', *Journal of Experimental Marine Biology and Ecology,* 249(2), pp. 235-248.
Mohammed, E. H. (2013) 'Biochemical response of the cyclopoida copepod *Apopcyclops borneoensis* exposed to nickel', *Jordan Journal of Biological Sciences,* 7(1), pp. 41 - 47.
Mohammed, E. H., Wang, G. and Jiang, J. (2010) 'The effects of nickel on the reproductive ability of three different marine copepods', *Ecotoxicology,* 19(5), pp. 911-916.
Monteiro, C. M., Castro, P. M. L. and Malcata, F. X. (2012) 'Metal uptake by microalgae: Underlying mechanisms and practical applications', *Biotechnology Progress,* 28(2), pp. 299-311.
Morcillo, P., Esteban, M. Á. and Cuesta, A. (2016) 'Heavy metals produce toxicity, oxidative stress and apoptosis in the marine teleost fish SAF-1 cell line', *Chemosphere,* 144, pp. 225-233.
Mosley, L. and Liss, P. (2019) 'Particle aggregation, pH changes and metal behaviour during estuarine mixing; review and integration', *Marine and Freshwater Research,* 71(3), pp. A - K.
Nagy, K., Duca, R. C., Lovas, S., Creta, M., Scheepers, P. T. J., Godderis, L. and Ádám, B. (2020) 'Systematic review of comparative studies assessing the toxicity of pesticide active ingredients and their product formulations', *Environmental Research,* 181, pp. 1 - 19.
Nassiri, Y., Ginsburger-Vogel, T., Mansot, J. L. and Wéry, J. (1996) 'Effects of heavy metals on *Tetraselmis suecica*: Ultrastructural and energy-dispersive X-ray spectroscopic studies', *Biology of the Cell,* 86(2), pp. 151-160.
Nations, U. (1987) *Montreal Protocol on Substances that Deplete the Ozone Layer*, Montreal, Canada.
Naveed, S., Li, C., Lu, X., Chen, S., Yin, B., Zhang, C. and Ge, Y. (2019) 'Microalgal extracellular polymeric substances and their interactions with metal(loid)s: A review', *Critical Reviews in Environmental Science and Technology,* 49(19), pp. 1769-1802.
Nazari, E. M., Ammar, D., Bem, A. F. d., Latini, A., M¸ller, Y. M. R. and Allodi, S. (2010) 'Effects of environmental and artificial UV-B radiation on freshwater prawn *Macrobrachium olfersi* embryos', *Aquatic Toxicology,* 98(1), pp. 25-33.
Neale, R. E., Barnes, P. W., Robson, T. M., Neale, P. J., Williamson, C. E., Zepp, R. G., Wilson, S. R., Madronich, S., Andrady, A. L., Heikkilä, A. M., Bernhard, G. H., Bais, A. F., Aucamp, P. J., Banaszak, A. T., Bornman, J. F., Bruckman, L. S., Byrne, S. N., Foereid, B., Häder, D. P., Hollestein, L. M., Hou, W. C., Hylander, S., Jansen, M. A. K., Klekociuk, A. R., Liley, J. B., Longstreth, J., Lucas, R. M., Martinez-Abaigar, J., McNeill, K., Olsen, C. M., Pandey, K. K., Rhodes, L. E., Robinson, S. A., Rose, K. C., Schikowski, T., Solomon, K. R., Sulzberger, B., Ukpebor, J. E., Wang, Q. W., Wängberg, S. Å., White, C. C., Yazar, S., Young, A. R., Young, P. J., Zhu, L. and Zhu, M. (2021) 'Environmental effects of stratospheric ozone depletion, UV radiation, and interactions with climate change: UNEP Environmental Effects Assessment Panel, Update 2020', *Photochemical & Photobiological Sciences,* 20(1), pp. 1-67.

Newsham, K. K. and Robinson, S. A. (2009) 'Responses of plants in polar regions to UVB exposure: a meta-analysis', *Global Change Biology,* 15(11), pp. 2574-2589.
Nguyen, T. V., Alfaro, A. C., Merien, F., Lulijwa, R. and Young, T. (2018) 'Copper-induced immunomodulation in mussel (*Perna canaliculus*) haemocytes', *Metallomics,* 10(7), pp. 965-978.
Nimse, S. B. and Pal, D. (2015) 'Free radicals, natural antioxidants, and their reaction mechanisms', *RSC Advances,* 5(35), pp. 27986-28006.
NIVA (2019) 'NIVA Risk Assessment database'. Available at: https://niva.no/radb (Accessed: 11/2019).
Niyogi, K. K. (1999) 'Photoprotection revisited: genetic and molecular approaches', *Annu Rev Plant Physiol Plant Mol Biol,* 50, pp. 333-359.
Niyogi, S. and Wood, C. M. (2004) 'Biotic Ligand Model, a Flexible Tool for Developing Site-Specific Water Quality Guidelines for Metals', *Environmental Science & Technology,* 38(23), pp. 6177-6192.
Nogueira, P. F. M., Lombardi, A. T. and Nogueira, M. M. (2012) '*Cylindrospermopsis raciborski*i exudate–Cu complexes: impact on copper dynamics and bioavailability in an aquatic food chain', *Environmental Science and Pollution Research,* 19(4), pp. 1245-1251.
Nowicka, B. (2022) 'Heavy metal–induced stress in eukaryotic algae—mechanisms of heavy metal toxicity and tolerance with particular emphasis on oxidative stress in exposed cells and the role of antioxidant response', *Environmental Science and Pollution Research,* 29(12), pp. 16860-16911.
NRC, N. R. C. (1983) *Risk assessment in the federal government: managing the process.* Washington, DC: The National Academies Press.
NRC, N. R. C. (2009) *Science and decisions: advancing risk assessment*, Washington, DC: The National Academies Press (978-0-309-12046-3. Available at: https://www.nap.edu/catalog/12209/science-and-decisions-advancing-risk-assessment.
Nys, C., Asselman, J., Hochmuth, J. D., Janssen, C. R., Blust, R., Smolders, E. and De Schamphelaere, K. A. (2015) 'Mixture toxicity of nickel and zinc to *Daphnia magna* is noninteractive at low effect sizes but becomes synergistic at high effect sizes', *Environ Toxicol Chem,* 34(5), pp. 1091-102.
Obermuller, B. (2006) *Effects of UV-radiation on crustaceans from polar and temperate coastal ecosystems.* PhD Thesis, University of Bremen, Bremen, Germany [Online] Available at: https://media.suub.uni-bremen.de/bitstream/elib/2275/1/00010462.pdf (Accessed.
Obermuller, B., Karsten, U. and Abele, D. (2005) 'Response of oxidative stress parameters and sunscreening compounds in Arctic amphipods during experimental exposure to maximal natural UVB radiation', *Journal of Experimental Marine Biology and Ecology,* 323(2), pp. 100-117.
Obermuller, B., Puntarulo, S. and Abele, D. (2007) 'UV-tolerance and instantaneous physiological stress responses of two Antarctic amphipod species *Gondogeneia antarctica* and *Djerboa furcipes* during exposure to UV radiation', *Marine Environmental Research,* 64(3), pp. 267-285.
OECD (2011) 'Test no. 201: freshwater alga and cyanobacteria, growth inhibition test', *OECD Guidelines for the Testing of Chemicals, Section 2*. Paris, France: OECD Publishing.
OECD (2018) ''Users' handbook supplement to the guidance document for developing and assessing Adverse Outcome Pathways', *OECD Series on Adverse Outcome Pathways*. Paris, France: OECD Publishing.
Olaniran, A. O., Balgobind, A. and Pillay, B. (2013) 'Bioavailability of heavy metals in soil: impact on microbial biodegradation of organic compounds and possible improvement strategies', *International journal of molecular sciences,* 14(5), pp. 10197-10228.
OSPAR (2016) *Metals in sediment and biota: status and trend of copper burden* 677/2016). Available at: https://www.ospar.org/documents?v=35698 (Accessed: 12.01.2023).
Oukarroum, A., Zaidi, W., Samadani, M. and Dewez, D. (2017) 'Toxicity of nickel oxide nanoparticles on a freshwater green algal strain of *Chlorella vulgaris*', *BioMed Research International,* 2017, pp. 1 - 9.
Ouyang, H., Kong, X., He, W., Qin, N., He, Q., Wang, Y., Wang, R. and Xu, F. (2012) 'Effects of five heavy metals at sub-lethal concentrations on the growth and photosynthesis of *Chlorella vulgaris*', *Chinese Science Bulletin,* 57(25), pp. 3363-3370.

Paffenhöfer, G.-A. (1993) 'On the ecology of marine cyclopoid copepods (Crustacea, Copepoda)', *Journal of Plankton Research,* 15(1), pp. 37-55.
Pan, K. and Wang, W.-X. (2012) 'Trace metal contamination in estuarine and coastal environments in China', *Science of The Total Environment,* 421-422, pp. 3-16.
Pane, E. F., Smith, C., McGeer, J. C. and Wood, C. M. (2003) 'Mechanisms of Acute and Chronic Waterborne Nickel Toxicity in the Freshwater Cladoceran, *Daphnia magna*', *Environmental Science & Technology,* 37(19), pp. 4382-4389.
Pane, L., Mariottini, G., Lodi, A. and Giacco, E. (2008) 'Effects of heavy metals on laboratory reared *tigriopus fulvus* fischer (Copepoda: Harpacticoida)', in Brown, S.E. and Welton, W.C. (eds.) *Heavy Metal Pollution*. New York, NY: Nova Science Publishers, pp. 157-165.
Papanastasiou, D. K., Beltrone, A., Marshall, P. and Burkholder, J. B. (2018) 'Global warming potential estimates for the C_1–C_3 hydrochlorofluorocarbons (HCFCs) included in the Kigali Amendment to the Montreal Protocol', *Atmospheric Chemistry and Physics,* 18(9), pp. 6317-6330.
Pavlaki, M. D., Araújo, M. J., Cardoso, D. N., Silva, A. R. R., Cruz, A., Mendo, S., Soares, A., Calado, R. and Loureiro, S. (2016a) 'Ecotoxicity and genotoxicity of cadmium in different marine trophic levels', *Environ Pollut,* 215, pp. 203-212.
Pavlaki, M. D., Araújo, M. J., Cardoso, D. N., Silva, A. R. R., Cruz, A., Mendo, S., Soares, A. M. V. M., Calado, R. and Loureiro, S. (2016b) 'Ecotoxicity and genotoxicity of cadmium in different marine trophic levels', *Environmental Pollution,* 215, pp. 203-212.
Pavlaki, M. D., Morgado, R. G., van Gestel, C. A. M., Calado, R., Soares, A. and Loureiro, S. (2017) 'Influence of environmental conditions on the toxicokinetics of cadmium in the marine copepod *Acartia tonsa*', *Ecotoxicol Environ Saf,* 145, pp. 142-149.
Pedroso, M. S., Pinho, G. L. L., Rodrigues, S. C. and Bianchini, A. (2007) 'Mechanism of acute silver toxicity in the euryhaline copepod *Acartia tonsa*', *Aquatic toxicology (Amsterdam, Netherlands),* 82(3), pp. 173-180.
Peperzak, L. and Brussaard, C. (2011) 'Flow cytometry applicability of fluorescent vitality probes on phytoplankton', *Journal of Phycology,* 47(3), pp. 692-702.
Perales-Vela, H. V., Peña-Castro, J. M. and Cañizares-Villanueva, R. O. (2006) 'Heavy metal detoxification in eukaryotic microalgae', *Chemosphere,* 64(1), pp. 1-10.
Petersen, K., Heiaas, H. H. and Tollefsen, K. E. (2014) 'Combined effects of pharmaceuticals, personal care products, biocides and organic contaminants on the growth of *Skeletonema pseudocostatum*', *Aquatic Toxicology,* 150(2014), pp. 45-54.
Petersen, K. and Tollefsen, K. E. (2011) 'Assessing combined toxicity of estrogen receptor agonists in a primary culture of rainbow trout (*Oncorhynchus mykiss*) hepatocytes', *Aquat Toxicol,* 101(1), pp. 186-95.
Pirrie, D., Power, M. R., Rollinson, G., Camm, G. S., Hughes, S. H., Butcher, A. R. and Hughes, P. (2003) 'The spatial distribution and source of arsenic, copper, tin and zinc within the surface sediments of the Fal Estuary, Cornwall, UK', *Sedimentology,* 50(3), pp. 579-595.
Pitombeira de Figuerêdo, L., Nilin, J., Queiroz da Silva, A., Pinheiro Damasceno, É., Loureiro, S. and Veras Costa-Lotufo, L. (2016) 'Zinc and nickel binary mixtures act additively on the tropical mysid *Mysidopsis juniae*', *Marine and Freshwater Research,* 67(3), pp. 301-308.
Prado, R., García, R., Rioboo, C., Herrero, C. and Cid, Á. (2015) 'Suitability of cytotoxicity endpoints and test microalgal species to disclose the toxic effect of common aquatic pollutants', *Ecotoxicology and Environmental Safety,* 114, pp. 117-125.
Prato, E., Parlapiano, I., Biandolino, F., Rotini, A., Manfra, L., Berducci, M. T., Maggi, C., Libralato, G., Paduano, L., Carraturo, F., Trifuoggi, M., Carotenuto, M. and Migliore, L. (2020) 'Chronic sublethal effects of ZnO nanoparticles on *Tigriopus fulvus* (Copepoda, Harpacticoida)', *Environ Sci Pollut Res Int,* 27(25), pp. 30957-30968.
Prego, R. and Cobelo-García, A. (2003) 'Zinc concentrations in the water column influenced by the oil spill in the vicinity of the Prestige shipwreck', *Ciencias Marinas,* 29, pp. 103-108.
Puthumana, J., Lee, M.-C., Park, J. C., Kim, H.-S., Hwang, D.-S., Han, J. and Lee, J.-S. (2017) 'Ultraviolet B radiation induces impaired lifecycle traits and modulates expression of cytochrome P450 (CYP) genes in the copepod *Tigriopus japonicus*', *Aquatic Toxicology,* 184, pp. 116-122.

Rainbow, P. S. (2018a) 'Coastal seas and oceans', in Rainbow, P.S. (ed.) *Trace metals in the environment and living organisms: the British Isles as a case study*. Cambridge: Cambridge University Press, pp. 565-654.
Rainbow, P. S. (2018b) 'Introduction', in Rainbow, P.S. (ed.) *Trace metals in the environment and living organisms: the British Isles as a case study*. Cambridge: Cambridge University Press, pp. 1-21.
Rainbow, P. S. and Luoma, S. N. (2011) 'Trace metals in aquatic invertebrates', in W. Nelson Bey, J.P.M. (ed.) *Environmental Contaminants in Biota - Interpreting Tissue Concentrations*. New York, NY: CRC Press, pp. 231-254.
Rastogi, R. P., Richa, Kumar, A., Tyagi, M. B. and Sinha, R. P. (2010) 'Molecular mechanisms of ultraviolet radiation-induced DNA damage and repair', *Journal of nucleic acids,* 2010, pp. 592980-592980.
Rath, B. (2011) 'Microalgal bioremediation: current practices and perspectives', *Journal of Biochemical Technology,* 3.
Rautio, M. and Korhola, A. (2002) 'UV-induced pigmentation in subarctic *Daphnia*', *Limnology and Oceanography,* 47(1), pp. 295-299.
Rhee, J.-S., Yu, I. T., Kim, B.-M., Jeong, C.-B., Lee, K.-W., Kim, M.-J., Lee, S.-J., Park, G. S. and Lee, J.-S. (2013a) 'Copper induces apoptotic cell death through reactive oxygen species-triggered oxidative stress in the intertidal copepod *Tigriopus japonicus*', *Aquatic Toxicology,* 132-133(2013), pp. 182-189.
Rhee, J.-S., Yu, I. T., Kim, B.-M., Jeong, C.-B., Lee, K.-W., Kim, M.-J., Lee, S.-J., Park, G. S. and Lee, J.-S. (2013b) 'Copper induces apoptotic cell death through reactive oxygen species-triggered oxidative stress in the intertidal copepod *Tigriopus japonicus*', *Aquatic Toxicology,* 132-133, pp. 182-189.
Richir, J., Bray, S., McAleese, T. and Watson, G. J. (2021) 'Three decades of trace element sediment contamination: The mining of governmental databases and the need to address hidden sources for clean and healthy seas', *Environment International,* 149, pp. 106362.
Rodea-Palomares, I., González-Pleiter, M., Martín-Betancor, K., Rosal, R. and Fernández-Piñas, F. (2015) 'Additivity and interactions in ecotoxicity of pollutant mixtures: some patterns, conclusions, and open questions', *Toxics,* 3(4), pp. 342-369.
Rodogiannis, K., Duong, J. T. and Kovarik, M. L. (2018) 'Microfluidic single-cell analysis of oxidative stress in *Dictyostelium discoideum*', *Analyst,* 143(15), pp. 3643-3650.
Rodriguez, C. A., Howard, I. B., Jeffrey, A. R. and Jean-FranÃ□Â§ois, S.-P. (2000) 'Impact of solar ultraviolet radiation on hatching of a marine copepod, *Calanus finmarchicus*', *Marine Ecology Progress Series,* 193, pp. 85-93.
Romano, G., Russo, G. L., Buttino, I., Ianora, A. and Miralto, A. (2003) 'A marine diatom-derived aldehyde induces apoptosis in copepod and sea urchin embryos', *The Journal of Experimental Biology,* 206(19), pp. 3487-3494.
Sabatini, S. E., Juárez, Á. B., Eppis, M. R., Bianchi, L., Luquet, C. M. and Ríos de Molina, M. d. C. (2009) 'Oxidative stress and antioxidant defenses in two green microalgae exposed to copper', *Ecotoxicology and Environmental Safety,* 72(4), pp. 1200-1206.
Sachana, M. (2019) 'Chapter 9 - Adverse Outcome Pathways and their role in revealing biomarkers', in Gupta, R.C. (ed.) *Biomarkers in Toxicology (Second Edition)*. London, UK: Academic Press, pp. 163-170.
Sahlmann, A., Lode, T., Heuschele, J., Borgå, K., Titelman, J. and Hylland, K. (2019) 'Genotoxic response and mortality in 3 marine copepods exposed to waterborne copper', *Environmental Toxicology and Chemistry,* 38(10), pp. 2224-2232.
Sahlmann, A., Wolf, R., Holth, T. F., Titelman, J. and Hylland, K. (2017) 'Baseline and oxidative DNA damage in marine invertebrates', *Journal of Toxicology and Environmental Health, Part A,* 80(16-18), pp. 807-819.
Salbu, B. (2009) 'Fractionation of radionuclide species in the environment', *Journal of Environmental Radioactivity,* 100(4), pp. 283-289.
Salbu, B. S., L; and Lind, O. C. (2015) 'Sources contributing to radionuclides in the environment: with focus on radioactive particles', in Clemens Walther, D.K.G. (ed.) *Radionuclides in the Environment - influence of chemical speciation and plant uptake on radionuclide migration*. London, UK: Springer International Publishing AG Switzerland, pp. 2-30.

Santas, R., Kousoulaki, K. and Häder, D. (1997) 'In assessing biological UV-B effects, natural fluctuations of solar radiation should be taken into account', *Plant Ecology,* 128, pp. 93-97.
Satoh, A., Vudikaria, L. Q., Kurano, N. and Miyachi, S. (2005) 'Evaluation of the sensitivity of marine microalgal strains to the heavy metals, Cu, As, Sb, Pb and Cd', *Environment International,* 31(5), pp. 713-722.
Schminke, H. K. (2007) 'Entomology for the copepodologist', *Journal of Plankton Research,* 29, pp. i149-i162.
Schneider, K., Schwarz, M., Burkholder, I., Kopp-Schneider, A., Edler, L., Kinsner-Ovaskainen, A., Hartung, T. and Hoffmann, S. (2009) '"ToxRTool", a new tool to assess the reliability of toxicological data', *Toxicology Letters,* 189(2), pp. 138-144.
Schramm, H., Jaramillo, M. L., Quadros, T. d., Zeni, E. C., Müller, Y. M. R., Ammar, D. and Nazari, E. M. (2017) 'Effect of UVB radiation exposure in the expression of genes and proteins related to apoptosis in freshwater prawn embryos', *Aquatic Toxicology,* 191, pp. 25-33.
Schreiber, U., Quayle, P., Schmidt, S., Escher, B. I. and Mueller, J. F. (2007) 'Methodology and evaluation of a highly sensitive algae toxicity test based on multiwell chlorophyll fluorescence imaging', *Biosensors and Bioelectronics,* 22(11), pp. 2554-2563.
Serreze, M. C. and Meier, W. N. (2019) 'The Arctic's sea ice cover: trends, variability, predictability, and comparisons to the Antarctic', *Annals of the New York Academy of Sciences,* 1436(1), pp. 36-53.
Sharma, K. V., Sarvalingam, B. K. and Marigoudar, S. R. (2021) 'A review of mesocosm experiments on heavy metals in marine environment and related issues of emerging concerns', *Environmental Science and Pollution Research,* 28(2), pp. 1304-1316.
Sharma, P., Jha, A. B., Dubey, R. S. and Pessarakli, M. (2012) 'Reactive Oxygen Species, oxidative damage, and antioxidative defense mechanism in plants under stressful conditions', *Journal of Botany,* 2012, pp. 1-26.
Shi, D., Lv, D., Liu, W., Shen, R., Li, D. and Hong, H. (2017) 'Accumulation and developmental toxicity of hexabromocyclododecanes (HBCDs) on the marine copepod *Tigriopus japonicus*', *Chemosphere,* 167, pp. 155-162.
Silva, J. C., Echeveste, P. and Lombardi, A. T. (2018) 'Higher biomolecules yield in phytoplankton under copper exposure', *Ecotoxicology and Environmental Safety,* 161, pp. 57-63.
Silva, S. J., Carman, K. R., Fleeger, J. W., Marshall, T. and Marlborough, S. J. (2009) 'Effects of phenanthrene- and metal-contaminated sediment on the feeding activity of the Harpacticoid Copepod, *Schizopera knabeni*', *Arch Environ Contam Toxicol,* 56(3), pp. 434-41.
Simonsen, M., Teien, H.-C., Lind, O. C., Saetra, Ø., Albretsen, J. and Salbu, B. (2019) 'Modeling key processes affecting Al speciation and transport in estuaries', *Science of The Total Environment,* 687, pp. 1147-1163.
Smith, K. S., Balistrieri, L. S. and Todd, A. S. (2015) 'Using biotic ligand models to predict metal toxicity in mineralized systems', *Applied Geochemistry,* 57, pp. 55-72.
Sobrino-Figueroa, A., Hernández, S. and Álvarez, C. (2020) 'Evaluation of the freshwater copepod *Acanthocyclops americanus* (Marsh, 1983) (Cyclopidae) response to Cd, Cr, Cu, Hg, Mn, Ni and Pb', *AIMS Environmental Science,* 7(6), pp. 449-463.
Soh, N. (2006) 'Recent advances in fluorescent probes for the detection of reactive oxygen species', *Analytical and Bioanalytical Chemistry,* 386(3), pp. 532-543.
Song, Y., Xie, L., Lee, Y., Brede, D. A., Lyne, F., Kassaye, Y., Thaulow, J., Caldwell, G., Salbu, B. and Tollefsen, K. E. (2020a) 'Integrative assessment of low-dose gamma radiation effects on *Daphnia magna* reproduction: Toxicity pathway assembly and AOP development', *Science of The Total Environment,* 705, pp. 135912.
Song, Y., Xie, L., Lee, Y. and Tollefsen, K. E. (2020b) 'De novo development of a Quantitative Adverse Outcome Pathway (qAOP) network for Ultraviolet B (UVB) radiation using targeted laboratory tests and automated data mining', *Environmental Science & Technology,* 54(20), pp. 13147 - 13156.
Sørensen, J. G., Kristensen, T. N. and Loeschcke, V. (2003) 'The evolutionary and ecological role of heat shock proteins', *Ecology Letters,* 6(11), pp. 1025-1037.

Souza, M. S., Balseiro, E., Laspoumaderes, C. and Modenutti, B. (2010) 'Effect of ultraviolet radiation on acetylcholinesterase activity in freshwater copepods', *Photochemistry and Photobiology,* 86(2), pp. 367-373.
Souza, M. S., Hansson, L.-A., Hylander, S., Modenutti, B. and Balseiro, E. (2012) 'Rapid enzymatic response to compensate UV radiation in copepods', *PloS one,* 7(2), pp. 1 - 6.
Stábile, F., Brönmark, C., Hansson, L.-A. and Lee, M. (2021) 'Fitness cost from fluctuating ultraviolet radiation in *Daphnia magna*', *Biology letters,* 17(8), pp. 1 - 6.
Stachowski-Haberkorn, S., Jérôme, M., Rouxel, J., Khelifi, C., Rincé, M. and Burgeot, T. (2013) 'Multigenerational exposure of the microalga *Tetraselmis suecica* to diuron leads to spontaneous long-term strain adaptation', *Aquatic Toxicology,* 140-141, pp. 380-388.
Stibor, H., Vadstein, O., Diehl, S., Gelzleichter, A., Hansen, T., Hantzsche, F., Katechakis, A., Lippert, B., L¯seth, K., Peters, C., Roederer, W., Sandow, M., Sundt-Hansen, L. and Olsen, Y. (2004) 'Copepods act as a switch between alternative marine pelagic food webs', *Ecology Letters,* 7(4), pp. 321-328.
Stock, W., Blommaert, L., Daveloose, I., Vyverman, W. and Sabbe, K. (2019) 'Assessing the suitability of Imaging-PAM fluorometry for monitoring growth of benthic diatoms', *Journal of Experimental Marine Biology and Ecology,* 513, pp. 35-41.
Stone, S., McKnight, K., Legendre, L., Koppel, D. J., Binet, M. T., Simpson, S. L. and Jolley, D. F. (2021) 'The effects of pulse exposures of metal toxicants on different life stages of the tropical copepod *Acartia sinjiensis*', *Environmental Pollution,* 285, pp. 1 - 10.
Sullivan, B. K., Buskey, E., Miller, D. C. and Ritacco, P. J. (1983) 'Effects of copper and cadmium on growth, swimming and predator avoidance in *Eurytemora affinis* (Copepoda)', *Marine Biology,* 77(3), pp. 299-306.
Sunda, W. G., Tester, P. A. and Huntsman, S. A. (1987) 'Effects of cupric and zinc ion activities on the survival and reproduction of marine copepods', *Marine Biology,* 94(2), pp. 203-210.
Suter II, G. W. (2008) 'Ecological risk assessment in the United States environmental protection agency: A historical overview', *Integrated Environmental Assessment and Management,* 4(3), pp. 285-289.
Takami, R., Almeida, J. V., Vardaris, C. V., Colepicolo, P. and Barros, M. P. (2012) 'The interplay between thiol-compounds against chromium (VI) in the freshwater green alga *Monoraphidium convolutum*: Toxicology, photosynthesis, and oxidative stress at a glance', *Aquatic Toxicology,* 118-119, pp. 80-87.
Tan, Y.-M., Leonard, J. A., Edwards, S., Teeguarden, J., Paini, A. and Egeghy, P. (2018) 'Aggregate Exposure Pathways in support of risk assessment', *Current opinion in toxicology,* 9, pp. 8-13.
Tao, W., Li, H., Peng, X., Zhang, W., Lou, Q., Gong, J. and Ye, J. (2021) 'Characteristics of heavy metals in seawater and sediments from Daya Bay (South China): environmental fates, source apportionment and ecological risks', *Sustainability,* 13(18), pp. 1 - 15.
Tartarotti, B. and Torres, J. (2009) 'Sublethal stress: Impact of solar UV radiation on protein synthesis in the copepod *Acartia tonsa*', *Journal of experimental marine biology and ecology,* 375(1-2), pp. 106-113.
Tchounwou, P. B., Yedjou, C. G., Patlolla, A. K. and Sutton, D. J. (2012) 'Heavy metal toxicity and the environment', *Experientia supplementum (2012),* 101, pp. 133-164.
Tedetti, M. and Sempere, R. (2006) 'Penetration of ultraviolet radiation in the marine environment. A review', *Photochemistry and Photobiology,* 82(2), pp. 389-397.
Teien, H.-C., Pettersen, M., Kassaye, Y., Hindar, A., Lind, O. and Håvardstun, J. (2017) *Aluminum and trace metals in the Kaldvellfjord - state forms and uptake in fish. - MINA academic report*, Ås, Norway: Norwegian University of Life Sciences.
Teien, H.-C., Standring, W. J. F. and Salbu, B. (2006) 'Mobilization of river transported colloidal aluminium upon mixing with seawater and subsequent deposition in fish gills', *Science of The Total Environment,* 364(1), pp. 149-164.
Thomas, K. V., Barnard, N., Collins, K. and Eggleton, J. (2003) 'Toxicity characterisation of sediment porewaters collected from UK estuaries using a *Tisbe battagliai* bioassay', *Chemosphere,* 53(9), pp. 1105-1111.
Tian, K., Wu, Q., Liu, P., Hu, W., Huang, B., Shi, B., Zhou, Y., Kwon, B.-O., Choi, K., Ryu, J., Seong Khim, J. and Wang, T. (2020) 'Ecological risk assessment of heavy metals in

sediments and water from the coastal areas of the Bohai Sea and the Yellow Sea', *Environment International,* 136, pp. 1 - 15.
Tlili, S., Ovaert, J., Souissi, A., Ouddane, B. and Souissi, S. (2016) 'Acute toxicity, uptake and accumulation kinetics of nickel in an invasive copepod species: *Pseudodiaptomus marinus*', *Chemosphere,* 144, pp. 1729-37.
Tollefsen, K. E., Scholz, S., Cronin, M. T., Edwards, S. W., de Knecht, J., Crofton, K., Garcia-Reyero, N., Hartung, T., Worth, A. and Patlewicz, G. (2014) 'Applying Adverse Outcome Pathways (AOPs) to support Integrated Approaches to Testing and Assessment (IATA)', *Regulatory Toxicology and Pharmacology,* 70(3), pp. 629-640.
Tollefsen, K. E., Song, Y., Høgåsen, T., Øverjordet, I. B., Altin, D. and Hansen, B. H. (2017) 'Mortality and transcriptional effects of inorganic mercury in the marine copepod *Calanus finmarchicus*', *Journal of Toxicology and Environmental Health, Part A,* 80(16-18), pp. 845-861.
Torres, E., Cid, A., Herrero, C. and Abalde, J. (2000) 'Effect of Cadmium on Growth, ATP Content, Carbon Fixation and Ultrastructure in the Marine Diatom *Phaeodactylum tricornutum* Bohlin', *Water, Air, and Soil Pollution,* 117(1), pp. 1-14.
Tovar-Sánchez, A., Duarte, C. M., Alonso, J. C., Lacorte, S., Tauler, R. and Galbán-Malagón, C. (2010) 'Impacts of metals and nutrients released from melting multiyear Arctic sea ice', *Journal of Geophysical Research: Oceans,* 115(C7), pp. 1 - 7.
Town, R. M. and Filella, M. (2002) 'Size fractionation of trace metal species in freshwaters: implications for understanding their behaviour and fate', *Reviews in Environmental Science and Biotechnology,* 1(4), pp. 277-297.
Trevisan, R., Flesch, S., Mattos, J. J., Milani, M. R., Bainy, A. C. D. and Dafre, A. L. (2014) 'Zinc causes acute impairment of glutathione metabolism followed by coordinated antioxidant defenses amplification in gills of brown mussels *Perna perna*', *Comparative Biochemistry and Physiology Part C: Toxicology & Pharmacology,* 159, pp. 22-30.
Trombini, C., Hampel, M. and Blasco, J. n. (2016) 'Evaluation of acute effects of four pharmaceuticals and their mixtures on the copepod *Tisbe battagliai*', *Chemosphere,* 155, pp. 319-328.
Turner, J. (2004) 'The importance of small planktonic copepods and their roles in pelagic marine food webs', *Zoological Studies,* 43(2), pp. 255-266.
Tvermoes, B. E., Bird, G. S. and Freedman, J. H. (2011) 'Cadmium induces transcription independently of intracellular calcium mobilization', *PLoS One,* 6(6), pp. e20542.
Uhoraningoga, A., Kinsella, G. K., Frias, J. M., Henehan, G. T. and Ryan, B. J. (2019) 'The statistical optimisation of recombinant β-glucosidase production through a two-stage, multi-model, Design of Experiments approach', *Bioengineering,* 6(3), pp. 1 - 23.
United Nations Environment Programme, E. E. A. P. (2012) 'Environmental effects of ozone depletion and its interactions with climate change: progress report, 2011', *Photochemical & Photobiological Sciences,* 11(1), pp. 13-27.
Valavanidis, A., Vlahogianni, T., Dassenakis, M. and Scoullos, M. (2006) 'Molecular biomarkers of oxidative stress in aquatic organisms in relation to toxic environmental pollutants', *Ecotoxicology and Environmental Safety,* 64(2), pp. 178-189.
Valko, M., Jomova, K., Rhodes, C. J., Kuča, K. and Musílek, K. (2016) 'Redox- and non-redox-metal-induced formation of free radicals and their role in human disease', *Archives of Toxicology,* 90(1), pp. 1-37.
Van den Brink, P. J. (2008) 'Ecological risk assessment: From book-keeping to chemical stress ecology', *Environmental Science & Technology,* 42(24), pp. 8999-9004.
Velders, G. J. M., Andersen, S. O., Daniel, J. S., Fahey, D. W. and McFarland, M. (2007) 'The importance of the Montreal Protocol in protecting climate', *Proceedings of the National Academy of Sciences,* 104(12), pp. 4814.
Venkataraman, Y. R., White, S. J. and Roberts, S. B. (2022) 'Differential DNA methylation in Pacific oyster reproductive tissue in response to ocean acidification', *BMC Genomics,* 23(1), pp. 556.
Verriopoulos, G. and Dimas, S. (1988) 'Combined toxicity of copper, cadmium, zinc, lead, nickel, and chrome to the copepod *Tisbe holothuriae*', *Bulletin of Environmental Contamination and Toxicology,* 41(3), pp. 378-384.

Verriopoulos, G. and Moraïtou-Apostolopoulou, M. (1982) 'Differentiation of the sensitivity to copper and cadmium in different life stages of a copepod', *Marine Pollution Bulletin,* 13(4), pp. 123-125.
Vignati, D. A. L., Dworak, T., Ferrari, B., Koukal, B., Loizeau, J.-L., Minouflet, M., Camusso, M. I., Polesello, S. and Dominik, J. (2005) 'Assessment of the geochemical role of colloids and their impact on contaminant toxicity in freshwaters: An example from the Lambro−Po system (Italy)', *Environmental Science & Technology,* 39(2), pp. 489-497.
Villagran, D., Fernandez Severini, M., Biancalana, F., Spetter, C., Fernandez, E. and Marcovecchio, J. (2019) 'Bioaccumulation of heavy metals in mesozooplankton from a human-impacted south western Atlantic estuary (Argentina)', *Journal of Marine Research,* 77(1-2), pp. 217-241.
Villeneuve, D. L., Crump, D., Garcia-Reyero, N., Hecker, M., Hutchinson, T. H., LaLone, C. A., Landesmann, B., Lettieri, T., Munn, S., Nepelska, M., Ottinger, M. A., Vergauwen, L. and Whelan, M. (2014) 'Adverse outcome pathway (AOP) development I: strategies and principles', *Toxicological sciences : an official journal of the Society of Toxicology,* 142(2), pp. 312-320.
Wang, J., Wang, Q., Li, J., Shen, Q., Wang, F. and Wang, L. (2012) 'Cadmium induces hydrogen peroxide production and initiates hydrogen peroxide-dependent apoptosis in the gill of freshwater crab, *Sinopotamon henanense*', *Comparative Biochemistry and Physiology Part C: Toxicology & Pharmacology,* 156(3), pp. 195-201.
Wang, L., Liu, J., Filipiak, M., Mungunkhuyag, K., Jedynak, P., Burczyk, J., Fu, P. and Malec, P. (2021) 'Fast and efficient cadmium biosorption by *Chlorella vulgaris* K-01 strain: The role of cell walls in metal sequestration', *Algal Research,* 60, pp. 102497.
Wang, M., Jeong, C.-B., Lee, Y. H. and Lee, J.-S. (2018) 'Effects of ocean acidification on copepods', *Aquatic Toxicology,* 196, pp. 17-24.
Wang, M., Jeong, C. B., Li, Y. and Lee, J. S. (2017) 'Different transcriptomic responses of two marine copepods, *Tigriopus japonicus* and *Pseudodiaptomus annandalei*, to a low dose of mercury chloride (HgCl(2))', *Aquat Toxicol,* 187(2017), pp. 124-131.
Wang, M. and Wang, G. (2010) 'Oxidative damage effects in the copepod *Tigriopus japonicus* Mori experimentally exposed to nickel', *Ecotoxicology,* 19(2), pp. 273-284.
Wang, M., Zhang, C. and Lee, J.-S. (2018) 'Quantitative shotgun proteomics associates molecular-level cadmium toxicity responses with compromised growth and reproduction in a marine copepod under multigenerational exposure', *Environmental Science & Technology,* 52(3), pp. 1612-1623.
Wang, M., Zhao, W., Wei, J., Wang, S. and Xie, X. (2019) 'Acute effects of UVB radiation on the survival, growth, development, and reproduction of *Daphniopsis tibetana* Sars (Crustacea: Cladocera)', *Environmental Science and Pollution Research,* 26(11), pp. 10916-10925.
Wang, W.-X. and Fisher, N. S. (1999) 'Delineating metal accumulation pathways for marine invertebrates', *Science of The Total Environment,* 237-238, pp. 459-472.
Wang, X., Luo, X., Wang, Q., Liu, Y. and Naidu, R. (2020) 'Predicting the combined toxicity of binary metal mixtures (Cu–Ni and Zn–Ni) to wheat', *Ecotoxicology and Environmental Safety,* 205, pp. 111334.
Wei, H., Qian, J., Xie, Z.-X., Lin, L., Wang, D.-Z. and Wang, M.-H. (2022) 'Diel Fluctuation Superimposed on Steady High pCO2 Generates the Most Serious Cadmium Toxicity to Marine Copepods', *Environmental Science & Technology,* 56(18), pp. 13179-13188.
Williamson, C. E., Fischer, J. M., Bollens, S. M., Overholt, E. P. and Breckenridge, J. K. (2011) 'Toward a more comprehensive theory of zooplankton diel vertical migration: Integrating ultraviolet radiation and water transparency into the biotic paradigm', *Limnology and Oceanography,* 56(5), pp. 1603-1623.
Williamson, C. E., Neale, P. J., Hylander, S., Rose, K. C., Figueroa, F. L., Robinson, S. A., Häder, D.-P., Wängberg, S.-Å. and Worrest, R. C. (2019) 'The interactive effects of stratospheric ozone depletion, UV radiation, and climate change on aquatic ecosystems', *Photochemical & Photobiological Sciences,* 18(3), pp. 717-746.
Wolinski, L., Modenutti, B., Souza, M. S. and Balseiro, E. (2016) 'Interactive effects of temperature, ultraviolet radiation and food quality on zooplankton alkaline phosphatase activity', *Environmental Pollution,* 213, pp. 135-142.

Wolinski, L., Souza, M. S., Modenutti, B. and Balseiro, E. (2020) 'Effect of chronic UVR exposure on zooplankton molting and growth', *Environmental Pollution,* 267, pp. 115448.
Won, E.-J., Lee, Y., Han, J., Hwang, U.-K., Shin, K.-H., Park, H. G. and Lee, J.-S. (2014) 'Effects of UV radiation on hatching, lipid peroxidation, and fatty acid composition in the copepod *Paracyclopina nana*', *Comparative Biochemistry and Physiology Part C: Toxicology & Pharmacology,* 165, pp. 60-66.
Wong, S. W. Y., Zhou, G.-J., Leung, P. T. Y., Han, J., Lee, J.-S., Kwok, K. W. H. and Leung, K. M. Y. (2020) 'Sunscreens containing zinc oxide nanoparticles can trigger oxidative stress and toxicity to the marine copepod *Tigriopus japonicus*', *Marine Pollution Bulletin,* 154, pp. 1 - 10.
Xie, F., Lampi, M. A., Dixon, D. G. and Greenberg, B. M. (2007) 'Assessment of the toxicity of mixtures of nickel or cadmium with 9,10-phenanthrenequinone to *Daphnia magna*: impact of a reactive oxygen-mediated mechanism with different redox-active metals', *Environ Toxicol Chem,* 26(7), pp. 1425-32.
Xie, L., Solhaug, K. A., Song, Y., Johnsen, B., Olsen, J. E. and Tollefsen, K. E. (2020) 'Effects of artificial ultraviolet B radiation on the macrophyte *Lemna minor*: a conceptual study for toxicity pathway characterization', *Planta,* 252(5), pp. 1 - 19.
Yoo, J.-W., Cho, H., Lee, K.-W., Won, E.-J. and Lee, Y.-M. (2021) 'Combined effects of heavy metals (Cd, As, and Pb): Comparative study using conceptual models and the antioxidant responses in the brackish water flea', *Comparative Biochemistry and Physiology Part C: Toxicology & Pharmacology,* 239(2021), pp. 1 - 8.
Zhang, F., Ye, N., Wang, S., Meng, Y., Fang, H., Wang, Z. and Wang, D.-G. (2019) 'Dissolved Organic Matter Modulates Algal Oxidative Stress and Membrane System Responses to Binary Mixtures of Nano-Metal-Oxides (nCeO2, nMgO and nFe3O4) and Sulfadiazine', *Nanomaterials*, 9(5). DOI: 10.3390/nano9050712.
Zhuang, Y., Yang, F., Xu, D., Chen, H., Zhang, H. and Liu, G. (2017) 'Spliced leader-based analyses reveal the effects of polycyclic aromatic hydrocarbons on gene expression in the copepod *Pseudodiaptomus poplesia*', *Aquatic Toxicology,* 183, pp. 114-126.

Appendix A

The following code was written in node.js version 14, making use of the *Axios, CSVWriter* and *CleanStr* packages.

```
/*
Scopus Search Tool

Author: Kieran Cutting
Date: 08/10/2020

This code uses the Scopus Search API to find all papers which match a given query
string and outputs them into a .csv file, 'scopus.csv'.

It requires an API key for the Scopus Search API, which can be retrieved from:
https://dev.elsevier.com/

The documentation for the Scopus Search API can be found here:
https://dev.elsevier.com/documentation/ScopusSearchAPI.wadl

Before running this code, ensure you have installed node.js and run 'npm install'
to install the project's dependencies.

In order to extract full data from the API, you will need to be on the wifi of a
Scopus subscriber university.
*/

// Axios makes requests to web addresses
let axios = require("axios");

// Creating an instance of axios to use, allowing us to search
const scopusSearch = axios.create({
    baseURL: "http://api.elsevier.com/content/search/scopus",
    headers: { "X-ELS-APIKey": 'enter_API_key_here' },
  });

// CSV Writer performs operations to write to CSV files
const createCsvWriter = require("csv-writer").createObjectCsvWriter;

// Setting up the headers of the CSV file
const scopusWriter = createCsvWriter({
  path: "scopus.csv",
  header: [
    { id: "author", title: "Author" },
    { id: "title", title: "Title" },
    { id: "publication", title: "Publication" },
    { id: "abstract", title: "Abstract" },
    { id: "date", title: "Date" },
    { id: "doi", title: "DOI" },
  ],
});
```

```
// Removes non-standard characters which may interfere with CSV output
const cleaner = require("cleanstr");

// Setting the search string
let scopusQuery =
  "?query=" + "TITLE-ABS-KEY%28copepods+AND+metal+AND+effects%29";

// To speed up response times, optionally use these modifiers
// let modifiers = "&field=dc:title,dc:description,authkeywords";

// On the wifi of a university with Scopus access, these modifiers ensure full
record data is found
let modifiers = "&view=complete";

// Initialising counters for search loops
let totalResults = 0; /* Total number of results*/
let startPoint = 0; /* The record number to start searching from, incrementing by
25*/
let start = "&start=" + startPoint; /* The string of the starting point*/
let iterations = 1; /* The loop end-point; must be non-zero but is reset within the
loop to be totalResults / 25*/

let scopusData = []; /* Array for the data to be stored in*/
let sanitisedScopus = []; /* Array for the sanitised data to be stored in before
writing to CSV */

// Begins the search
run();

async function run() {
  await getScopusData();
  outputData();
}

// Gets the data from Scopus API and stores in data variable
async function getScopusData() {
  // Loops for 'iteration' times - iteration is reset within the context of
  // the loop to be the number of results / 25
  for (let i = 0; i < iterations; i++) {

    // Axios searches with variableName.get()
    await scopusSearch
      .get(scopusQuery + start + modifiers)
      .then(function (res) {

        // sets searchData as the data of retrieved from axios
        let searchData = res.data["search-results"];

        // if totalResults is zero, i.e. the code is running for the first time,
        // sets totalResults to the number of total results, and sets iterations
        // to total results / 25 in order to chunk up the requests
```

```
        if (totalResults == 0) {
          totalResults = searchData["opensearch:totalResults"];
          iterations = searchData["opensearch:totalResults"] / 25;
        }

        // For each entry of the data, pushes to the 'messy' data array
        for (let items of searchData.entry) {
          scopusData.push(items);
        }

        // Adds 25 to startPoint to change where the loop searches from
        startPoint = startPoint + 25;
        start = "&start=" + startPoint; /* The string of the starting point*/
      })
      .catch(function (err) {
        // Outputs any errors
        console.log(err);
      });
  }
}

// Sanitises data and then writes to CSV
function outputData() {
  sanitiseData();
  scopusWriter
    .writeRecords(sanitisedScopus)
    .then(() => console.log("Scopus data written successfully!"));
}

// Makes data CSV friendly by pushing to the sanitised array
function sanitiseData() {
  for (let items of scopusData) {
    sanitisedScopus.push({
      author: items["dc:creator"],
      title: items["dc:title"],
      publication: items["prism:publicationName"],
      abstract: items["dc:description"],
      date: items["prism:coverDate"],
      doi: items["prism:doi"],
    });
  }
}

// If needed within multiple runs of the code, this resets the search counters
function reset() {
    totalResults = 0; /* Total number of results */
    startPoint = 0; /* The record number to start searching from, incrementing by
25 by default*/
    start = "&start=" + startPoint; /* The string of the starting point */
    iterations = 1; /* The loop end-point; must be non-zero but is reset within the
loop to be totalResults / 25 */
  }
```